frontiers | Research Topics

Chemoradiotherapy in locally advanced rectal cancer patients

Edited by
Davide Bellini, Marco Rengo and Vincenza Granata

Published in
Frontiers in Oncology

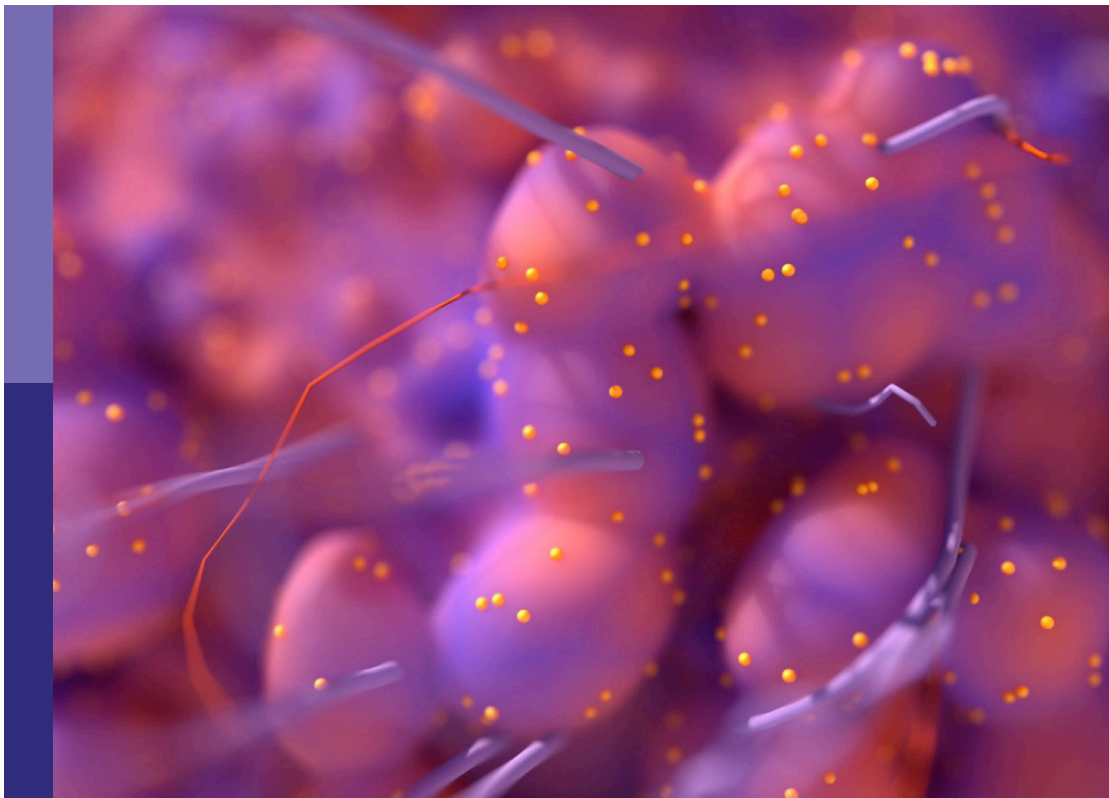

ISSN 1664-8714
ISBN 978-2-8325-4728-1
DOI 10.3389/978-2-8325-4728-1

About Frontiers

Frontiers is more than just an open access publisher of scholarly articles: it is a pioneering approach to the world of academia, radically improving the way scholarly research is managed. The grand vision of Frontiers is a world where all people have an equal opportunity to seek, share and generate knowledge. Frontiers provides immediate and permanent online open access to all its publications, but this alone is not enough to realize our grand goals.

Frontiers journal series

The Frontiers journal series is a multi-tier and interdisciplinary set of open-access, online journals, promising a paradigm shift from the current review, selection and dissemination processes in academic publishing. All Frontiers journals are driven by researchers for researchers; therefore, they constitute a service to the scholarly community. At the same time, the *Frontiers journal series* operates on a revolutionary invention, the tiered publishing system, initially addressing specific communities of scholars, and gradually climbing up to broader public understanding, thus serving the interests of the lay society, too.

Dedication to quality

Each Frontiers article is a landmark of the highest quality, thanks to genuinely collaborative interactions between authors and review editors, who include some of the world's best academicians. Research must be certified by peers before entering a stream of knowledge that may eventually reach the public - and shape society; therefore, Frontiers only applies the most rigorous and unbiased reviews. Frontiers revolutionizes research publishing by freely delivering the most outstanding research, evaluated with no bias from both the academic and social point of view. By applying the most advanced information technologies, Frontiers is catapulting scholarly publishing into a new generation.

What are Frontiers Research Topics?

Frontiers Research Topics are very popular trademarks of the *Frontiers journals series*: they are collections of at least ten articles, all centered on a particular subject. With their unique mix of varied contributions from Original Research to Review Articles, Frontiers Research Topics unify the most influential researchers, the latest key findings and historical advances in a hot research area.

Find out more on how to host your own Frontiers Research Topic or contribute to one as an author by contacting the Frontiers editorial office: frontiersin.org/about/contact

Chemoradiotherapy in locally advanced rectal cancer patients

Topic editors

Davide Bellini — Sapienza University of Rome, Italy

Marco Rengo — Sapienza University of Rome, Italy

Vincenza Granata — Radiological department, National Cancer of Naples, IRCCS, Italy

Citation

Bellini, D., Rengo, M., Granata, V., eds. (2024). *Chemoradiotherapy in locally advanced rectal cancer patients*. Lausanne: Frontiers Media SA.

doi: 10.3389/978-2-8325-4728-1

Table of contents

frontiers | Frontiers in Oncology

ORIGINAL RESEARCH
published: 27 May 2022
doi: 10.3389/fonc.2022.886101

Combining Clinicopathology, IVIM-DWI and Texture Parameters for a Nomogram to Predict Treatment Response to Neoadjuvant Chemoradiotherapy in Locally Advanced Rectal Cancer Patients

Rixin Su[1†], Shusheng Wu[2†], Hao Shen[1], Yaolin Chen[1], Jingya Zhu[1], Yu Zhang[1], Haodong Jia[3], Mengge Li[2], Wenju Chen[2], Yifu He[1,2] and Fei Gao[3*]*

[1] Department of Medical Oncology, Anhui Provincial Hospital Affiliated to Anhui Medical University, Hefei, China, [2] Department of Medical Oncology, The First Affiliated Hospital of University of Science and Technology of China (USTC), Division of Life Sciences and Medicine, University of Science and Technology of China, Anhui Provincial Cancer Hospital, Hefei, China, [3] Department of Radiology, The First Affiliated Hospital of University of Science and Technology of China (USTC), Division of Life Sciences and Medicine, University of Science and Technology of China, Anhui Provincial Cancer Hospital, Hefei, China

OPEN ACCESS

Edited by:
Marco Rengo,
Sapienza University of Rome, Italy

Reviewed by:
Mariarita Tarallo,
Sapienza University of Rome, Italy
Ning Mao,
Yantai Yuhuangding Hospital, China

***Correspondence:**
Yifu He
yifuhe@fsyy.ustc.edu.cn
Fei Gao
15956912758@163.com

[†]These authors have contributed equally to this work

Specialty section:
This article was submitted to Gastrointestinal Cancers: Colorectal Cancer, a section of the journal Frontiers in Oncology

Received: *28 February 2022*
Accepted: *25 April 2022*
Published: *27 May 2022*

Citation:
Su R, Wu S, Shen H, Chen Y, Zhu J, Zhang Y, Jia H, Li M, Chen W, He Y and Gao F (2022) Combining Clinicopathology, IVIM-DWI and Texture Parameters for a Nomogram to Predict Treatment Response to Neoadjuvant Chemoradiotherapy in Locally Advanced Rectal Cancer Patients. Front. Oncol. 12:886101. doi: 10.3389/fonc.2022.886101

Objectives: This study aimed to create a nomogram for the risk prediction of neoadjuvant chemoradiotherapy (nCRT) resistance in locally advanced rectal cancer (LARC).

Methods: Clinical data in this retrospective study were collected from a total of 135 LARC patients admitted to our hospital from June 2016 to December 2020. After screening by inclusion and exclusion criteria, 62 patients were included in the study. Texture analysis (TA) was performed on T2WI and DWI images. Patients were divided into response group (CR+PR) and no-response group (SD+PD) according to efficacy assessment. Multivariate analysis was performed on clinicopathology, IVIM-DWI and texture parameters for screening of independent predictors. A nomogram was created and model fit and clinical net benefit were assessed.

Results: Multivariate analysis of clinicopathology parameters showed that the differentiation and T stage were independent predictors (OR values were 14.516 and 11.589, resp.; $P<0.05$). Multivariate analysis of IVIM-DWI and texture parameters showed that f value and Rads-score were independent predictors (OR values were 0.855, 2.790, resp.; $P<0.05$). In this study, clinicopathology together with IVIM-DWI and texture parameters showed the best predictive efficacy (AUC=0.979). The nomogram showed good predictive performance and stability in identifying high-risk LARC patients who are resistant to nCRT (C-index=0.979). Decision curve analyses showed that the nomogram had the best clinical net benefit. Ten-fold cross-validation results showed that the average AUC value was 0.967, and the average C-index was 0.966.

Conclusions: The nomogram combining the differentiation, T stage, f value and Rads-score can effectively estimate the risk of nCRT resistance in patients with LARC.

Keywords: locally advanced rectal cancer, clinicopathology, intravoxel incoherent motion diffusion weighted imaging, texture analysis, nomogram, prediction, response to nCRT

INTRODUCTION

Rectal cancer is the third most common malignancy in terms of morbidity and mortality worldwide, and nearly half of rectal cancers are diagnosed as locally advanced rectal cancer (LARC) (1). Total mesorectal excision (TME) after neoadjuvant chemoradiotherapy (nCRT) for LARC is the current standard treatment modality, which can improve the local control rate, sphincter preservation rate, and reduce the local recurrence rate of LARC. And 10% to 20% of patients can achieve pathological complete remission after nCRT (2). Early assessment of nCRT efficacy and preservation of anal sphincter function can significantly improve the quality of life for patients (3, 4). Therefore, it becomes an urgent issue to find markers that can predict the efficacy of nCRT for LARC, then differentiate patients who are sensitive or resistant to nCRT at an early stage, and formulate individualized treatment for different patients.

Since the introduction of conventional MRI to local staging of rectal cancer, many efforts have been made to find predictive imaging signatures so as to identify patients with good or poor response to nCRT and patients at higher risk of recurrence (5, 6). However, as conventional MRI has poor sensitivity and specificity in assessing and predicting treatment response, it is hard to distinguish post-treatment fibrosis and edema from tumor tissue after nCRT, and even harder to accurately predict complete pathological remission (7–9). Without the use of exogenous contrast agents, intravoxel incoherent motion diffusion weighted imaging (IVIM-DWI) based on the biexponential model can assess the pure diffusion motion and perfusion-related motion of water molecules separately. Compared to conventional MRI, IVIM-DWI can more accurately display tissue microenvironment information and non-invasively and quantitatively diagnose tumor malignancy, pathological differentiation, and lymph node metastasis (10–12). In recent years, several studies have proved the superiority of IVIM-DWI in predicting treatment response in various tumors (13–15). It was found that IVIM-DWI was effective in predicting tumor size changes in patients with breast cancer liver metastases who were undergoing radioembolization, and that treatment-induced changes in f value could be a potential biomarker in the prediction of treatment response (16). Studies have also shown that IVIM-DWI parameters, especially pretreatment D value could predict patients' response to induction chemotherapy with locally advanced hypopharyngeal carcinoma (17). However, no conclusive results have been obtained about the efficacy of IVIM-DWI in predicting the response of patients with LARC to nCRT.

Texture analysis (TA) is an emerging image analysis method that extracts quantitative imaging features from images through high throughput analysis. It can reflect the spatial variation and heterogeneity of voxel intensities within the tumor and can provide valuable references for disease diagnosis, treatment, and efficacy prediction of therapies (18, 19), thus a promising method for assessing response to various cancer treatments. Studies have found that texture analysis of magnetic resonance imaging (MRI) could predict early recurrence after hepatectomy for solitary hepatocellular carcinoma (20). It was also found that MRI texture features could predict pathological complete response (pCR) to neoadjuvant chemotherapy in breast cancer (21). In rectal cancer, TA can work as a supplement to conventional MR imaging, especially in identifying staging, assessing treatment response, and predicting lymph node metastasis and prognosis (22–24).

The purpose of this study was to combine clinicopathology, IVIM-DWI and texture parameters to establish a nomogram for treatment response prediction to nCRT in patients with LARC, which can be used to identify patients at high risk of nCRT resistance.

MATERIALS AND METHODS

Patients

A total of 135 LARC patients admitted to Anhui Provincial Hospital from June 2016 to December 2020 were retrospectively collected, among whom 62 patients with complete clinical data were included in this study. Inclusion criteria included (1) Locally advanced rectal primary adenocarcinoma was confirmed by colonoscopy biopsy; (2) All patients received pelvic nCRT before surgery; (3) The lower edge of the tumor is within 15 cm of the anal verge; (4) Patients completed routine MRI and IVIM-DWI examinations before nCRT. Exclusion criteria were (1) Patients who have not received complete nCRT; (2) Patients with a history of other tumors; (3) The image quality is poor, with significant artifacts, and cannot be used for image segmentation or image histology feature extraction. The flow chart of this study is shown in **Figure 1**.

Imaging Examination

Before receiving nCRT, patients underwent MRI examination which was performed in the supine position utilizing a 3.0-T scanner (Signa HDXT, General Electric Healthcare, Waukesha, WI, USA) with an 8-channel phased array coil. All patients fasted for at least 8 hours and received intramuscular injection of hyoscine butylbromide 20 mg half an hour before MRI examination to reduce gastrointestinal motility artifacts. The sequences include axial T_1-weighted imaging (T1WI) fast spin-echo (FSE), axial T_2-weighted imaging (T2WI) FSE, sagittal T2WI FSE, coronal T2WI FSE. IVIM-DWI was acquired using single-shot echo-planar imaging (EPI) pulse sequence with 10 b

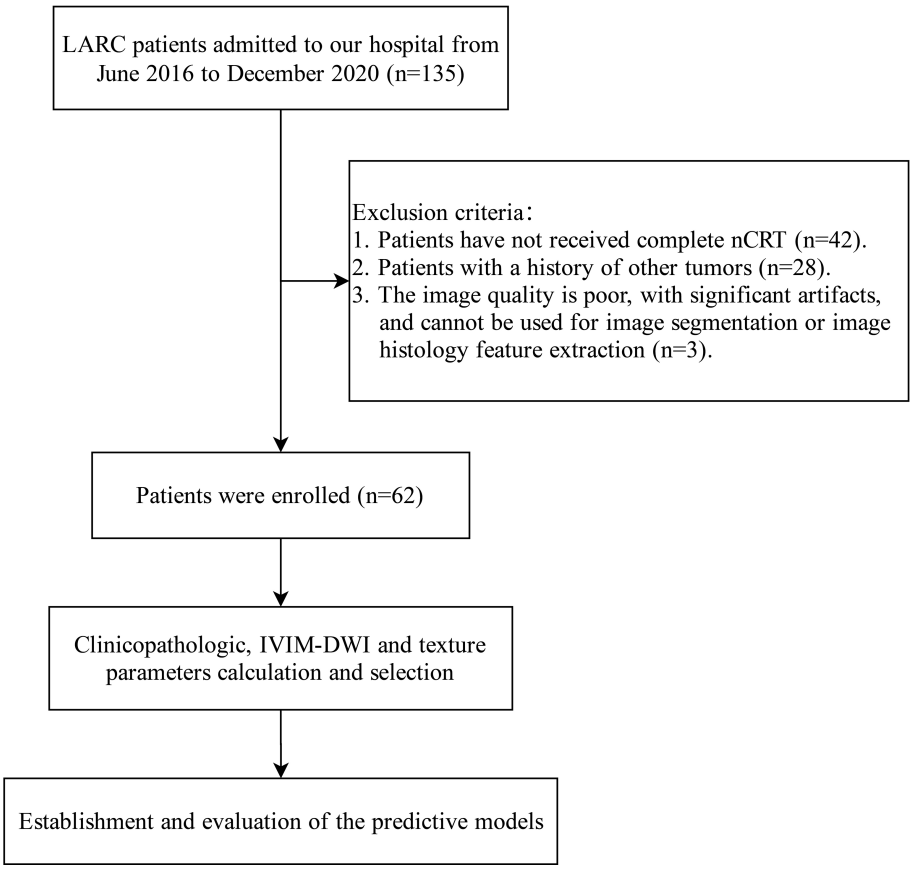

FIGURE 1 | Flow chart for establishing a nomogram for predicting nCRT resistant in LARC patients.

values (0, 10, 20, 50, 100, 200, 400, 800, 1,200, and 2000 s/mm^2). The scan parameters of each sequence in MRI are shown in **Table 1**.

IVIM-DWI Measurement

The IVIM-DWI measurement was performed by two radiologists. They used FunctionTool to build regions of interest (ROI) on a post-processing workstation (version ADW 4.5, GE Healthcare) without knowledge of clinicopathological results. To acquire the parameters, the ROI of IVIM-DWI was selected on the maximum transverse plane of each lesion (b value=800 s/mm^2) (**Figure 2**). Referring to the axial T2WI image, the ROI was manually delineated along the tumor margin, avoiding the hemorrhage, necrosis, and cystic change of the tumor. All parameters were measured three times and the average value was calculated. To assess interobserver agreement, each radiologist plotted twice to obtain values and calculate intraclass correlation coefficients (ICC). Parameters with ICC value > 0.75 were selected for subsequent analysis.

Texture Features Analyses

Patients underwent tumor delineation and texture features extraction. The raw data was transferred to the PACS system, and axis IVIM-DWI (b=800 s/mm^2) and T_2WI images (DICOM

TABLE 1 | Scan parameters of each sequence in MRI.

Sequences	T1WI FSE	T2WI FSE	T2WI FSE	T2WI FSE	IVIM-DWI
Plane	Axial	Axial	Sagittal	Coronal	Axial
TR/TE (ms)	500/7.2	3500/109.1	3500/109.1	3500/109.1	4000/75
NEX	1	4	4	4	–
FOV (mm)	320 × 320	240 × 240	240 × 240	240 × 240	420 × 420
Slice thickness (mm)	6	3	3	3	4
Slice interval (mm)	2	0	0	0	1

T1WI, T_1-weighted imaging; FSE, fast spin-echo; T2WI, T_2-weighted imaging; TR/TE, repetition time/echo time; NEX, number of excitations; FOV, field of view.

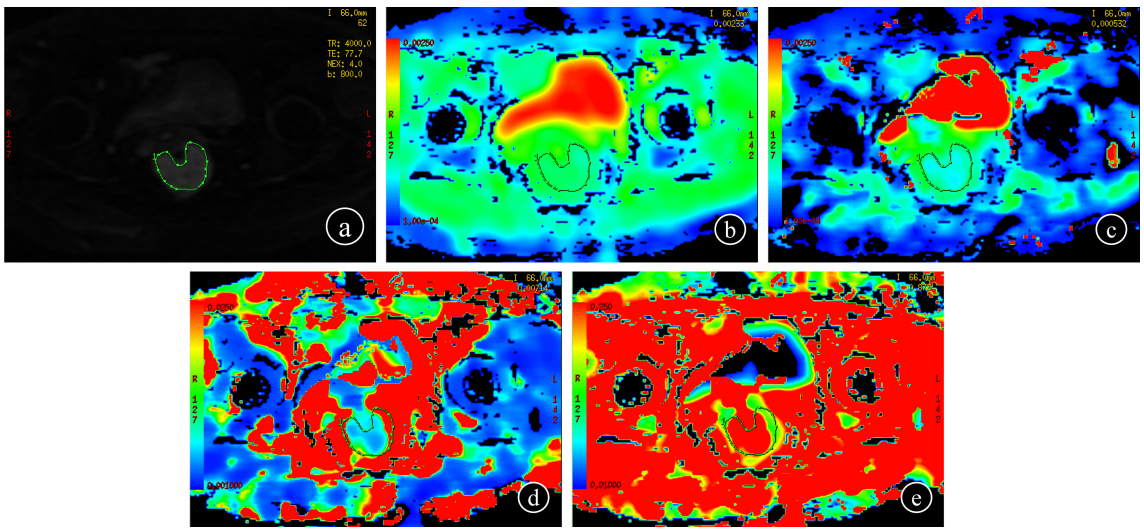

FIGURE 2 | IVIM-DWI measurement (b = 800 s/mm^2) **(A)**; each radiologist drew ROI three times to get the values on the maps of ADC, D, D*, and f, respectively **(B–E)**.

format) were imported into the ITK-SNAP software. Two radiologists segmented the tumor's 3-dimensional volume of interest (3D-VOI), and all lesions were delineated layer by layer. The definition of ROI included areas of hemorrhage, necrosis, and cystic degeneration while avoiding normal anatomy. The original images and ROIs were imported into A.K (Analysis Kit, Kinetics Version 2.1, GE Healthcare). Then a series of texture features for all lesions were automatically acquired by the software. Finally, 1 656 texture features (828 on T2WI, 828 on IVIM-DWI) of the entire tumor were extracted. **Figure 3** shows the texture feature extraction. Features with ICC value > 0.75 were selected for subsequent analysis.

nCRT Regimen

nCRT regimen: radiotherapy (5 days a week, 1.8 ~ 2.0 Gy/d, total dose of 45 ~ 50 Gy) + chemotherapy [capecitabine 825 mg/m^2, twice a day (Monday to Friday)].

nCRT Efficacy Evaluation

nCRT efficacy on patients was assessed 6-8 weeks after they received nCRT. Two senior physicians with rich experience in

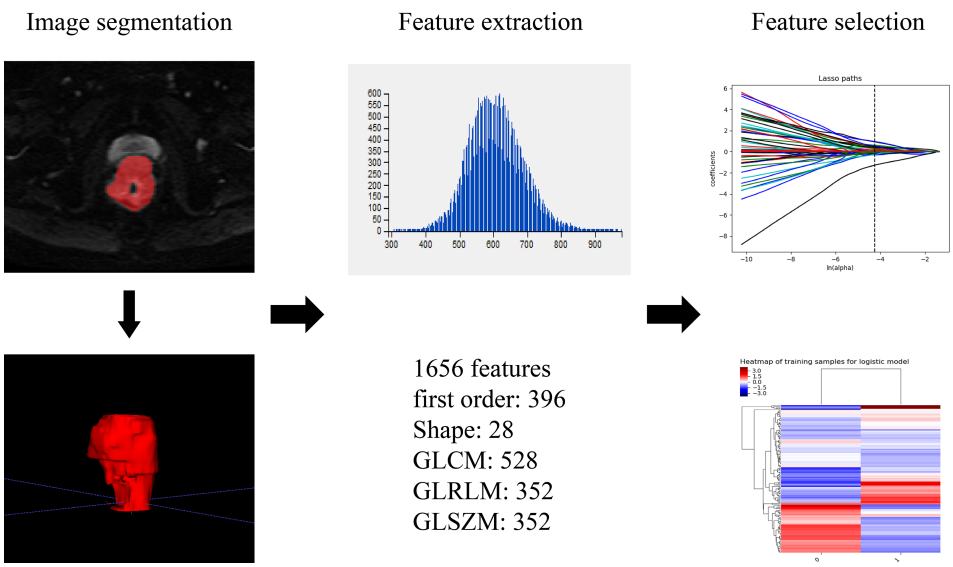

FIGURE 3 | Texture features acquisition workflow.

pelvic MR diagnosis performed image evaluation on fat suppressed T2WI (T2WI-FS) sequences under double-blind conditions. They used histology as the reference standard to identify responders or not. The efficacy evaluation was based on the revised RECIST guidelines (version 1.1) criteria (25): (1) Complete response (CR) refers to the disappearance of all target lesions, the appearance of no lesions, and the normal tumor markers for at least 4 weeks. (2) Partial remission (PR) is the reduction of the sum of the maximum diameters of target lesions ≥30% for at least 4 weeks. (3) Stable disease (SD) is the sum of the largest diameters of target lesions and the reduction does not reach PR, or the enlargement does not reach disease progression (PD). (4) PD refers to an increase of 20% at least in the sum of the largest diameters of target lesions, or the appearance of new lesions. Response group = CR+PR, No-Response group = SD+PD.

Statistical Analysis

All data were statistically analyzed using Graphpad Prism 9.0, SPSS 26.0, R 4.0.5 and IPMS 2.4.0 software. For continuous variables, Kolmogorov-Smirnov was used to test the normality of the data. If the data followed normal distribution, x ± s was used for statistical description, and independent sample t-test was conducted to compare two groups; otherwise, median ± interquartile range was used for statistical description, and Mann-Whitney U test was conducted to compare two groups. For categorical variables, the number and percentage of cases were used for statistical description, and the chi-square test or Fisher's exact probability was adopted for comparison between two groups. ICC assessed the inter-observer and intra-observer agreement of IVIM-DWI values and texture feature measurements (ICC>0.75 indicated good agreement) (26, 27). Radiomic features were screened by independent samples t-test or Mann-Whitney U test and multivariate logistic regression. Each set of texture features was developed using multi-factor linear weighting based on the regression coefficients of the selected features, and a radiomics score (Rads-score) was calculated for each patient. A nomogram model was established on the basis of clinicopathology, IVIM-DWI and Rads-score parameters. Ten-fold cross-validation was performed to assess discrimination and prediction ability of the nomogram model. All statistical tests were two-sided probability tests, and P <0.05 was considered statistically significant.

Ethical Approval and Informed Consent

This study was approved by the Ethics Committee of Anhui Provincial Hospital and the requirement for informed consent was waived due to the retrospective nature of this study.

RESULTS

Clinicopathology Characteristics

A total of 62 patients' data were collected. The average age of the patients was 58.77 ± 15.66 years. The clinical characteristics of the patients were shown in **Table 2**. All patients completed the efficacy evaluation, including 6 cases of CR (9.68%), 38 cases of PR (61.29%), 18 cases of SD (29.03%), 0 cases of PD (0%); ORR was 70.97% and DCR was 100%. There were no significant differences in age, gender, tumor diameter, N stage, CA199, and HB between the two groups (P>0.05).

Intra- and Inter-Observer Agreement

Among the 1 656 texture features extracted from T2WI and IVIM-DWI (b=800 s/mm^2) images, there were 1 054 text features with

TABLE 2 | Clinicopathologic characteristics in rectal cancer Patients.

Characteristics	Response group (n = 44)	No-Response group (n = 18)	*P* value
Age (year)	59.4 ± 15.5	57.2 ± 16.5	0.609
Sex			0.954
Male	29	12	
Female	15	6	
Differentiation			0.022
Well/Moderate	41	12	
Poor	3	6	
Tumor diameter (cm)	4.4 ± 2.1	5.2 ± 2.2	0.178
T stage			0.003
T2~3	28	4	
T4	16	14	
N stage			0.492
N0	7	1	
N1~2	37	17	
CEA (ng/ml)			0.008
<5	26	4	
≥5	18	14	
CA199 (U/ml)			0.068
<37	36	10	
≥37	8	8	
HB (g/l)	120.5 ± 17.6	119.4 ± 20	0.829

CEA, carcinoembryonic antigen; CA199, carbohydrate antigen 19-9; HB, Hemoglobin; CR, complete response; PR, partial response; SD, stable disease; PD, disease progression; Response group, the first-time evaluation results was CR or PR; No-Response group, the first-time evaluation results was SD or PD.

high stability. The ICC (inter) and ICC (intra) of IVIM-DWI values and texture features ranged from 0.775 to 0.996 and from 0.764 to 0.998, respectively, with good repeatability.

Calculating the Radsscore

Among the texture features extracted from axial T_2WI and IVIM-DWI (b=800 s/mm^2), two statistically significant texture feature parameters [glrlm_LongRunEmphasis (T_2WI), firstorder_Median (IVIM)] were retained for diagnostic efficacy after feature selection analysis. The Rads-score formula of the radiomics is as follows:

$$\text{Rads} - \text{score} = -6.627 + 0.269 * \text{glrlm}\_\text{LongRunEmphasis}(T_2\text{WI}) + 0.003 * \text{firstorder}\_\text{Median}(\text{IVIM})$$

Predictive Performance of Clinicopathology Parameters

Univariate analysis showed that tumor differentiation, T stage, CEA and CA199 were significantly correlated with the efficacy of nCRT in patients (P<0.05). Multivariate logistic analysis showed that tumor differentiation (OR: 14.516, 95%CI: 1.726-122.057, P=0.014) and T stage (OR: 11.589, 95%CI: 2.103-63.860, P=0.005) were independent factors affecting nCRT efficacy (**Table 3**). Therefore, a predictive model (model 1) was developed.

Predictive Performance of IVIM-DWI and Texture Parameters

Univariate analysis showed that D, D*, f and Rads-score were significantly correlated with the efficacy of nCRT in patients (P<0.05). Multivariate logistic analysis showed that f (OR: 0.855, 95%CI: 0.752-0.971, P=0.016) and Rads-score (OR: 2.790, 95% CI: 1.163-6.696, P=0.022) were independent factors influencing nCRT efficacy in patients (**Table 4**). Therefore, a predictive model (model 2) was built to describe the relations between independent factors and nCRT efficacy.

Development and Performance of the Nomogram

Based on combination of the differentiation, T stage, f value and Rads-score, a nomogram was created to predict tumor resistance to nCRT in patients with LARC (**Figure 4**). AUCs of differentiation, T stage, differentiation and T stage, f, Rads-score, f and Rads-score and the nomogram were 0.633, 0.707, 0.778, 0.857, 0.783, 0.917, 0.979, respectively (**Figure 5**) (**Table 5**). The nomogram calibration curve revealed that the observation and prediction were conducted in a good agreement (**Figure 6A**). C-index was 0.979, and Brier score was 0.052. Decision curve analysis (DCA) showed that the model developed by combining the differentiation, T stage, f value and Rads-score had the largest net benefit (**Figure 6B**).

Internal Validation of the Nomogram Model

To assess model's discrimination and prediction ability, the nomogram model was internally validated using ten-fold cross-validation. The results showed that the average AUC value was 0.967, and the average C-index was 0.966.

DISCUSSION

In this study, it was found that the differentiation, T stage, f value and Rads-score were related to tumor resistance to nCRT in patients with LARC. We developed and validated a nomogram which incorporated the differentiation, T stage, f value and Rads-score. The results showed that the nomogram could yield the highest AUC. Calibration curve of the nomogram revealed that the observation and prediction were in a good agreement. DCA indicated that the nomogram model had the largest net benefit.

Since the introduction of quantitative imaging, an increasing number of studies on quantitative imaging have been conducted to improve the diagnosis and treatment of cancer and many of these studies had demonstrated the widespread use of quantitative imaging in the clinical setting (28, 29). For instance, Ren et al. established an MRI-based radiomic signature from combined contrast-enhanced T1-weighted and T2-weighted images to predict the preoperative staging of head and neck cancers (30). Zheng et al. combined the IVIM-DWI

TABLE 3 | Statistical analysis results of clinicopathologic characteristics in rectal cancer patients.

Characteristics	Univariate analysis (*P*)	Multivariate logistic regression analysis		
		OR	95%CI	*P*
Age (year)	0.603			
Sex	0.954			
Differentiation	0.014	14.516	1.726-122.057	0.014*
Tumor diameter (cm)	0.179			
T stage	0.005	11.589	2.103-63.860	0.005*
N stage	0.292			
CEA (ng/ml)	0.012	3.825	0.764-19.142	0.103
CA199 (U/ml)	0.037	2.464	0.460-13.208	0.292
HB (g/l)	0.825			

*$P < 0.05$.

CEA, carcinoembryonic antigen; CA199, carbohydrate antigen 19-9; HB, Hemoglobin; CR, complete response; PR, partial response; SD, stable disease; PD, disease progression; Response group, the first-time evaluation results was CR or PR; No-Response group, the first-time evaluation results was SD or PD.

TABLE 4 | Statistical analysis results of the IVIM-DWI and texture parameters in rectal cancer patients.

Parameters	Response group	No-Response group	Univariate analysis (*P*)	Multivariate logistic regression analysis		
				OR	95%CI	*P*
ADC ($\times10^{-3}$ mm^2/s)	0.935 ± 0.256	0.996 ± 0.193	0.364			
D ($\times10^{-3}$ mm^2/s)	0.593 ± 0.194	0.846 ± 0.308	0.002	2.717	0.019-380.669	0.692
D*($\times10^{-3}$ mm^2/s)	14.62 ± 13.73	24.74 ± 20.05	0.038	0.976	0.906-1.052	0.530
f (%)	47.01 ± 13.95	27.03 ± 10.33	<0.001	0.855	0.752-0.971	0.016*
Rads-score	4.67 ± 1.19	6.14 ± 1.31	0.002	2.790	1.163-6.696	0.022*

*$P < 0.05$.

IVIM-DWI, intravoxel incoherent motion diffusion weighted imaging; CR, complete response; PR, partial response; SD, stable disease; PD, disease progression; Response group, the first-time evaluation results was CR or PR; No-Response group, the first-time evaluation results was SD or PD; OR, odds ratio; CI, confidence interval; ADC, apparent diffusion coefficient; D, slow diffusion coefficient; D, fast diffusion coefficient; f, perfusion-related diffusion fraction.*

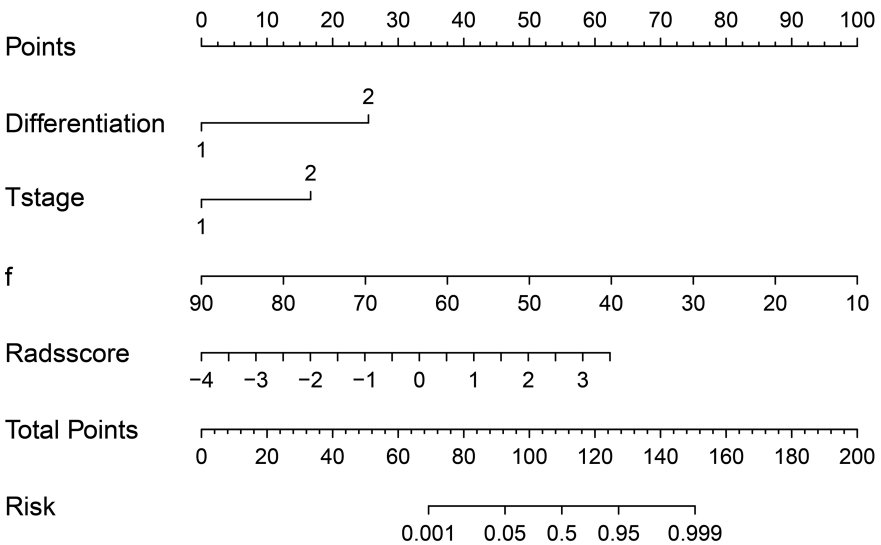

FIGURE 4 | A regression coefficient-based nomogram to predict the possibility of nCRT resistant in LARC patients. f, perfusion-related diffusion fraction.

parameters (D, f) and texture features (GLCM-correlation, GLRLM-LRE, and GLSZM-ZE) to establish a nomogram for early treatment response prediction in patients with cervical cancer after concurrent chemoradiotherapy (AUC=0.975) (31). Jia et al. performed IVIM-DWI measurement and MRI radiomics feature extraction on 123 rectal adenocarcinoma patients and established a nomogram. The nomogram model of D* and f values combined with Rads-score achieved a good performance in assessing non-enlarged lymph node metastasis of rectal adenocarcinoma preoperatively (AUC=0.864) (26). In this study, we combined the differentiation, T stage, f value and Rads-score to establish a nomogram and our nomogram showed good performance in predicting treatment response to nCRT in LARC patients (AUC=0.967).

This study found that poor differentiation and high T stage were associated with poor response to nCRT in patients with LARC, and these two factors were also independent predictors of tumor resistance to nCRT. Therefore, we established a predictive model (model 1) which combined the differentiation and T stage. The AUC of the model was 0.778, suggesting that the model had a certain predictive value. In a previous study, Huang et al. found that patients in the poorly differentiated group had a worse prognosis than the non-poorly differentiated group who received nCRT for rectal cancer treatment (32). Xu et al. found that in T2N0M0 colorectal cancer patients, the well-differentiated group had a better prognosis than the poorly differentiated group, and the differentiation was an independent prognostic factor in T2N0M0 colorectal cancer (33). The poor differentiation has been shown to be associated with bowel penetration, lymph node involvement and vascular invasion, suggesting that it is a risk factor for colorectal cancer invasion and dissemination (34). T stage reflects the depth of tumor infiltration and correlates with cancer invasion, and several studies have explored the prognostic value of T stage in the colorectum (35–37). It was found that the T4 stage was an independent risk factor for tumor resistance to nCRT in LARC. In a retrospective study, Xu et al. found that the T4 stage was an independent risk factor for shorter overall survival (OS) in patients with colorectal cancer

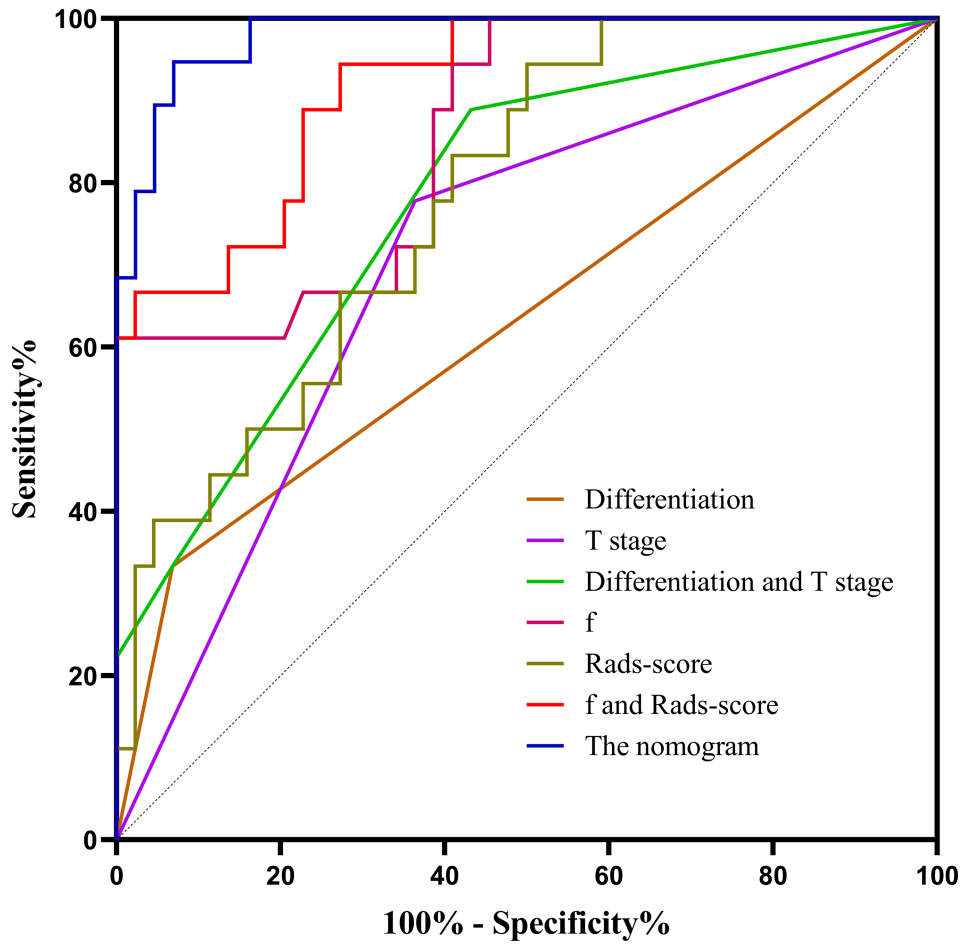

FIGURE 5 | The ROC curves of different parameters and models. f, perfusion-related diffusion fraction; Rads-score, radiomics score.

TABLE 5 | The predictive performance of the model in rectal cancer patients.

Parameters	AUC	Sensitivity (%)	Specificity (%)	Accuracy (%)
Differentiation	0.633	0.333	0.932	0.774
T stage	0.707	0.778	0.636	0.661
Differentiation and T stage	0.778	0.889	0.568	0.661
f	0.857	1.000	0.611	0.887
Rads-score	0.783	0.944	0.500	0.629
f and Rads-score	0.917	0.944	0.727	0.790
The nomogram	0.979	0.944	0.909	0.919

f, perfusion-related diffusion fraction; Rads-score, radiomics score.

(38). Chen et al. evaluated several microscopic features of stage T4 cancers and suggested that tumors that penetrate the visceral peritoneum and directly invade other organs or structures through malignant invasion were associated with poor survival (39). In summary, the poor differentiation and high T stage of rectal cancer may reflect the high degree of malignancy, which may lead to tumor resistance to nCRT and poor efficacy.

In addition to clinicopathological parameters, this study also found that low f value and high Rads-score were significantly associated with poor efficacy. We combined f and Rads-score to establish the second prediction model (model 2) of tumor resistance to nCRT in LARC and the model had a good predictive performance, AUC=0.917. The f value represents the voxel's blood volume fraction, which can reflect the capillary density and is related to the blood perfusion in the tissue (40).

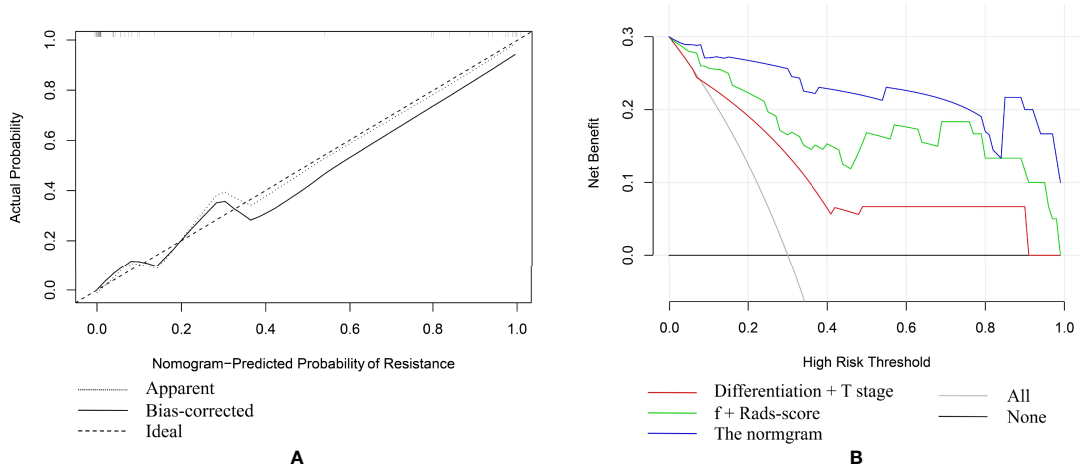

FIGURE 6 | **(A)** The fivefold cross-validation plot of the nomogram. **(B)** Decision curve analysis (DCA) of different models.

A previous study had shown that a higher f value may reflect a stronger blood supply to the tumor, which can deliver more chemotherapeutic medications to the tumor tissue, promoting tumor regression (41). Hu et al. found that in rectal cancer patients who received nCRT, the f value of the pCR group was significantly higher than that of the non-pCR group (42). Bakke et al. found that IVIM-DWI could be used to clarify the degree of histopathological regression of LARC after nCRT, and patients with high pre-treatment f value had better tumor regression (43). These studies confirmed that LARC patients with high pre-treatment f value had a better response to nCRT.

TA is a quantitative image post-processing technique, which can objectively reflect the underlying biological characteristics and heterogeneity of tumors due to its quantitative extraction and analysis of the pixel distribution of the lesion area (44). In a previous study, Lu et al. found that High DISS (gray-level run-length matrix_Dissimilarity) on sagittal fat-suppression T2WI and high DISS and ENTR (gray-level co-occurrence matrix_Entropy) on transverse T2WI could predict high T stage in rectal cancer (45). In a study of TA for early prediction of patients' response to nCRT in LARC, Park et al. found that GLRLM_LRLGE (gray-level run-length matrix_Long Run Low Gray Level Emphasis) on T2WI images could predict tumor recurrence after treatment (46). In this study, the texture parameters of DWI and T2WI images were analyzed and we filter out these two parameters [glrlm_LongRunEmphasis (T2WI) and firstorder_Median (IVIM)] through texture features and calculated the Rads-score, both of which were found to be positively correlated with Rads-score. Multivariate results showed that Rads-score was an independent risk factor for tumor resistance to nCRT in LARC. The glrlm_LongRun Emphasis is a measure of long run length distribution, with a higher value indicating longer run lengths and coarser structural textures. The firstorder_Median is the ROI's median gray level intensity. These two parameters can represent heterogeneity and subtle changes within the tumor. The results of this study showed that the rough texture and gray intensity in the RIO were more resistant to nCRT.

Most previous studies on rectal cancer only explored the role of IVIM-DWI or texture parameters of a single sequence image (47–49). In this study, two sequence image texture parameters were analyzed and combined with clinicopathology, IVIM-DWI and texture parameters to establish a nomogram for predicting tumor resistance to nCRT in LARC, thus richer and more accurate than the results obtained in previous studies. Compared with model 1 and model 2, the nomogram had higher predictive power and larger net benefit. The nomogram established a risk prediction system for tumor resistance to nCRT in LARC, so that appropriate treatment can be formulated for different patients, which is beneficial to patient recovery.

There are several limitations of this study. First, the manual image segmentation process might be affected by some subjective and objective factors. Second, some cases with small lesions were excluded due to the need for sufficient pixels to ensure the reliability of IVIM-DWI and TA parameter measurements, therefore, the results we obtained might be biased. Third, this study lacks validation with an external cohort. Finally, the present study was a single-center retrospective study with small sample size. Thus, it is necessary to conduct a multi-center prospective study with a large sample size for verification in the future.

CONCLUSIONS

In conclusion, the differentiation, T stage, f value and Rads-score were independent predictors of tumor resistance to nCRT in LARC. The nomogram model combining the differentiation, T stage, f value and Rads-score showed promising performance in estimating the risk of tumor resistance to nCRT in patients with LARC.

DATA AVAILABILITY STATEMENT

The raw data supporting the conclusions of this article will be made available by the authors, without undue reservation.

ETHICS STATEMENT

The studies involving human participants were reviewed and approved by Anhui Provincial Hospital Ethics Committee. Written informed consent for participation was not required for this study in accordance with the national legislation and the institutional requirements.

AUTHOR CONTRIBUTIONS

RS, SW, YH, FG, ML and WC: conception and design. RS, SW, HS, YC, JZ and HJ: collection and arrangement of data. RS, SW, YH, FG and YZ: data analysis and manuscript writing. All authors contributed to the article and approved the submitted version.

FUNDING

This work was supported by Natural Science Foundation of Anhui Province (No. 1808085MH234 and 1408085MH179), Anhui Province Key Research and Development Program Project (No. 202104j07020044), Health Commission of Anhui Province Scientific Research Project (No. AHWJ2021b105) and Hefei Key Common Technology Research and Major Scientific and Technological Achievement Project (No. 2021YL005).

ACKNOWLEDGMENTS

We thank all patients who participated in this study and all staff involved in the working process of this study.

REFERENCES

1. Liang M, Cai Z, Zhang H, Huang C, Meng Y, Zhao L, et al. Machine Learning-Based Analysis of Rectal Cancer Mri Radiomics for Prediction of Metachronous Liver Metastasis. *Acad Radiol* (2019) 26(11):1495–504. doi: 10.1016/j.acra.2018.12.019
2. European Society of Coloproctology collaborating. Evaluating the Incidence of Pathological Complete Response in Current International Rectal Cancer Practice: The Barriers to Widespread Safe Deferral of Surgery. *Colorect Dis* (2018) 20 Suppl 6:58–68. doi: 10.1111/codi.14361
3. Dizdarevic E, Frostrup Hansen T, Ploen J, Henrik Jensen L, Lindebjerg J, Rafaelsen S, et al. Long-Term Patient-Reported Outcomes After High-Dose Chemoradiation Therapy for Nonsurgical Management of Distal Rectal Cancer. *Int J Radiat Oncol Biol Phys* (2020) 106(3):556–63. doi: 10.1016/j.ijrobp.2019.10.046
4. van der Valk MJM, Hilling DE, Bastiaannet E, Meershoek-Klein Kranenbarg E, Beets GL, Figueiredo NL, et al. Long-Term Outcomes of Clinical Complete Responders After Neoadjuvant Treatment for Rectal Cancer in the International Watch & Wait Database (Iwwd): An International Multicentre Registry Study. *Lancet* (2018) 391(10139):2537–45. doi: 10.1016/s0140-6736(18)31078-x
5. Beets-Tan RG, Beets GL. Local Staging of Rectal Cancer: A Review of Imaging. *J Magn Reson Imaging* (2011) 33(5):1012–9. doi: 10.1002/jmri.22475
6. Oberholzer K, Menig M, Kreft A, Schneider A, Junginger T, Heintz A, et al. Rectal Cancer: Mucinous Carcinoma on Magnetic Resonance Imaging Indicates Poor Response to Neoadjuvant Chemoradiation. *Int J Radiat Oncol Biol Phys* (2012) 82(2):842–8. doi: 10.1016/j.ijrobp.2010.08.057
7. Klessen C, Rogalla P, Taupitz M. Local Staging of Rectal Cancer: The Current Role of MRI. *Eur Radiol* (2007) 17(2):379–89. doi: 10.1007/s00330-006-0388-x
8. Schafer AO, Baumann T, Pache G, Wiech T, Langer M. [Preoperative Staging of Rectal Cancer]. *Radiologe* (2007) 47(7):635–51. doi: 10.1007/s00117-007-1516-6
9. Caruso D, Zerunian M, De Santis D, Biondi T, Paolantonio P, Rengo M, et al. Magnetic Resonance of Rectal Cancer Response to Therapy: An Image Quality Comparison Between 3.0 and 1.5 Tesla. *BioMed Res Int* (2020) 2020:9842732. doi: 10.1155/2020/9842732
10. Mao X, Zou X, Yu N, Jiang X, Du J. Quantitative Evaluation of Intravoxel Incoherent Motion Diffusion-Weighted Imaging (Ivim) for Differential Diagnosis and Grading Prediction of Benign and Malignant Breast Lesions. *Med (Baltim)* (2018) 97(26):e11109. doi: 10.1097/MD.0000000000011109
11. Surov A, Meyer HJ, Hohn AK, Behrmann C, Wienke A, Spielmann RP, et al. Correlations Between Intravoxel Incoherent Motion (Ivim) Parameters and Histological Findings in Rectal Cancer: Preliminary Results. *Oncotarget* (2017) 8(13):21974–83. doi: 10.18632/oncotarget.15753
12. Liang L, Luo X, Lian Z, Chen W, Zhang B, Dong Y, et al. Lymph Node Metastasis in Head and Neck Squamous Carcinoma: Efficacy of Intravoxel Incoherent Motion Magnetic Resonance Imaging for the Differential Diagnosis. *Eur J Radiol* (2017) 90:159–65. doi: 10.1016/j.ejrad.2017.02.039
13. Liu ZC, Yan LF, Hu YC, Sun YZ, Tian Q, Nan HY, et al. Combination of Ivim-Dwi and 3d-Asl for Differentiating True Progression From Pseudoprogression of Glioblastoma Multiforme After Concurrent Chemoradiotherapy: Study Protocol of a Prospective Diagnostic Trial. *BMC Med Imaging* (2017) 17 (1):10. doi: 10.1186/s12880-017-0183-y
14. Sun H, Xu Y, Song A, Shi K, Wang W. Intravoxel Incoherent Motion Mri of Rectal Cancer: Correlation of Diffusion and Perfusion Characteristics With Prognostic Tumor Markers. *AJR Am J Roentgenol* (2018) 210(4):W139–W47. doi: 10.2214/AJR.17.18342
15. Song T, Yao Q, Qu J, Zhang H, Zhao Y, Qin J, et al. The Value of Intravoxel Incoherent Motion Diffusion-Weighted Imaging in Predicting the Pathologic Response to Neoadjuvant Chemotherapy in Locally Advanced Esophageal Squamous Cell Carcinoma. *Eur Radiol* (2021) 31(3):1391–400. doi: 10.1007/s00330-020-07248-z
16. Pieper CC, Sprinkart AM, Meyer C, Konig R, Schild HH, Kukuk GM, et al. Evaluation of a Simplified Intravoxel Incoherent Motion (Ivim) Analysis of Diffusion-Weighted Imaging for Prediction of Tumor Size Changes and Imaging Response in Breast Cancer Liver Metastases Undergoing Radioembolization: A Retrospective Single Center Analysis. *Med (Baltim)* (2016) 95(14):e3275. doi: 10.1097/MD.0000000000003275
17. Guo W, Luo D, Lin M, Wu B, Li L, Zhao Y, et al. Pretreatment Intra-Voxel Incoherent Motion Diffusion-Weighted Imaging (Ivim-Dwi) in Predicting Induction Chemotherapy Response in Locally Advanced Hypopharyngeal Carcinoma. *Med (Baltim)* (2016) 95(10):e3039. doi: 10.1097/MD.0000000000003039
18. Aker M, Ganeshan B, Afaq A, Wan S, Groves AM, Arulampalam T. Magnetic Resonance Texture Analysis in Identifying Complete Pathological Response to Neoadjuvant Treatment in Locally Advanced Rectal Cancer. *Dis Colon Rectum* (2019) 62(2):163–70. doi: 10.1097/DCR.0000000000001224
19. Chitalia RD, Kontos D. Role of Texture Analysis in Breast Mri as a Cancer Biomarker: A Review. *J Magn Reson Imaging* (2019) 49(4):927–38. doi: 10.1002/jmri.26556
20. Zhang J, Liu X, Zhang H, He X, Liu Y, Zhou J, et al. Texture Analysis Based on Preoperative Magnetic Resonance Imaging (Mri) and Conventional Mri Features for Predicting the Early Recurrence of Single Hepatocellular Carcinoma After Hepatectomy. *Acad Radiol* (2019) 26(9):1164–73. doi: 10.1016/j.acra.2018.10.011

21. Eun NL, Kang D, Son EJ, Park JS, Youk JH, Kim JA, et al. Texture Analysis With 3.0-T Mri for Association of Response to Neoadjuvant Chemotherapy in Breast Cancer. *Radiology* (2020) 294(1):31–41. doi: 10.1148/radiol.2019182718
22. Sun Y, Hu P, Wang J, Shen L, Xia F, Qing G, et al. Radiomic Features of Pretreatment Mri Could Identify T Stage in Patients With Rectal Cancer: Preliminary Findings. *J Magn Reson Imaging* (2018) 48(3):615–21. doi: 10.1002/jmri.25969
23. Li M, Zhang J, Dan Y, Yao Y, Dai W, Cai G, et al. A Clinical-Radiomics Nomogram for the Preoperative Prediction of Lymph Node Metastasis in Colorectal Cancer. *J Transl Med* (2020) 18(1):46. doi: 10.1186/s12967-020-02215-0
24. Coppola F, Giannini V, Gabelloni M, Panic J, Defeudis A, Lo Monaco S, et al. Radiomics and Magnetic Resonance Imaging of Rectal Cancer: From Engineering to Clinical Practice. *Diagnost (Basel)* (2021) 11(5):756. doi: 10.3390/diagnostics11050756
25. Eisenhauer EA, Therasse P, Bogaerts J, Schwartz LH, Sargent D, Ford R, et al. New Response Evaluation Criteria in Solid Tumours: Revised Recist Guideline (Version 1.1). *Eur J Cancer* (2009) 45(2):228–47. doi: 10.1016/j.ejca.2008.10.026
26. Jia H, Jiang X, Zhang K, Shang J, Zhang Y, Fang X, et al. A Nomogram of Combining Ivim-Dwi and Mri Radiomics From the Primary Lesion of Rectal Adenocarcinoma to Assess Nonenlarged Lymph Node Metastasis Preoperatively. *J Magn Reson Imaging* (2022). doi: 10.1002/jmri.28068
27. Liu Z, Zhang XY, Shi YJ, Wang L, Zhu HT, Tang Z, et al. Radiomics Analysis for Evaluation of Pathological Complete Response to Neoadjuvant Chemoradiotherapy in Locally Advanced Rectal Cancer. *Clin Cancer Res* (2017) 23(23):7253–62. doi: 10.1158/1078-0432.CCR-17-1038
28. Liu Z, Wang S, Dong D, Wei J, Fang C, Zhou X, et al. The Applications of Radiomics in Precision Diagnosis and Treatment of Oncology: Opportunities and Challenges. *Theranostics* (2019) 9(5):1303–22. doi: 10.7150/thno.30309
29. Park H, Lim Y, Ko ES, Cho HH, Lee JE, Han BK, et al. Radiomics Signature on Magnetic Resonance Imaging: Association With Disease-Free Survival in Patients With Invasive Breast Cancer. *Clin Cancer Res* (2018) 24(19):4705–14. doi: 10.1158/1078-0432.CCR-17-3783
30. Ren J, Tian J, Yuan Y, Dong D, Li X, Shi Y, et al. Magnetic Resonance Imaging Based Radiomics Signature for the Preoperative Discrimination of Stage I-Ii and Iii-Iv Head and Neck Squamous Cell Carcinoma. *Eur J Radiol* (2018) 106:1–6. doi: 10.1016/j.ejrad.2018.07.002
31. Zheng X, Li C, Zhang L, Cao F, Fang X, Qian L, et al. Combining Intravoxel Incoherent Motion Diffusion Weighted Imaging and Texture Analysis for a Nomogram to Predict Early Treatment Response to Concurrent Chemoradiotherapy in Cervical Cancer Patients. *J Oncol* (2021) 2021:9345353. doi: 10.1155/2021/9345353
32. Huang Q, Qin H, Xiao J, He X, Xie M, He X, et al. Association of Tumor Differentiation and Prognosis in Patients With Rectal Cancer Undergoing Neoadjuvant Chemoradiation Therapy. *Gastroenterol Rep (Oxf)* (2019) 7 (4):283–90. doi: 10.1093/gastro/goy045
33. Xu B, Yu L, Zhao LZ, Ma DW. Prognostic Factors in the Patients With T2n0m0 Colorectal Cancer. *World J Surg Oncol* (2016) 14:76. doi: 10.1186/s12957-016-0826-4
34. Blumberg D, Paty PB, Picon AI, Guillem JG, Klimstra DS, Minsky BD, et al. Stage I Rectal Cancer: Identification of High-Risk Patients. *J Am Coll Surg* (1998) 186(5):574–80. doi: 10.1016/s1072-7515(98)00018-0
35. Li J, Guo BC, Sun LR, Wang JW, Fu XH, Zhang SZ, et al. Tnm Staging of Colorectal Cancer Should be Reconsidered by T Stage Weighting. *World J Gastroenterol* (2014) 20(17):5104–12. doi: 10.3748/wjg.v20.i17.5104
36. Merkel S, Wein A, Gunther K, Papadopoulos T, Hohenberger W, Hermanek P. High-Risk Groups of Patients With Stage Ii Colon Carcinoma. *Cancer* (2001) 92(6):1435–43. doi: 10.1002/1097-0142(20010915)92:6<1435::aid-cncr1467>3.0.co;2-n
37. Elsaleh H, Iacopetta B. Re: Pooled Analysis of Fluorouracil-Based Adjuvant Therapy of Stage Ii and Iii Colon Cancer: Who Benefits and by How Much? *J Clin Oncol* (2005) 23(3):653–4. doi: 10.1200/JCO.2005.05.190
38. Xu W, Zhu Y, Shen W, Ding W, Wu T, Guo Y, et al. Combination of Cdx2 Expression and T Stage Improves Prognostic Prediction of Colorectal Cancer. *J Int Med Res* (2019) 47(5):1829–42. doi: 10.1177/0300060518819620
39. Chen YG, Liu YL, Jiang SX, Wang XS. Adhesion Pattern and Prognosis Studies of T4n0m0 Colorectal Cancer Following En Bloc Multivisceral Resection: Evaluation of T4 Subclassification. *Cell Biochem Biophys* (2011) 59(1):1–6. doi: 10.1007/s12013-010-9106-z
40. Meyer HJ, Hohn AK, Woidacki K, Andric M, Powerski M, Pech M, et al. Associations Between Ivim Histogram Parameters and Histopathology in Rectal Cancer. *Magn Reson Imaging* (2021) 77:21–7. doi: 10.1016/j.mri.2020.12.008
41. Zhou Y, Liu J, Liu C, Jia J, Li N, Xie L, et al. Intravoxel Incoherent Motion Diffusion Weighted Mri of Cervical Cancer - Correlated With Tumor Differentiation and Perfusion. *Magn Reson Imaging* (2016) 34(8):1050–6. doi: 10.1016/j.mri.2016.04.009
42. Hu H, Jiang H, Wang S, Jiang H, Zhao S, Pan W. 3.0 T Mri Ivim-Dwi for Predicting the Efficacy of Neoadjuvant Chemoradiation for Locally Advanced Rectal Cancer. *Abdom Radiol (NY)* (2021) 46(1):134–43. doi: 10.1007/s00261-020-02594-4
43. Bakke KM, Hole KH, Dueland S, Groholt KK, Flatmark K, Ree AH, et al. Diffusion-Weighted Magnetic Resonance Imaging of Rectal Cancer: Tumour Volume and Perfusion Fraction Predict Chemoradiotherapy Response and Survival. *Acta Oncol* (2017) 56(6):813–8. doi: 10.1080/0284186X.2017.1287951
44. Liu L, Liu Y, Xu L, Li Z, Lv H, Dong N, et al. Application of Texture Analysis Based on Apparent Diffusion Coefficient Maps in Discriminating Different Stages of Rectal Cancer. *J Magn Reson Imaging* (2017) 45(6):1798–808. doi: 10.1002/jmri.25460
45. Lu HC, Wang F, Yin JD. Texture Analysis Based on Sagittal Fat-Suppression and Transverse T2-Weighted Magnetic Resonance Imaging for Determining Local Invasion of Rectal Cancer. *Front Oncol* (2020) 10:1476. doi: 10.3389/fonc.2020.01476
46. Park H, Kim KA, Jung JH, Rhie J, Choi SY. Mri Features and Texture Analysis for the Early Prediction of Therapeutic Response to Neoadjuvant Chemoradiotherapy and Tumor Recurrence of Locally Advanced Rectal Cancer. *Eur Radiol* (2020) 30(8):4201–11. doi: 10.1007/s00330-020-06835-4
47. Yang L, Xia C, Zhao J, Zhou X, Wu B. The Value of Intravoxel Incoherent Motion and Diffusion Kurtosis Imaging in the Assessment of Tumor Regression Grade and T Stages After Neoadjuvant Chemoradiotherapy in Patients With Locally Advanced Rectal Cancer. *Eur J Radiol* (2021) 136:109504. doi: 10.1016/j.ejrad.2020.109504
48. Li H, Yuan Y, Chen XL, Chen GW, Liu H, Liu YS, et al. Value of Intravoxel Incoherent Motion for Assessment of Lymph Node Status and Tumor Response After Chemoradiation Therapy in Locally Advanced Rectal Cancer. *Eur J Radiol* (2022) 146:110106. doi: 10.1016/j.ejrad.2021.110106
49. Liu S, Wen L, Hou J, Nie S, Zhou J, Cao F, et al. Predicting the Pathological Response to Chemoradiotherapy of Non-Mucinous Rectal Cancer Using Pretreatment Texture Features Based on Intravoxel Incoherent Motion Diffusion-Weighted Imaging. *Abdom Radiol (NY)* (2019) 44(8):2689–98. doi: 10.1007/s00261-019-02032-0

Conflict of Interest: The authors declare that the research was conducted in the absence of any commercial or financial relationships that could be construed as a potential conflict of interest.

frontiers | Frontiers in Oncology

ORIGINAL RESEARCH
published: 08 June 2022
doi: 10.3389/fonc.2022.807264

Deep Learning Model for Predicting the Pathological Complete Response to Neoadjuvant Chemoradiotherapy of Locally Advanced Rectal Cancer

Xiaoying Lou[1,2†], Niyun Zhou[3†], Lili Feng[2,4†], Zhenhui Li[5†], Yuqi Fang[3,6†], Xinjuan Fan[1,2], Yihong Ling[7], Hailing Liu[1,2], Xuan Zou[1,2], Jing Wang[1,2], Junzhou Huang[3], Jingping Yun[7], Jianhua Yao[3*] and Yan Huang[1,2*]*

[1] Department of Pathology, The Sixth Affiliated Hospital of Sun Yat-sen University, Guangzhou, China, [2] Guangdong Institute of Gastroenterology, The Sixth Affiliated Hospital of Sun Yat-sen University, Guangzhou, China, [3] Tencent AI Lab, Shenzhen, China, [4] Department of Radiation Oncology, The Sixth Affiliated Hospital of Sun Yat-sen University, Guangzhou, China, [5] Department of Pathology, Yunnan Cancer Hospital, Kunming, China, [6] Department of Electronic Engineering, The Chinese University of Hong Kong, Hong Kong, Hong Kong SAR, China, [7] Department of Pathology, Cancer Center of Sun Yat-sen University, Guangzhou, China

Objective: This study aimed to develop an artificial intelligence model for predicting the pathological complete response (pCR) to neoadjuvant chemoradiotherapy (nCRT) of locally advanced rectal cancer (LARC) using digital pathological images.

Background: nCRT followed by total mesorectal excision (TME) is a standard treatment strategy for patients with LARC. Predicting the PCR to nCRT of LARC remine difficulty.

Methods: 842 LARC patients treated with standard nCRT from three medical centers were retrospectively recruited and subgrouped into the training, testing and external validation sets. Treatment response was classified as pCR and non-pCR based on the pathological diagnosis after surgery as the ground truth. The hematoxylin & eosin (H&E)-stained biopsy slides were manually annotated and used to develop a deep pathological complete response (DeepPCR) prediction model by deep learning.

Results: The proposed DeepPCR model achieved an AUC-ROC of 0.710 (95% CI: 0.595, 0.808) in the testing cohort. Similarly, in the external validation cohort, the DeepPCR model achieved an AUC-ROC of 0.723 (95% CI: 0.591, 0.844). The sensitivity and specificity of the DeepPCR model were 72.6% and 46.9% in the testing set and 72.5% and 62.7% in the external validation cohort, respectively. Multivariate logistic regression analysis showed that the DeepPCR model was an independent predictive factor of nCRT (P=0.008 and P=0.004 for the testing set and external validation set, respectively).

Conclusions: The DeepPCR model showed high accuracy in predicting pCR and served as an independent predictive factor for pCR. The model can be used to assist in clinical treatment decision making before surgery.

Keywords: rectal cancer, deep learning, neoadjuvant chemoradiotherapy, pathological complete response, artificial intelligence

OPEN ACCESS

Edited by:
Qi Liu,
Fudan University, China

Reviewed by:
Fevzi Cengiz,
Tınaztepe University, Turkey
Simon J. Furney,
Royal College of Surgeons in Ireland, Ireland
Jacopo Lenkowicz,
Agostino Gemelli University Polyclinic (IRCCS), Italy

***Correspondence:**
Yan Huang
huangy@mail.sysu.edu.cn
Jianhua Yao
jianhuayao@tencent.com
Jingping Yun
yunjp@sysucc.org.cn

†These authors have contributed equally to this work and share first authorship

Specialty section:
This article was submitted to Gastrointestinal Cancers: Colorectal Cancer, a section of the journal Frontiers in Oncology

Received: *01 November 2021*
Accepted: *02 May 2022*
Published: *08 June 2022*

Citation:
Lou X, Zhou N, Feng L, Li Z, Fang Y, Fan X, Ling Y, Liu H, Zou X, Wang J, Huang J, Yun J, Yao J and Huang Y (2022) Deep Learning Model for Predicting the Pathological Complete Response to Neoadjuvant Chemoradiotherapy of Locally Advanced Rectal Cancer. Front. Oncol. 12:807264. doi: 10.3389/fonc.2022.807264

INTRODUCTION

Colorectal cancer remains one of the leading causes of cancer death (1). For patients with locally advanced rectal cancer (LARC), neoadjuvant chemoradiotherapy (nCRT) followed by total mesorectal excision (TME) is recommended as a standard treatment strategy. nCRT can significantly reduce local recurrence and treatment-associated toxicity and more importantly, make tumors more amenable to resection. However, the treatment response to nCRT varies greatly among patients. Approximately 15-38% of patients could obtain a pathological complete response (pCR) and are recommended the watch and wait approach to avoid the side effects of surgery (2), while 20% of patients have little to no response to nCRT and might even suffer significant side effects and miss their best opportunity for surgery (3–5). More importantly, patients with pCR have better long-term outcomes, indicating a favorable prognosis (6). However, how to predict treatment response, especially to identify pCR candidates prior to nCRT, remains challenging for LARC.

Previous studies have shown that tumor stage, serum tumor markers before neoadjuvant therapy, and lymphocyte infiltration in the tumor microenvironment are associated with tumor regression to nCRT (7). Recently, with the development of artificial intelligence algorithms, radiological imaging has been used to evaluate the treatment response of LARC (8–14). The commonly adopted imaging techniques include diffusion-weighted magnetic resonance imaging (MRI) (11), diffusion kurtosis and T2-weighted MRI (8), and a multiparametric MRI protocol with dynamic-contrast-enhanced MRI (13). For instance, Zhang *et al.* (10) developed a pCR prediction model based on diffusion kurtosis and T2-weighted MRI, and the area under the curve (AUC) was 0.70 (95% confidence interval (CI): 0.59, 0.79). Histopathological images prevail as the gold standard for patient diagnosis and contain abundant biological information. Therefore, we anticipate that more accurate predictions can be achieved by analyzing pathological images than by analyzing radiological images.

Compared with conventional machine learning, deep learning can automatically extract features from an image without the necessity of feature predefinition and is suitable for mining the most relevant feature representations. Multi-instance learning (MIL), as a weakly supervised deep learning technique, has achieved promising results on the topic of patient prognosis and outcome prediction (15–18). MIL enables the network to learn more holistic information from whole-slide images (WSIs). To the best of our knowledge, there has been little investigation on the prediction of pCR based on histopathological images prior to nCRT with the MIL technique. The aim of this study was to develop a deep pathological complete response (DeepPCR) prediction model for the prediction of pCR directly from conventional hematoxylin & eosin (H&E)-stained histopathological images.

MATERIALS AND METHODS

Study Cohort and Availability

Two different cohorts, i.e., the primary cohort and external validation cohort, were adopted for training and internal and external validation and included retrospectively identified LARC patients from January 1, 2010, to January 1, 2018, from three hospitals in China (the Sixth Affiliated Hospital of Sun Yat-sen University, Cancer Center of Sun Yat-sen University, and Yunnan Cancer Hospital). A total of 842 patients were recruited; among them, the primary cohort (783 patients from the Sixth Affiliated Hospital of Sun Yat-sen University and Cancer Center of Sun Yat-sen University) was randomly subgrouped into the training set (666 patients, 85%) and testing set (117 patients, 15%), and the external validation cohort (from Yunnan Cancer Hospital) contained 102 patients. The inclusion criteria were as follows: (1) patients had locally advanced disease determined by pretreatment TNM stage (T3/T4, and/or N+); (2) biopsy was performed, and the biopsy specimen was pathologically diagnosed as adenocarcinoma; and (3) patients underwent nCRT followed by rectal resection. The exclusion criteria were as follows: (1) patients with familial adenomatous polyposis, distant metastases, or Lynch syndrome; and (2) patients with no information on tumor regression grade (TRG) and no available H&E-stained slides.

All patients accepted a standard treatment strategy based on the National Comprehensive Cancer Network (NCCN) guidelines (version 3, 2017). The nCRT regimen was 50 Gy pelvic radiation therapy with concurrent 5-fluorouracil-based chemotherapy (FOLFIRI or FOLFOX regimens). TME was performed by either anterior resection or abdominoperineal resection after nCRT of 4-8 weeks. The TRG after nCRT was used to divide patients into two groups based on H&E-stained slides after surgery: pCR (with no remaining viable cancer cells) and non-pCR (with small clusters of cancer cells or no response with extensive residual cancer). The flow diagram of patient enrollment into the two cohorts is shown in **Figure 1**.

Clinicopathological variables, such as age, sex, TNM stage, histological grade, TRG after surgery, and blood testing parameters, including lymphocytes, neutrophils, carcinoembryonic antigen (CEA), carbohydrate antigen 19-9 (CA19-9), and lactate dehydrogenase (LDH) prior to nCRT treatment, were collected. This study was approved by the Institutional Review Board of the Sixth Affiliated Hospital of Sun Yat-sen University.

Data Preparation

Formalin-fixed paraffin-embedded (FFPE) biopsy tissue blocks were cut into 4-μm sections for H&E staining. All slides were checked by a pathologist who ascertained that they contained tumor areas. WSIs were acquired at a magnification of 20× on an Aperio scanner.

Tumor tissue regions were hand-delineated by pathologists (Dr. XYL and Dr. HLL) using Aperio Image Scope software and subsequently cropped into patches with a size of 299×299 pixels at a magnification of 20×. The distribution of the number of patches per slide followed a long-tail distribution, with the majority of slides containing approximately 100 patches. For slides with more than 1000 patches, we randomly chose 1000 cropped patches.

pCR Candidate Classification

Four models were designed for classifying the input biopsy histological images, with patients' distinct TRG outcomes as

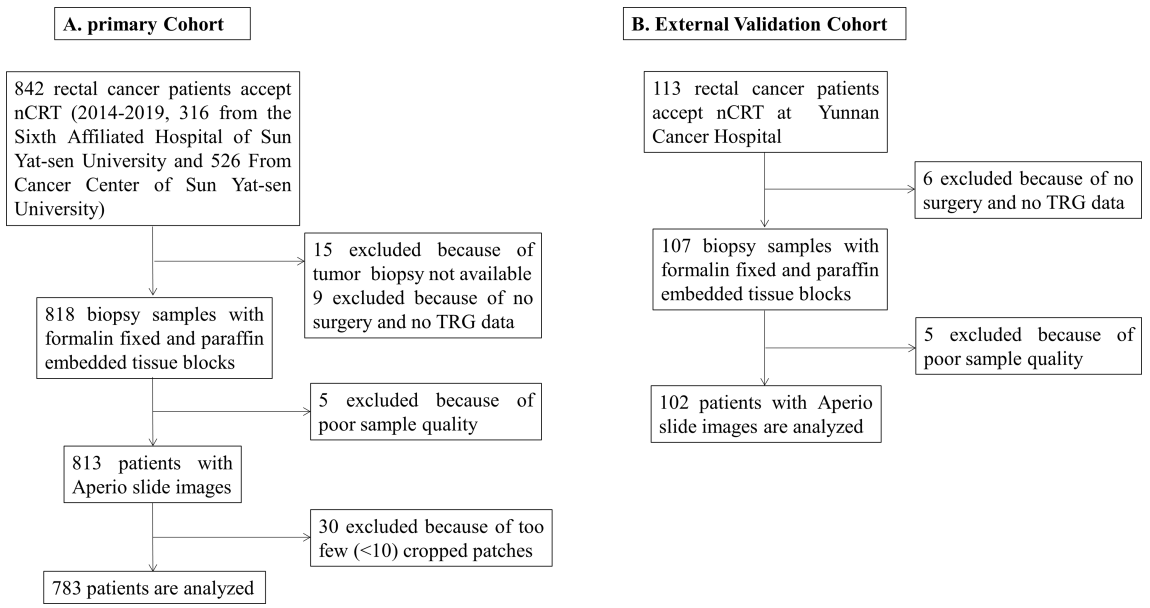

FIGURE 1 | The flow diagram of patient enrollment. **(A)** Primary cohort, **(B)** External validation cohort.

the ground truth. The first three models were trained on 102,728 patches and tested on 18475 patches in the primary cohort, namely, the DeepPCR model, *patch-based combined* model, and *patch-based individual model*. The DeepPCR model was built upon the MIL strategy (**Figure 2**). Specifically, a pretrained ResNet-18 model (19) was leveraged to extract the pathological feature representations of each cropped patch, i.e., the patch-wise phenotype representation (patchPR). Based on the patchPRs, the unsupervised K-means algorithm was used to categorize these features into six clusters (see **Supplementary Figure 1**). Each cluster occupied a subspace of the features and comprised a distinctive phenotype group. The patches in each cluster were further processed by a multi-instance fully convolutional model (MI-FCM) (20) to generate cluster-wise phenotype representation (clusPR). Herein, the MI-FCM was comprised of two pairs of *Conv-ReLU* layers, followed by a *pooling* layer. Afterwards, WSI-wise phenotype representation (wsiPR) was constructed by concatenating the clusPRs from the same WSI. The wsiPR sufficiently exploited the intercluster feature difference and intracluster feature dependence, constituting the most informative phenotype representation. Based on wsiPR, a two-layer fully connected network was leveraged to generate the final prediction. The DeepPCR model built a hierarchical feature structure from patch to WSI and explicitly modeled the mutual dependence between different phenotype groups for patient outcome prediction.

The patch-based combined model and *patch-based individual model* used patch-based approaches in which the cropped patches shared the same label with the original histopathological WSI and the prediction of patch-based methods was made for each patch rather than each WSI. Similar to DeepPCR, the pretrained ResNet-18 model was adopted to extract the phenotype representations of each cropped patch. According to the aggregation method of the patch-level prediction, we implemented these patch-based models in two ways. One was to predict each individual patch's label, and then combined them *via* majority voting, which was called the *patch-based individual model*. The other was to aggregate the patch-level predictions of each subject by removing the clustering step in DeepPCR, called the *patch-based combined model* (remaining modules are the same as DeepPCR). To validate the effectiveness of pathological imaging data in pCR outcome prediction compared with nonpathological data, the fourth model (*hematology model*), based on clinical hematology data, including CEA, CA19-9, LDH, lymphocytes, and neutrophils, was built. A two-layer multilayer perceptron (MLP) model was adopted in the hematology model.

Phenotype Visualization

To visualize the representative phenotypes in each K-means cluster, t-distributed Stochastic Neighbor Embedding (t-SNE) (21) and the Raster Fairy method (22) were applied on the patchPRs. t-SNE is a technique for dimensionality reduction that is particularly well suited for the visualization of high-dimensional data. The Raster Fairy method aims to transform the two-dimensional clustering data derived from t-SNE into a regular grid without destroying the neighborhood relations emerging from the clustering. The GradCAM method (23) was used to calculate the patch importance for target prediction.

Statistical Analysis

The predictive efficacy of the model was evaluated by the area under the receiver operating characteristic curve (AUC-ROC), area under the precision-recall curve (AUC-PR), sensitivity, specificity, positive predictive value (PPV), and negative predictive value (NPV). Univariate and multivariate logistic regression analyses

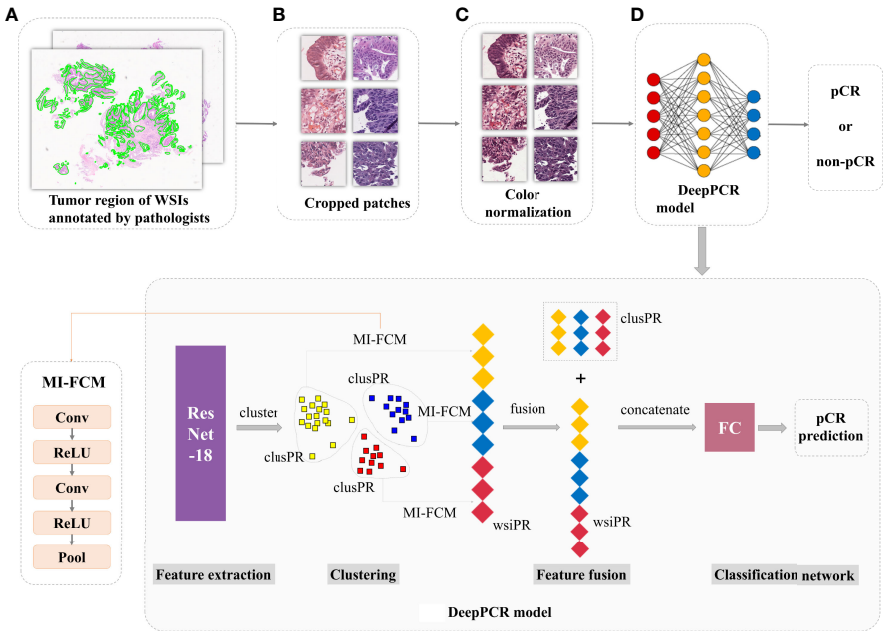

FIGURE 2 | The proposed deep learning framework (DeepPCR) for pCR prediction. **(A)** WSIs with tumors annotated by expert pathologists. **(B)** All WSIs were cropped into small patches with a size of 299×299 pixels at a magnification of 20×. **(C)** An in-house deep learning-based color normalization method was applied to ensure the color consistency of the cropped patches. **(D)** Illustration of the proposed DeepPCR model for pCR candidate prediction. Three scales of phenotype feature representations (i.e., patchPR, clusPR, and wsiPR) were integrated to derive the final prediction.

were performed to investigate the predictive value for all biomarkers. The statistical significance of the differences in the clinicopathological characteristics of pCR and non-pCR patients were calculated using the Mann-Whitney test (two-tailed) for continuous variables and Fisher's exact test (two-tailed) for dichotomous variables. Comparisons of clinicopathological factors in the primary and external validation cohorts were performed using Student's t test for continuous variables and Fisher's exact test (two-tailed) for dichotomous variables. A two-sided p value of less than 0.05 was considered statistically significant.

RESULTS

Patient Characteristics

The primary cohort included 783 patients: 295 patients from the Sixth Affiliated Hospital of Sun Yat-sen University and 488 patients from the Cancer Center of Sun Yat-sen University. A total of 201 and 582 patients were classified as pCR and non-pCR, respectively. The external validation cohort from Yunnan Cancer Hospital included 102 patients, of which 24 and 78 patients were classified as pCR and non-pCR, respectively. The clinicopathological characteristics of the patients in the primary and external validation cohorts are provided in **Table 1**. The clinicopathological characteristics, including clinical T stage and histological grade, were different between the primary and external validation cohorts (P<0.001 and P<0.001, respectively) (**Supplementary Table 1**).

pCR Candidate Prediction in the Primary Cohort

The DeepPCR model had a higher discriminative power, with an AUC-ROC of 0.710 (95% CI: 0.595, 0.808) and an AUC-PR of 0.875 (95% CI: 0.795, 0.935) in the primary cohort (**Figure 3A** and **Table 2A**). The sensitivity, specificity, PPV and NPV were 72.6%, 46.9%, 70.4%, and 54.0%, respectively (**Table 2A**). The other three models showed inferior performance. Specifically, the *hematology model* had an AUC-ROC of 0.403 (95% CI: 0.274, 0.534) and an AUC-PR of 0.698 (95% CI: 0.591, 0.805). *The patch-based individual* model and *patch-based combined* model achieved an AUC-ROC of 0.544 (95% CI: 0.432, 0.653) and an AUC-PR of 0.805 (95% CI: 0.717, 0.885) and an AUC-ROC of 0.627 (95% CI: 0.516, 0.733) and an AUC-PR of 0.842 (95% CI: 0.762, 0.909), respectively (**Figures 3A, C** and **Table 2A**). As shown in **Figure 3E**, the AUC-ROC of the DeepPCR model was significantly higher than that of the *hematology model* ($P < 0.001$) and *patch-based individual model* ($P < 0$ .05).

pCR Candidate Prediction in the External Validation Cohort

To investigate the effectiveness and generalizability of the DeepPCR model, it was validated in the external cohort. In the external validation cohort, the DeepPCR model achieved a similar AUC-ROC of 0.723 (95% CI: 0.591, 0.844) and an AUC-PR of 0.887 (95% CI: 0.805, 0.949) (**Figures 3B, D** and **Table 2B**). The sensitivity, specificity, PPV and NPV were 0.725 (95% CI: 0.637, 0.814), 0.627 (95% CI: 0.463, 0.773), 0.758 (95%

TABLE 1 | Clinicopathological characteristics of patients in the training, testing, and external validation cohorts.

	Training set (n=666)			Testing set (n=117)			ExternalValidation set (n=102)		
	PCR (%) (n=171)	Non-PCR (%) (n=495)	*P* value	PCR (%) (n=30)	Non-PCR (%) (n=87)	*P* value	PCR (%) (n=24)	Non-PCR (%) (n=78)	*P* value
Age, mean(SD), y	52.77 ± 12.02	54.71 ± 11.78	0.078	53.90 ± 11.71	55.38 ± 11.47	0.549	54.08 ± 11.01	57.17 ± 10.37	0.182
Sex, No. (%)			0.849			0.376			0.081
Female	55(32.2)	154(31.1)		8(26.7)	32(36.8)		12(50.0)	22(28.2)	
Male	116(67.8)	341(68.9)		22(73.3)	55(63.2)		12(50.0)	56(71.8)	
Clinical T stage									
cT2	10(5.9)	16(3.2)	0.124	2(6.7)	2(2.3)	0.271	1(4.2)	0(0.0)	0.235
cT3	113(66.1)	323(65.3)	0.926	20(66.7)	55(63.2)	0.827	9(37.5)	24(30.8)	0.612
cT4	48(28.0)	156(31.5)	0.442	8(26.6)	30(34.5)	0.503	14(58.3)	54(69.2)	0.333
Clinical N stage									
cN0	34(19.9)	76(15.4)	0.189	5(16.7)	13(14.9)	0.777	0(0.0)	18(23.1)	0.006
cN1	86(50.3)	249(50.3)	1	13(43.3)	40(46.0)	0.834	17(70.8)	43(55.1)	0.236
cN2	51(29.8)	170(34.3)	0.301	12(40.0)	34(39.1)	1	7(29.2)	17(21.8)	0.582
TNM stage									
Stage II	35(20.5)	76(15.3)	0.167	5(16.6)	13(14.9)	0.777	0(0.0)	18(23.1)	0.006
Stage III	136(79.5)	419(84.7)	0.124	25(83.4)	74(85.1)	0.777	24(100.0)	60(76.9)	0.006
Histological grade									
1	22(12.9)	55(11.1)	0.579	3(10.0)	16(18.4)	0.394	1(4.2)	0(0)	0.235
2	125(73.1)	382(77.2)	0.299	22(73.3)	65(74.7)	1	23(95.8)	71(91.0)	0.677
3	24(14.0)	58(11.7)	0.421	5(16.7)	6(6.9)	0.147	0(0)	7(9.0)	0.194
Patch No.	102,728			18475			46599		

CI: 0.671, 0.847), and 0.536 (95% CI: 0.368, 0.688), respectively (**Table 2B**). In external cohorts, the AUC-ROC of the DeepPCR model was significantly higher than that of the hematology model (P < 0.001) and patch-based individual model (P < 0 .05) (**Figure 3F**).

Univariate and Multivariate Analyses

In the primary cohort, the univariate logistic regression analysis showed that CEA and DeepPCR model were significantly correlated with pCR (*P=0*.033 and 0.0001, respectively) (**Table 3A**). Multivariate logistic regression analysis showed that only DeepPCR was an independent factor for predicting pCR (95% CI: 1.646, 28.743; *P*=0.008) (**Table 3B**).

In the external validation cohort, age, CEA, neutrophil-to-lymphocyte ratio (NLR), patch-based combined model and DeepPCR model were significantly correlated with pCR (*P=0*.042, 0.029, 0.04, 0.023, and 0.0001, respectively) (**Table 3A**). Multivariate logistic regression analysis showed that only DeepPCR was an independent factor for predicting pCR (95% CI: 2.138, 51.186; *P*=0.004) (**Table 3B**).

Histological Patterns Associated With TRG

To find some important clinical insights based on the DeepPCR model, we determined which types of histological patterns were most relevant to patient TRG, and the pipeline of this process is displayed in **Figure 4**. In **Figure 4A**, each grid represented an individual patch, and the patchPRs obtained from all these patches were categorized into six phenotype clusters (**Figure 4B**), which were reduced into a two-dimensional feature space based on t-SNE and the Raster Fairy method. Here, the phenotypes could be color, edges, texture, curve and/or shape of cancer and normal tissues. To conduct an investigation into which types of phenotypes contribute the most to pCR prediction, the GradCAM method (23) was adopted to calculate the importance of patches. The importance heatmap is shown in **Figure 4C**, and darker colors indicate that the patches played a more important role in pCR prediction. We also calculated the sum of the importance values of the patches in each cluster (**Figure 4D**). It can be seen that different clusters had different predictive powers for pCR prediction, and a larger value indicated that the corresponding cluster contributed more to DeepPCR. The size of bubbles represents the number of patches in the corresponding cluster. We found that patches in clusters 0 and l played more important roles in pCR candidate prediction. Specifically, the patch importance value of cluster 1 was significantly larger than that of clusters 2, 3, 4, and 5 (*P*<0.001, *P*<0.05, *P*<0.01, and *P*<0.001, respectively). There were no significant differences between cluster 0 and cluster 1 in terms of the patch importance value (**Figure 4D**). **Figure 4E** shows the representative patches of cluster 1 and their distribution in a WSI, which also represented a special histological pattern and spatial pattern highly associated with pCR. Similarly, **Figures 4F–J** demonstrates the same patchPR visualization process but for the non-pCR group. The patch importance value of cluster 2 was significantly larger than that of clusters 0, 1, 3, 4, and 5 (*P*<0.001, *P*<0.001, *P*<0.001, *P*<0.001, and *P*<0.001, respectively) (**Figure 4I**) in non-pCR candidate prediction.

DISCUSSION

In the present study, we developed a novel model to predict pCR in LARC using digital pathological images. We found that the DeepPCR model could achieve a relatively high AUC-ROC score of 0.710. Multivariate logistic analysis showed that the DeepPCR model was indeed an independent factor for predicting pCR,

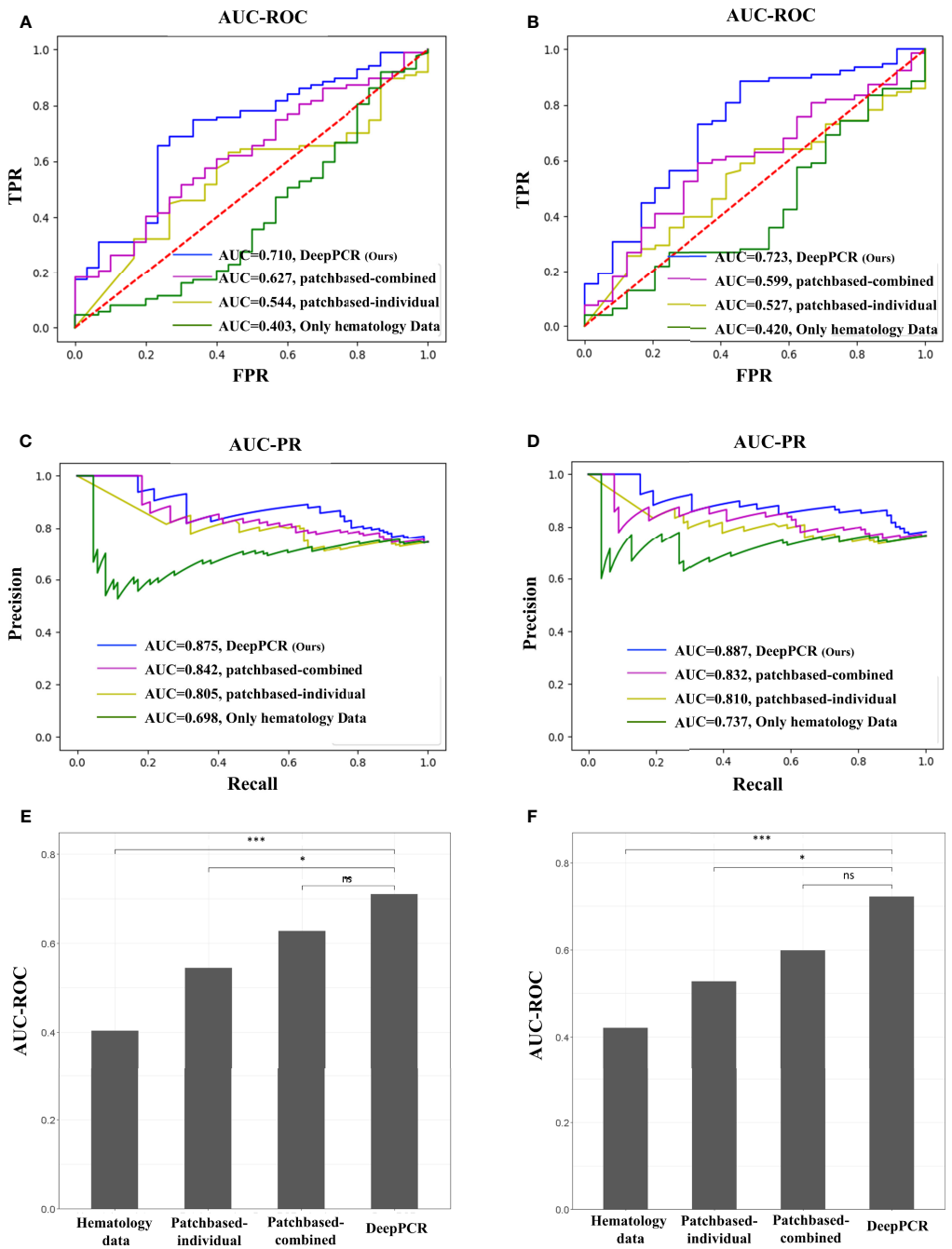

FIGURE 3 | **(A, B)** AUC-ROC of the four comparative methods in the **(A)** primary and **(B)** external validation cohorts (top row). **(C, D)** AUC-PR of the four comparative methods in the **(C)** primary and **(D)** external validation cohorts (middle row). **(E, F)** DeLong test for the four comparative methods in the **(E)** primary and **(F)** external validation cohorts (bottom row). In this work, we used a probability threshold of 0.7 (that is, any patient with a pCR prediction probability greater than 0.7 was reported as a pCR candidate). No significant difference (ns): $P > 0.05$, $^{*}P < 0.05$, $^{***}P < 0.001$.

indicating that the model could assist in treatment decision making prior to surgery for LARC.

In recent years, there has been increasing interest in digital pathology image analysis based on machine learning algorithms to assist in pathological diagnosis (24, 25). With the development of deep learning, an increasing number of studies have focused on clinical-grade detection and the prediction of outcomes. For example, Cao et al. (24) developed a pathomics-based model for microsatellite instability prediction from pathological images. Ole-Johan Skrede et al. (25) developed a deep learning-based

TABLE 2 | Results of DeepPCR and the comparative models in the (a) primary and (b) external validation cohorts.

(a) Model/Outcome	AUC-ROC	AUC-PR	Sen (%)	Spe (%)	PPV (%)	NPV (%)
Hematology model	0.403 (0.274, 0.534)	0.698 (0.591, 0.805)	72.6 (64.1, 80.3)	27.2 (18.8, 36.2)	61.7 (60.0, 71.1)	37.7 (30.8, 51.2)
Patch-based individual model	0.544 (0.432, 0.653)	0.805 (0.717, 0.885)	68.4 (59.8, 76.9)	25.8 (17.0, 34.7)	57.2 (45.2, 69.6)	27.0 (15.4, 46.8)
Patch-based combined model	0.627 (0.516, 0.733)	0.842 (0.762, 0.909)	69.2 (60.7, 77.8)	30.4 (20.7, 40.7)	61.6 (50.5, 73.1)	37.6 (18.0, 59.4)
DeepPCR model	0.710 (0.595, 0.808)	0.875 (0.795, 0.935)	72.6 (64.1, 80.3)	46.9 (32.6, 61.0)	70.4 (61, 79.9)	54.0 (35.8, 70.9)
(b) Model/Outcome	**AUC-ROC**	**AUC-PR**	**Sen (%)**	**Spe (%)**	**PPV (%)**	**NPV (%)**
Hematology model	0.420 (0.293, 0.548)	0.737 (0.623, 0.846)	70.6 (61.8, 79.4)	21. 7 (14.2, 30.0)	57.4 (48.5, 67.4)	17.6 (14.3, 20.4)
Patch-based individual model	0.527 (0.402, 0.657)	0.810 (0.712, 0.895)	73.5 (64.7, 81.4)	22.6 (15.3, 31.4)	57.9 (62.6, 72.4)	17.8 (17.4, 18.1)
Patch-based combined model	0.599 (0.474, 0.726)	0.832 (0.732, 0.919)	69.6 (60.8, 78.4)	27.2 (16.3, 38)	62.3 (49.9, 74.5)	31.7 (14.8, 54.1)
DeepPCR model	0.723 (0.591, 0.844)	0.887 (0.805, 0.949)	72.5 (63.7, 81.4)	62.7 (46.3, 77.3)	75.8 (67.1, 84.7)	53.6 (36.8, 68.8)

The CI value is inside the parentheses. Sen, sensitivity; Spe, specificity; PPV, positive predictive value; NPV, negative predictive value. In this work, we used a probability threshold of 0.7 (that is, any patient with a pCR prediction probability greater than 0.7 was reported as a pCR candidate).

TABLE 3 | Univariate and multivariate logistic regression analyses.

(a) Univariate logistic regression	Testing Set		External Validation Set	
	P value	**Exp (B) (95% CI)**	**P value**	**Exp (B) (95% CI)**
Sex	0.316	1.6 (0.638, 4.011)	0.051	0.393 (0.153, 1.006)
Age	0.051	2.679 (0.995, 7.212)	0.042	2.768 (1.039, 7.376)
TNM stage	0.822	1.138 (0.369, 3.513)	0.998	0 (0, -)
CEA	0.033	2.796 (1.087, 7.197)	0.029	3.667 (1.145, 11.74)
CA-199	0.087	2.128 (0.896, 5.055)	0.054	2.505 (0.985, 6.37)
CRP	0.198	2.348 (0.639, 8.621)	–	
LDH	0.999	5.80e8 (0, -)	0.207	2.4 (0.617, 9.339)
Lymphocytes	0.24	2.186 (0.593, 8.062)	0.133	2.2 (0.788, 6.146)
Neutrophils	0.414	1.524 (0.555, 4.186)	0.097	2.508 (0.846, 7.436)
NLR	0.142	3.155 (0.681, 14.623)	0.04	3.045 (1.054, 8.804)
Patch-indi	0.06	2.248 (0.967, 5.224)	0.219	1.786 (0.709, 4.5)
Patch-comb	0.053	2.548 (0.989, 6.564)	0.023	3.143 (1.171, 8.437)
DeepPCR	0.0001	6.125 (2.462, 15.239)	0.0001	7 (2.575, 19.028)
(b) Multivariate logistic regression	**Test Cohort**		**External Validation Cohort**	
	Sig.	**Exp (B) (95% CI)**	**Sig.**	**Exp (B) (95% CI)**
Sex	0.143	2.45 (0.739, 8.124)	0.011	0.122 (0.024, 0.621)
Age	0.489	1.576 (0.434, 5.72)	0.705	1.346 (0.289, 6.261)
TNM stage	0.965	1.034 (0.233, 4.582)	0.998	0 (0, -)
CEA	0.101	2.718 (0.823, 8.973)	0.189	3.211 (0.564, 18.284)
CA-199	0.124	2.413 (0.785, 7.415)	0.059	4.137 (0.945, 18.108)
CRP	0.104	4.607 (0.732, 29.003)		
LDH	0.999	2.6e8 (0, -)	0.118	7.334 (0.604, 89.051)
Lymphocytes	0.128	3.412 (0.704, 16.539)	0.203	3.418 (0.514, 22.723)
Neutrophils	0.979	0.981 (0.239, 4.023)	0.874	0.846 (0.107, 6.699)
NLR	0.138	4.242 (0.628, 28.678)	0.05	8.854 (0.995, 78.749)
Patch-indi	0.346	1.657 (0.58, 4.732)	0.831	0.855 (0.204, 3.591)
Patch-comb	0.8	0.819 (0.175, 3.842)	0.642	1.453 (0.301, 7.023)
DeepPCR	0.008	6.879 (1.646, 28.743)	0.004	10.461 (2.138, 51.186)

(a) Univariate logistic regression analysis of the testing set and external validation set. (b) Multivariate logistic regression analysis of the testing set and external validation set. The covariates were sex, age, TNM stage, CEA, CA19-9, CRP, LDH, lymphocytes, neutrophils, neutrophil-to-lymphocyte ratio (NLR), patch-based individual (patch-indi) model, patch-based combined (patch-comb) model, and DeepPCR model.

biomarker model for colorectal cancer outcome by analyzing H&E-stained sections. The successful applications of artificial intelligence in digital pathology indicate that digital pathology images contain important information for the diagnosis and prognosis of cancer. Due to the complexity of pathological imaging, there have been few relevant studies on the prediction of neoadjuvant efficacy based on preoperative pathological biopsy with artificial intelligence. Some studies used MRI to predict neoadjuvant efficacy. For instance, Petresc et al. (8) utilized pretreatment T2-weighted radiomic features to predict LARC responders, and least absolute shrinkage and selection operator (LASSO) regression analysis was applied to derive a predicted AUC of 0.80 (95% CI: 0.58, 0.94). Although their model's performance was better than ours, they used a small cohort of patients. In a retrospective study, Zhang et al. (10) developed a deep learning-based model for pCR prediction based on diffusion kurtosis and T2-weighted MRI, and the AUC was 0.70 (95% CI: 0.59, 0.79), which was similar to that of our proposed model. The limitation of their model was that they did not validate the model in independent external cohorts.

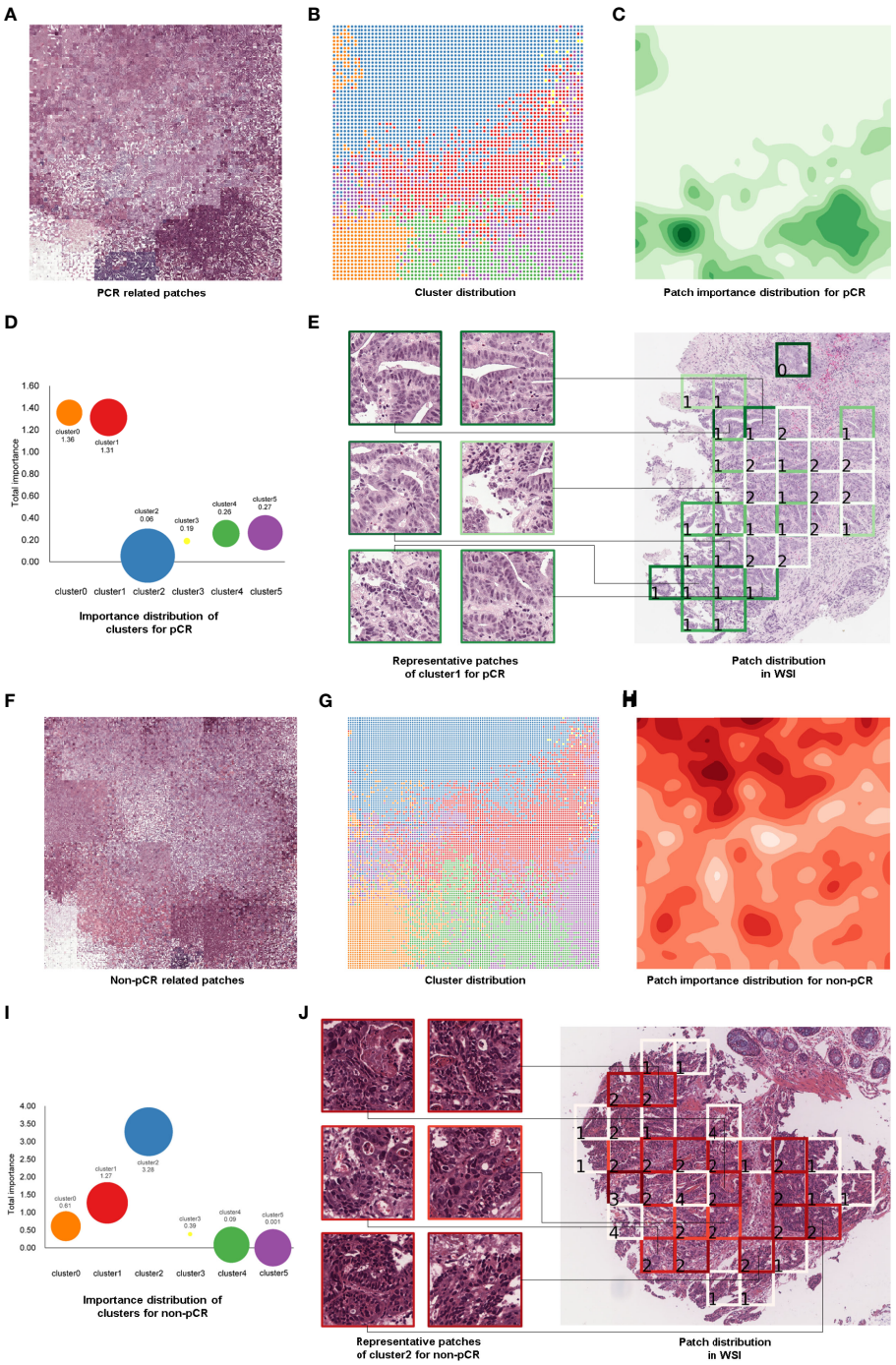

FIGURE 4 | Patch-level feature interpretation in the pCR group **(A–E)** and non-pCR group **(F–J)**. Patches in the correctly predicted pCR group **(A)** and correctly predicted non-pCR group **(F)**. PatchPRs were categorized into six phenotype clusters based on t-SNE and the Raster Fairy method, and each grid represented an individual patch **(B, G)**. The importance distribution of the patches in the pCR group **(C)** and non-pCR group **(H)**. Darker colors represent the patches that played a more important role in pCR or non-pCR prediction. Demonstration of patch importance and the number of patches in each cluster; the size of the bubble represents the number of patches in the corresponding cluster **(D, I)**. Representative patches of cluster 1 **(E)** and cluster 2 **(J)** and the part of the WSI from which they were selected.

Radiological imaging has its own limitation in distinguishing inflammatory lesions from neoplastic lesions. As the gold standard of disease diagnosis, conventional preoperative pathological biopsy is of great significance for the diagnosis and prognosis of tumors.

The discriminative power of DeepPCR model was significantly higher than that of the hematology model ($P<0.001$) and the other two patch-based models ($P<0.001$ and $P<0.001$, respectively). The number of patients in our study was larger than other reported works (8–14). Moreover, the DeepPCR model was evaluated in independent cohorts. The external validation cohort came from another center with a different sample handling procedure and using a different scanner. Although the external validation cohort was different from the primary cohort in terms of the clinicopathological characteristics, such as clinical T stage and histological grade ($P<0.001$ and $P<0.001$, respectively), the proposed model achieved similar results as those in the primary cohort, indicating its generalizability and robustness.

The proposed model leveraged an MIL-based deep learning model and showed a superior performance compared to previous patch-based learning methods. Existing patch-based approaches can be categorized into two classes based on the level of the employed annotations. For the first class, patch-wise annotations are used to train deep learning models (26–30), and strong supervision is typically performed, benefiting from the precise labeling information. Nevertheless, these methods depend on pixel-level annotations by expert pathologists, and it would be labor intensive and hard to obtain sufficient high-quality annotation data. For the second class of methods, the ground-truth labels are provided for the whole images rather than the patches (31, 32). When performing the learning process, the global image-level label of each WSI is taken as the patch-level label directly, and the final prediction is generated by combining the patch-level outputs. Although this type of method is very straightforward, there are two crucial problems. First, the cropped patches of WSIs are processed independently, and the spatial constraints of these patches are neglected. The second problem is that the patches in the same image indiscriminately share the same label and thus introduce a substantial disturbance to model training. To address these problems, several MIL-based approaches that aim to leverage the feature representations of all image patches to collaboratively predict the patient outcome have been developed (15–18, 33). Building upon these methods, our proposed model can effectively mine the dependence of feature representations at three different scales, i.e., patch-level, cluster-level, and WSI-level phenotype representations. In this patient outcome prediction task, the MIL-based learning method outperformed the patch-based learning methods. Specifically, the MIL-based methods were able to jointly consider intrapatch dependence; thus, the spatial relationships between tumor tissues (including cancer cells and surrounding stromal cells) were exploited. These tissues form the tumor microenvironment (34), and the characterization of the microenvironment plays an important role in tumor progression and the response to treatment. However, the patch-based learning methods only processed patches independently, and the spatial information among patches was neglected; thus, these methods showed poor performance. Our findings suggest that MIL-based learning models can handle the spatial information inherent in the tumor microenvironment.

Some deep learning-based studies visualized and interpreted the learned feature representations (31, 35–38), which may provide some important clinical insights. For instance, Courtiol et al. (35) identified regions that contributed to patient outcome prediction (mesothelioma classification) by visualizing various scenarios predicted by the deep learning model. They found that these regions are mostly located in the stroma and are associated with inflammation, cellular diversity and vacuolization. Campanella et al. (36) assessed the model by visualizing the features reduced in a 2D space and found that a set of top-ranked patches with probabilities close to 0.5 contained glands suspicious of being malignant. In our study, patchPRs were categorized into six phenotype clusters based on the DeepPCR model. We determined that different clusters had different predictive powers for pCR prediction. We calculated the sum of the importance values of the patches in each cluster and found that the patches in cluster 0 and cluster 1 played more important roles in pCR candidate prediction. Although we did not analyze each cluster in more detail, we proposed that some histological patterns may be associated with the predicted TRG. The novel histological pattern may be associated with the morphological features and microenvironment of the tumor.

Previous studies showed that pretreatment serum CEA levels were significantly correlated with pCR (39). In our study, the univariate logistic regression analysis showed that CEA levels significantly correlated with pCR in the primary cohort ($P=0.033$) and in the external validation cohort ($P=0.042$). However, in multivariate logistic regression analysis, this association did not persist, and only the DeepPCR model was an independent factor for predicting pCR (95% CI: 1.646, 28.743; $P=0.008$). We also conducted pCR prediction experiments based on clinical data, i.e., CEA, CA19-9, LDH, lymphocytes, and neutrophils. In the experimental studies, an AUC-ROC of 0.403 was achieved based on these nonpathological data, showing that they may not be sufficient for prognostic pCR prediction.

Although promising results and relevant clinical insights were found, there are some limitations in this study. First, this study was a retrospective study. A multicenter prospective study is needed to confirm the performance of the prediction model. Second, due to the prevalence of tumor heterogeneity, the representativeness of biopsy specimens was limited. Another limitation of this study was that deep learning has the disadvantage of its black-box nature. Although we determined some histological patterns relevant to patient TRG, the morphological features and microenvironment of each histological pattern should be further investigated.

In conclusion, our study was the first to investigate the nCRT outcome prediction problem in LARC patients using presurgical biopsy pathological images. A clinically useful prediction model was developed using deep learning. The DeepPCR model was evaluated in an independent cohort and achieved stable results. This model has the potential to guide clinicians in making nCRT choices.

DATA AVAILABILITY STATEMENT

The original contributions presented in the study are included in the article/**Supplementary Material**. Further inquiries can be directed to the corresponding authors.

ETHICS STATEMENT

This study was approved by the Institutional Review Board of the Sixth Affiliated Hospital of Sun Yat-sen University.

AUTHOR CONTRIBUTIONS

JH, JPY, JHY, and YH contribute to conception and design. LF, ZL, XZ, JW, and YL contribute to acquisition of data. NZ and YF contribute to analysis and interpretation of data. NZ, YF, XL, and XF participate in drafting the article. All authors give final approval of the version to be published.

FUNDING

This work was supported by the Guangdong Science and Technology Project (No. 2019B030316003 to XF), Natural Science Foundation of Guangdong Province (No. 2019A1515010901 to XF), the National Science Fund for Excellent Young Scholars (No.82122057 to XF); Guangdong Natural Science Funds for Distinguished Young Scholars (No. 2021B1515020022 to XF).

SUPPLEMENTARY MATERIAL

The Supplementary Material for this article can be found online at: https://www.frontiersin.org/articles/10.3389/fonc.2022.807264/full#supplementary-material

Supplementary Figure 1 | Effects of the number of clusters on pCR prediction. The AUC-ROC in the test cohort was optimal when the number of clusters was set to 6.

Supplementary Figure 2 | Demonstration of pCR and non-pCR patient differentiation using **(A)** patch-level, **(B)** cluster-level, **(C)** WSI-level feature representations based on the t-SNE results. With the increase in level, pCR and non-pCR candidates were easier to differentiate.

REFERENCES

1. Bray F, Ferlay J, Soerjomataram I, Siegel R, Torre LA, Jemal A. Global Cancer Statistics 2018: GLOBOCAN Estimates of Incidence and Mortality Worldwide for 36 Cancers in 185 Countries. *CA: Cancer J Clin* (2018) 68(6):394–424. doi: 10.3322/caac.21492
2. Roh MS, Colangelo LH, O'Connell MJ, Yothers G, Deutsch M, Allegra CJ, et al. Preoperative Multimodality Therapy Improves Disease-Free Survival in Patients With Carcinoma of the Rectum: NSABP R-03. *J Clin Oncol* (2009) 27 (31):5124. doi: 10.1200/JCO.2009.22.0467
3. Capirci C, Valentini V, Cionini L, Paoli AD, Rodel C, Jones RG, et al. Prognostic Value of Pathologic Complete Response After Neoadjuvant Therapy in Locally Advanced Rectal Cancer: Long-Term Analysis of 566 ypCR Patients. *Int J Radiat Oncol Biol Phys* (2008) 72(1):99–107. doi: 10.1016/j.ijrobp.2007.12.019
4. Ciccocioppo A, Stephens JH, Hewett PJ, Rieger NA. Complete Pathologic Response After Preoperative Rectal Cancer Chemoradiotherapy. *ANZ J Surg* (2009) 79(6):481–4. doi: 10.1111/j.1445-2197.2009.04950.x
5. Yeo SG, Kim DY, Kim TH, Chang HJ, Oh JH, Park W, et al. Pathologic Complete Response of Primary Tumor Following Preoperative Chemoradiotherapy for Locally Advanced Rectal Cancer: Long-Term Outcomes and Prognostic Significance of Pathologic Nodal Status (KROG 09-01). *Ann Surg* (2010) 252(6):998–1004. doi: 10.1097/SLA.0b013e3181f3f1b1
6. Maas M, Nelemans PJ, Valentini V, Das P, Rödel C, Kuo LJ, et al. Long-Term Outcome in Patients With a Pathological Complete Response After Chemoradiation for Rectal Cancer: A Pooled Analysis of Individual Patient Data. *Lancet Oncol* (2010) 11(9):835–44. doi: 10.1016/S1470-2045(10)70172-8
7. Huang Y, Lou X, Zhu Y, Wang YC, Zhang L, Liu HL, et al. Local Environment in Biopsy Better Predict the Pathological Response to Neoadjuvant Chemoradiotherapy in Rectal Cancer. *Biosci Rep* (2019) 39(3). doi: 10.1042/BSR20190003
8. Petresc B, Lebovici A, Caraiani C, Feier DS, Graur F, Buruian MM. Pre-Treatment T2-WI Based Radiomics Features for Prediction of Locally Advanced Rectal Cancer Non-Response to Neoadjuvant Chemoradiotherapy: A Preliminary Study. *Cancers* (2020) 12(7):1894. doi: 10.3390/cancers12071894
9. Shaish H, Aukerman A, Vanguri R, Spinelli A, Armenta P, Jambawalikar S, et al. Radiomics of MRI for Pretreatment Prediction of Pathologic Complete Response, Tumor Regression Grade, and Neoadjuvant Rectal Score in Patients With Locally Advanced Rectal Cancer Undergoing Neoadjuvant Chemoradiation: An International Multicenter Study. *Eur Radiol* (2020) 1–11. doi: 10.1007/s00330-020-06968-6
10. Zhang XY, Wang L, Zhu HT, Li ZW, Ye M, Li XT, et al. Predicting Rectal Cancer Response to Neoadjuvant Chemoradiotherapy Using Deep Learning of Diffusion Kurtosis MRI. *Radiology* (2020) 190936. doi: 10.1148/radiol.2020190936
11. Fu J, Zhong X, Li N, Lewis J, Sung K, Raldow AC, et al. Deep Learning-Based Radiomic Features for Improving Neoadjuvant Chemoradiation Response Prediction in Locally Advanced Rectal Cancer. *Phys Med Biol* (2020) 65 (7):075001. doi: 10.1088/1361-6560/ab7970
12. Shayesteh SP, Alikhassi A, Farhan F, Ghalehtaki R, Soltanabadi M, Haddad P, et al. Prediction of Response to Neoadjuvant Chemoradiotherapy by MRI-Based Machine Learning Texture Analysis in Rectal Cancer Patients. *J gastrointest Cancer* (2020) 51(2):601–9. doi: 10.1007/s12029-019-00291-0
13. Shi L, Zhang Y, Nie K, Sun X, Niu T, Yue N, et al. Machine Learning for Prediction of Chemoradiation Therapy Response in Rectal Cancer Using Pre-Treatment and Mid-Radiation Multi-Parametric MRI. *Magn reson Imaging* (2019) 61:33–40. doi: 10.1016/j.mri.2019.05.003
14. Liao W, Pei H. MRI-Based Radiomics Predicts Tumor Response to Neoadjuvant Chemoradiotherapy in Locally Advanced Rectal Cancer. *Front Oncol* (2019) 9:552. doi: 10.3389/fonc.2019.00552
15. Mercan C, Aksoy S, Mercan E, Shapiro LG, Weaver DL, Elmore JG. Multi-Instance Multi-Label Learning for Multi-Class Classification of Whole Slide Breast Histopathology Images. *IEEE Trans Med Imaging* (2017) 37(1):316–25. doi: 10.1109/TMI.2017.2758580
16. Sudharshan PJ, Petitjean C, Spanhol F, Oliveira LE, Heutte L, Honeine P, et al. Multiple Instance Learning for Histopathological Breast Cancer Image Classification. *Expert Syst Appl* (2019) 117:103–11. doi: 10.1016/j.eswa.2018.09.049
17. Zhu W, Lou Q, Vang YS, Xie XH. Deep Multi-Instance Networks With Sparse Label Assignment for Whole Mammogram Classification. In: *International Conference on Medical Image Computing and Computer-Assisted Intervention*. Cham: Springer (2017). p. 603–11.
18. Das K, Conjeti S, Roy AG, Chatterjee J, Sheet D. Multiple Instance Learning of Deep Convolutional Neural Networks for Breast Histopathology Whole Slide Classification. In: *2018 IEEE 15th International Symposium on Biomedical Imaging (ISBI 2018)*. IEEE (2018). p. 578–81.
19. He K, Zhang X, Ren S. Deep Residual Learning for Image Recognition. In: *Proceedings of the IEEE Conference on Computer Vision and Pattern Recognition* (2016). p. 770–8.

20. Yang H, Tianyi Zhou J, Cai J, Ong YS. Miml-Fcn+: Multi-Instance Multi-Label Learning via Fully Convolutional Networks With Privileged Information. In: *Proceedings of the IEEE Conference on Computer Vision and Pattern Recognition* (2017). p. 1577–85.
21. Maaten L, Hinton G. Visualizing Data Using T-SNE. *J Mach Learn Res* (2008) 9(Nov):2579–605.
22. Available at: https://github.com/Quasimondo/RasterFairy.
23. Selvaraju RR, Cogswell M, Das A, Vedantam R, Parikh D, Batra D, et al. Grad-Cam: Visual Explanations From Deep Networks via Gradient-Based Localization. In: *Proceedings of the IEEE International Conference on Computer Vision* (2017). p. 618–26.
24. Cao R, Yang F, Ma SC, Liu L, Zhao Y, Li Y, et al. Development and Interpretation of a Pathomics-Based Model for the Prediction of Microsatellite Instability in Colorectal Cancer. *Theranostics* (2020) 10 (24):11080–91. doi: 10.7150/thno.49864
25. Skrede OJ, De Raedt S, Kleppe A, Hveem TS, Liestøl K, Maddison J, et al. Deep Learning for Prediction of Colorectal Cancer Outcome: A Discovery and Validation Study. *Lancet* (2020) 395(10221):350–60. doi: 10.1016/S0140-6736 (19)32998-8
26. Roy K, Banik D, Bhattacharjee D, Nasipuri M. Patch-Based System for Classification of Breast Histology Images Using Deep Learning. *Comput Med Imaging Graphics* (2019) 71:90–103. doi: 10.1016/j.compmedimag.2018.11.003
27. Bandi P, Geessink O, Manson Q, Van Dijk M, Balkenhol M, Hermsen M, et al. From Detection of Individual Metastases to Classification of Lymph Node Status at the Patient Level: The Camelyon17 Challenge[J]. *IEEE Trans Med Imaging* (2018) 38(2):550–60. doi: 10.1109/TMI.2018.2867350
28. Bejnordi BE, Veta M, Van Diest PJ, Ginneken BV, Karssemeijer N, Litjens G. Diagnostic Assessment of Deep Learning Algorithms for Detection of Lymph Node Metastases in Women With Breast Cancer. *JAMA* (2017) 318(22):2199–210. doi: 10.1001/jama.2017.14580
29. Kong B, Wang X, Li Z, Qi S, Zhang S. Cancer Metastasis Detection via Spatially Structured Deep Network. In: *International Conference on Information Processing in Medical Imaging*. Cham: Springer (2017). p. 236–48.
30. Zanjani FG, Zinger S, With P. Cancer Detection in Histopathology Whole-Slide Images Using Conditional Random Fields on Deep Embedded Spaces. In: *Medical Imaging 2018: Digital Pathology* (2018) 105810I. doi: 10.1117/12.2293107
31. Kather JN, Pearson AT, Halama N. Deep Learning can Predict Microsatellite Instability Directly From Histology in Gastrointestinal Cancer. *Nat Med* (2019) 25(7):1054–6. doi: 10.1038/s41591-019-0462-y
32. Hou L, Samaras D, Kurc TM, Gao Y, Davis JE, Saltz JH. Patch-Based Convolutional Neural Network for Whole Slide Tissue Image Classification. In: *Proceedings of the Ieee Conference on Computer Vision and Pattern Recognition* (2016). p. 2424–33.
33. Yao J, Zhu X, Huang J. Deep Multi-Instance Learning for Survival Prediction From Whole Slide Images. In: *International Conference on Medical Image Computing and Computer-Assisted Intervention*. Cham: Springer (2019). p. 496–504.
34. Hanahan D, Weinberg RA. Hallmarks of Cancer: The Next Generation. *cell* (2011) 144(5):646–74. doi: 10.1016/j.cell.2011.02.013
35. Courtiol P, Maussion C, Moarii M, Pronier E, Pilcer S, Sefta M, et al. Deep Learning-Based Classification of Mesothelioma Improves Prediction of Patient Outcome. *Nat Med* (2019) 25(10):1519–25. doi: 10.1038/s41591-019-0583-3
36. Campanella G, Hanna MG, Geneslaw L, Miraflor A, Silva VWK, Busam KJ, et al. Clinical-Grade Computational Pathology Using Weakly Supervised Deep Learning on Whole Slide Images. *Nat Med* (2019) 25(8):1301–9. doi: 10.1038/s41591-019-0508-1
37. Lee H, Yune S, Mansouri M, Kim M, Tajmir SH, Guerrier CE, et al. An Explainable Deep-Learning Algorithm for the Detection of Acute Intracranial Haemorrhage From Small Datasets. *Nat Biomed Eng* (2019) 3(3):173. doi: 10.1038/s41551-018-0324-9
38. Mitani A, Huang A, Venugopalan S, Corrado GS, Peng L, Webster DR, et al. Detection of Anaemia From Retinal Fundus Images *via* Deep Learning. *Nat Biomed Eng* (2020) 4(1):18–27. doi: 10.1038/s41551-019-0487-z
39. Garland ML, Vather R, Bunkley N, Pearse M, Bissett IP. Clinical Tumour Size and Nodal Status Predict Pathologic Complete Response Following Neoadjuvant Chemoradiotherapy for Rectal Cancer. *Int J Colorectal Dis* (2014) 29(3):301–7. doi: 10.1007/s00384-013-1821-7

Conflict of Interest: The authors declare that the research was conducted in the absence of any commercial or financial relationships that could be construed as a potential conflict of interest.

frontiers | Frontiers in Oncology

TYPE Original Research
PUBLISHED 16 September 2022
DOI 10.3389/fonc.2022.953790

OPEN ACCESS

EDITED BY
Xinxiang Li,
Fudan University, China

REVIEWED BY
J. Joshua Smith,
Memorial Sloan Kettering Cancer Center, United States
Ri Na Yoo,
The Catholic University of Korea, South Korea
Charles Ternent,
American Society of Colon and Rectal Surgeons, United States

*CORRESPONDENCE
Minhua Zheng
zhengmhrjhospital@163.com
Zirui He
hezirui@aliyun.com

†These authors have contributed equally to this work and share first authorship

SPECIALTY SECTION
This article was submitted to Gastrointestinal Cancers: Colorectal Cancer, a section of the journal Frontiers in Oncology

RECEIVED 26 May 2022
ACCEPTED 25 August 2022
PUBLISHED 16 September 2022

CITATION
Zhao X, Han P, Zhang L, Ma J, Dong F, Zang L, He Z and Zheng M (2022) Prolonged neoadjuvant chemotherapy without radiation versus total neoadjuvant therapy for locally advanced rectal cancer: A propensity score matched study.
Front. Oncol. 12:953790.
doi: 10.3389/fonc.2022.953790

Prolonged neoadjuvant chemotherapy without radiation versus total neoadjuvant therapy for locally advanced rectal cancer: A propensity score matched study

Xuan Zhao[1,2†], Peiyi Han[1,2†], Luyang Zhang[1,2†], Junjun Ma[1,2], Feng Dong[1,2], Lu Zang[1,2], Zirui He[1,2*] and Minhua Zheng[1,2*]

[1]Department of General Surgery, Ruijin Hospital, Shanghai Jiao Tong University School of Medicine, Shanghai, China, [2]Shanghai Minimally Invasive Surgery Center, Shanghai, China

Background: Although neoadjvuant chemoradiotherapy (CRT) improves the local control rate of locally advanced rectal cancer (LARC), it fails to significantly improve disease-free survival (DFS) and overall survival (OS). We explored the efficacy of prolonged neoadjuvant chemotherapy (pNCT) without radiation and compared this schema with total neoadjuvant therapy (TNT).

Material and methods: Patients diagnosed with LARC and received TNT (4 cycles of induction CapeOX/FOLFOX followed with CRT) or pNCT (6~8 cycles of CapeOX/FOLFOX) between June 2016 and October 2021 were retrospective analyzed. All patients underwent total mesorectal excision (TME). A 1:1 propensity score match was performed to adjust baseline potential confounders. The tumor response, toxicity, recurrence-free survival (RFS) and OS were observed.

Results: A total of 184 patients with 92 patients in each group were finally enrolled. The median follow-up time was 35 months. TNT showed better pathological complete response (pCR) rate (25.0% vs 16.3%) and objective regression rate (73.9% vs 59.8%) than pNCT. TNT and pNCT produce similar 3-year RFS and OS rates in patients with mid-to-upper rectal cancer. TNT was associated with improved tumor responsiveness in all patients and improved 3-year RFS rates in those with low rectal cancer.

Conclusion: pNCT is an option for patients with mid-to-upper rectal cancer, but radiation is still necessary for low rectal cancer. To determine optimal

schema for neoadjuvant therapy and patient selection, additional randomized controlled studies are needed.

KEYWORDS

chemoradiotherapy, rectal cancer, neoadjuvant chemotherapy, recurrence, propensity score

1 Introduction

Neoadjuvant chemoradiotherapy (CRT) followed by total mesorectal excision (TME) and adjuvant systemic chemotherapy comprise the general paradigm of locally aggressive rectal cancer (LARC) treatment. Although the treatment strategy improves the local control of disease (1–4), it fails to significantly improve disease-free survival (DFS) and overall survival (OS) (5). Distant recurrence remains the leading cause of death for patients and is inadequately controlled by the current treatment mode (6, 7).

Recent evidence suggests that neoadjuvant chemotherapy may be used for controlling distant recurrence. Combined chemotherapy and chemoradiation, referred to as total neoadjuvant therapy (TNT), is used worldwide, and several high-quality trials showed that TNT improves oncological outcomes in two aspects (8–11). First, short-term recurrence rates decreased in those who underwent TNT, especially at 3-year follow up. Second, pathological complete response (pCR) rates increased after treatment with TNT, with the therapy nearly doubling pCR rates compared with CRT.

In recent years, use of neoadjuvant chemotherapy alone was reported to result in promising survival outcomes (12, 13). The FORWARC (13) study showed that 3-year DFS rates in those undergoing mFOLFOX6 with and without routine radiation did not significantly differ, and the elimination of radiation was unlikely to increase local recurrence risk after R0/1 resection. Especially in low-risk patients whose response to chemotherapy was good, the need for radiotherapy remains unclear. Findings of the trials have the potential to update clinical practice guidelines regarding the use of radiotherapy. To date, the optimal use of neoadjuvant chemotherapy and its target patient population remains controversial. The ideal way to maintain a balance between the benefits of TNT and overtreatment is of particular importance, and is likely to be debated well into the future.

In this study, we retrospectively reviewed records of 257 patients who were diagnosed with resectable LARC and treated with either TNT or prolonged neoadjuvant chemotherapy (pNCT) without radiation. We aimed to assess the safety, efficacy, and survival outcomes of pNCT versus TNT in patients with baseline resectable LARC.

2 Material and methods

2.1 Study population

This retrospective study utilized the data of consecutive patients who underwent TNT/pNCT followed with radical surgery for rectal cancer between June 2016 and October 2021 at Ruijin Hospital, Shanghai, China. Patients were randomly assigned to receive TNT or pNCT and were staged using preoperative imaging, including enhanced magnetic resonance imaging (MRI) and computed tomography (CT). Other clinical data were obtained from the patients' medical history at Ruijin Hospital.

Patients meeting the following eligibility criteria were included: (I) aged between 18 and 80 years; (II) diagnosis of rectal adenocarcinoma *via* colonoscopy and a pathological examination (the lower tumor edge within 12 cm of the anal verge); (III) underwent TNT or pNCT, and (IV) postoperative pathological results showing R0 resection. Exclusion criteria were as follows: (I) the presence of concomitant malignant disease, (II) history of malignant disease, (III) failure to complete planned cycles of neoadjuvant or adjuvant treatment, and (IV) unresectable tumors or difficult to get R0 resection after neoadjuvant therapy.

2.2 Treatment

2.2.1 Neoadjuvant therapy and adjuvant therapy

All patients received oxaliplatin- and fluorouracil-based neoadjuvant chemotherapy (mFOLFOX6 or CapeOX). The mFOLFOX6 regimen consisted of an intravenous infusion of oxaliplatin (85 mg/ m^2) followed by leucovorin (400 mg/m^2), an intravenous bolus of 5-FU (400 mg/m^2), and a continuous intravenous infusion of 5-FU (2,400 mg/m^2) for 2 days. The CapeOX regimen consisted of intravenous infusion of oxaliplatin (130 mg/m^2). Capecitabine (1,000 mg/m^2) was orally administered twice daily for 14 days. The pNCT group received six to eight cycles of chemotherapy. After surgery, patients diagnosed with pathological stage III or high-risk stage II rectal adenocarcinoma received adjuvant therapy

similar to the preoperative treatment for an additional four cycles. The high-risk factors included: CRM<1mm, ypN2/N1c, poor mesorectal quality, poor tumor differentiation.

2.2.2 Synchronous chemoradiotherapy

The TNT group received CRT after four cycles of induction chemotherapy. Patients received 50 Gy radiation throughout 5 weeks (2 Gy five times per week). During radiotherapy, continuous oral capecitabine was administered twice daily, on days 1–14 and 22–35. This procedure was performed by specific radiation oncologists.

2.3 Surgery and pathological examination

CT and enhanced rectal MRI imaging were repeated after preoperative treatment. Surgery was performed if the tumor was considered resectable. In the pNCT group, the median interval between the last treatment and surgery was 2 week (range, 2-3 weeks). In the TNT group, the median interval between CRT and surgery was 6 weeks (range, 4-6 weeks), with one cycle of chemotherapy during the interval. All included patients underwent laparoscopic TME with R0 resection. The surgical specimens were examined by pathologists from the Department of Pathology. Pathological features such as ypT stage, ypN stage, tumor differentiation, and tumor response were determined *via* routine methods, and a mismatch repair status (MMR) test was performed, if necessary. The radiological response to neoadjuvant therapy was evaluated based on response evaluation criteria for solid tumors (RECIST v1.1).

2.4 Post-treatment surveillance

All patients were followed-up every 3 months for the first year after surgery, and every 6 months for the next 4 years. Enhanced CT scans (chest, abdomen, and pelvis), serum tests for tumor markers (CEA, CA19-9, CA125, and CA242), and colonoscopies were performed every six months. Survival outcomes and the recurrence status of patients were also noted. Recurrence-free survival (RFS) was defined as the time between the end of treatment and date of recurrence. OS was defined as the time from surgery to the date of all-cause death.

2.5 Statistical analysis

Statistical analyses were performed using IBM SPSS Statistics version 26 (IBM Corporation, Armonk, NY, USA) or R version 4.1.3. Propensity scores matching (PSM) at a ratio of 1:1 was completed using SPSS. The chi-square test was used to compare categorical variables, and continuous variables were analyzed using the Student's t-test. Kaplan–Meier curves were used to analyze survival and recurrence. A Cox regression model was used to calculate hazard ratios of OS and RFS. Survival curves and forest plots were constructed using the R packages *survminer*, *forestmodel* and *forestplot*. P-values were two-sided, and $P < 0.05$ was considered statistically significant.

3 Results

3.1 Patient characteristics

A total of 257 patients with LARC who underwent TNT or pNCT from April 2016 to August 2021 were enrolled in this study (Figure 1). A total of 229 patients were included after screening, with 131 and 98 being treated with pNCT and TNT, respectively. Among the excluded patients, 4 and 2 patients in the pNCT and TNT groups (2.96% vs 1.72%), respectively, were excluded due to unsatisfied tumor response, and underwent additional treatment later (Supplementary Table1). Finally, 92 patients of each group were studied after a 1:1 PSM. Baseline clinical characteristics of patients before and after PSM are shown in Table 1. Overall, 176 of 184 patients (96%) had cT3 and cT4 tumors, and 174 of 184 patients (95%) had clinically involved lymph nodes. The mean distance to the anal verge was 5.95 cm, and 71 of 184 patients (39%) had low rectal cancer (within 5 cm from the anal verge).

3.2 Pathology staging and response to chemotherapy

All patients underwent laparoscopic TME and a pathological examination to evaluate their responsiveness to treatment preoperatively. Similar ypT and ypN stages were observed after both TNT and pNCT. TRG findings revealed that the TNT group had a higher rate of TRG0 and TRG1 than the pNCT group; however, the difference was not statistically significant ($p = 0.095$, Table 2). Patients in the TNT group had higher pathological complete response (pCR; 25.0% and 16.3%, respectively) and objective regression rates (73.9% and 59.8%, respectively) than those of the pNCT group. TNT and pNCT groups showed promising disease control rates (93.5% and 95.7%, respectively). As for toxicity, no patient died of chemotherapy-related adverse events. Grade 3/4 adverse events in preoperative chemotherapy and postoperative hospitalization were rare in both groups (Table 3). The most common severe adverse event was leukopenia, which was similar between the two groups (4 in pNCT vs. 3 in TNT, p=0.702).

3.3 Surgical outcomes and survival

The permanent diversion rate was 20.65% (19/92) and 27.17% (25/92) in the pNCT and TNT group, and the

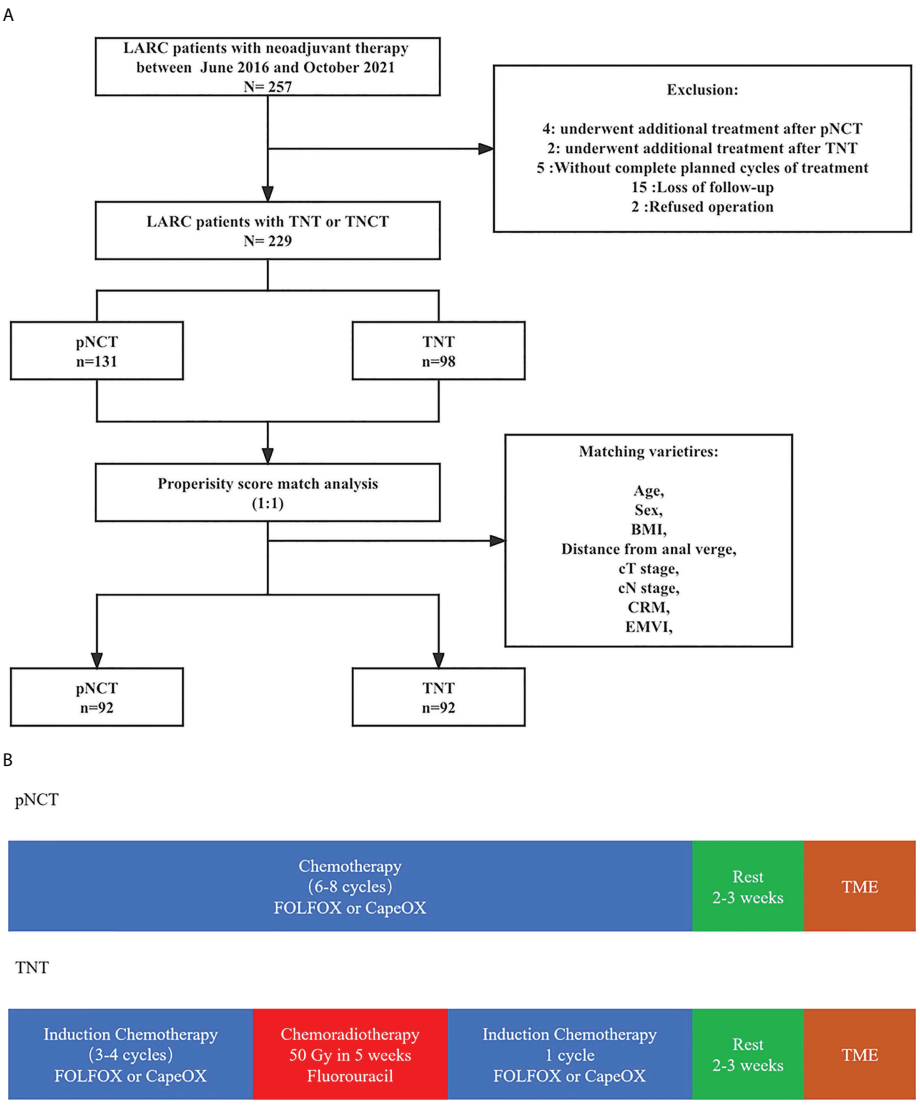

FIGURE 1
The diagram of total study **(A)** Neoadjuvant treatment; **(B)** Study population.The diagram of total study **(A)** Neoadjuvant treatment; **(B)** Study population. pNCT prolonged neoadjuvant chemotherapy; TNT, total neoadjuvant therapy; BMI, Body mass index; CRM, circumference resection margin; EMVI, extramural vascular invasion; TME, total mesorectal excision.

temporary stoma rate was 29.35% (27/92) and 26.09% (24/92), respectively. Anastomosis bleeding and leakage were the most common short-term complications. Five patients in pNCT group and seven patients in TNT group suffered from grade 3/4 anastomosis leakage and showed no significant difference between two groups (5.43 vs. 7.61, p=0.234).

The median follow-up period was 35 months (5–64 months), with that for the pNCT and TNT groups being 34.5 months (9–61 months) and 36 months (5–64 months), respectively. As shown in Figure 2, 6 of 92 patients of the pNCT group (6.5%) and 8 (8.7%) of the TNT group died. Recurrence was reported in 40 (43.5%) and 29 (31.5%) patients of the pNCT and TNT groups, respectively (Table 4). Among these patients, local recurrence events were reported in 11 (12.0%) and 5 (5.4%) patients of the pNCT and TNT groups, respectively, and distant metastasis was reported in 30 (33.6%) and 26 (28.3%) patients.

Subgroup analysis of survival outcomes showed that low rectal cancer (within 5 cm of the anal verge) was a strong indicator of TNT (P <0.01, Figure 3), while other factors assessed failed to show statistical significance. We further investigated survival outcomes of patients with and without low rectal cancer. Results showed that for patients with low rectal cancer, better RFS was associated with the use of TNT; however, this result was

10.3389/fonc.2022.953790

TABLE 1 Baseline clinical characteristics of patients before and after propensity scoring matching.

Characteristic		Before matching			After matching		
		pNCT N=131	TNT n=98	P	pNCT N=92	TNT N=92	P
Sex (%)	Male	103 (78.6)	76 (77.6)	0.974	74 (80.4)	70 (76.1)	0.592
	Female	28 (21.4)	22 (22.4)		18 (19.6)	22 (23.9)	
Age, years (SD)		60.91 (9.23)	60.90 (8.68)	0.993	61.23 (8.64)	60.60 (8.61)	0.621
BMI (SD)		22.93 (3.32)	22.92 (2.53)	0.993	22.87 (3.08)	22.93 (2.56)	0.871
Distance from anal verge, cm (SD)		6.34 (2.32)	6.02 (1.99)	0.282	5.95 (1.97)	6.01 (2.01)	0.853
Pretreatment CEA level, ng/ml (SD)		7.31 (13.69)	4.52 (7.76)	0.071	4.42 (5.63)	3.61 (4.76)	0.293
cT (%)	cT1	0 (0.0)	2 (2.0)	0.208	0 (0.0)	2 (2.2)	0.275
	cT2	4 (3.1)	4 (4.1)		3 (3.3)	3 (3.3)	
	cT3	65 (49.6)	39 (39.8)		48 (52.2)	38 (41.3)	
	cT4	62 (47.3)	53 (54.1)		41 (44.6)	49 (53.3)	
cN (%)	cN0	10 (7.6)	4 (4.1)	0.516	6 (6.5)	4 (4.3)	0.718
	cN1	49 (37.4)	40 (40.8)		34 (37.0)	38 (41.3)	
	cN2	72 (55.0)	54 (55.1)		52 (56.5)	50 (54.3)	
CRM (%)	Negative	52 (39.7)	32 (32.7)	0.339	29 (31.5)	31 (33.7)	0.875
	Positive	79 (60.3)	66 (67.3)		63 (68.5)	61 (66.3)	
EMVI (%)	Negative	53 (40.5)	37 (37.8)	0.781	35 (38.0)	35 (38.0)	1
	Positive	78 (59.5)	61 (62.2)		57 (62.0)	57 (62.0)	
Median Follow-up Time months (min-max)					34.5 (9-61)	36 (5-64)	

pNCT, prolonged neoadjuvant chemotherapy; TNT, total neoadjuvant therapy; BMI, Body mass index; CRM, circumference resection margin; EMVI, extramural vascular invasion.

not observed in patients with mid-to-upper rectal cancer (Figure 4). In univariable and multivariable analysis, effects of these factors on RFS and OS were assessed (Table 5). Worsened RFS was associated with pNCT, cT4, ypT4, ypN2, and unfavorable tumor response, while ypT4 (HR, 2.00; CI,1.20–3.50) and ypN2 (HR,2.20; CI, 1.30–3.60) were independent risk factors.

4 Discussion

Recently, TNT has been widely used to treat patients with LARC, which results in promising survival outcomes. One of the advantages of TNT is that it allows for the early use of systemic chemotherapy, which may improve the efficiency by which micro-metastases at early stages of tumor development are targeted (14, 15). However, with increasing focus on neoadjuvant chemotherapy, the value of preoperative radiation, especially in patients with initially resectable tumors that undergo high-quality TME surgery, is under question. Recently, several randomized studies have reported non-inferior survival outcomes in those receiving neoadjuvant chemotherapy without radiation (12, 13, 16, 17), which has prompted a reexamination of the significance of preoperative radiation.

In our study, we compared prolonged neoadjuvant chemotherapy without radiation to TNT composed of induction CapeOX/FOLFOX and CRT. All patients underwent R0 resection, as confirmed *via* a pathological examination. Results showed that the pCR and 3-year RFS rates of the TNT group were longer than those of the pNCT group; however, TNT failed to improve survival in those with middle and high rectal cancer. This result showed that TNT may related with improved tumor responsiveness and promising survival outcomes; however, preoperative radiation might not be necessary for initially resectable mid-to-upper rectal cancer.

Previous studies have reported that although neoadjuvant radiotherapy may improve the pCR rate, it fails to improve the prognosis. Moreover, radiation may damage normal tissue adjacent to the tumor, a process that may be related to several complications, including radiation-induced rectal injury, anastomosis leakage, sexual dysfunction, and bowel dysfunction (18, 19). Recently, several prospective clinical studies have assessed the effectiveness of radiotherapy-free regimens. The FOWARC trial compared the following treatment regimens: neoadjuvant mFOLFOX6 alone, fluorouracil plus radiotherapy, and mFOLFOX6 plus radiotherapy. Results showed that outcomes of those undergoing mFOLFOX6 with or without radiation and fluorouracil with radiation did not significantly differ (13). Deng et al. (16) assessed outcomes in those given neoadjuvant CapeOX alone, reporting that promising tumor response rates were observed. Zhang et al. (12) administered neoadjuvant chemotherapy alone with triplet regimens of mFOLFOXIRI, which also produced similar oncologic outcomes. On the other

10.3389/fonc.2022.953790

TABLE 2 Pathological result of tumor response to neoadjuvant therapy.

Characteristics		Overall N=184	pNCT N=92	TNT N=92	P value
ypT (%)	ypT0	40 (21.7)	16 (17.4)	24 (26.1)	0.512
	ypT1	1 (0.5)	0 (0.0)	1 (1.1)	
	ypT2	24 (13.0)	12 (13.0)	12 (13.0)	
	ypT3	82 (44.6)	44 (47.8)	38 (41.3)	
	ypT4	37 (20.1)	20 (21.7)	17 (18.5)	
ypN (%)	ypN0	106 (57.6)	50 (54.3)	56 (60.9)	0.112
	ypN1	43 (23.4)	19 (20.7)	24 (26.1)	
	ypN2	35 (19.0)	23 (25.0)	12 (13.0)	
Differentiation (%)	No tumor*	42 (22.8)	16 (17.4)	26 (28.3)	0.02
	Poor	22 (12.0)	15 (16.3)	7 (7.6)	
	Moderate	76 (41.3)	33 (35.9)	43 (46.7)	
	Well	44 (23.9)	28 (30.4)	16 (17.4)	
TRG (%)	0	39 (21.2)	15 (16.3)	24 (26.1)	0.095
	1	13 (7.1)	4 (4.3)	9 (9.8)	
	2	100 (54.3)	53 (57.6)	47 (51.1)	
	3	32 (17.4)	20 (21.7)	12 (13.0)	
Response (%)	CR*	38 (20.7)	15 (16.3)	23 (25.0)	0.408
	PR	76 (41.3)	40 (43.5)	36 (39.1)	
	SD	60 (32.6)	33 (35.9)	27 (29.3)	
	PD	10 (5.4)	4 (4.3)	6 (6.5)	
ORR (%)	SD+PD	70 (38.0)	37 (40.2)	24 (26.1)	0.06
	CR+PR	114 (62.0)	55 (59.8)	68 (73.9)	
DCR (%)	PD	10 (5.4)	4 (4.3)	6 (6.5)	0.745
	CR+PR+SD	174 (94.6)	88 (95.7)	86 (93.5)	
pCR (%)	PR+SD+PD	146 (79.3)	77 (83.7)	69 (75.0)	0.202
	CR	38 (20.7)	15 (16.3)	23 (25.0)	

pNCT, prolonged neoadjuvant chemotherapy; TNT, total neoadjuvant therapy; ypT, Pathological T stage after neoadjuvant therapy; ypN, Pathological N stage after neoadjuvant therapy; TRG, tumor regression grade; CR, complete response; PR, partial response; SD, stable disease; PD, progressive disease; ORR, Objective regression rate; DCR, Disease control rate; pCR, Pathological complete regression.
*The number of "No tumor" patients were more than "CR" patients because four patients had complete tumor regression but still had positive lymph nodes.

TABLE 3 Comparison of toxicity and adverse event.

Adverse Event	pNCT n=92	TNT n=92	P
Chemotherapy-related adverse event (%)			
Death	0	0	
Leukopenia (Grade 3, 4[†])	4 (4.35)	3 (3.26)	0.702
Anemia (Grade 3, 4[†])	0	1 (1.09)	0.319
Thrombocytopenia (Grade 3, 4[†])	1 (1.09)	0	0.319
Diarrhea (Grade 3, 4[†])	2 (2.18)	1 (1.09)	0.563
	Postoperative complications (%)		
Death	0	0	
Bleeding (Grade 3, 4[#])	1 (1.09)	2 (2.18)	0.563
Anastomosis leakage (Grade B, C*)	5 (5.43)	7 (7.61)	0.234
Wound infection (Grade 3, 4[#])	0	1 (1.09)	0.319

[†]Common Terminology Criteria for Adverse Events (CTCAE).
[#]Clavien-Dindo classification.
*Classification of International Study Group of Rectal Cancer (ISREC).

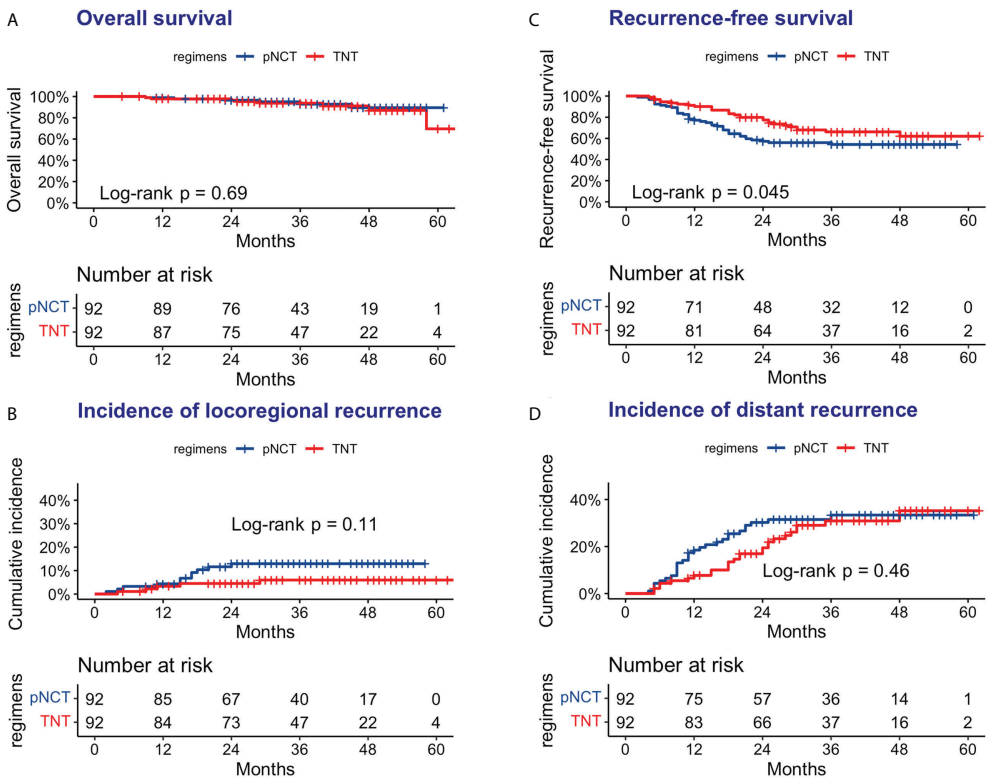

FIGURE 2
Oncologic outcomes of pNCT group and TNT group **(A)** Overall survival **(B)** Disease-free survival; **(C)** Cumulative incidence of locoregional recurrence; **(D)** Cumulative incidence of distant metastases. pNCT prolonged neoadjuvant chemotherapy; TNT total neoadjuvant therapy.

hand, it is still not clear whether all patients with LARC need chemoradiotherapy. The QuickSilver trial studied MRI-predicted good prognosis rectal patients, and suggested that CRT might not be necessary for stage II and III rectal cancer (20). The prospective multicenter OCUM trial compared surgery alone versus neoadjuvant CRT, and showed a better DFS and OS for high-risk patients (CRM+ or lower third rectal cancer) (21).These studies indicated that the application of radiotherapy needs more accurate selection of patients.

Our study shows that chemotherapy alone produces similar RFS and OS in patients with middle and high rectal cancer; however, chemoradiotherapy remained necessary in those undergoing low rectal cancer treatment. The following three explanations for this result are possible. First, the lower pelvic cavity is narrower than the upper pelvic cavity. Performing lower rectal cancer radical resection of the complete mesorectum with a sufficiently resection margin is difficult. In these cases, preoperative radiation could improve tumor downstaging

TABLE 4 Comparison of outcomes of patients.

Relapse Type	pNCT n=92	TNT n=92	P
Death (%)	6 (6.5)	8 (8.7)	0.781
Total (%)	40 (43.5)	29 (31.5)	0.128
Locally recurrence (%)	11 (12.0)	5 (5.4)	0.191
Distant metastasis (%)	30 (33.6)	26 (28.3)	0.747
Liver (%)	21 (22.8)	17 (18.5)	0.585
Lung (%)	4 (4.3)	4 (4.3)	1.000
Liver+Lung(%)	4 (4.3)	3 (3.3)	1.000
Other (%)	1 (1.1)	2 (2.2)	1.000

pNCT, prolonged neoadjuvant chemotherapy; TNT, total neoadjuvant therapy.

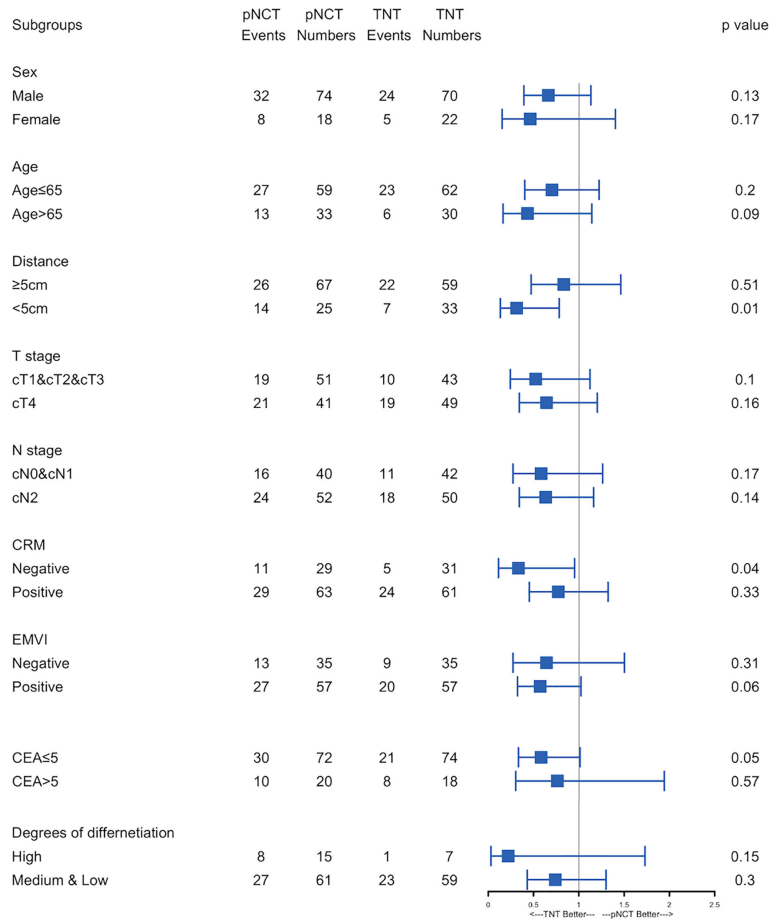

FIGURE 3
Forest plot of recurrence-free survival.Forest plot of recurrence-free survival. Subgroups analyses of recurrence-free survival was performed. pNCT, prolonged neoadjuvant chemotherapy; TNT, total neoadjuvant therapy; CRM, circumference resection margin; EMVI, extramural vascular invasion; ypT, Pathological T stage after neoadjuvant therapy; ypN, Pathological N stage after neoadjuvant therapy; CR, complete response; PR, partial response; SD, stable disease; PD, progressive disease.

more than chemotherapy alone, thereby limiting the risk of residual tumors. Second, the tumor location is a prognostic factor for assessing the treatment efficacy (22). Patients with lower rectal cancer may benefit from neoadjuvant radiation more than those undergoing upper rectal cancer therapy (23). Third, the increased rate of postoperative complications in low rectal cancer may delay treatment after surgery.

Although several clinical trials have focused on assessing the use of neoadjuvant treatment, the optimal treatment schema remains uncertain due to data heterogeneity among published studies. Most studies assessing TNT provided patients with fluorouracil- and oxaliplatin-based chemotherapy (10, 24, 25). In addition, irinotecan-based chemotherapy, including doublet regimen CAPIRI (26, 27) and triplet regimen FOFIRINOX (11), showed good toxicity, tumor response rates, and survival outcomes. Most studies that considered neoadjuvant chemotherapy alone provided patients with CapeOX/FOLFOX, with or without monoclonal antibodies. However, whether all patients are eligible for neoadjuvant chemotherapy alone remains debatable. Good tumor response rates were observed when Deng et al. (16) provided CapeOX alone to patients with low- and intermediate-risk LARC. However, the Japanese N-SOG 03 trial revealed that CapeOX plus bevacizumab was associated with a poorer local recurrence and OS rates in patients with cT4b LARC, indicating that chemotherapy alone might not be suitable for the cT4b population (17). In our study, we used CapeOX or mFOLFOX6 regimens for TNT and prolonged neoadjuvant chemotherapy. All patients had baseline resectable tumors, meaning that no cT4b patients were enrolled. We found that doublet regimen CapeOX/mFOLFOX6 was a safe and effective treatment as induction chemotherapy or pNCT alone, but the pCR rate of TNT patients in our study was lower than triplet regimen FOLFIRINOX reported in PRODIGE 23 trial (25% vs 28%) (11).

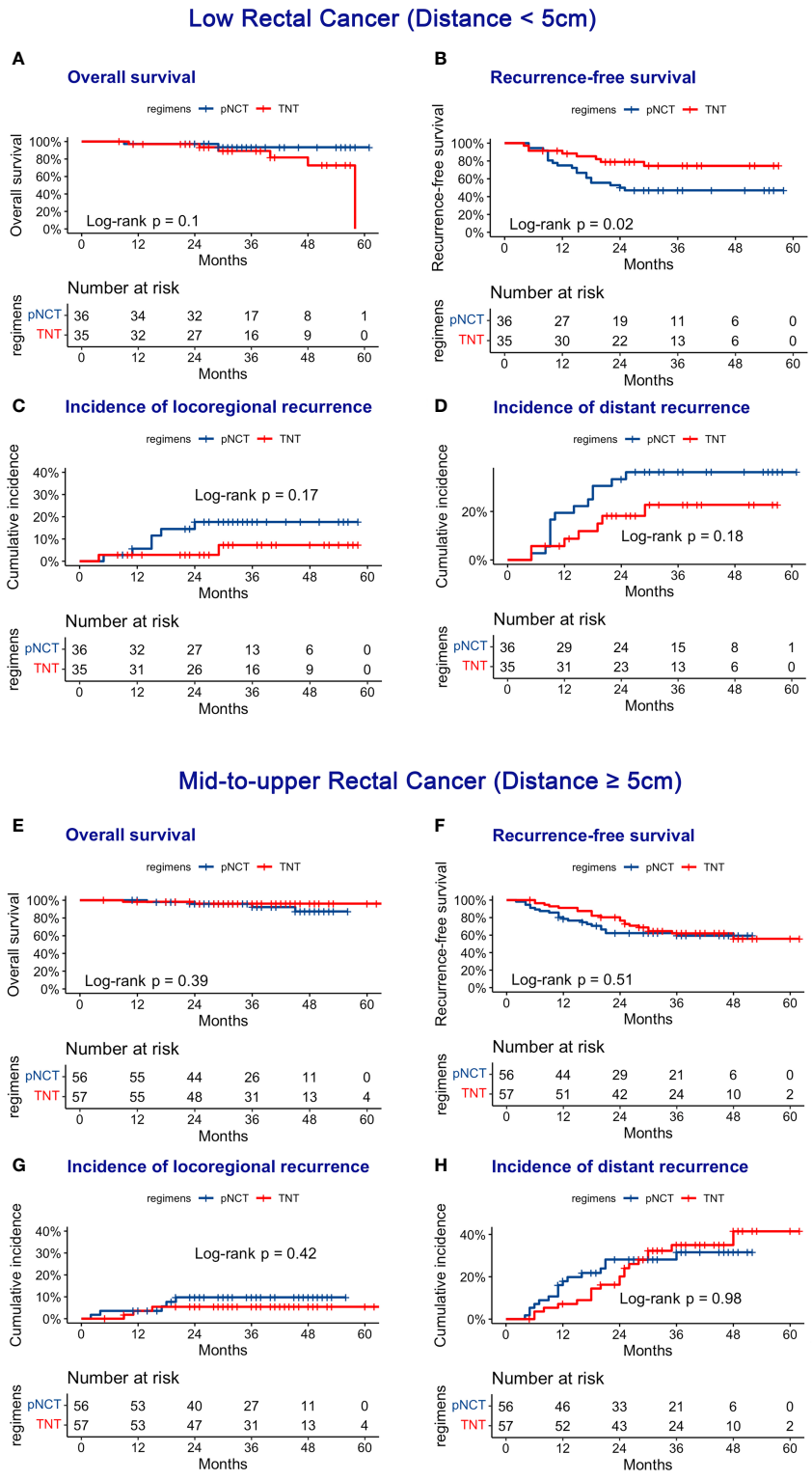

FIGURE 4
Oncologic Outcomes of pNCT and TNT in subgroup. Subgroup was divided according to the distance between tumor and anal verge. **(A)** Overall survival **(B)** Disease-free survival; **(C)** cumulative incidence of locoregional recurrence; **(D)** cumulative incidence of distant metastases in low group (distance <5 cm). **E** Overall survival **(F)** Disease-free survival; **(G)** cumulative incidence of locoregional recurrence; **(H)** cumulative incidence of distant metastases in mid-to-upper group (distance ≥5 cm).

TABLE 5 Univariable and multivariable analysis of the effects of prognostic factors on recurrence-free survival and overall survival.

Chatacteristic	RFS				OS	
	uni-HR (HR.95L-HR.95H)	pvalue	Multi-HR (HR.95L-HR.95H)	pvalue	HR (HR.95L-HR.95H)	pvalue
Regimens (pNCT vs TNT)	0.66 (0.38-0.99)	0.047	0.67 (0.41-1.10)	0.110	0.66 (0.43-3.60)	0.689
Sex (Female vs Male)	1.20 (0.63-2.12)	0.634	——	——	1.20 (0.45-26.14)	0.237
Age (Age<=65 vs Age>65)	0.65 (0.40-1.16)	0.155	——	——	0.65 (0.34-3.01)	0.991
cT_Stage (cT1&cT2&cT3 vs cT4)	1.30 (1.02-2.66)	0.04	1.30 (0.79-2.20)	0.300	1.30 (1.11-11.99)	0.033
cN_Stage (cN0 vs cN1&cN2)	1.00 (0.52-27.22)	0.187	——	——	1.00 (0-Inf)	0.998
MMR (unknown&pMMR vs dMMR)	1.50 (0.44-1.15)	0.165	——	——	1.50 (0.44-3.62)	0.665
CEA (CEA ≤ 5 vsCEA>5)	0.86 (0.87-2.56)	0.143	——	——	0.86 (0.04-2.47)	0.277
CRM (negative vs positive)	2.00 (0.96-2.95)	0.067	——	——	2.00 (0.50-6.49)	0.365
EMVI (negative vs positive)	2.20 (0.81-2.23)	0.252	——	——	2.20 (0.22-1.83)	0.405
ypT_Stage (ypT1&ypT2&ypT3 vs ypT4)	0.77 (1.53-4.23)	<0.001	2.00 (1.20-3.50)	0.012	0.77 (0.61-6.20)	0.265
ypN_Stage (ypN0 vs ypN1&ypN2)	1.20 (1.57-4.13)	<0.001	2.20 (1.30-3.60)	0.003	1.20 (1.00-8.98)	0.05
Response (CR&PR vs SD&PD)	1.30 (1.21-3.11)	0.006	1.40 (0.86-2.30)	0.180	1.30 (0.43-3.64)	0.68
Distance (≥5cm vs <5cm)	1.20 (0.60-1.67)	0.997	——	——	1.20 (0.75-6.12)	0.156

pNCT, prolonged neoadjuvant chemotherapy; TNT, total neoadjuvant therapy; CRM, circumference resection margin; EMVI, extramural vascular invasion; MMR, mismatch repair; ypT, Pathological T stage after neoadjuvant therapy; ypN, Pathological N stage after neoadjuvant therapy; CR, complete response; PR, partial response; SD, stable disease; PD, progressive disease.

Chemotherapy cycles are also important. For postoperative chemotherapy, the IDEA study found that 6-months of adjuvant chemotherapy increased the cost and toxicity without improving survival outcomes when compared with 3-month chemotherapy. However, outcomes associated with neoadjuvant chemotherapy may differ from those of adjuvant chemotherapy. Patients who do not undergo surgery have improved the health status and compliance to chemotherapy. In our study, the pNCT group underwent two to four additional cycles of CapeOX/mFOLFOX6 instead of radiation. A comparison of our results with other published studies that assessed the use of neoadjuvant chemotherapy showed that pNCT failed to improve rates of pCR (16.3% versus 6.5%–21.0% for pNCT versus other neoadjuvant therapies, respectively) (13, 16, 17, 28–30). This difference may be explained by differences in the selection of patients and therapy regimens. To determine whether prolonged chemotherapy improves response rates, further prospective studies are needed.

The arrangement of chemoradiotherapy and chemotherapy regimens was another consideration. There are two major modes of TNT: induction chemotherapy plus chemoradiotherapy and chemoradiotherapy plus consolidation chemotherapy. The CAO/ARO/AIO-12 trial compared induction and consolidation chemotherapy in TNT (31, 32). Findings showed that chemoradiotherapy with consolidation chemotherapy was associated with higher pCR rates than induction chemotherapy (25% vs 17%). This can be explained by the longer interval between chemoradiotherapy and surgery. Nevertheless, improvement to pCR failed to improve survival outcomes according to final results of CAO/ARO/AIO-12. In our study, we applied the induction chemotherapy plus chemoradiotherapy followed with an extra cycle of chemotherapy, and achieved a pCR rate of 25% (23/92). Compared with relevant studies (32), our results showed that the additional chemotherapy could probably improve the pCR rate of induction chemotherapy mode. Moreover, based on our experience, induction chemotherapy is more suitable for a "neoadjuvant chemotherapy plus selective radiation" mode. When the scheme was used, patients underwent chemotherapy before their tumor response status was re-evaluated to determine whether additional radiation was needed.

Another consideration is the interval between the last treatment and surgery. The optimal radiotherapy fractionation and timing to surgery is still undetermined. The Stockholm III trial compared short interval (1 week before surgery) with long interval (4-8 weeks before surgery), and showed a comparable oncological outcome between the two groups (33). In a recent randomized study, Akgun et al. (34) compared outcomes of patients for whom intervals between surgery and chemotherapy were either less or more than 8 weeks. The results showed that patients with an interval of more than 8 weeks had improved disease regression and pCR rates compared to those with a surgery-to-chemotherapy interval of less than 8 weeks. Related systematic reviews also showed that surgical delay may improve pCR rates. However, the delayed surgery was not significantly associated with long-term prognosis. The timing to surgery and the best arrangement of neoadjuvant treatment and surgery worth more investigations.

We are aware that this study has some limitations. First, this was a retrospective study with a limited amount of patients. Although we found difference in RFS between the two groups, the study was likely not powered to detect the difference in terms of the recurrence patterns. Second, the functional outcomes of patients after surgery (sexual dysfunction, urinary dysfunction, etc.) were absent, and we failed to evaluate the functional complications between two groups. Third, all enrolled patients were diagnosed with baseline resectable LARC. The efficacy of pNCT for the conversion of unresectable tumors or lateral lymph node metastases was unable to be evaluated. Finally, since patients of both groups completed all cycles of neoadjuvant treatment, we were unable to compare the compliance differences between the two schemas.

In summary, the results of our study show that TNT and pNCT produce similar 3-year RFS and OS rates in patients with mid-to-upper rectal cancer. TNT was associated with improved tumor responsiveness in all patients and improved 3-year RFS rates in those with low rectal cancer. This result indicates that neoadjuvant chemotherapy without radiation might be an option for patients with mid-to-upper rectal cancer. More randomized controlled studies are needed to determine better schema for neoadjuvant therapy.

Data availability statement

The original contributions presented in the study are included in the article/Supplementary Material. Further inquiries can be directed to the corresponding authors.

Ethics statement

The studies involving human participants were reviewed and approved by Ethics committee of Shanghai Ruijin Hospital. The patients/participants provided their written informed consent to participate in this study.

Author contributions

MZ and ZH contributed to conception and design of the study. JM, FD and LZ recruited the patients. XZ, PH and LYZ collected the database and performed the statistical analysis. XZ and PH wrote the first draft of the manuscript. MZ and ZH edited the draft. All authors contributed to manuscript revision, read, and approved the submitted version. All authors contributed to the article and approved the submitted version.

Funding

This study was supported by the National Natural Science Foundation of China (No.82072614).

Conflict of interest

The authors declare that the research was conducted in the absence of any commercial or financial relationships that could be construed as a potential conflict of interest.

Publisher's note

Supplementary material

The Supplementary Material for this article can be found online at: https://www.frontiersin.org/articles/10.3389/fonc.2022.953790/full#supplementary-material

References

1. Brændengen M, Tveit KM, Berglund Å, Birkemeyer E, Frykholm G, Påhlman L, et al. Randomized phase III study comparing preoperative radiotherapy with chemoradiotherapy in nonresectable rectal cancer. *J Clin Oncol* (2008) 26 (22):3687–94. doi: 10.1200/jco.2007.15.3858

2. Gérard J-P, Conroy T, Bonnetain F, Bouché O, Chapet O, Closon-Dejardin MT, et al. Preoperative radiotherapy with or without concurrent fluorouracil and leucovorin in T3-4 rectal cancers: Results of FFCD 9203. *J Clin Oncol* (2006) 24 (28):4620–25. doi: 10.1200/jco.2006.06.7629

3. Sauer R, Becker H, Hohenberger W, Rödel C, Wittekind C, Fietkau R, et al. Preoperative versus postoperative chemoradiotherapy for rectal cancer. *New Engl J Med* (2004) 351(17):1731–40. doi: 10.1056/nejmoa040694

4. Bosset J-F, Collette L, Calais G, Mineur L, Maingon P, Radosevic-Jelic L, et al. Chemotherapy with preoperative radiotherapy in rectal cancer. *New Engl J Med* (2006) 355(11):1114–23. doi: 10.1056/nejmoa060829

5. Rahbari NN, Elbers H, Askoxylakis V, Motschall E, Bork U, Büchler MW, et al. Neoadjuvant radiotherapy for rectal cancer: Meta-analysis of randomized controlled trials. *Ann Surg Oncol* (2013) 20(13):4169–82. doi: 10.1245/s10434-013-3198-9

6. Sebag-Montefiore D, Stephens RJ, Steele R, Monson J, Grieve R, Khanna S, et al. Preoperative radiotherapy versus selective postoperative chemoradiotherapy in patients with rectal cancer (MRC CR07 and NCIC-CTG C016): A multicentre, randomised trial. *Lancet* (2009) 373(9666):811–20. doi: 10.1016/s0140-6736(09) 60484-0

7. Gollins S, Sebag-Montefiore D. Neoadjuvant treatment strategies for locally advanced rectal cancer. *Clin Oncol* (2016) 28(2):146–51. doi: 10.1016/j.clon.2015.11.003

8. Garant A, Kavan P, Martin A-G, Azoulay L, Vendrely V, Lavoie C, et al. Optimizing treatment sequencing of chemotherapy for patients with rectal cancer: The KIR randomized phase II trial. *Radiotherapy Oncol* (2021) 155:237–45. doi: 10.1016/j.radonc.2020.11.008

9. Moore J, Price T, Carruthers S, Selva-Nayagam S, Luck A, et al. Prospective randomized trial of neoadjuvant chemotherapy during the 'wait period' following preoperative chemoradiotherapy for rectal cancer: Results of the WAIT trial. *Colorectal Dis* (2017) 19(11):973–79. doi: 10.1111/codi.13724

10. Bahadoer RR, Dijkstra EA, van Etten B, Marijnen CAM, Putter H, Kranenbarg EM, et al. Short-course radiotherapy followed by chemotherapy before total mesorectal excision (TME) versus preoperative chemoradiotherapy, TME, and optional adjuvant chemotherapy in locally advanced rectal cancer (RAPIDO): A randomised, open-label, phase 3 trial. *Lancet Oncol* (2021) 22 (1):29–42. doi: 10.1016/s1470-2045(20)30555-6

11. Conroy T, Bosset JF, Etienne PL, Rio E, François É, Mesgouez-Nebout N, et al. Neoadjuvant chemotherapy with FOLFIRINOX and preoperative chemoradiotherapy for patients with locally advanced rectal cancer (UNICANCER-PRODIGE 23): A multicentre, randomised, open-label, phase 3 trial. *Lancet Oncol* (2021) 22(5):702–15. doi: 10.1016/s1470-2045(21)00079-6

12. Zhang J, Huang M, Cai Y, Wang L, Xiao J, Lan P, et al. Neoadjuvant chemotherapy with mFOLFOXIRI without routine use of radiotherapy for locally advanced rectal cancer. *Clin Colorectal Canc* (2019) 18(4):238–44. doi: 10.1016/j.clcc.2019.07.001

13. Deng Y, Chi P, Lan P, Wang L, Chen W, Cui L, et al. Neoadjuvant modified FOLFOX6 with or without radiation versus fluorouracil plus radiation for locally advanced rectal cancer: Final results of the Chinese FOWARC trial. *J Clin Oncol* (2019) 37(34):3223–33. doi: 10.1200/jco.18.02309

14. Giunta EF, Bregni G, Pretta A, Deleporte A, Liberale G, Bali AM, et al. Total neoadjuvant therapy for rectal cancer: Making sense of the results from the RAPIDO and PRODIGE 23 trials. *Cancer Treat Rev* (2021) 96:102177. doi: 10.1016/j.ctrv.2021.102177

15. Schrag D, Weiser MR, Goodman KA, et al. Neoadjuvant chemotherapy without routine use of radiation therapy for patients with locally advanced rectal cancer: a pilot trial. *J Clin oncology: Off J Am Soc Clin Oncol* (2014) 32(6):513–18. doi: 10.1200/JCO.2013.51.7904

16. Deng X, Wu Q, Bi L, Yu Y, Huang S, He D, et al. Early response to upfront neoadjuvant chemotherapy (CAPOX) alone in low- and intermediate-risk rectal cancer: A single-arm phase II trial. *Br J Surg* (2021) 109(1):121–28. doi: 10.1093/bjs/znab388

17. Tomida A, Uehara K, Hiramatsu K, Maeda A, Sakamoto E, Okada Y, et al. Neoadjuvant CAPOX and bevacizumab alone for locally advanced rectal cancer: Long-term results from the n-SOG 03 trial. *Int J Clin Oncol* (2019) 24(4):403–10. doi: 10.1007/s10147-018-1372-6

18. Sun W, Dou R, Chen J, Lai S, Zhang C, Ruan L, et al. Impact of long-course neoadjuvant radiation on postoperative low anterior resection syndrome and quality of life in rectal cancer: *Post hoc* analysis of a randomized controlled trial. *Ann Surg Oncol* (2019) 26(3):746–55. doi: 10.1245/s10434-018-07096-8

19. Kumagai T, Rahman F, Smith AM. The microbiome and radiation induced-bowel injury: Evidence for potential mechanistic role in disease pathogenesis. *Nutrients* (2018) 10(10):1405. doi: 10.3390/nu10101405

20. Kennedy ED, Simunovic M, Jhaveri K, Kirsch R, Brierley J, Drolet S, et al. Safety and feasibility of using magnetic resonance imaging criteria to identify patients with "Good prognosis" rectal cancer eligible for primary surgery: The phase 2 nonrandomized QuickSilver clinical trial. *JAMA Oncol* (2019) 5(7):961–66. doi: 10.1001/jamaoncol.2019.0186

21. Ruppert R, Junginger T, Ptok H, Strassburg J, Maurer CA, Brosi P, et al. Oncological outcome after MRI-based selection for neoadjuvant chemoradiotherapy in the OCUM rectal cancer trial. *Br J Surg* (2018) 105(11):1519–29. doi: 10.1002/bjs.10879

22. Glynne-Jones R, Wyrwicz L, Tiret E, Brown G, Rödel C, Cervantes A, et al. Rectal cancer: ESMO clinical practice guidelines for diagnosis, treatment and follow-up. *Ann Oncol* (2018) 29(Suppl 4):iv263. doi: 10.1093/annonc/mdy161

23. Li Y, Wang J, Ma X, Tan L, Yan Y, Xue C, et al. A review of neoadjuvant chemoradiotherapy for locally advanced rectal cancer. *Int J Biol Sci* (2016) 12 (8):1022–31. doi: 10.7150/ijbs.15438

24. Bujko K, Wyrwicz L, Rutkowski A, Malinowska M, Pietrzak L, Kryński J, et al. Long-course oxaliplatin-based preoperative chemoradiation versus 5 × 5 gy and consolidation chemotherapy for cT4 or fixed cT3 rectal cancer: results of a randomized phase III study. *Ann Oncol* (2016) 27(5):834–42. doi: 10.1093/annonc/mdw062

25. Jin J, Tang Y, Hu C, Jiang LM, Jiang J, Li N, et al. Multicenter, randomized, phase III trial of short-term radiotherapy plus chemotherapy versus long-term chemoradiotherapy in locally advanced rectal cancer (STELLAR). *J Clin Oncol* (2022), 40(15):Jco2101667. doi: 10.1200/jco.21.01667

26. Zhu J, Liu A, Sun X, Liu L, Zhu Y, Zhang T, et al. Multicenter, randomized, phase III trial of neoadjuvant chemoradiation with capecitabine and irinotecan guided by UGT1A1 status in patients with locally advanced rectal cancer. *J Clin Oncol* (2020) 38(36):4231–39. doi: 10.1200/jco.20.01932

27. Wang J, Fan J, Li C, Yang L, Wan J, Zhang H, et al. The impact of chemotherapy completion on the efficacy of irinotecan in the preoperative chemoradiotherapy of locally advanced rectal cancer: An expanded analysis of the CinClare phase III trial. *Clin Colorectal Cancer* (2020) 19(2):e58–69. doi: 10.1016/j.clcc.2020.01.004

28. Kamiya T, Uehara K, Nakayama G, Ishigure K, Kobayashi S, Hiramatsu K, et al. Early results of multicenter phase II trial of perioperative oxaliplatin and capecitabine without radiotherapy for high-risk rectal cancer: CORONA I study. *Eur J Surg Oncol* (2016) 42(6):829–35. doi: 10.1016/j.ejso.2016.02.014

29. Oshiro T, Uehara K, Aiba T, Mukai T, Ebata T, Nagino M. Impact of RAS/BRAF mutation status in locally advanced rectal cancer treated with preoperative chemotherapy. *Int J Clin Oncol* (2018) 23(4):681–88. doi: 10.1007/s10147-018-1253-z

30. Nishimura J, Hasegawa J, Kato T, Yoshioka S, Noura S, Kagawa Y, et al. Phase II trial of capecitabine plus oxaliplatin (CAPOX) as perioperative therapy for locally advanced rectal cancer. *Cancer Chemother Pharmacol* (2018) 82(4):707–16. doi: 10.1007/s00280-018-3663-z

31. Fokas E, Allgäuer M, Polat B, Klautke G, Grabenbauer GG, Fietkau R, et al. Randomized phase II trial of chemoradiotherapy plus induction or consolidation chemotherapy as total neoadjuvant therapy for locally advanced rectal cancer: CAO/ARO/AIO-12. *J Clin Oncol* (2019) 37(34):3212–22. doi: 10.1200/jco.19.00308

32. Fokas E, Schlenska-Lange A, Polat B, Klautke G, Grabenbauer GG, Fietkau R, et al. Chemoradiotherapy plus induction or consolidation chemotherapy as total neoadjuvant therapy for patients with locally advanced rectal cancer: Long-term results of the CAO/ARO/AIO-12 randomized clinical trial. *JAMA Oncol* (2022) 8 (1):e215445. doi: 10.1001/jamaoncol.2021.5445

33. Erlandsson J, Holm T, Pettersson D, Berglund Å, Cedermark B, Radu C, et al. Optimal fractionation of preoperative radiotherapy and timing to surgery for rectal cancer (Stockholm III): A multicentre, randomised, non-blinded, phase 3, non-inferiority trial. *Lancet Oncol* (2017) 18(3):336–46. doi: 10.1016/s1470-2045(17)30086-4

34. Akgun E, Caliskan C, Bozbiyik O, Yoldas T, Sezak M, Ozkok S, et al. Randomized clinical trial of short or long interval between neoadjuvant chemoradiotherapy and surgery for rectal cancer. *Br J Surg* (2018) 105(11):1417–25. doi: 10.1002/bjs.10984

frontiers | Frontiers in Oncology

TYPE Original Research
PUBLISHED 21 February 2023
DOI 10.3389/fonc.2023.1119323

OPEN ACCESS

EDITED BY
Marco Rengo,
Sapienza University of Rome, Italy

REVIEWED BY
Francesco Ricchetti,
Sacro Cuore Don Calabria Hospital, Scientific Institute for Research, Hospitalization and Healthcare (IRCCS), Italy
Jesus C. Fabregas,
University of Florida, United States

*CORRESPONDENCE
Changlin Zou
zcl19670115@163.com

†These authors have contributed equally to this work

SPECIALTY SECTION
This article was submitted to Gastrointestinal Cancers: Colorectal Cancer, a section of the journal Frontiers in Oncology

RECEIVED 08 December 2022
ACCEPTED 06 February 2023
PUBLISHED 21 February 2023

CITATION
Xu Y, Zou H, Shao Z, Zhang X, Ren X, He H, Zhang D, Du D and Zou C (2023) Efficacy and safety of different radiotherapy doses in neoadjuvant chemoradiotherapy in patients with locally advanced rectal cancer: A retrospective study. *Front. Oncol.* 13:1119323. doi: 10.3389/fonc.2023.1119323

Efficacy and safety of different radiotherapy doses in neoadjuvant chemoradiotherapy in patients with locally advanced rectal cancer: A retrospective study

Yuyan Xu[1†], Haizhou Zou[2†], Zhenyong Shao[1], Xuebang Zhang[1], XiaoLin Ren[1], Huijuan He[3], Dahai Zhang[4], Dexi Du[5] and Changlin Zou[1*]

[1]Department of Radiotherapy, The First Affiliated Hospital of Wenzhou Medical University, Wenzhou, China, [2]Department of Oncology, Wenzhou Hospital of Traditional Chinese Medicine, Wenzhou, China, [3]Department of Radiotherapy, Quzhou People's Hospital, Quzhou, China, [4]Department of Radiotherapy, Dongyang People's Hospital, Jinhua, China, [5]Department of Radiotherapy Oncology, Lishui Central Hospital, Lishui, China

Background: This study aims to compare the efficacy and safety of neoadjuvant chemoradiotherapy (nCRT) with different radiotherapy doses (45Gy and 50.4Gy) in patients with locally advanced rectal cancer (LARC).

Methods: Herein, 120 patients with LARC were retrospectively enrolled between January 2016 and June 2021. All patients underwent two courses of induction chemotherapy (XELOX), chemoradiotherapy, and total mesorectum excision (TME). A total of 72 patients received a radiotherapy dose of 50.4 Gy, while 48 patients received a dose of 45 Gy. Surgery was then performed within 5-12 weeks following nCRT.

Results: There was no statistically significant difference between the baseline characteristics of the two groups. The rate of good pathological response in the 50.4Gy group was 59.72% (43/72), while in the 45Gy group achieved 64.58% (31/48) (P>0.05). The disease control rate (DCR) in the 50.4Gy group was 88.89% (64/72), compared to 89.58% (43/48) in the 45Gy group (P>0.05). The incidence of adverse reactions for radioactive proctitis, myelosuppression, and intestinal obstruction or perforation differed significantly between the two groups (P<0.05). The anal retention rate in the 50.4Gy group was significantly higher in contrast to the 45Gy group (P<0.05).

Conclusions: Patients receiving a radiotherapy dose of 50.4Gy have a better anal retention rate but also a higher incidence of adverse events such as radioactive proctitis, myelosuppression, and intestinal obstruction or perforation, and a comparable prognosis to patients treated with a radiotherapy dose of 45Gy.

KEYWORDS

locally advanced rectal cancer, radiotherapy dose, intensity-modulated radiation therapy, neoadjuvant chemoradiotherapy, adverse reactions

Introduction

Colorectal cancer incidence and mortality ranked third and second overall in 2020, according to cancer statistics (1). It is common for patients with rectal cancer to be asymptomatic in the early stages, so many patients are already in an advanced stage upon diagnosis. Neoadjuvant chemoradiotherapy (nCRT) plays an important role for patients with locally advanced rectal cancer (LARC), and clinical trials like the CAO/ARO/AIO-94 Study, the Swedish Trial, and the CAO/ARO/AIO-04 Study have demonstrated its effectiveness in LARC patients (2–5). Neoadjuvant chemoradiotherapy combined with total mesorectum excision (TME) is the first-line treatment for LARC patients, and while it can reduce tumor burden, induce downstaging, and improve the local control rate, it does not improve the overall survival (OS) (4, 6–8).

In recent years, the development of total neoadjuvant therapy (TNT) has also provided new options for LARC patients. CAO/ARO/AIO-12 Trial assessed the outcomes of 311 LARC patients treated with chemotherapy plus chemoradiotherapy (CRT) plus TME or CRT plus chemotherapy plus TME, and showed that if organ preservation is a priority, then TNT with consolidation chemotherapy (CNCT) after CRT is the preferred modality and this trial provides important evidence for the clinical use of TNT and has influenced the concept of organ preservation (9). RAPIDO trial looked at the efficacy of preoperative short-course radiotherapy (SCRT) plus nCRT compared to preoperative concurrent chemoradiotherapy (CCRT) and concluded that SCRT combined with nCRT reduced the probability of treatment failure in rectal cancer compared to standard treatment (10). The findings suggest that preoperative chemotherapy may be more effective than adjuvant chemotherapy and that this treatment modality may become the new standard of care for high-risk LARC (10). OPRA trial analyzed the outcomes of 324 LARC patients treated with induction chemotherapy (INCT) followed by CRT or CRT followed by CNCT, and concluded that half of the patients who received neoadjuvant treatment achieved organ preservation with no significant impairment in survival compared to previous controls who received radiotherapy, TME, and post-operative chemotherapy (11).

Notably, outcomes of nCRT vary widely among LARC patients, with more than one-third of patients experiencing recurrent or metastatic diseases (12). Moreover, some patients can achieve pathological complete remission (pCR) while others barely respond to nCRT. The proportion of patients who achieve pCR after nCRT is usually used as a reliable indicator of treatment response, Roh et al. reported that about 10-30% of patients achieved pCR (13), while Sanghera et al. concluded that 42% reached pCR (14) after nCRT. There is a strong correlation between clinical stage, tumor differentiation, and treatment regimens (6, 15, 16) in determining the outcomes of patients. Given that patients respond differently to nCRT, more research is needed to identify the most effective follow-up treatments.

Generally, surgery, chemotherapy, and radiotherapy are all crucial treatments for LARC, and each of these methods has made significant progress in recent years (17–23). The National Comprehensive Cancer Network (NCCN) guidelines and European Society for Medical Oncology (ESMO) guidelines recommend a total dose of 45-50.4Gy delivered in 25-28 fractions (24). In clinical practice, both radiotherapy doses are frequently used, but studies assessing their efficacy and safety are scarce. More studies focus on radiotherapy dose intensification versus conventional fractionation (25–28). Higher radiotherapy doses are known to be associated with improved efficacy but are also associated with an increased incidence of adverse events. A comparative analysis of radiotherapy doses of 45 Gy and 50.4 Gy was performed in the present study. Patients were divided into the 45Gy group and the 50.4Gy group according to the radiotherapy dose. Notably, pathological responses, imaging assessments, anal retention rate, local control, adverse reactions, and survival were analyzed across the two groups (45Gy and 50.4Gy).

Abbreviations: LARC, Locally advanced rectal cancer; nCRT, Neoadjuvant chemoradiotherapy; TME, Total mesorectum excision; OS, Overall survival; NCCN, National Comprehensive Cancer Network; AJCC, American Joint Committee on Cancer; DMFS, Distant metastasis free survival; PFS, progression-free survival; IMRT, Intensity-modulated radiation; RTOG, Radiation Therapy Oncology Group; GTV, Gross tumor volume; CTV, Clinical target volume; PTV, Planning target volume; XELOX regimen, Oxaliplatin in combination with capecitabine; pCR, Pathological complete response; DFS, Disease-free survival; CTCAE, Common Terminology Criteria for Adverse Events; MR, magnetic resonance; CR, Complete response; PR, Partial response; SD, Stable disease; PD, Progressive disease; DCR, Disease control rate; CRM, Circumferential resection margin; EMVI, Extramural venous invasion; SCRT, Short-course radiotherapy.

Materials and methods

Patient selection

144 patients were recruited in total, but 24 were excluded due to loss of follow-up or distant metastases before treatment, and 120 patients were enrolled eventually. The patient flow diagram is shown in Figure 1.

The inclusion criteria were as follows: (I) patients aged 18 to 75 years old; (II) rectal adenocarcinoma was diagnosed by colonoscopy; (III) Eastern Cooperative Oncology Group performance status (ECOG PS) was 0 or 1; (IV) defined as stage II/III according to the 8th edition of the American Joint Committee on Cancer (AJCC) staging; (V) no distant metastases or concurrent malignancy; (VI) normal heart, liver and kidney function; (VII) underwent complete chemoradiotherapy and radical surgical treatment.

The exclusion criteria were as follows: (I) diagnosed with distant metastasis; (II) prior chemoradiotherapy or targeted therapy or immunotherapy; (III) patients with other malignancy and incomplete clinical data.

Data collection

Patients baseline characteristics like age, gender, clinical stage, tumor location, tumor differentiation, circumferential resection margin (CRM) status, and extramural venous invasion (EMVI) status were collected on diagnosis. Adverse events, imaging assessments in pre- and post-nCRT, and pathological responses including epidermal growth factor receptor (EGFR) status, human

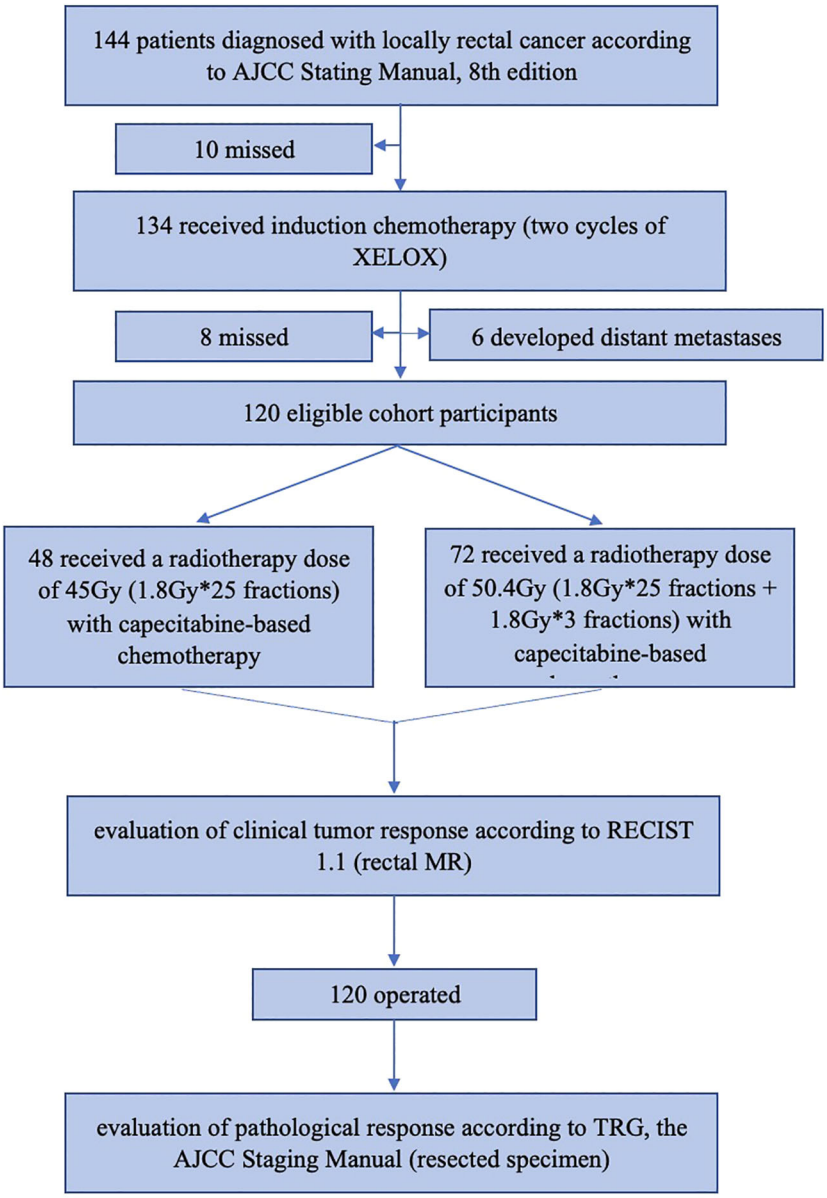

FIGURE 1
The patients flow diagram. AJCC, American Joint Committee on Cancer; XELOX regimen, Oxaliplatin in combination with capecitabine; MR, magnetic resonance.

epidermal growth factor receptor-2 (Her-2) status, and mismatch repair (MMR) status were recorded during follow-up observation. The time window for local recurrence rate, distant metastasis-free survival (DMFS), disease-free survival (DFS), and overall survival (OS) was from the date of surgery to the date of final follow-up. The last follow-up date was in November 2021. This study employed the outpatient system, the inpatient system, and telephone consultations to collect accurate patient information and to check for gaps through various collection methods. Regarding tumor location, tumors less than 5cm from the anus were considered low, tumors between 5-10cm from the anus were considered median, and tumors 10-12cm from the anus were considered high. The research was approved by the local ethics committee of The First Affiliated Hospital of Wenzhou Medical University and the Hospital Reviewing Board.

Radiotherapy

Intensity-modulated radiation (IMRT) technology with the Elekta Synergy system (Elekta AB, Stockholm, Sweden) was utilized in this study. All patients were in the supine position. The CT scan range was from the upper boundary of the 2-3 lumbar vertebrae to the lower boundary of the upper 1/3 of the femur, with a thickness of 5mm. Contrast-enhanced venography was recommended if there were no contraindications. Calibration radiographs were taken for each patient at the first session and at regular intervals (once a week).

Radiotherapy targets for both groups (45Gy and 50.4Gy) were performed with the Monaco planning system according to the Radiation Therapy Oncology Group (RTOG) criteria. All patients were treated with 6 MV-X-rays. The specific target areas are

outlined below. The gross tumor volume (GTV) was radiographically identified as gross lesions, including primary and metastatic lymph nodes. Clinical target volume (CTV) was defined as GTV + selective lymph node drainage area. CTV included the rectum and mesangial region, the presacral region, the internal iliac lymph nodes, and some obturator lymph nodes. The external iliac lymph nodes need to be irradiated when the tumor invades the bladder, prostate, and gynecological organs, and the external iliac and inguinal lymph nodes need to be irradiated when the tumor invades the anal canal or the lower 1/3 vagina. The upper boundary was the bifurcation of the common iliac artery, the lower boundary included the whole mesentery and was at least 2cm away from the lower edge of the tumor, the left and the right boundary was the inner edge of the true pelvis, the anterior boundary was 1cm in front of the posterior wall of the bladder or the anterior wall of the rectal organ; the internal iliac artery and vein were expanded by 0.7cm, and the posterior boundary was the front edge of the sacrum. Planning target volume (PTV) was defined as CTV+0.5-1.0cm.

The prescribed doses of PTV in the two groups were 45Gy and 50.4Gy, respectively. Patients in the 45Gy group received a total pelvic irradiation dose of 25×1.8Gy. Patients in the 50.4Gy group received a total pelvic irradiation dose of 45Gy (25×1.8Gy), and then the field was reduced to the mesenteric region for a supplement dose of 5.4Gy (3×1.8Gy). It should be pointed out that at least 95% of PTV received the specified dose. Radiotherapy was administered five times a week, from Monday to Friday. Organs at risk (OAR) mainly consisted of the femoral head, bladder and small intestine, the limited doses for each organ were as follows: femoral head Dmax <45Gy, bladder V50 <50Gy, and small intestine Dmax <50Gy.

Chemotherapy regimens

XELOX- oxaliplatin at 135 mg/m^2 and capecitabine at 1,000 mg/m^2-was administrated twice a day for 14 days, every 21 days for 2 cycles before chemoradiotherapy. Based on several clinical studies like STAR-01, ACCORD, NSABP R-04, and PETACC 6, the addition of oxaliplatin to capecitabine-based chemoradiotherapy failed to improve the rates of pathological complete response(pCR) and OS as expected. Furthermore, it could increase grade 3/4 side effects, thereby affecting patient tolerance (29–31). According to the results of the ACCORD trial, there was no significant difference between the groups in terms of 3-year local recurrence (4%, 6%), DFS (74%, 69%), and OS (both 88%). Fluorouracil-based chemotherapy is still considered to be the first-line regimen during radiotherapy in LARC patients. Therefore, capecitabine was given simultaneously during radiotherapy, twice a day, on weekdays. Patients were assessed 5-12 weeks following nCRT, and surgery was performed.

Adverse reactions monitoring

A variety of nCRT-related adverse reactions were evaluated, including bone marrow suppression, radioactive proctitis, intestinal obstruction or perforation, narrow lumen, anastomotic fistula, perianal skin injury, emesis, and hand-foot syndrome. Hand-foot syndrome was mainly associated with capecitabine treatment. During concurrent chemoradiotherapy, blood routine examinations and biochemical examinations were conducted weekly. RTOG radiation injury classification and Common Terminology Criteria for Adverse Events (CTCAE, Version 5) were adopted to assess adverse events. Grades 1 and 2 myelosuppression were considered mild, while grades 3 and 4 were considered moderate to severe. Similarly, grades 1 and 2 were defined as mild radiation proctitis, and grades 3 and 4 were defined as moderate to severe radiation proctitis. The remaining adverse reactions including intestinal obstruction or perforation, narrow lumen, anastomotic fistula, perianal skin injury, emesis, and hand-foot syndrome were evaluated by their occurrence or not.

Therapeutic effect evaluation

Clinical tumor response was determined by senior radiologists using rectal magnetic resonance (MR) imaging after nCRT and in keeping with RECIST 1.1. Complete response(CR) or clinical complete response (cCR) is defined as the disappearance of all targets lesions; partial response(PR) is achieved when the sum of the target diameter is reduced by at least 30% from baseline; progressive disease (PD) is characterized by an increase of at 20% in minimum diameter of all target lesions, while stable disease (SD) is the state between PR and PD. Disease control rate (DCR) is defined as a radiographic assessment of CR, PR, and SD. Postoperatively, the efficacy was evaluated by the pathological response. Pathological tumor response was evaluated by two experienced pathologists using resected specimens after TME and in accordance with TRG (the AJCC Staging Manual), with the four-tier AJCC Staging Manual being our study's preferred evaluation method (32). Grade 0-pCR- is complete regression with the absence of cancer cells; grade 1 is moderate regression with single or few cancer cells remaining; grade 2 is mild regression and surplus tumor with extensive fibrotic stroma; grade 3 is no regression and extensive tumor residue accompanied by no or little tumor cell necrosis. Grades 0 and 1 are considered good pathological regression, while grades 2 and 3 are considered poor pathological regression.

Statistical analysis

SPSS 23.0 software (USA) was used for statistical analysis. Age, gender, clinical stage, tumor location, tumor differentiation, imaging reports, pathological response, imaging assessment, anal retention rate, disease control rate, and adverse events were compared using the $\chi 2$ test for the two groups. Univariate and multivariate Cox regression analyses were conducted to identify characteristics that related to survival in patients. Age, gender, clinical stage, tumor location, tumor differentiation, CRM status, EMVI status, EGFR status, MMR status, Her-2 status, and radiation dose were the included variable. The Kaplan-Meier method was used to estimate the survival curves, and

the log-rank test was used for comparative analysis. A P-value<0.05 was considered statistically significant.

Results

Baseline characteristics

The baseline characteristics are shown in Table 1. The 45Gy group consisted of patients with a median age of 59.5years (from 36 to79 years) while the 50.4Gy group consisted of patients with a median age of 58 years (from 38 to 77 years), with a male predominance in both groups. No significant difference was observed between the 50.4Gy group and the 45Gy group in terms of clinical stage, tumor location, tumor differentiation, and several biological features.

Treatment outcomes

The rate of good pathological response (grade 0/1) was 59.72% in the 50.4Gy group (43/72), while it was 64.58% in the 45Gy group (31/48). The DCR in the 50.4Gy group was 91.67% (66/72), compared to 89.58% in the 45Gy group (43/48). The anal preservation rate in the 50.4Gy group was 79.17% (57/72), compared to 60.42% (29/48) in the 45Gy group (P<0.05). The efficacy of nCRT is shown in Table 2. Imaging evaluation in pre- and post-nCRT for patients is shown in Figure 2.

As demonstrated in Table 3, the local recurrence rate in the 50.4Gy group was 6.94% (5/72), the distant metastasis rate was 18.06% (13/72), and the DCR was 88.89% (64/72), compared with 4.17% (2/48), 22.92% (11/48), and 89.58% (43/48) in the 45Gy group, respectively. No statistical difference was found between the two groups.

TABLE 1 Baseline characteristics of patients.

Characteristics	45Gy group	50.4Gy group	χ2	p
Age (years)			0.051	0.821
Median (Range)	59.5 (36-79)	58 (38-77)		
>55	27	42		
≤55	21	30		
Gender			0.068	0.794
Male	37	54		
Female	11	18		
Clinical stage				
T3	36	51	0.251	0.617
T4	12	21		
N0	6	8	1.001	0.606
N1	17	20		
N2	25	44		
Tumor location			1.066	0.587
Low	22	27		
Mid	25	42		
High	1	3		
Tumor differentiation			0.988	0.610
Poorly differentiated	9	12		
Moderately differentiated	23	41		
Well differentiated	16	19		
CRM			1.442	0.230
(+)	18	35		
(-)	30	37		
EMVI			0.050	0.823
(+)	23	33		

(Continued)

TABLE 1 Continued

Characteristics	45Gy group	50.4Gy group	χ2	p
(-)	25	39		
EGFR			4.300	0.116
(+)	24	46		
(-)	13	19		
N/A	11	7		
Her-2			3.952	0.157
(+)	9	15		
(-)	28	50		
N/A	11	7		
MMR			4.263	0.122
pMMR	29	54		
dMMR	8	11		
N/A	11	7		

CRM, circumferential resection margin; EMVI, extramural venous invasion; EGFR, epidermal growth factor receptor; Her-2, human epidermal growth factor receptor-2; MMR, mismatch repair; dMMR, mismatch-repair-deficient; pMMR, mismatch-repair-proficient; N/A, not applicable.

Univariate Cox regression analysis showed that tumor differentiation, Her-2 status, and MMR status were associated with DFS, HR=0.312 (tumor differentiated), 0.505 (Her-2), 0.344 (MMR) (tumor differentiated 95% CI: 0.176–0.555, Her-2 95% CI: 0.263–0.968, MMR 95% CI: 0.147–0.804). Multivariate Cox regression analysis implied that tumor differentiation was an independent predictor for DFS (see Table 4). Univariate and multivariate Cox regression analysis revealed that only tumor differentiation was closely related to OS, HR=0.232 (95% CI: 0.068-0.794). However, Cox regression analysis showed that the radiation dose was not an independent predictor for DFS (HR=1.118, 95% CI: 0.559-2.525) or OS (HR=1.321, 95% CI: 0.293-5.945). Notably, the base variables of univariate and multivariate Cox regression analyses have been bolded and skewed in Tables 4, 5.

Herein, higher radiation doses did not confer longer DFS (see Figure 3). As shown in Figure 4, there was no statistical difference between the two groups regarding OS. Radiotherapy dose intensification was not significant in this study, the long-term survival outcomes in the 45Gy group were comparable to outcomes in the 50.4Gy group.

Adverse reactions

CTCAE assessment of myelosuppression and radiation proctitis was evaluated by the RTOG radiation injury classification. The incidence of myelosuppression, radiation proctitis, and intestinal obstruction or perforation in the high-dose group was higher than

TABLE 2 Efficacy evaluation of nCRT.

Characteristics	45Gy group	50.4Gy group	χ2	p
TRG stage			0.288	0.592
Grade 0,1	31	43		
Grade 2,3	17	29		
Imaging evaluation			0.005	0.945
DCR (CR+PR+SD)	43	64		
PD	5	8		
Operation			4.986	0.026
Anal-preservation	29	57		
Non-anal-preservation	19	15		

DCR, disease control rate; CR, complete response; PR, partial response; SD, disease stability; PD, disease progression; nCRT, neoadjuvant chemoradiotherapy.

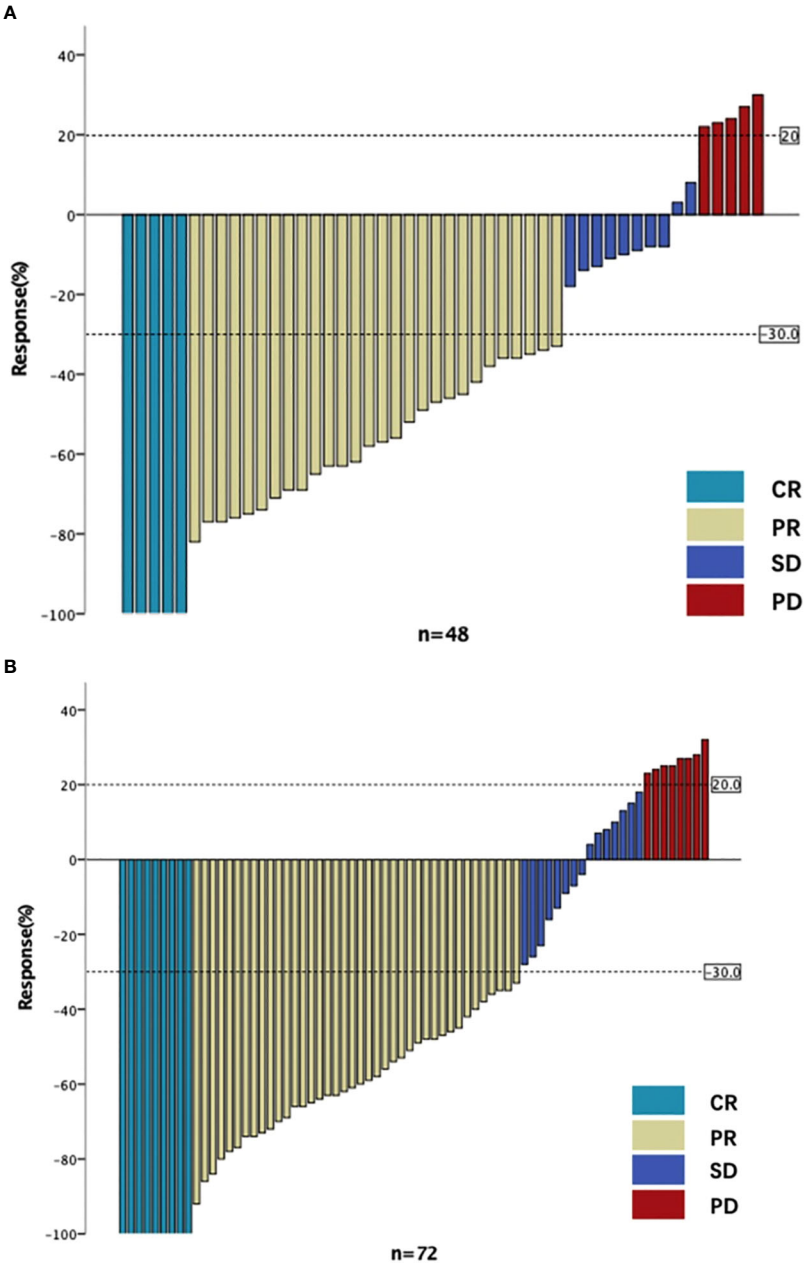

FIGURE 2
The imaging evaluation in two groups. **(A)** The imaging evaluation in 45Gy group. **(B)** The imaging evaluation in 50.4Gy group. CR, complete response; PR, partial response; SD, stable disease; PD, progressive disease.

TABLE 3 Disease control situation.

Control condition	45Gy group	50.4Gy group	$\chi 2$	p
Local recurrence rate (%)	4.17 (2/48)	6.94 (5/72)	0.057	0.811
Distant metastasis rate (%)	22.92 (11/48)	18.06 (13/72)	0.425	0.514
Disease control rate (%)	89.58 (43/48)	91.67 (66/72)	0.151	0.698

TABLE 4 Univariate and multivariate Cox regression analyses for different variables and DFS in LARC patients.

Variables	Disease free survival (n=120)			
	Univariate analysis		Multivariate analysis	
	HR (95% CI)	p	HR (95% CI)	p
Age (≤55 vs. ***>55years***)	3.120 (0.941-10.343)	0.063		
Gender (***male*** vs. female)	0.876 (0.413-1.859)	0.730		
Clinical stage (***T3*** vs. T4)	1.394 (0.642-3.024)	0.401		
Clinical stage (***N0*** vs. N1 vs. N2)	1.111 (0.645-1.912)	0.704		
Tumor location (***low*** vs. mid vs. high)	1.050 (0.529-2.087)	0.888		
Tumor differentiated (***poorly*** vs. moderately vs. well)	0.312 (0.176-0.555)	<0.001	0.380 (0.204-0.708)	0.002
CRM (***positive*** vs. negative)	0.703 (0.334-1.479)	0.353		
EMVI (***positive*** vs. negative)	0.695 (0.330-1.464)	0.339		
EGFR (positive vs. ***negative*** vs. N/A)	0.588 (0.335-1.031)	0.064		
MMR (***pMMR*** vs. dMMR vs. N/A)	0.344 (0.147-0.804)	0.014	1.246 (0.494-3.147)	0.641
Her-2 (positive vs. ***negative*** vs. N/A)	0.505 (0.263-0.968)	0.040	0.427 (0.147-1.244)	0.119
Radiation dose (***45Gy*** vs. 50.4Gy)	1.118 (0.559-2.525)	0.655		

DFS, disease-free survival; LARC, locally advanced rectal cancer; CRM, circumferential resection margin; EMVI, extramural venous invasion; EGFR, epidermal growth factor receptor; MMR, mismatch repair; dMMR, mismatch-repair-deficient; pMMR, mismatch-repair-proficient; N/A, not applicable; Her-2, human epidermal growth factor receptor-2.

that in the low-dose group, and the differences were statistically significant. Incidence of narrow lumen, anastomotic fistula, perianal skin injury, emesis, and the hand-foot syndrome showed no significant difference between the two groups. The incidence of specific adverse events is listed in Table 6.

Discussion

In our retrospective study, we found that the survival outcomes of LARC patients treated with 50.4Gy were similar to those of patients treated with 45Gy. In the 50.4Gy group, the rates of pCR and cCR were

TABLE 5 Univariate and multivariate Cox regression analyses for different variables and OS in LARC patients.

Variables	Overall survival (n=120)			
	Univariate analysis		Multivariate analysis	
	HR (95% CI)	p	HR (95% CI)	p
Age (≤55 vs. ***>55years***)	4.778 (0.570-40.067)	0.149		
Gender (***male*** vs. female)	0.030 (0.000-36.221)	0.334		
Clinical stage (***T3*** vs. T4)	1.941 (0.430-8.756)	0.388		
Clinical stage (***N0*** vs. N1 vs. N2)	1.345 (0.426-4.245)	0.614		
Tumor location (***low*** vs. mid vs. high)	1.675 (0.454-6.178)	0.439		
Tumor differentiated (***poorly*** vs. moderately vs. well)	0.232 (0.068-0.794)	0.020	0.232 (0.068-0.794)	0.020
CRM (***positive*** vs. negative)	0.256 (0.050-1.326)	0.105		
EMVI (***positive*** vs. negative)	0.298 (0.058-1.538)	0.148		
EGFR (positive vs. ***negative*** vs. N/A)	0.457 (0.138-1.515)	0.200		
MMR (***pMMR*** vs. dMMRvs. N/A)	0.327 (0.057-1.888)	0.211		
Her-2 (positive vs. ***negative*** vs. N/A)	0.356 (0.064-1.979)	0.238		
Radiation dose (***45Gy*** vs. 50.4Gy)	1.321 (0.293-5.945)	0.717		

OS, overall survival; LARC, locally advanced rectal cancer; CRM, circumferential resection margin; EMVI, extramural venous invasion; EGFR, epidermal growth factor receptor; MMR, mismatch repair; dMMR, mismatch-repair-deficient; pMMR, mismatch-repair-proficient; N/A, not applicable; Her-2, human epidermal growth factor receptor-2.

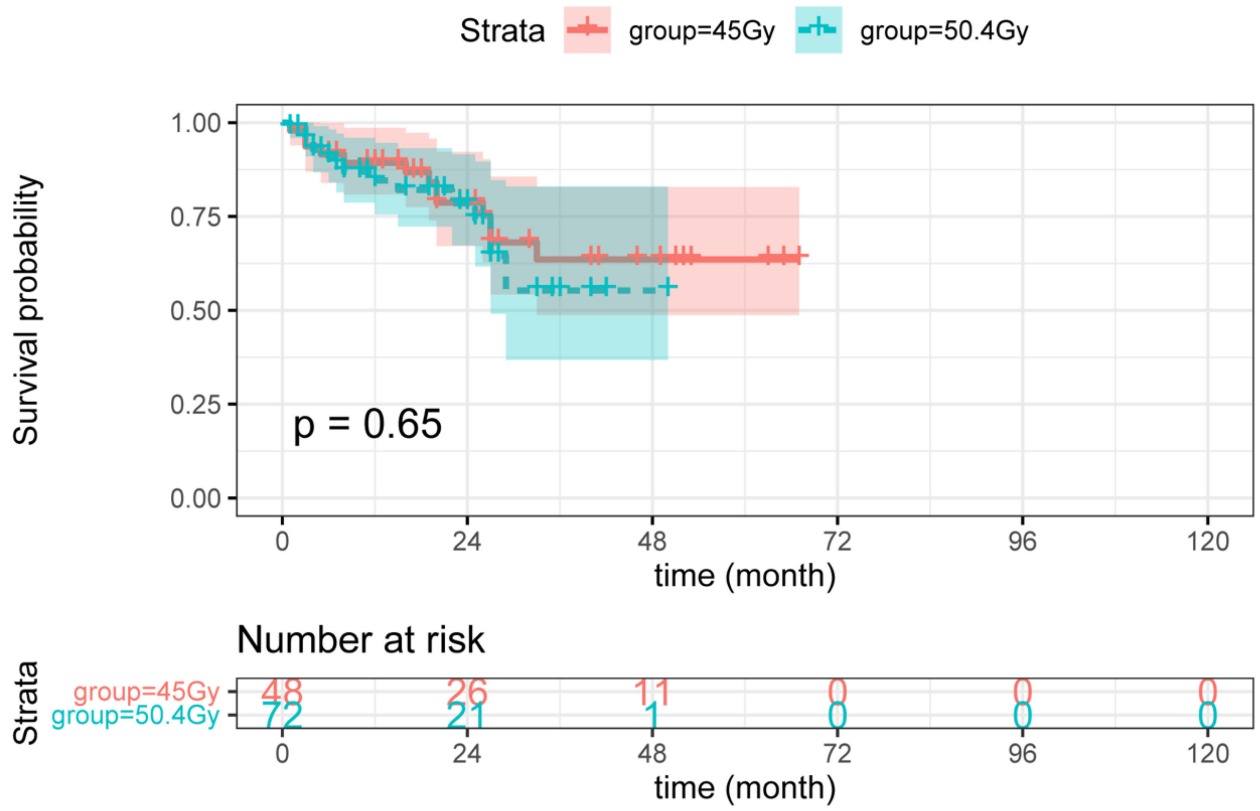

FIGURE 3
The DFS between LARC patients with different radiation doses. DFS, disease-free survival; LARC, locally advanced rectal cancer.

19.4% (14 of 72), and 12.5% (9 of 72), respectively, while in the 45Gy group, the rates were 22.9% (11 of 48), and 10.4% (5 of 48), showing no statistical significance. After radiotherapy dose transmutation from 45Gy to 50.4Gy, we observed no improvement in the rate of pCR, while there was a slight improvement in the rate of cCR. The rate of cCR in our study in question was partly based on data from a randomized phase 2 trial, where the rate of clinical complete/near-complete tumor response at MR did not increase after dose escalation from 50Gy to 65Gy (27). Radiotherapy dose intensification was not significant in this study. The statistics from a randomized trial showed that brachytherapy boost supplementation to conventional radiotherapy dose could improve the rate of near-complete response, but not that of pCR (33). Previously reported dose-response relationships may largely be directed by grade 0 and grade 1 (TRG, the AJCC Staging Manual), which could partly explain the rates of pCR in our study.

A radiotherapy dose of 50.4Gy was associated with higher rates of adverse reactions such as radioactive proctitis, myelosuppression, and intestinal obstruction or perforation. In the 45Gy group, 2.1% (1 of 48) of patients experienced intestinal obstruction, while 6.9% (5 of 72) of patients had intestinal obstruction, and 8.3% (6 of 72) had intestinal perforation in the 50.4Gy group. Due to a significant disadvantage relative to the rate of radioactive proctitis, the intestinal perforation rate was higher in the 50.4Gy group than in the 45Gy group. Among the patients in the 45Gy group, 14.6% (7 of 48) had severe myelosuppression compared with 37.5% (27 of 72) in the 50.4Gy ($P<0.05$). The districts of radiotherapy for LARC generally include the pelvis and pelvic lymph node areas, which exposes to hematological toxicity in the range of 30%-70% and there is a dose-likelihood efficiency (34, 35).

Colorectal cancer is an intractable worldwide public health issue due to its huge disease burden. The prevalence of western lifestyles, dietary changes, and reduced physical activity are the main reasons for the continued rise in colorectal cancer incidence worldwide (36). Multidisciplinary-based treatment is strongly recommended since advancements in diagnostic imaging and an evidence-based combination of chemotherapy, radiotherapy, and TME can markedly improve the prognosis of LARC patients. Especially in the case of a resectable lesion, the integration of chemotherapy and radiotherapy can achieve favorable tumor downstaging and local control rate (37, 38). However, owing to metastasis to other organs or local recurrence, the long-term survival of LARC is unsatisfactory (4, 17). To achieve a better prognosis, imaging (39, 40), carcinoembryonic antigen (CEA) combined with carbohydrate antigen 19-9 (CA19-9) (41), platelet-associated biomarkers (42), and circulating tumor DNA (ctDNA) (43) must be dynamically estimated and promptly evaluated. A more personalized treatment regimen is preferable for high risk patients, and novel combination regimens should be further investigated.

SCRT, which is the conventional treatment in European countries, is developing rapidly. Generally, patients receive pelvic radiotherapy at a dose of 5×5Gy during the first week, followed by surgical intervention

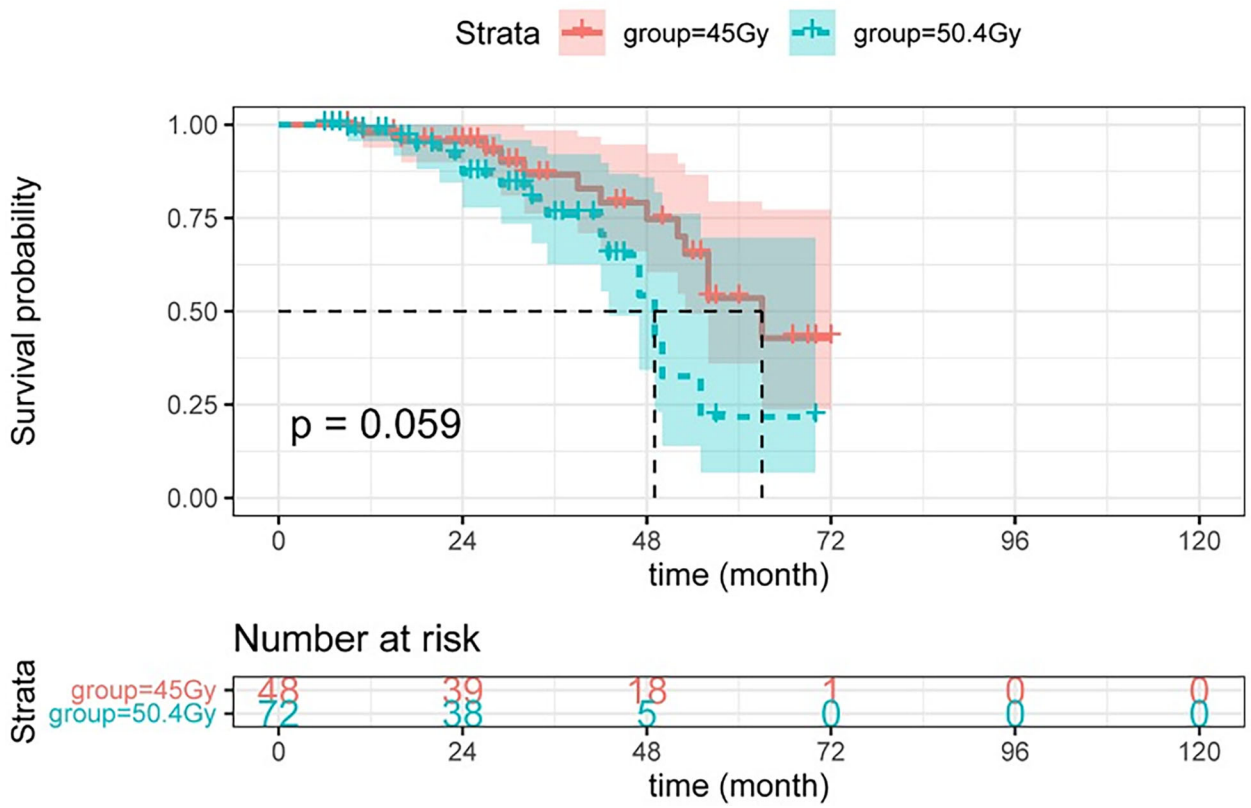

FIGURE 4
The OS between LARC patients with different radiation doses. OS, overall survival; LARC, locally advanced rectal cancer.

and six sessions of adjuvant chemotherapy. Interestingly, no significant difference in recurrence rates, distant metastasis, or late adverse events compared to long-term radiotherapy was observed (44). Moreover, a single-arm phase II clinical research (45) concluded that SCRT followed by chemotherapy plus immunotherapy and surgery demonstrated an impressive pCR rate with good tolerance in patients. Furthermore, SCRT treatment resulted in fewer late adverse events and rectal injury (46, 47). However, another randomized trial concluded that SCRT with delayed surgery was associated with an increased risk of local recurrence after a 10-year follow-up period (48).

Given the association between treatment intensification-tumor response and tumor prognosis, more consolidated treatment options are needed. TNT-chemotherapy combined with chemoradiotherapy before surgery-is a novel treatment approach for LARC patients, achieving improved downstaging, patient compliance, and micrometastases elimination rate (49–51). TNT is a promising systemic strategy to target micrometastases, especially for patients unfit for surgery (49). The pCR rate in patients treated with TNT (36%) was found to be higher compared to patients receiving nCRT (21%) (49). Patients who achieved pCR may choose non-operative treatment, sphincter-sparing surgery, or observation and periodic review. Nowadays, chemotherapy is administrated before or after radiotherapy, and the sequence of radiotherapy, chemotherapy and surgery has been extensively explored. In general, INCT combined with CRT is a preferred method since it is associated with better compliance and fewer acute adverse reactions (13, 50, 52). In our study, all patients underwent two cycles of induction chemotherapy and fluorouracil-based chemoradiotherapy.

Cancer is more averse to becoming a “chronic disease” as medical technology advances and therapeutic methods evolve. Functional needs and survival needs (46) are two central issues we should aim to address in future treatment prospects of rectal cancer. Our goal at the moment is to achieve a complete resection of the lesion while sparing the functioning sphincter complex of the anus, thereby improving the quality of life of patients. Notably, surgical improvements have helped reduce the local recurrence rate from above 50% to below 10% (53, 54). Herein, we noticed a significantly higher rate of anal retention in the 50.4Gy group compared to the 45Gy group (79.2% (57 of 72) vs. 60.4% (29 of 48)).

CRM and EMVI are important factors that predict survival outcomes and contribute to clinical treatment planning (55, 56). As a result, no significant difference between the two groups was observed. The survival curve in this study was not statistically significant, but the 45Gy group had a higher 80-month survival rate, which may be related to the higher incidence of adverse reactions in the 50.4Gy group, particularly intestinal obstruction or perforation and myelosuppression. Furthermore, according to our findings, a radiotherapy dose of 50.4Gy resulted in a favorable anal retention rate

TABLE 6 Adverse reactions to treatment.

Characteristics	45Gy group	50.4Gy group	χ2	p
Radioactive proctitis			6.699	0.010
Grade 1,2	43	50		
Grade 3,4	5	22		
Myelosuppression			5.412	0.020
Grade 1,2	32	41		
Grade 3,4	7	27		
Intestinal obstruction or perforation	1	11	4.201	0.040
Narrow lumen	2	4	0.119	0.730
Anastomotic fistula	5	12	0.925	0.336
Skin lesions around the anus	17	24	0.056	0.814
Emesis	15	24	0.057	0.811
Hand-foot syndrome	8	13	0.038	0.844

but at the expense of increased rates of several adverse reactions, with no improvement in the rate of good pathological response, DFS or OS.

Nevertheless, our study has several limitations. We included a small number of patients from a single center, and the follow-up time was not long enough to obtain long-term survival statistics. Moreover, our study was retrospective in nature, which may have resulted in bias to some extent. Nonetheless, to our knowledge, this is the first study that concluded the rate of pCR in the 45Gy group was higher than that of the 50.4Gy group. This study has clinical guiding significance and, to some extent, provides the basis for choosing radiotherapy doses in LARC patients. A radiotherapy dose of 50.4Gy is preferred for a higher likelihood of anal retention if a patient-centered outcome is prioritized. Meanwhile, if an efficacy-centered outcome is preferred, a radiotherapy dose of 45Gy is desired for a greater degree of pCR and a lower likelihood of adverse reactions. Combined with the trend of individualized treatment of the tumor, the radiotherapy dose needs to be considered according to the tolerance of the patient, which includes age, ECOG PS, and underlying disease. In the follow-up treatment, the efficacy and quality of life are the focus of doctors.

Conclusion

A radiation dose of 50.4Gy contributes to a better anal retention rate but at the cost of serious adverse events and failure to improve the rate of good pathological response, imaging remission, DFS or OS.

Data availability statement

The raw data supporting the conclusions of this article will be made available by the authors, without undue reservation.

Author contributions

(I) Conception and design: XZ, CZ; (II) Administrative support: HZ; (III) Provision of study materials or patients: YX, ZS; (IV) Collection and assembly of data: All authors; (V) Data analysis and interpretation: XR; (VI) Manuscript writing: All authors. (VII) All authors contributed to the article and approved the submitted version.

Funding

The research was funded by Wenzhou Science Technology Bureau (grant number Y20180220) and Zhejiang Medical Association (grant number 2022ZYC-Z27).

Conflict of interest

The authors declare that the research was conducted in the absence of any commercial or financial relationships that could be construed as a potential conflict of interest.

Publisher's note

References

1. Ferlay J, Colombet M, Soerjomataram I, Parkin D, Piñeros M, Znaor A, et al. Cancer statistics for the year 2020: An overview. *Int J Cancer* (2021). doi: 10.1002/ijc.33588

2. Folkesson J, Birgisson H, Pahlman L, Cedermark B, Glimelius B, Gunnarsson U. Swedish Rectal cancer trial: Long lasting benefits from radiotherapy on survival and local recurrence rate. *J Clin Oncol* (2005) 23(24):5644–50. doi: 10.1200/JCO.2005.08.144

3. Rödel C, Graeven U, Fietkau R, Hohenberger W, Hothorn T, Arnold D, et al. Oxaliplatin added to fluorouracil-based preoperative chemoradiotherapy and postoperative chemotherapy of locally advanced rectal cancer (the German CAO/ARO/AIO-04 study): Final results of the multicentre, open-label, randomised, phase 3 trial. *Lancet Oncol* (2015) 16(8):979–89. doi: 10.1016/S1470-2045(15)00159-X

4. Sauer R, Liersch T, Merkel S, Fietkau R, Hohenberger W, Hess C, et al. Preoperative versus postoperative chemoradiotherapy for locally advanced rectal cancer: Results of the German CAO/ARO/AIO-94 randomized phase III trial after a median follow-up of 11 years. *J Clin Oncol* (2012) 30(16):1926–33. doi: 10.1200/JCO.2011.40.1836

5. van der Valk M, Marijnen C, van Etten B, Dijkstra E, Hilling D, Kranenbarg E, et al. Compliance and tolerability of short-course radiotherapy followed by preoperative chemotherapy and surgery for high-risk rectal cancer - results of the international randomized RAPIDO-trial. *Radiother Oncol* (2020) 147:75–83. doi: 10.1016/j.radonc.2020.03.011

6. Bosset J, Calais G, Mineur L, Maingon P, Radosevic-Jelic L, Daban A, et al. Enhanced tumorocidal effect of chemotherapy with preoperative radiotherapy for rectal cancer: preliminary results–EORTC 22921. *J Clin Oncol* (2005) 23(24):5620–7. doi: 10.1200/JCO.2005.02.113

7. Bosset J, Calais G, Daban A, Berger C, Radosevic-Jelic L, Maingon P, et al. Preoperative chemoradiotherapy versus preoperative radiotherapy in rectal cancer patients: assessment of acute toxicity and treatment compliance. report of the 22921 randomised trial conducted by the EORTC radiotherapy group. *Eur J Cancer (Oxford Engl 1990)* (2004) 40(2):219–24. doi: 10.1016/j.ejca.2003.09.032

8. Gérard J, Conroy T, Bonnetain F, Bouché O, Chapet O, Closon-Dejardin M, et al. Preoperative radiotherapy with or without concurrent fluorouracil and leucovorin in T3-4 rectal cancers: results of FFCD 9203. *J Clin Oncol* (2006) 24(28):4620–5. doi: 10.1200/JCO.2006.06.7629

9. Fokas E, Schlenska-Lange A, Polat B, Klautke G, Grabenbauer GG, Fietkau R, et al. Chemoradiotherapy plus induction or consolidation chemotherapy as total neoadjuvant therapy for patients with locally advanced rectal cancer: Long-term results of the CAO/ARO/AIO-12 randomized clinical trial. *JAMA Oncol* (2022) 8(1):e215445. doi: 10.1001/jamaoncol.2021.5445

10. Bahadoer RR, Dijkstra EA, van Etten B, Marijnen CAM, Putter H, Kranenbarg EM, et al. Short-course radiotherapy followed by chemotherapy before total mesorectal excision (TME) versus preoperative chemoradiotherapy, TME, and optional adjuvant chemotherapy in locally advanced rectal cancer (RAPIDO): A randomised, open-label, phase 3 trial. *Lancet Oncol* (2021) 22(1):29–42. doi: 10.1016/S1470-2045(20)30555-6

11. Garcia-Aguilar J, Patil S, Gollub MJ, Kim JK, Yuval JB, Thompson HM, et al. Organ preservation in patients with rectal adenocarcinoma treated with total neoadjuvant therapy. *J Clin Oncol* (2022) 40(23):2546–56. doi: 10.1200/JCO.22.00032

12. Rahma O, Yothers G, Hong T, Russell M, You Y, Parker W, et al. Use of total neoadjuvant therapy for locally advanced rectal cancer: Initial results from the pembrolizumab arm of a phase 2 randomized clinical trial. *JAMA Oncol* (2021) 7(8):1225–30. doi: 10.1001/jamaoncol.2021.1683

13. Roh MS, Colangelo LH, O'Connell MJ, Yothers G, Deutsch M, Allegra CJ, et al. Preoperative multimodality therapy improves disease-free survival in patients with carcinoma of the rectum: NSABP r-03. *J Clin Oncol* (2009) 27(31):5124–30. doi: 10.1200/JCO.2009.22.0467

14. Sanghera P, Wong DW, McConkey CC, Geh JI, Hartley A. Chemoradiotherapy for rectal cancer: an updated analysis of factors affecting pathological response. *Clin Oncol (R Coll Radiol)* (2008) 20(2):176–83. doi: 10.1016/j.clon.2007.11.013

15. Mo S, Dai W, Xiang W, Huang B, Li Y, Feng Y, et al. Survival contradiction between stage IIA and stage IIIA rectal cancer: A retrospective study. *J Cancer* (2018) 9(8):1466–75. doi: 10.7150/jca.23311

16. Huang Q, Qin H, Xiao J, He X, Xie M, He X, et al. Association of tumor differentiation and prognosis in patients with rectal cancer undergoing neoadjuvant chemoradiation therapy. *Gastroenterol Rep (Oxf)* (2019) 7(4):283–90. doi: 10.1093/gastro/goy045

17. Glimelius B. Multidisciplinary treatment of patients with rectal cancer: Development during the past decades and plans for the future. *Upsala J Med Sci* (2012) 117(2):225–36. doi: 10.3109/03009734.2012.658974

18. Lichthardt S, Wagner J, Löb S, Matthes N, Kastner C, Anger F, et al. Pathological complete response due to a prolonged time interval between preoperative chemoradiation and surgery in locally advanced rectal cancer: analysis from the German StuDoQ|Rectalcarcinoma registry. *BMC cancer* (2020) 20(1):49. doi: 10.1186/s12885-020-6538-8

19. Stijns R, de Graaf E, Punt C, Nagtegaal I, Nuyttens J, van Meerten E, et al. Long-term oncological and functional outcomes of chemoradiotherapy followed by organ-sparing transanal endoscopic microsurgery for distal rectal cancer: The CARTS study. *JAMA surg* (2019) 154(1):47–54. doi: 10.1001/jamasurg.2018.3752

20. Hofheinz R, Wenz F, Post S, Matzdorff A, Laechelt S, Hartmann J, et al. Chemoradiotherapy with capecitabine versus fluorouracil for locally advanced rectal cancer: a randomised, multicentre, non-inferiority, phase 3 trial. *Lancet Oncol* (2012) 13(6):579–88. doi: 10.1016/S1470-2045(12)70116-X

21. Ng S, Chu J, Chander S, Bressel M, McKendrick J, Wong R, et al. Results of phase II trial of intensified neoadjuvant treatment with interdigitating radiotherapy and chemotherapy with oxaliplatin, 5-fluorouracil and folinic acid in patients with locally advanced rectal cancer (PROARCT trial). *Radiother Oncol* (2021) 155:27–32. doi: 10.1016/j.radonc.2020.10.012

22. Sun Y, Lin Y, Liu Z, Jiang W, Chi P. Combined laparoscopic lymphoadenectomy of lateral pelvic and inguinal nodal metastases using indocyanine green fluorescence imaging guidance in low rectal cancer after preoperative chemoradiotherapy: a case report. *BMC gastroenterol* (2022) 22(1):123. doi: 10.1186/s12876-022-02193-1

23. Schellenberg A, Moravan V, Christian F. A competing risk analysis of colorectal cancer recurrence after curative surgery. *BMC gastroenterol* (2022) 22(1):95. doi: 10.1186/s12876-022-02161-9

24. Glynne-Jones R, Wyrwicz L, Tiret E, Brown G, Rödel C, Cervantes A, et al. Rectal cancer: ESMO clinical practice guidelines for diagnosis, treatment and follow-up. *Ann Oncol* (2017) 28(suppl_4):iv22–40. doi: 10.1093/annonc/mdx224

25. Delishaj D, Fumagalli IC, Ursino S, Cristaudo A, Colangelo F, Stefanelli A, et al. Neoadjuvant radiotherapy dose escalation for locally advanced rectal cancers in the new era of radiotherapy: A review of literature. *World J Clin Cases* (2021) 9(30):9077–89. doi: 10.12998/wjcc.v9.i30.9077

26. Alongi F, Fersino S, Mazzola R, Fiorentino A, Giaj-Levra N, Ricchetti F, et al. Radiation dose intensification in pre-operative chemo-radiotherapy for locally advanced rectal cancer. *Clin Transl Oncol* (2017) 19(2):189–96. doi: 10.1007/s12094-016-1522-0

27. Couwenberg AM, Burbach JPM, Berbee M, Lacle MM, Arensman R, Raicu MG, et al. Efficacy of dose-escalated chemoradiation on complete tumor response in patients with locally advanced rectal cancer (RECTAL-BOOST): A phase 2 randomized controlled trial. *Int J Radiat Oncol Biol Phys* (2020) 108(4):1008–18. doi: 10.1016/j.ijrobp.2020.06.013

28. Bertocchi E, Barugola G, Nicosia L, Mazzola R, Ricchetti F, Dell'Abate P, et al. A comparative analysis between radiation dose intensification and conventional fractionation in neoadjuvant locally advanced rectal cancer: A monocentric prospective observational study. *Radiol Med* (2020) 125(10):990–8. doi: 10.1007/s11547-020-01189-9

29. Schmoll H, Stein A, Van Cutsem E, Price T, Hofheinz R, Nordlinger B, et al. Pre- and postoperative capecitabine without or with oxaliplatin in locally advanced rectal cancer: PETACC 6 trial by EORTC GITCG and ROG, AIO, AGITG, BGDO, and FFCD. *J Clin Oncol* (2021) 39(1):17–29. doi: 10.1200/JCO.20.01740

30. Gérard J, Azria D, Gourgou-Bourgade S, Martel-Laffay I, Hennequin C, Etienne P, et al. Comparison of two neoadjuvant chemoradiotherapy regimens for locally advanced rectal cancer: results of the phase III trial ACCORD 12/0405-prodige 2. *J Clin Oncol* (2010) 28(10):1638–44. doi: 10.1200/JCO.2009.25.8376

31. Aschele C, Cionini L, Lonardi S, Pinto C, Cordio S, Rosati G, et al. Primary tumor response to preoperative chemoradiation with or without oxaliplatin in locally advanced rectal cancer: Pathologic results of the STAR-01 randomized phase III trial. *J Clin Oncol* (2011) 29(20):2773–80. doi: 10.1200/JCO.2010.34.4911

32. Trakarnsanga A, Gönen M, Shia J, Nash G, Temple L, Guillem J, et al. Comparison of tumor regression grade systems for locally advanced rectal cancer after multimodality treatment. *J Natl Cancer Institute* (2014) 106(10):2773–2780. doi: 10.1093/jnci/dju248

33. Jakobsen A, Ploen J, Vuong T, Appelt A, Lindebjerg J, Rafaelsen SR. Dose-effect relationship in chemoradiotherapy for locally advanced rectal cancer: a randomized trial comparing two radiation doses. *Int J Radiat Oncol Biol Phys* (2012) 84(4):949–54. doi: 10.1016/j.ijrobp.2012.02.006

34. Kuntz L, Noel G. [Pelvic irradiation and hematopoietic toxicity: A review of the literature]. *Cancer Radiother* (2021) 25(1):77–91. doi: 10.1016/j.canrad.2020.05.018

35. Sini C, Fiorino C, Perna L, Noris Chiorda B, Deantoni CL, Bianchi M, et al. Dose-volume effects for pelvic bone marrow in predicting hematological toxicity in prostate cancer radiotherapy with pelvic node irradiation. *Radiother Oncol* (2016) 118(1):79–84. doi: 10.1016/j.radonc.2015.11.020

36. Dekker E, Tanis P, Vleugels J, Kasi P, Wallace M. Colorectal cancer. *Lancet (London England)* (2019) 394(10207):1467–80. doi: 10.1016/S0140-6736(19)32319-0

37. Valentini V, Glimelius B, Haustermans K, Marijnen CA, Rödel C, Gambacorta MA, et al. EURECCA consensus conference highlights about rectal cancer clinical management: the radiation oncologist's expert review. *Radiother Oncol* (2014) 110(1):195–8. doi: 10.1016/j.radonc.2013.10.024

38. Lupattelli M, Matrone F, Gambacorta MA, Osti M, Macchia G, Palazzari E, et al. Preoperative intensity-modulated radiotherapy with a simultaneous integrated boost combined with capecitabine in locally advanced rectal cancer: short-term results of a multicentric study. *Radiat Oncol* (2017) 12(1):139. doi: 10.1186/s13014-017-0870-4

39. Wan L, Peng W, Zou S, Ye F, Geng Y, Ouyang H, et al. MRI-Based delta-radiomics are predictive of pathological complete response after neoadjuvant chemoradiotherapy in locally advanced rectal cancer. *Acad Radiol* (2021) 28 Suppl 1: S95–s104. doi: 10.1016/j.acra.2020.10.026

40. Caruso R, Vicente E, Quijano Y, Duran H, Fabra I, Diaz E, et al. Role of 18F-PET-CT to predict pathological response after neoadjuvant treatment of rectal cancer. *Discovery Oncol* (2021) 12(1):16. doi: 10.1007/s12672-021-00405-w

41. Zheng Z, Wang X, Lu X, Huang Y, Chi P. Prognostic significance of carcinoembryonic antigen combined with carbohydrate antigen 19-9 following neoadjuvant chemoradiotherapy in patients with locally advanced rectal cancer. *Colorectal Dis* (2021) 23(9):2320–30. doi: 10.1111/codi.15694

42. Wang P, Wang Z, Liu Y, Xie J, Ren Y. Prognostic value of platelet-associated biomarkers in rectal cancer patients received neoadjuvant chemoradiation: A retrospective study. *Cancer Radiother* (2021) 25(2):147–54. doi: 10.1016/j.canrad.2020.06.030

43. McDuff SGR, Hardiman KM, Ulintz PJ, Parikh AR, Zheng H, Kim DW, et al. Circulating tumor DNA predicts pathologic and clinical outcomes following neoadjuvant chemoradiation and surgery for patients with locally advanced rectal cancer. *JCO Precis Oncol* (2021) 5. doi: 10.1200/PO.20.00220

44. Ngan S, Burmeister B, Fisher R, Solomon M, Goldstein D, Joseph D, et al. Randomized trial of short-course radiotherapy versus long-course chemoradiation comparing rates of local recurrence in patients with T3 rectal cancer: Trans-Tasman radiation oncology group trial 01.04. *J Clin Oncol* (2012) 30(31):3827–33. doi: 10.1200/JCO.2012.42.9597

45. Lin Z, Cai M, Zhang P, Li G, Liu T, Li X, et al. Phase II, single-arm trial of preoperative short-course radiotherapy followed by chemotherapy and camrelizumab in locally advanced rectal cancer. *J immunother Cancer* (2021) 9(11):147–154. doi: 10.1136/jitc-2021-003554

46. Ahmed K, Correa C, Dilling T, Rao N, Shridhar R, Trotti A, et al. Altered fractionation schedules in radiation treatment: A review. *Semin Oncol* (2014) 41 (6):730–50. doi: 10.1053/j.seminoncol.2014.09.012

47. Michalski J, Gay H, Jackson A, Tucker S, Deasy J. Radiation dose-volume effects in radiation-induced rectal injury. *Int J Radiat oncol biol phys* (2010) 76:S123–9. doi: 10.1016/j.ijrobp.2009.03.078

48. Pach R, Sierzega M, Szczepanik A, Popiela T, Richter P. Preoperative radiotherapy 5×5 gy and short versus long interval between surgery for resectable rectal cancer: 10-year follow-up of the randomised controlled trial. *Radiother Oncol* (2021) 9(11). doi: 10.1016/j.radonc.2021.10.006

49. Cercek A, Roxburgh CSD, Strombom P, Smith JJ, Temple LKF, Nash GM, et al. Adoption of total neoadjuvant therapy for locally advanced rectal cancer. *JAMA Oncol* (2018) 4(6):e180071. doi: 10.1001/jamaoncol.2018.0071

50. Fernandez-Martos C, Garcia-Albeniz X, Pericay C, Maurel J, Aparicio J, Montagut C, et al. Chemoradiation, surgery and adjuvant chemotherapy versus induction chemotherapy followed by chemoradiation and surgery: Long-term results of the Spanish GCR-3 phase II randomized trial†. *Ann Oncol* (2015) 26(8):1722–8. doi: 10.1093/annonc/mdv223

51. Cercek A, Goodman KA, Hajj C, Weisberger E, Segal NH, Reidy-Lagunes DL, et al. Neoadjuvant chemotherapy first, followed by chemoradiation and then surgery, in the management of locally advanced rectal cancer. *J Natl Compr Canc Netw* (2014) 12 (4):513–9. doi: 10.6004/jnccn.2014.0056

52. Fokas E, Allgäuer M, Polat B, Klautke G, Grabenbauer GG, Fietkau R, et al. Randomized phase II trial of chemoradiotherapy plus induction or consolidation chemotherapy as total neoadjuvant therapy for locally advanced rectal cancer: CAO/ARO/AIO-12. *J Clin Oncol* (2019) 37(34):3212–22. doi: 10.1200/JCO.19.00308

53. Martling AL, Holm T, Rutqvist LE, Moran BJ, Heald RJ, Cedemark B. Effect of a surgical training programme on outcome of rectal cancer in the county of Stockholm. Stockholm Colorectal cancer study group, Basingstoke bowel cancer research project. *Lancet* (2000) 356(9224):93–6. doi: 10.1016/S0140-6736(00)02469-7

54. Wibe A, Syse A, Andersen E, Tretli S, Myrvold HE, Søreide O. Oncological outcomes after total mesorectal excision for cure for cancer of the lower rectum: Anterior vs. abdominoperineal resection. *Dis Colon Rectum* (2004) 47(1):48–58. doi: 10.1007/s10350-003-0012-y

55. Taylor F, Quirke P, Heald R, Moran B, Blomqvist L, Swift I, et al. Preoperative magnetic resonance imaging assessment of circumferential resection margin predicts disease-free survival and local recurrence: 5-year follow-up results of the MERCURY study. *J Clin Oncol* (2014) 32(1):34–43. doi: 10.1200/JCO.2012.45.3258

56. Patel U, Brown G, Machado I, Santos-Cores J, Pericay C, Ballesteros E, et al. MRI Assessment and outcomes in patients receiving neoadjuvant chemotherapy only for primary rectal cancer: long-term results from the GEMCAD 0801 trial. *Ann Oncol* (2017) 28(2):344–53. doi: 10.1093/annonc/mdw616

frontiers | Frontiers in Oncology

TYPE Original Research
PUBLISHED 30 March 2023
DOI 10.3389/fonc.2023.1099168

OPEN ACCESS

EDITED BY
Marco Rengo,
Sapienza University of Rome, Italy

REVIEWED BY
Simone Vicini,
Sapienza University of Rome, Italy
Gian Paolo Spinelli,
Sapienza University of Rome, Italy

*CORRESPONDENCE
Jaw-Yuan Wang
cy614112@ms14.hinet.net;
jawyuanwang@gmail.com
Hsiang-Lin Tsai
chunpin870132@yahoo.com.tw

SPECIALTY SECTION
This article was submitted to Gastrointestinal Cancers: Colorectal Cancer, a section of the journal Frontiers in Oncology

RECEIVED 13 December 2022
ACCEPTED 21 March 2023
PUBLISHED 30 March 2023

CITATION
Yin T-C, Chen P-J, Yeh Y-S, Li C-C, Chen Y-C, Su W-C, Chang T-K, Huang C-W, Huang C-M, Tsai H-L and Wang J-Y (2023) Efficacy of concurrent radiotherapy in patients with locally advanced rectal cancer and synchronous metastasis receiving systemic therapy. *Front. Oncol.* 13:1099168. doi: 10.3389/fonc.2023.1099168

Efficacy of concurrent radiotherapy in patients with locally advanced rectal cancer and synchronous metastasis receiving systemic therapy

Tzu-Chieh Yin[1,2,3], Po-Jung Chen[3], Yung-Sung Yeh[4,5,6], Ching-Chun Li[1,7], Yen-Cheng Chen[3,8], Wei-Chih Su[3,8], Tsung-Kun Chang[3,8,9], Ching-Wen Huang[3,10], Chun-Ming Huang[11,12,13,14], Hsiang-Lin Tsai[3,10]* and Jaw-Yuan Wang[3,8,10,11,15,16]*

[1]Division of General and Digestive Surgery, Department of Surgery, Kaohsiung Medical University Hospital, Kaohsiung Medical University, Kaohsiung, Taiwan, [2]Department of Surgery, Kaohsiung Municipal Tatung Hospital, Kaohsiung Medical University, Kaohsiung, Taiwan, [3]Division of Colorectal Surgery, Department of Surgery, Kaohsiung Medical University Hospital, Kaohsiung Medical University, Kaohsiung, Taiwan, [4]Division of Trauma and Surgical Critical Care, Department of Surgery, Kaohsiung Medical University Hospital, Kaohsiung Medical University, Kaohsiung, Taiwan, [5]Department of Emergency Medicine, Faculty of Post-Baccalaureate Medicine, College of Medicine, Kaohsiung Medical University, Kaohsiung, Taiwan, [6]Graduate Institute of Injury Prevention and Control, College of Public Health, Taipei Medical University, Taipei, Taiwan, [7]Department of Surgery, Kaohsiung Municipal Hsiaokang Hospital, Kaohsiung, Taiwan, [8]Graduate Institute of Clinical Medicine, College of Medicine, Kaohsiung Medical University, Kaohsiung, Taiwan, [9]Department of Surgery, Faculty of Post-Baccalaureate Medicine, College of Medicine, Kaohsiung Medical University, Kaohsiung, Taiwan, [10]Department of Surgery, Faculty of Medicine, College of Medicine, Kaohsiung Medical University, Kaohsiung, Taiwan, [11]Graduate Institute of Medicine, College of Medicine, Kaohsiung Medical University, Kaohsiung, Taiwan, [12]Department of Radiation Oncology, Kaohsiung Medical University Hospital, Kaohsiung, Taiwan, [13]Department of Radiation Oncology, Faculty of Medicine, College of Medicine, Kaohsiung Medical University, Kaohsiung, Taiwan, [14]Department of Radiation Oncology, Kaohsiung Municipal Ta-Tung Hospital, Kaohsiung Medical University, Kaohsiung, Taiwan, [15]Center for Cancer Research, Kaohsiung Medical University, Kaohsiung, Taiwan, [16]Pingtung Hospital, Ministry of Health and Welfare, Pingtung, Taiwan

Background: Neoadjuvant chemoradiotherapy followed by total mesorectal excision is the standard treatment for patients with nonmetastatic locally advanced rectal cancer (LARC). However, for patients with LARC and synchronous metastasis, the optimal treatment strategy and sequence remain inconclusive. In the present study, we evaluated the efficacy and safety of concurrent radiotherapy in patients with *de novo* metastatic rectal cancer who received chemotherapy and targeted therapy.

Methods: We retrospectively reviewed the data of 63 patients with LARC and synchronous metastasis who received intensive therapy at the study hospital between April 2015 and November 2018. The included patients were divided into two groups: RT-CT, those who received systemic chemotherapy with targeted therapy and concurrent radiotherapy (for primary rectal cancer), and CT, those who received only systemic chemotherapy with targeted therapy.

Results: Treatment response was better in the RT-CT group than in the CT group. The rate of primary tumor resection (PTR) was higher in the RT-CT group than in the CT group (71.4% and 42.9%, respectively; P = .0286). The RT-CT group exhibited considerably longer local recurrence-free survival (P = .0453) and progression-free survival (PFS; from 13.3 to 22.5 months) than did the CT group (P = .0091); however, the groups did not differ in terms of overall survival (OS; P = .49). Adverse events were almost similar between the groups, except frequent diarrhea, the prevalence of which was higher in the RT-CT group than in the CT group (59.5% and 23.8%, respectively; P = .0075).

Conclusions: In the era of biologics, radiotherapy may increase the resectability of primary rectal tumors, reducing the risk of locoregional failure and prolonging PFS. Concurrent pelvic radiotherapy may not substantially improve OS, which is indicated by metastasis. Hence, the resection of the distant metastases may be essential for improving long-term OS. To further determine the efficacy of concurrent radiotherapy, additional prospective, randomized studies must combine preoperative pelvic radiotherapy with PTR and metastectomy to treat patients with stage IV LARC.

KEYWORDS

metastatic rectal cancer, locally advanced rectal cancer, concurrent radiotherapy, primary tumor resection (PTR), systemic chemotherapy, systemic targeted therapy

Introduction

Approximately 704 000 new cases of rectal cancer are reported worldwide every year; of them, approximately 20% to 30% present with synchronous metastasis upon initial diagnosis (1). The liver and lungs are the most common sites of metastasis, and approximately 80% of the total cases of stage IV cancer are associated with unresectable metastatic tumor burden (2). Currently, neoadjuvant concurrent chemoradiotherapy (CCRT) followed by total mesorectal excision (TME) is the standard treatment for patients with nonmetastatic locally advanced rectal cancer (LARC). This approach results in pathological downstaging and ensures improved local control, longer disease-free survival (DFS), and tolerable toxicity (3–7). Short-course preoperative radiotherapy also reduces the risk of local failure in patients receiving TME (8, 9).

Owing to the advancement of chemotherapy and biologics, therapeutic outcomes in patients with metastatic colorectal cancer (mCRC) have improved (10–12). Highly aggressive treatment of metastatic diseases, particularly colon cancer with liver metastasis, with hepatic resection and various regional therapy improves mCRC and prolongs overall survival (OS) (13–16).

To the best of our knowledge, the optimal treatment strategy and sequence for patients with LARC with *de novo* metastasis have not been standardized or documented. The potential benefit of concurrent radiotherapy in this population remains unclear and may be overshadowed by the effects of multiagent systemic therapy. Thus, in the present study, we evaluated the efficacy and safety of concurrent radiotherapy in patients with stage IV LARC receiving systemic chemotherapy and targeted therapy.

Materials and methods

We retrospectively reviewed the data of 63 patients with *de novo* metastatic LARC who underwent intensive therapy at our institution between April 2015 and November 2018. Figure 1 illustrates the data collection process. This study was approved by the Institutional Review Board of Kaohsiung Medical University Hospital, Taiwan (approval number: KMUHIRB-E(II)-20220041). The inclusion criteria for patient selection were as follows: diagnosis of T3 or T4 and/or N1 or N2 rectal cancer, presence of systemic metastasis, and ongoing systemic chemotherapy. Patients with synchronous secondary cancer, histological malignancy other than adenocarcinoma, or metachronous metastasis or those receiving only postoperative chemotherapy were excluded from this study. The included patients were divided into two groups: RT-CT and CT. The RT-CT group comprised patients who received systemic chemotherapy with targeted therapy and concurrent radiotherapy (for primary rectal cancer), whereas the CT group comprised patients who received only systemic chemotherapy with targeted therapy. Treatments were selected by surgeons or radiation oncologists.

All patients underwent initial workups, which involved taking their medical history, physical examinations, laboratory examinations, carcinoembryonic antigen (CEA) testing, diagnostic colonoscopy, and chest to pelvic computer tomography for preoperative clinical staging. TNM classes were defined in accordance with the criteria outlined by the American Joint Commission on Cancer (AJCC)/International Union Against Cancer (17). Pelvic magnetic resonance imaging (MRI) was

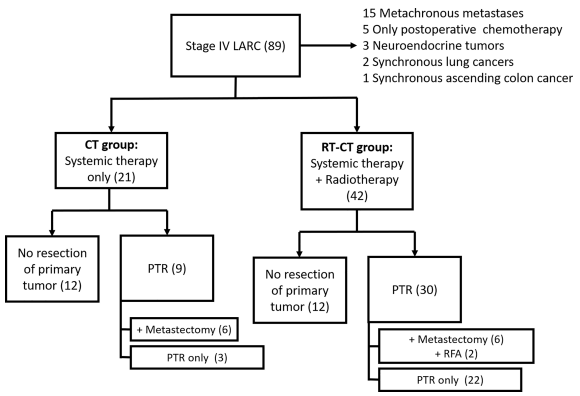

FIGURE 1
Consort Diagram of Data Collection Process. LARC, locally advanced rectal cancer; PTR, primary tumor resection; and RFA, radiofrequency ablation.

performed to evaluate the local status of the primary rectal tumor. To evaluate therapeutic response, MRI was performed again 8 to 10 weeks after pelvic radiotherapy and/or repeatedly performed every 3 months thereafter before primary tumor excision (PTR). Computed tomography was performed at 2- to 3-month intervals to evaluate the progression of distant metastasis and the patients' response to systemic therapy.

The patients received biweekly systemic therapy comprising chemotherapy with 5-fluorouracil, leucovorin, and irinotecan and targeted therapy with monoclonal antibody against vascular endothelial growth factor (anti-VEGF; bevacizumab) or epidermal growth factor receptor (anti-EGFR; cetuximab or panitumumab). *KRAS* and *NRAS* mutations were detected at diagnosis. The dose of irinotecan was in accordance of *UGT1A1* polymorphism and was reduced by 20% during the addition of concurrent radiotherapy (12, 18). The interval between the last dose of bevacizumab and elective surgery was at least 5 weeks, and bevacizumab was restarted at least 5 weeks postoperatively. Patients who underwent PTR subsequently received chemotherapy and targeted therapy. Long-course radiotherapy was concurrently administered with and at the beginning of systemic therapy in the RT-CT group in accordance with the procedure described in a previously published study (19). The total dose of radiation was 45 to 50.4 Gy (delivered in 25 to 30 fractions). Three-dimensional conformal or intensity- modulated radiation therapy was used for external-beam irradiation.

The response to systemic therapy and radiotherapy was evaluated on the basis of the Response Evaluation Criteria in Solid Tumors (RECIST) (20). Complete response (CR) was defined as the disappearance of all target lesions, whereas partial response (PR) was defined as a ≥30% decrease in the sum of the longest diameters of target lesions from the baseline value. Progressive disease (PD) was defined as a ≥20% increase in the sum of the longest diameters of target lesions from the value recorded at the initiation of treatment or the appearance of ≥1 new lesions. Stable disease (SD) was defined as neither PR nor PD.

The decision to perform surgery for PTR and the timing of surgery depended on the objective outcome of primary tumors and the control of distant metastases after neoadjuvant therapy. In all patients who underwent PTR, TME was performed through conventional laparotomy or minimally invasive surgery (MIS). The procedures were low anterior resection (LAR), intersphincteric resection (ISR), and abdominal perineal resection (APR). Colostomy was performed if the patients were at risk of total lumen obstruction or bowel rupture or when they underwent PTR and were at risk of anastomotic insufficiency (defunctioning stoma). Colostomy was taken down approximately 3 months after PTR (21). The options for liver-directed therapy were the surgical resection of liver metastases and radiofrequency ablation (RFA).

Postoperative and follow-up surveillance involved routine history taking, physical examinations, CEA testing, and CT at 3-month intervals. Annular colonoscopy was performed and positron emission tomography was executed (if needed). Local recurrence (LR) was defined as recurrence in the pelvic cavity or bowel lumen near an anastomosis. LR-free survival (LRFS) was defined as the interval between PTR and the first radiographic evidence of LR. Progression-free survival (PFS) was defined as the interval between the initiation of treatment and PD or the recurrence of distant metastasis. OS was defined as the between-diagnosis and all-cause death or final follow-up.

We collected data regarding the patients' demographics and tumor characteristics, namely age, sex, TNM stage, body mass index (BMI), tumor location (distance between a tumor's caudal margin and anal verge), tumor size, synchronous metastatic site, *RAS* mutation status, and presence of comorbidities. Data regarding treatment and response were biologics used, chemotherapy cycles, and RECIST findings for primary tumors and metastases. Perioperative data and surgical outcomes comprised the records of PTR, curative resection of metastases, site of metastectomy, procedures and methods performed for PTR, physical status based on the classification system of the American Society of Anesthesiologists, preservation of the anal sphincter, addition of defunctioning stoma, and nonclosure of stoma. Histopathological characteristics comprised the status of surgical margin; rate of R0 resection; rate of pathological CR (pCR); histological grading of differentiation; pathological stage of disease; number of harvested lymph nodes; lympho-vascular invasion (LVI), and perineural invasion. The tumor regression grade (TRG) was assessed using the guidelines of the AJCC (22).

Adverse events (AEs) associated with systemic therapy, radiotherapy, and surgical complications were evaluated using the US National Cancer Institute Common Terminology Criteria for Adverse Events (version 4.0; http://ctep.cancer.gov/reporting/ctc.html). AEs associated with systemic therapy were hematologic (e.g., anemia, leukopenia, and thrombocytopenia) and nonhematologic (e.g., nausea or vomiting, diarrhea, fatigue, mucositis, peripheral neuropathy, skin manifestations, alopecia, infection, abnormal liver function, and bowel perforation) events. AEs associated with radiotherapy primarily were radiation dermatitis. Surgical complications were defined as complications developed within 30 days after PTR.

Data were analyzed using JMP for Windows (version 16.0; SAS Institute, Cary, NC, USA). Continuous variables are presented in terms of median and interquartile region (IQR) values, and dichotomous variables are presented in terms of number and

percentage values. Between-group comparisons were performed using the $\chi 2$ test for categorical variables and Student's *t* test for quantitative variables. A *P* value of ≤.05 was considered statistically significant. Survival plots (LRFS, PFS, and OS) were constructed using the Kaplan–Meier method, and a log-rank test was used to compare the groups in terms of time-to-event distribution.

Results

A total of 89 patients were initially identified; of them, 15 had metachronous metastasis, 5 received only postoperative chemotherapy, 3 had neuroendocrine tumors, 2 had synchronous lung cancer, and 1 had synchronous ascending colon cancer (Figure 1). After the exclusion of these patients, 63 patients remained for our analysis. Of them, 42 received systemic chemotherapy with targeted therapy and concurrent radiotherapy; they constituted the RT-CT group. The remaining 21 patients received only systemic chemotherapy with targeted therapy and constituted the CT group. In the RT-CT group, 30 patients (71.4%) underwent PTR, whereas 12 received no surgery for primary rectal tumor after radiotherapy. A total of 6 patients underwent curative resection of metastases (3 underwent partial hepatectomy for liver metastases, whereas the remaining 3 underwent lobectomy for lung metastases), and 2 patients underwent RFA for liver metastases. In the CT group, 9 (42.9%) underwent PTR, whereas 12 did not. Of the 9 patients, 6 underwent staged metastectomy (2 patients underwent partial hepatectomy, whereas 4 patients underwent lung lobectomy) after PTR. The patients were followed up until their death, final follow-up, or March 2022.

Table 1 summarizes the patients' demographics and tumor characteristics. Not surprisingly, tumor location was more low-lying in the RT-CT group than in the CT group (*P* = .0011); 21.4% of the patients in the RT-CT group had a tumor location of <5 cm; this proportion was 4.8% in the CT group. *KRAS* or *NRAS* mutation was detected in 15 (35.7%) patients in the RT-CT group, which was slightly more than the proportion noted on the CT group (3 patients; 14.3%; *P* = .0904). The groups did not differ considerably in terms of age, sex, clinical stage, tumor size, BMI, *BRAF* mutation status, or the presence of comorbidities (all *P* >.05). The most frequent site of synchronous metastasis was the liver in the RT-CT group (27 patients; 64.3%), followed by the lungs. 12 (57.1%) patients in the CT group exhibited liver or lung metastasis.

In both groups, most patients received bevacizumab (Table 2). In the RT-CT group, 26 patients (61.9%) received bevacizumab, and 14 (33.3%) received cetuximab. A total of 13 (61.9%) and 7 (33.3%) patients in the CT group received bevacizumab and cetuximab, respectively. The RT-CT and CT groups received 14 (median; IQR, 9 to 16) and 12 (IQR, 9 to 13) cycles of chemotherapy, respectively. The groups did not differ substantially in terms biologics used or systemic therapy cycles (both *P* >.05). A total of 12 patients (28.6%) in the RT-CT group were at a risk of total lumen obstruction before or during treatment; loop colostomy was performed to avoid such a situation. In the CT group, 11 (52.4%) patients underwent loop colostomy. The RT-CT group exhibited no increased tendency of acute bowel obstruction after the addition of concurrent radiotherapy to their systemic therapy regimen (*P* = .0663). The response rate (CR + PR) of primary rectal tumor was significantly higher in the RT-CT group than in the CT group (73.8% and 47.6%, respectively; *P* = .0398). The disease control rate (CR + PR + SD) of distant metastases was similar between the RT-CT and CT groups (88.1% and 85.7%, respectively; *P* = .63); distant metastasis remained at-least stable during the first-line therapy in 37 patients in the RT-CT group and 18 patients in the CT group (*P* = .63).

The proportion of patients who underwent PTR was significantly higher in the RT- CT group than in the CT group (*P* = .0286; Table 3). A total of 30 (71.4%) patients in the RT-CT group underwent PTR after receiving concurrent radiotherapy with systemic therapy, whereas 9 patients (42.9%) in the CT group underwent PTR after receiving systemic therapy. In the RT-CT group, 24 (80%), 4 (13.3%), and 2 (6.7%) patients underwent LAR, ISR, and APR, respectively. All patients in the CT group received LAR. MIS was performed in 16 (53.4%) and 7 (77.8%) patients in the RT-CT and CT groups, respectively; the groups did not differ in terms of surgical method (*P* = .34). The rates of anal preservation in the RT-CT and CT groups were 93.3% and 100%, respectively. Defunctioning stoma was created during PTR performed in 13 patients (43.3%) in the RT-CT group and 1 patient (11.1%) in the CT group. This was expected because the number of patients with low-lying rectal cancer was higher in the RT-CT group than in the CT group. Metastectomy or liver-directed local therapy (RFA) was performed in 8 patients (19.1%) in the RT-CT group; of them, 3 underwent partial hepatectomy, 2 underwent RFA, and 3 underwent lung lobectomy. Curative resection of metastases was performed in 6 patients (28.6%) in the CT group; of them, 2 underwent partial hepatectomy, and 4 underwent lung lobectomy. In both groups, metastectomy was performed in a staged manner; the number patients who underwent metastectomy didn't vary significantly between the groups (*P* = .40).

Table 4 summarizes the histopathological characteristics of primary tumors. The status of resection margin in terms of distal resection margin and circumferential resection margin (CRM) was similar between the groups. A total of 2 patients in the RT-CT group and 1 patient in the CT group exhibited positive CRM. The rate of R0 resection in the RT-CT and CT groups was 93.3% and 88.9%, respectively. In the RT-CT group, 4 patients exhibited pCR (13.3%) after concurrent radiotherapy and TME; this number was 1 in the CT group (*P* = .67). TRGs 0, 1, 2, and 3 were detected in, respectively, 4 (13.3%), 7 (23.3%), 14 (46.7%), and 5 (16.7%) patients in the RT-CT group and 1 (12.5), 1 (12.5%), 3 (37.5%), and 3 (37.5) patients in the CT group (*P* = .65). After preoperative radiotherapy, tumor size markedly reduced with a median size of 2.5 cm compared with 3.5 cm without radiotherapy (*P* = .0105). Regarding pathological stages, the groups did not vary significantly in terms of ypT stage (*P* = .64). However, significant between-group differences were noted in terms of ypN stage (*P* = .0197); the proportion of patients with ypN2 stage tumor was higher in the CT group (33.3%) than in the RT-CT group (6.7%). The number of harvested lymph nodes was lower in the RT-CT group (median number, 7) than in the CT group (median number, 16; *P* = .0365).

Table 5 summarizes the AEs associated with concurrent radiotherapy and systemic therapy. Anemia was identified to be the most common hematologic AE in both the RT- CT (90.5%) and CT (95.2%) groups. In the RT-CT group, the most prevalent

TABLE 1 Demographics of patients with stage IV locally advanced rectal cancer and the characteristics of their disease in the RT-CT[1] and CT[2] groups.

	RT-CT (N = 42)	CT (N = 21)	*P*-value
Age, median (IQR)	62 (54 – 68)	58 (54 - 68)	0.69
Male (%)	27 (64.3)	12 (57.1)	0.89
BMI, median (IQR)	24.1 (22.3 – 27)	22.3 (18.8 – 25.1)	0.13
Clinical TNM stage IVa/IVb/IVc (%)	20/20/2 (47.6/47.6/4.8)	8/9/4 (38.1/42.9/19.1)	0.21
cT1/cT2/cT3/cT4 (%)	0/1/26/15 (0/2.4/61.9/35.7)	0/1/13/7 (0/4.8/61.9/33.3)	0.88
cN0/cN1/cN2 (%)	2/13/27 (4.8/31.0/64.3)	1/9/11 (4.8/42.9/52.4)	0.64
cM1a/cM1b/cM1c (%)	20/20/2 (47.6/47.6/4.8)	8/9/4 (38.1/42.9/19.1)	0.21
Tumor location			0.0011*
<5 cm	9 (21.4)	1 (4.8)	
≧5 cm, < 10 cm	17 (40.5)	2 (9.5)	
≧10 cm	11 (26.2)	16 (76.2)	
NS	5 (11.9)	2 (9.5)	
Tumor size, median (IQR)	4.7 (3.4 – 7.3)	5.4 (4.9 – 6.2)	0.56
Metastases site			–
Liver (%)	27 (64.3)	12 (57.1)	
Lung (%)	15 (35.7)	12 (57.1)	
Non-regional lymph nodes (%)	13 (31.0)	5 (23.8)	
Peritoneum (%)	2 (4.8)	4 (19)	
Spine (%)	2 (4.8)	1 (4.8)	
Adrenal gland (%)	2 (4.8)	2 (9.5)	
Abdominal wall (%)	1 (2.4)	0	
Ovary (%)	0	2 (9.5)	
Bone (%)	1 (2.4)	0	
***KRAS* or *NRAS* mutant (%)**	15 (35.7)	3 (14.3)	0.0904
***BRAF* Mutant (%)**	0	1 (4.8)	0.15
Comorbidity (%)	27 (75)	11 (68.8)	0.64
Follow up, median (IQR)	28.1 (19.8 – 36.6)	24.5 (16.1 – 32.6)	0.27

[1]Group receiving systemic chemotherapy with targeted therapy plus concurrent radiotherapy.
[2]Group receiving systemic chemotherapy with only targeted therapy.
BMI, body mass index; NS, not stated; WD, well differentiated; MD, moderately differentiated; and PD, poorly differentiated.
*$P < .05$.

nonhematologic AEs were diarrhea (25 patients; 59.5%) and fatigue (18 patients; 42.9%). In the CT group, the leading AEs were nausea/vomiting and fatigue, which were observed in 10 (47.6%) patients. In the CT group, diarrhea (any grade) was noted in only 5 (23.8%) patients, which was significantly less than in the RT-CT group ($P = .0075$). Grade III or IV AEs were not frequently detected. Leukopenia and infectious complications were prominent AEs observed in 7 (16.7%) and 5 (11.9%) patients in the RT-CT group, respectively. 3 (14.3%) patients in the CT group developed leukopenia during the treatment course. Radiation dermatitis was observed in 13 (31%) patients in the RT-CT group. Notably, spontaneous rectal perforation developed during or shortly after preoperative radiotherapy in 3 patients (7.1%), and they immediately underwent loop colostomy. Of them, only 1 underwent subsequent PTR. In patients who received concurrent radiotherapy and underwent PTR, infectious complications and postoperative anastomotic leakage were noted in 3 (10%) and 2 (6.7%) patients despite the creation of defunctioning stoma during PTR. Bevacizumab was the monoclonal antibody used in systemic therapy in all the 3 patients of spontaneous rectal perforation and 2 patients of postoperative anastomotic leakage.

The median follow-up duration was 27 (range, 6.7 to 89.2) months. The 24-month LRFS rates of the RT-CT and CT groups were 82.6% and 50%, respectively (Figure 2A). In patients with stage IV LARC who underwent PTR, LRFS was significantly better ($P = .0453$) in those who received concurrent radiotherapy than in those

TABLE 2 Comparison of between the RT-CT[1] and CT[2] groups in terms of treatment and response.

	RT-CT (N = 42)	CT (N = 21)	*P*-value
Target therapy agent			1
Anti-EGFR (%)	16 (38.1)	8 (38.1)	
Anti-VEGF (%)	26 (61.9)	13 (61.9)	
Chemotherapy cycles, median (IQR)	14 (9 – 16)	12 (9 – 13)	0.11
Stomy for lumen obstruction (%)	12 (28.6)	11 (52.4)	0.0663
Response rate of primary tumor (CR + PR) (%)	31 (73.8)	10 (47.6)	0.0398*
Disease control rate of metastases (CR + PR + SD) (%)	37 (88.1)	18 (85.7)	0.63

[1]Group receiving systemic chemotherapy with targeted therapy plus concurrent radiotherapy.
[2]Group receiving systemic chemotherapy with only targeted therapy.
EGFR, epidermal growth factor receptor; VEGF, vascular endothelial growth factor; CR, complete response; PR, partial response; and SD, stable disease.
*$P < .05$.

who did not. The median PFS of the RT-CT group was 22.5 months, which was significantly better than that of the CT group (13.3 months; $P = .0091$; Figure 2B). However, the 2 groups did not differ significantly in terms of OS (RT-CT group, 31.5 months; CT group, 30.6 months; $P = .49$; Figure 2C).

Discussion

Our findings indicate that patients with relatively low-lying rectal tumors exhibit a high tendency of receiving radiotherapy in addition to systemic therapy even in stage IV of the disease. Although the 2 groups in our study varied in terms of metastatic tumor sites and load, they exhibited similarity in terms of M stage. The addition of concurrent radiotherapy enhanced tumor response. Consistent with the findings of studies on LARC (23) and locally advanced colon cancer (24), in our study, a prolonged interval between preoperative radiotherapy and surgery did not increase the risk of disease progression; this assertion is based on the fact that the disease control rate of distant metastases was noninferior in the RT-CT group. Improved response of primary rectal tumor facilitated PTR after radiotherapy. Histopathologically, no differences were noted between the group in terms of resection margin status, pCR rate, and TRG. However, tumor shrinkage was markedly higher in the RT-CT group than in the CT group. Furthermore, lymph nodes exhibited better response after pelvic irradiation since less ypN2 was obtained in the RT-CT group than in the CT group.

We observed satisfactory local control after concurrent radiotherapy and PTR. The addition of radiotherapy to the systemic chemotherapy regimen increased the rate of 24-month LRFS. It also prolonged (from 13.3 to 22.5 months) the PFS of patients with synchronous metastasis. Few studies have reported similar findings. Concurrent radiotherapy exerted no considerable positive effects on the OS of patients with stage IV LARC. The AEs

TABLE 3 Perioperative data and surgical outcomes recorded in the RT-CT[1] and CT[2] groups.

	RT-CT (N = 42)	CT (N = 21)	*P*-value
PTR (%)	30 (71.4)	9 (42.9)	0.0286*
Curative resection of metastases (%)	8[a] (19.1)	6 (28.6)	0.40
Site of metastectomy			–
Liver (%)	5 (11.9)	2 (9.5)	
Lung (%)	3 (7.1)	4 (19.1)	
Procedures performed for PTR LAR/ISR/APR (%)	24/4/2 (80/13.3/6.7)	9/0/0 (100/0/0)	0.18
Methods of PTR Open/MIS (%)	14/16 (46.7/53.4)	2/7 (22.2/77.8)	0.34
ASA 2/3/NS (%)	15/14/1 (50/46.7/3.3)	2/6/1 (22.2/66.7/11.1)	0.27
Sphincter preservation rate (%)	28 (93.3)	9 (100)	0.30
Defunctioning stoma with PTR (%)	13 (43.3)	1 (11.1)	0.13
Non-closure of stoma (%)	17 (40.5)	6 (28.6)	0.63

[1]Group receiving systemic chemotherapy with targeted therapy plus concurrent radiotherapy.
[2]Group receiving systemic chemotherapy with only targeted therapy.
PTR, primary tumor resection; RFA, radiofrequency ablation; LAR, low anterior resection; ISR, intersphincteric resection; APR, abdominal perineal resection; MIS, minimally invasive surgery; and ASA, American Society of Anesthesiologists.
*$P < .05$.
[a]Including 2 patients who underwent radiofrequency ablation.

TABLE 4 Comparison between the RT-CT and CT groups in terms of the histopathologic characteristics of resected primary tumors.

	RT-CT (N = 30)	CT (N = 9)	*P*-value
DRM, median (IQR)	2.0 (1.4 – 2.6)	1.8 (1 – 2.2)	0.35
DRM involvement (%)	0	0	–
CRM, median (IQR)	1.5 (0.4 – 2.5)	0.9 (0.7 – 3.3)	0.98
CRM involvement (%)	2 (6.7)	1 (11.1)	0.67
R0 resection (%)	28 (93.3)	8 (88.9)	0.67
pCR (%)	4 (13.3)	1 (11.1)	0.86
TRG 0/1/2/3 (%)	4/7/14/5 (13.3/23.3/46.7/16.7)	1/1/3/3 (12.5/12.5/37.5/37.5)	0.65
Tumor size, median (IQR)	2.5 (1.7 – 3)	3.5 (2.6 – 3.7)	0.0105*
Histology WD/MD/PD/NS (%)	4/22/2/2 (13.3/73.3/6.7/6.7)	0/8/1/0 (0/88.9/11.1/0)	0.32
pT stage pT0/pT1/pT2/pT3/pT4 (%)	4/1/7/16/2 (13.3/3.3/23.3/53.3/6.7)	1/0/1/5/2 (11.1/0/11.1/55.6/22.2)	0.64
pN stage pN0/pN1/pN2 (%)	19/9/2 (63.3/30/6.7)	6/0/3 (66.7/0/33.3)	0.0197*
Number of harvested LN, median (IQR)	7 (5 – 13.2)	16 (10 – 25)	0.0365*
LVI (%)	5 (16.7)	2 (22.2)	0.73
Perineural invasion (%)	4 (13.3)	4 (44.4)	0.13

[1]Group receiving systemic chemotherapy with targeted therapy plus concurrent radiotherapy.
[2]Group receiving systemic chemotherapy with only targeted therapy.
DRM, distal resection margin; CRM, circumferential margin; pCR, pathologic complete response; TRG, tumor regression grade; NS, not stated; LN, lymph nodes; and LVI, lympho-vascular invasion.
*$P < .05$.

associated with radiotherapy and systemic therapy were generally tolerable and easily manageable. However, clinicians must consider the risks of spontaneous rectal rupture and anastomotic insufficiency in patients with stage IV LARC receiving simultaneous radiotherapy and targeted therapy, particularly with bevacizumab.

Circulatory tumor cells (CTCs) accelerate micrometastases and are associated with disease progression and survival in breast cancer (25, 26). After preoperative chemoradiotherapy, the proportion of CTCs reportedly decrease in patients with rectal cancer, delaying disease progression (27). Sun et al. revealed considerably lower proportions of CTCs in patients with LARC receiving neoadjuvant CCRT, particularly the responders (28). As expected, we discovered that PFS improved after the addition of concurrent radiotherapy to the current multimodality treatment regimen for LARC with synchronous metastasis. This improvement may also be associated with changes in systemic inflammation and immune function. The neutrophil-to-lymphocyte ratio (NLR) is an indicator of systemic inflammation and may serve as a prognostic factor for various cancers, including rectal cancer (29). A strong correlation has been reported between tumor volume in rectal cancer and NLR (30); the high value of NLR observed in patients with rectal cancer after preoperative radiotherapy has been associated with poor pathological response and survival outcomes (31, 32).

Metastectomy is a key predictor of survival in patients with rectal cancer with metastasis; R0 resection of metastases confers the largest survival benefits (33, 34). In the present study, the improvement in PFS due to additional radiotherapy did not translate to long-term survival. The discrepancy between PFS and OS could be attributed to the low number of patients who underwent curative resection of metastases; in the RT-CT group, only 6 patients underwent metastectomy for liver or lung metastases, and 2 patients underwent RFA. Therefore, the major determinators of OS may depend on the control of distant metastasis. Hence, attempt should still be made for resection of distant metastases to prolong OS.

In patients with mCRC, the precise use of targeted therapy (on the basis of patients' genetic profiles) and liver-directed therapy results in improved treatment outcomes. In this cohort, late LR become noteworthy, and radiotherapy is a reasonable option for reducing locoregional failure. However, the results in the literature are inconclusive. Kim et al. analyzed data on patients with stage IV rectal cancer with synchronous liver metastasis who underwent TME and liver-directed therapy; LR rate (LRR) was lower in patients receiving postoperative chemoradiotherapy than in those receiving only chemotherapy (35). Fossum et al. demonstrated that neoadjuvant radiotherapy markedly decreased LRR in patients with LARC with resectable liver and/or lung metastasis (36). Chang et al. revealed a trend toward relatively low LRR in patients who underwent PTR treated with postoperative CCRT (37). In their propensity score matching study, Lin et al. indicated improved survival in patients with stage IV rectal cancer when the patients had received CCRT before PTR (34). However, several other studies have reported contradictory findings. A study indicated poor treatment responses and reduced pathological downstaging rates after neoadjuvant radiotherapy in patients with stage IV rectal

TABLE 5 Adverse effects related to systemic therapy, radiotherapy, and surgical complications in the RT-CT and CT groups.

	Grade III-IV			Any grade		
	RT-CT (N = 42)	CT (N = 21)	*P*-value	RT-CT (N = 42)	CT (N = 21)	*P*-value
Hematologic toxicity						
Anemia	3 (7.1)	2 (9.5)	0.75	38 (90.5)	20 (95.2)	0.49
Leukopenia	7 (16.7)	3 (14.3)	0.81	29 (69.1)	12 (57.1)	0.35
Thrombocytopenia	0	0	–	6 (14.3)	2 (9.5)	0.58
Non-hematologic toxicity						
Nausea/vomiting	1 (2.4)	0	0.37	13 (31)	10 (47.6)	0.20
Diarrhea	3 (7.1)	1 (4.8)	0.71	25 (59.5)	5 (23.8)	0.0075*
Fatigue	0	0	–	18 (42.9)	10 (47.6)	0.72
Mucositis	0	0	–	10 (23.8)	6 (28.6)	0.68
Parasthesia	0	0	–	3 (7.1)	1 (4.8)	0.71
Rash acneiform/palmar-plantar erythema	1 (2.4)	0	0.37	8 (19.1)	3 (14.3)	0.63
Alopesia	0	0	–	4 (9.5)	4 (19.1)	0.30
Infection	5 (11.9)	1 (4.8)	0.34	5 (13.9)	5 (11.9)	0.23
Abnormal liver function	2 (4.8)	0	0.20	13 (31)	7 (33.3)	0.85
Bowel perforation	3 (7.1)	0	0.11	3 (7.1)	0	0.11
Radiation dermatitis	0	–	–	13 (31)	–	–
Surgical complications						
Anastomotic leakage	2 (6.7)	0	0.30	2 (6.7)	0	0.30
Infectious complications	2 (6.7)	1 (11.1)	0.67	3 (10)	1 (11.1)	0.92

[1]Group receiving systemic chemotherapy with targeted therapy plus concurrent radiotherapy.
[2]Group receiving systemic chemotherapy with only targeted therapy.
*$P < .05$.

cancer compared with the findings observed in those with stage II or III disease (38). An et al. reported a nonsuperior LRR in patients who underwent TME and simultaneous metastectomy of limited liver metastases after additional radiotherapy than in those who underwent surgery after only systemic therapy (39). Lee et al. demonstrated that postoperative pelvic radiotherapy improved LRFS only in patients with pT4 disease with metastasis (33). Manyam et al. suggested that preoperative radiotherapy should be avoided in patients with metastatic rectal cancer because the pathological downstaging of rectal cancer for surgical resection is at the expense of increased postoperative complications (40). Consistent with the findings of our study, many studies have reported nonsignificant long-term survival benefits in patients with metastatic rectal cancer who received neoadjuvant or adjuvant radiotherapy, including those who exhibited improved local control (33, 35–41).

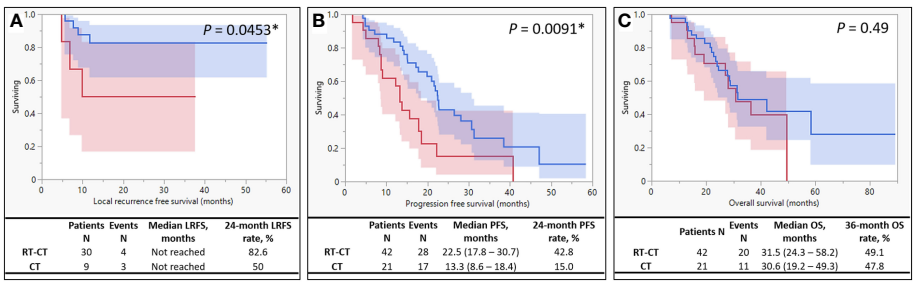

FIGURE 2
Kaplan–Meier Survival Curves. The survival curve of the RT-CT (systemic chemotherapy with targeted therapy plus pelvic radiotherapy) group is indicated by blue, and that of the CT (systemic chemotherapy with targeted therapy alone) group is indicated by red. **(A)** Local recurrence-free survival, **(B)** progression-free survival, and **(C)** overall survival.

In patients with limited liver metastasis burden and satisfactory performance status, prolonged DFS and favorable OS may be achieved after combined liver and colorectal resection (2, 42); PTR with TME should be performed in patients exhibiting good prognosis. However, the optimal management strategy for mCRC with unresectable metastasis remains debatable because of various heterogeneities. The *in-situ* retention of primary tumors in patients with mCRC rarely results in life-threatening events unless complete obstruction, intractable bleeding, or potential tumor perforation is evident. Therefore, the efficacy of PTR in unresectable metastases remains controversial. In patients with asymptomatic mCRC with unresectable metastasis, PTR may be more effective than palliative chemotherapy alone in terms of the superiority of median OS (43). A propensity score matching analysis revealed a 2-year increase in the median OS of patients who underwent PTR (44). In a population-based cohort study including more than 37 000 patients with mCRC who did not undergo metastectomy, PTR in asymptomatic patients was associated with prolonged OS and cancer-specific survival (45).

Except for the low-lying tumor location, patients of better performance status and low metastatic burden appear to be highly likely to receive a multimodality treatment including concurrent radiotherapy and PTR. However, in the present study, the considerable differences in PFS between-group were unlikely solely due to the effects of unadjusted confounders. Unlike in other studies, all the patients included in our study received biologics as part of systemic therapy; this might have controlled metastasis and highlighted the positive effects of concurrent radiotherapy on PFS.

Our study has some limitations, such as the relatively small sample size and between-group heterogeneity in terms of metastatic tumor sites and load. Nevertheless, the finding that concurrent radiotherapy may delay disease progression may help improve the management of patients with LARC with synchronous metastasis.

Conclusions

The combination of concurrent radiotherapy and systemic therapy may increase primary tumors' resectability and prolong LRFS in patients with LARC with *de novo* metastasis. Radiotherapy may also substantially improve PFS. However, the resection of distant metastases is recommended to improve OS. In the era of biologics, the combination of preoperative concurrent radiotherapy and subsequent PTR may be a promising multimodality treatment approach for patients with stage IV LARC.

Data availability statement

The raw data supporting the conclusions of this article will be made available by the authors, without undue reservation.

Ethics statement

The studies involving human participants were reviewed and approved by Institutional Review Board of Kaohsiung Medical University Hospital, Taiwan (approval number: KMUHIRB-E(II)-20220041). The patients/participants provided their written informed consent to participate in this study.

Author contributions

T-CY, being the first author of this manuscript, designed this study, analyzed the data, and wrote the manuscript. W-CS, P-JC, T-KC, Y-CC, C-CL, Y-SY, C-WH and C-MH made substantial contributions in terms of the data acquisition, interpretation and statistical analyses, in addition to assisting with the manuscript preparation. H-LT and J-YW, being the corresponding author for this manuscript, also participated in the study design and coordination, in addition to making critical revisions to the manuscript. All authors have reviewed and approved submission of the final version of the manuscript.

Funding

This work was supported by grants from the Ministry of Science and Technology (MOST109-2314-B-037-046-MY3, MOST 111-2314-B-037-070-MY3, and MOST 111-2314-B-037-049), Ministry of Health and Welfare (12D1-IVMOHW02), Health and Welfare Surcharge of Tobacco Products, Kaohsiung Municipal Tatung Hospital (KMTTH-104-023, KMTTH-111-007), Kaohsiung Medical University Hospital (KMUH111-1R31, KMUH111-1R32, KMUH111-1M28, KMUH111-1M29, KMUH111-1M31), and Kaohsiung Medical University. In addition, this study was supported by the Grant of Taiwan Precision Medicine Initiative and Taiwan Biobank, Academia Sinica, Taiwan, R.O.C.

Acknowledgments

We appreciate Kuan-Ting Lee's effort to this work.

Conflict of interest

The authors declare that the research was conducted in the absence of any commercial or financial relationships that could be construed as a potential conflict of interest.

Publisher's note

References

1. Bray F, Ferlay J, Soerjomataram I, Siegel RL, Torre LA, Jemal A. Global cancer statistics 2018: GLOBOCAN estimates of incidence and mortality worldwide for 36 cancers in 185 countries. *CA: Cancer J Clin* (2018) 68(6):394–424. doi: 10.3322/caac.21492

2. Venderbosch S, de Wilt JH, Teerenstra S, Loosveld OJ, van Bochove A, Sinnige HA, et al. Prognostic value of resection of primary tumor in patients with stage IV colorectal cancer: retrospective analysis of two randomized studies and a review of the literature. *Ann Surg Oncol* (2011) 18(12):3252–60. doi: 10.1245/s10434-011-1951-5

3. Sauer R, Becker H, Hohenberger W, Rödel C, Wittekind C, Fietkau R, et al. Preoperative versus postoperative chemoradiotherapy for rectal cancer. *N Engl J Med* (2004) 351(17):1731–40. doi: 10.1056/NEJMoa040694

4. Bosset JF, Collette L, Calais G, Mineur L, Maingon P, Radosevic-Jelic L, et al. Chemotherapy with preoperative radiotherapy in rectal cancer. *N Engl J Med* (2006) 355(11):1114–23. doi: 10.1056/NEJMoa060829

5. Sauer R, Liersch T, Merkel S, Fietkau R, Hohenberger W, Hess C, et al. Preoperative versus postoperative chemoradiotherapy for locally advanced rectal cancer: results of the German CAO/ARO/AIO-94 randomized phase III trial after a median follow-up of 11 years. *J Clin Oncol* (2012) 30(16):1926–33. doi: 10.1200/JCO.2011.40.1836

6. Guillem JG, Chessin DB, Cohen AM, Shia J, Mazumdar M, Enker W, et al. Long-term oncologic outcome following preoperative combined modality therapy and total mesorectal excision of locally advanced rectal cancer. *Ann Surg* (2005) 241(5):829–36; discussion 36-8. doi: 10.1097/01.sla.0000161980.46459.96

7. Theodoropoulos G, Wise WE, Padmanabhan A, Kerner BA, Taylor CW, Aguilar PS, et al. T-Level downstaging and complete pathologic response after preoperative chemoradiation for advanced rectal cancer result in decreased recurrence and improved disease-free survival. *Dis Colon Rectum.* (2002) 45(7):895–903. doi: 10.1007/s10350-004-6325-7

8. Sebag-Montefiore D, Stephens RJ, Steele R, Monson J, Grieve R, Khanna S, et al. Preoperative radiotherapy versus selective postoperative chemoradiotherapy in patients with rectal cancer (MRC CR07 and NCIC-CTG C016): A multicentre, randomised trial. *Lancet* (2009) 373(9666):811–20. doi: 10.1016/S0140-6736(09)60484-0

9. Kapiteijn E, Marijnen CA, Nagtegaal ID, Putter H, Steup WH, Wiggers T, et al. Preoperative radiotherapy combined with total mesorectal excision for resectable rectal cancer. *N Engl J Med* (2001) 345(9):638–46. doi: 10.1056/NEJMoa010580

10. Van Cutsem E, Köhne CH, Láng I, Folprecht G, Nowacki MP, Cascinu S, et al. Cetuximab plus irinotecan, fluorouracil, and leucovorin as first-line treatment for metastatic colorectal cancer: updated analysis of overall survival according to tumor KRAS and BRAF mutation status. *J Clin Oncol* (2011) 29(15):2011–9. doi: 10.1200/JCO.2010.33.5091

11. Kopetz S, Chang GJ, Overman MJ, Eng C, Sargent DJ, Larson DW, et al. Improved survival in metastatic colorectal cancer is associated with adoption of hepatic resection and improved chemotherapy. *J Clin Oncol* (2009) 27(22):3677–83. doi: 10.1200/JCO.2008.20.5278

12. Tsai HL, Chen YC, Yin TC, Su WC, Chen PJ, Chang TK, et al. Comparison of UGT1A1 polymorphism as guidance of irinotecan dose escalation in RAS wild-type metastatic colorectal cancer patients treated with cetuximab or bevacizumab plus FOLFIRI as the first-line therapy. *Oncol Res* (2022) 29(1):47–61. doi: 10.3727/096504022X16451187313084

13. Rees M, Tekkis PP, Welsh FK, O'Rourke T, John TG. Evaluation of long-term survival after hepatic resection for metastatic colorectal cancer: a multifactorial model of 929 patients. *Ann Surg* (2008) 247(1):125–35. doi: 10.1097/SLA.0b013e31815aa2c2

14. Ardito F, Vellone M, Cassano A, De Rose AM, Pozzo C, Coppola A, et al. Chance of cure following liver resection for initially unresectable colorectal metastases: analysis of actual 5-year survival. *J Gastrointest Surg* (2013) 17(2):352–9. doi: 10.1007/s11605-012-2103-3

15. Poultsides GA, Servais EL, Saltz LB, Patil S, Kemeny NE, Guillem JG, et al. Outcome of primary tumor in patients with synchronous stage IV colorectal cancer receiving combination chemotherapy without surgery as initial treatment. *J Clin Oncol* (2009) 27(20):3379–84. doi: 10.1200/JCO.2008.20.9817

16. Abdalla EK, Vauthey JN, Ellis LM, Ellis V, Pollock R, Broglio KR, et al. Recurrence and outcomes following hepatic resection, radiofrequency ablation, and combined resection/ablation for colorectal liver metastases. *Ann Surg* (2004) 239(6):818–25; discussion 25-7. doi: 10.1097/01.sla.0000128305.90650.71

17. Amin MB, Edge S, Greene F, Byrd DR, Brookland RK, Washington MK, et al. *AJCC cancer staging manual. 8th ed.* New York, NY: Springer (2017) p. 252–4.

18. Li CC, Chang TK, Chen YC, Tsai HL, Huang CW, Su WC, et al. Clinical outcomes of patients with peritoneal metastasis-only colorectal cancer treated with first-line bevacizumab and FOLFIRI through irinotecan dose escalation according to UGT1A1 polymorphism: Compared to liver metastasis-only, and lung metastasis-only. *Cancer Manag Res* (2022) 14:1541–9. doi: 10.2147/CMAR.S355318

19. Huang CM, Huang MY, Tsai HL, Huang CW, Ma CJ, Yeh YS, et al. An observational study of extending FOLFOX chemotherapy, lengthening the interval between radiotherapy and surgery, and enhancing pathological complete response rates in rectal cancer patients following preoperative chemoradiotherapy. *Ther Adv Gastroenterol* (2016) 9(5):702–12. doi: 10.1177/1756283X16656690

20. Therasse P, Arbuck SG, Eisenhauer EA, Wanders J, Kaplan RS, Rubinstein L, et al. New guidelines to evaluate the response to treatment in solid tumors. European organization for research and treatment of cancer, national cancer institute of the united states, national cancer institute of Canada. *J Natl Cancer Institute.* (2000) 92(3):205–16. doi: 10.1093/jnci/92.3.205

21. Yin TC, Tsai HL, Yang PF, Su WC, Ma CJ, Huang CW, et al. Early closure of defunctioning stoma increases complications related to stoma closure after concurrent chemoradiotherapy and low anterior resection in patients with rectal cancer. *World J Surg Oncol* (2017) 15(1):80. doi: 10.1186/s12957-017-1149-9

22. Edge SB, Byrd DR, Compton CC, Fritz AG, Greene FL, Trotti A3rd. *AJCC cancer staging manual. 7th ed.* New York: Springer-Verlag (2010).

23. Huang CW, Su WC, Yin TC, Chen PJ, Chang TK, Chen YC, et al. Time interval between the completion of radiotherapy and robotic-assisted surgery among patients with stage I-III rectal cancer undergoing preoperative chemoradiotherapy. *PloS One* (2020) 15(10):e0240742. doi: 10.1371/journal.pone.0240742

24. Chen YC, Tsai HL, Li CC, Huang CW, Chang TK, Su WC, et al. Critical reappraisal of neoadjuvant concurrent chemoradiotherapy for treatment of locally advanced colon cancer. *PloS One* (2021) 16(11):e0259460. doi: 10.1371/journal.pone.0259460

25. Wong NS, Kahn HJ, Zhang L, Oldfield S, Yang LY, Marks A, et al. Prognostic significance of circulating tumour cells enumerated after filtration enrichment in early and metastatic breast cancer patients. *Breast Cancer Res Treat* (2006) 99(1):63–9. doi: 10.1007/s10549-006-9181-4

26. Budd GT, Cristofanilli M, Ellis MJ, Stopeck A, Borden E, Miller MC, et al. Circulating tumor cells versus imaging–predicting overall survival in metastatic breast cancer. *Clin Cancer Res an Off J Am Assoc Cancer Res* (2006) 12(21):6403–9. doi: 10.1158/1078-0432.CCR-05-1769

27. Magni E, Botteri E, Ravenda PS, Cassatella MC, Bertani E, Chiappa A, et al. Detection of circulating tumor cells in patients with locally advanced rectal cancer undergoing neoadjuvant therapy followed by curative surgery. *Int J Colorectal Dis* (2014) 29(9):1053–9. doi: 10.1007/s00384-014-1958-z

28. Sun W, Li G, Wan J, Zhu J, Shen W, Zhang Z. Circulating tumor cells: A promising marker of predicting tumor response in rectal cancer patients receiving neoadjuvant chemo-radiation therapy. *Oncotarget* (2016) 7(43):69507–17. doi: 10.18632/oncotarget.10875

29. Huang CM, Huang MY, Tsai HL, Huang CW, Su WC, Chang TK, et al. Pretreatment neutrophil-to-Lymphocyte ratio associated with tumor recurrence and survival in patients achieving a pathological complete response following neoadjuvant chemoradiotherapy for rectal cancer. *Cancers (Basel)* (2021) 13(18):4589. doi: 10.3390/cancers13184589

30. Braun LH, Baumann D, Zwirner K, Eipper E, Hauth F, Peter A, et al. Neutrophil-to-Lymphocyte ratio in rectal cancer-novel biomarker of tumor immunogenicity during radiotherapy or confounding variable? *Int J Mol Sci* (2019) 20(10):2488. doi: 10.3390/ijms20102448

31. Ishikawa D, Nishi M, Takasu C, Kashihara H, Tokunaga T, Higashijima J, et al. The role of neutrophil-to-lymphocyte ratio on the effect of CRT for patients with rectal cancer. *In Vivo.* (2020) 34(2):863–8. doi: 10.21873/invivo.11850

32. Jeon BH, Shin US, Moon SM, Choi JI, Kim MS, Kim KH, et al. Neutrophil to lymphocyte ratio: A predictive marker for treatment outcomes in patients with rectal cancer who underwent neoadjuvant chemoradiation followed by surgery. *Ann Coloproctol.* (2019) 35(2):100–6. doi: 10.3393/ac.2018.10.01

33. Lee JH, Jo IY, Lee JH, Yoon SC, Kim YS, Choi BO, et al. The role of postoperative pelvic radiation in stage IV rectal cancer after resection of primary tumor. *Radiat Oncol J* (2012) 30(4):205–12. doi: 10.3857/roj.2012.30.4.205

34. Lin JK, Lee LK, Chen WS, Lin TC, Jiang JK, Yang SH, et al. Concurrent chemoradiotherapy followed by metastasectomy converts to survival benefit in stage IV rectum cancer. *J Gastrointest Surg* (2012) 16(10):1888–96. doi: 10.1007/s11605-012-1959-6

35. Kim JW, Kim YB, Kim NK, Min BS, Shin SJ, Ahn JB, et al. The role of adjuvant pelvic radiotherapy in rectal cancer with synchronous liver metastasis: a retrospective study. *Radiat Oncol* (2010) 5:75. doi: 10.1186/1748-717X-5-75

36. Fossum CC, Alabbad JY, Romak LB, Hallemeier CL, Haddock MG, Huebner M, et al. The role of neoadjuvant radiotherapy for locally-advanced rectal cancer with resectable synchronous metastasis. *J Gastrointest Oncol* (2017) 8(4):650–8. doi: 10.21037/jgo.2017.06.07

37. Chang CY, Kim HC, Park YS, Park JO, Choi DH, Park HC, et al. The effect of postoperative pelvic irradiation after complete resection of metastatic rectal cancer. *J Surg Oncol* (2012) 105(3):244–8. doi: 10.1002/jso.22109

38. Kim SH, Kim JH, Jung SH. Comparison of oncologic outcomes of metastatic rectal cancer patients with or without neoadjuvant chemoradiotherapy. *Int J Colorectal Dis* (2015) 30(9):1193–9. doi: 10.1007/s00384-015-2272-0

39. An HJ, Yu CS, Yun SC, Kang BW, Hong YS, Lee JL, et al. Adjuvant chemotherapy with or without pelvic radiotherapy after simultaneous surgical resection of rectal cancer with liver metastases: analysis of prognosis and patterns of recurrence. *Int J Radiat Oncol Biol Phys* (2012) 84(1):73–80. doi: 10.1016/j.ijrobp.2011.10.070

40. Manyam BV, Mallick IH, Abdel-Wahab MM, Reddy CA, Remzi FH, Kalady MF, et al. The impact of preoperative radiation therapy on locoregional recurrence in patients with stage IV rectal cancer treated with definitive surgical resection and contemporary chemotherapy. *J Gastrointest Surg* (2015) 19(9):1676–83. doi: 10.1007/s11605-015-2861-9

41. Huh JW, Kim HC, Park HC, Choi DH, Park JO, Park YS, et al. Is chemoradiotherapy beneficial for stage IV rectal cancer? *Oncology* (2015) 89(1):14–22. doi: 10.1159/000371390

42. Martin R, Paty P, Fong Y, Grace A, Cohen A, DeMatteo R, et al. Simultaneous liver and colorectal resections are safe for synchronous colorectal liver metastasis. *J Am Coll Surg* (2003) 197(2):233–41; discussion 41-2. doi: 10.1016/S1072-7515(03)00390-9

43. Huang L, Wei G, Chen N, Liu J, Wang Z, Yu Y, et al. Impact of upfront chemotherapy on the effect of primary tumour resection for asymptomatic synchronous colorectal cancer with unresectable metastases: A propensity-Score-Matched cohort analysis. *Clin Med Insights Oncol* (2022) 16:11795549221085054. doi: 10.1177/11795549221085054

44. Chen X, Hu W, Huang C, Liang W, Zhang J, Wu D, et al. Survival outcome of palliative primary tumor resection for colorectal cancer patients with synchronous liver and/or lung metastases: A retrospective cohort study in the SEER database by propensity score matching analysis. *Int J Surg* (2020) 80:135–52. doi: 10.1016/j.ijsu.2020.06.024

45. Tarantino I, Warschkow R, Worni M, Cerny T, Ulrich A, Schmied BM, et al. Prognostic relevance of palliative primary tumor removal in 37,793 metastatic colorectal cancer patients: A population-based, propensity score-adjusted trend analysis. *Ann Surg* (2015) 262(1):112–20. doi: 10.1097/SLA.0000000000000860

frontiers | Frontiers in Oncology

TYPE Original Research
PUBLISHED 31 March 2023
DOI 10.3389/fonc.2023.1125470

OPEN ACCESS

EDITED BY
Marco Rengo,
Sapienza University of Rome, Italy

REVIEWED BY
Sergey Achkasov,
Ryzhikh National Medical Research Centre of Coloproctology, Russia
Francesco Ricchetti,
Sacro Cuore Don Calabria Hospital (IRCCS), Italy

*CORRESPONDENCE
Fengpeng Wu
wfpzhj@126.com

†These authors have contributed equally to this work

‡These authors have contributed equally to this work

SPECIALTY SECTION
This article was submitted to Gastrointestinal Cancers: Colorectal Cancer, a section of the journal Frontiers in Oncology

RECEIVED 16 January 2023
ACCEPTED 21 March 2023
PUBLISHED 31 March 2023

CITATION
Zhou C, Wang K, Zhang X, Xiao Y, Yang C, Wang J, Qu F, Wang X, Liu M, Gao C, Xiao L and Wu F (2023) Assessing the predictive value of clinical factors to pathological complete response for locally advanced rectal cancer: An analysis of 124 patients.
Front. Oncol. 13:1125470.
doi: 10.3389/fonc.2023.1125470

Assessing the predictive value of clinical factors to pathological complete response for locally advanced rectal cancer: An analysis of 124 patients

Chaoxi Zhou[1†], Kanghua Wang[2,3†], Xiaoxiao Zhang[4], Yuting Xiao[3], Congrong Yang[3], Jun Wang[3], Fuyin Qu[3], Xuan Wang[3], Ming Liu[3], Chao Gao[3], Linlin Xiao[3‡] and Fengpeng Wu[3*‡]

[1]Department of General Surgery, Fourth Hospital of Hebei Medical University, Shijiazhuang, Hebei, China, [2]Department of Medical Oncology, Affiliated Hospital Of Hebei University, Baoding, China, [3]Department of Radiotherapy, Fourth Hospital of Hebei Medical University, Shijiazhuang, China, [4]Department of Radiation Oncology, Hebei Cancer Hospital Chinese Academy of Medical Sciences, Langfang, China

Purpose: To investigate the clinical factors affecting pathological complete response (pCR) after neoadjuvant chemoradiotherapy (nCRT) in locally advanced rectal cancer (LARC).

Methods: Clinical data of 124 LARC patients treated with nCRT and surgery in the fourth Hospital of Hebei Medical University from 2014 to 2019 were retrospectively analyzed. In this study, univariate analysis and logistic dichotomous multivariate regression analysis were used to study the clinical factors affecting pCR, and the receiver operator characteristic curve (ROC) analysis was used to further verify the accuracy of partial indexes in predicting pCR.

Results: Of the 124 enrolled patients, 19 patients (15.32%) achieved pCR. Univariate analysis showed that the number of cycles of consolidation chemotherapy, serum carcino-embryonic antigen (CEA) level before treatment, MRI longitudinal length of tumor, and extramural vascular invasion (EMVI) were statistically correlated with pCR. ROC analysis of the longitudinal length of tumor measured by MRI showed that the area under the curve (AUC) value, sensitivity and specificity were 0.735, 89.47% and 48.57% respectively, and the optimal cut-off value was 5.5cm. The ROC analysis showed that the AUC value, sensitivity and specificity of pCR prediction using CEA were 0.741, 63.16% and 90.48%, respectively, and the optimal cut-off value was 3.1ng/ml. Multivariate results showed that the number of cycles of consolidation chemotherapy, serum CEA level before treatment, and EMVI were independent predictors of pCR.

Conclusion: The number of cycles of consolidation chemotherapy, serum CEA level before treatment, and EMVI may be important determinants of LARC patients to reach pCR after nCRT.

KEYWORDS

locally advanced rectal cancer, neoadjuvant chemoradiotherapy, extramural vascular invasion, carcino-embryonic antigen (CEA), pathological complete response (PCR)

Introduction

Neoadjuvant chemoradiotherapy (nCRT) had the advantages of reducing local recurrence rate (LRR) and improving sphincter retention rate (1, 2). Therefore, the National Comprehensive Cancer Network (NCCN) guidelines recommended nCRT for patients with locally advanced rectal cancer (LARC) (3, 4). LARC patients have distinct individual differences in response to nCRT. About 54%-75% of patients could achieve tumor staging reduction after nCRT, and only 9%-25% could achieve pathological complete response (pCR) (5–7). Patients who achieved pCR had better prognosis, lower LRR, and lower distant metastasis rate, with a 5-year overall survival (OS) of 87.6% and a 5-year LRR of only 2.8% (8–10). At present, some studies suggested that when patients achieve clinical complete response (cCR), a "watch and wait", nonoperative (chemotherapy and/or RT) management approach may be considered to replace the total mesorectal excision (TME) in centers with experienced multidisciplinary teams (11, 12). By this management, surgery-related complications including intestinal function, urinary tract and sexual dysfunction could be avoided, thereby improving the quality of life of patients (13). Therefore, patients with pCR may be more suitable for this treatment strategy. However, patients who achieve cCR do not necessarily achieve pCR after surgery. Studies have shown that about 25% of patients with cCR are confirmed as pCR (14). At present, pCR is mainly confirmed by histopathological diagnosis of postoperative specimens. There are no accurate, reliable and non-invasive clinical predictors for pCR. Therefore, finding clinically relevant factors that predict pCR in LARC patients after nCRT may avoid unnecessary radical surgery, which has a significant meaning for individualized treatment of patients. This study aims to explore the clinical factors affecting the pCR of LARC patients after nCRT, so as to guide patients to optimize the treatment plan and predict the prognosis of patients.

Materials and methods

Patients

LARC patients who completed nCRT combined with TME surgery in the Fourth Hospital of Hebei Medical University from January 2014 to December 2019, were included in this retrospective case control study according. Patients were grouped according to tumor regression grading after nCRT.

The inclusion criteria were as follows: (1) Histopathology was confirmed rectal adenocarcinoma before neoadjuvant therapy; (2) T3-4, N0/N+, and M0 were diagnosed by imaging examination (chest CT, abdominal and pelvic MRI, PET-CT) at initial diagnosis; (3) Neoadjuvant therapy and TME surgery were completed before entering this study; (4) The mode of neoadjuvant therapy was long-course concurrent chemoradiotherapy recommended by NCCN guidelines.

The exclusion criteria were as follows: (1) Patients have other malignancies besides rectal cancer; (2) Distant metastases were found before surgery; (3) The neoadjuvant therapy was chemotherapy alone, radiotherapy alone, short-course radiotherapy (SCRT) or induction chemotherapy before radiotherapy; (4) Patients have incomplete clinical data.

All patients were treated with long-course preoperative RT by intensity-modulated radiation therapy (IMRT) using 6 MV photons. The median dose of radiotherapy was 50.4Gy (45-70Gy), including 114 cases with ≤50.4Gy and 10 cases with >50.4Gy, and the single dose was 1.8-2.0Gy. The target volume delineation and field setup were completed with reference to the ICRU Report 83 and the academic writings of Lee et al. (15). The chemotherapy regimens concurrently with irradiation were as follows: Capecitabine (82 cases), 5-FU+ calcium Leucovorin (3 cases), FOLFOX (9 cases), and XELOX (30 cases).

The collection of clinical data was approved by the ethics committee of the fourth hospital of Hebei Medical University. The data are anonymous, and the requirement for informed consent was therefore waived.

Statistical analysis

Statistical analysis was performed using SPSS software 22.0 (SPSS, Inc., Chicago, IL, USA). Chi-square test or Fisher exact test was used for univariate analysis. Logistic binary regression analysis (forward stepwise) was used for multivariate analysis to investigate the clinical factors affecting pCR, and the Hosmer-Lemeshow test was used to evaluate the goodness of fit of logistic regression model. In addition, the receiver operator characteristic curve (ROC) was used to calculate the area under the curve (AUC) to test some statistically significant variable values. In this study, $P < 0.05$ was considered statistically significant.

Results

Characteristics of patients

From January 2014 to December 2019, 203 LARC patients were found at the Fourth Hospital of Hebei Medical, of which 124 patients met the inclusion criteria of this study. The median patient age at the time of LARC diagnosis was 58 years old (30-87), including 95 males and 29 females. There were 87 patients with Dixon surgery, 34 patients with Miles surgery, and 3 patients with Hartman surgery. The anus preservation rate was 72.58%. In terms of the efficacy evaluation of nCRT, according to the tumor regression grading (AJCC 8th) standard (16), pathology experts identified 19 of 124 cases with tumor regression grading (TRG) 0, 13 with TRG 1, 78 with TRG 2, and 14 with TRG 3. In our study, patients with TRG 0-1 status were defined as good regression (GR). The main clinical characteristics of the patients were listed in Table 1.

Univariate and multivariate analysis

Univariate analysis demonstrated that the number of cycles of consolidation chemotherapy (P=0.035), CEA level before treatment (P=0.030), longitudinal length of the tumor on MRI (P=0.027), and extramural vascular invasion (EMVI) or not (P=0.014) were significantly associated with pCR (Table 1).

The significance of the Hosmer-Lemeshow goodness of fit was 0.327, indicating that the model had a good degree of fit (P>0.05). After all factors listed in Table 1 were brought into the logistic regression model as independent variables, we found that the cycle number of consolidation chemotherapy ≥1 (P=0.042), serum CEA before treatment <5ng/mL (P=0.005) and EMVI negative (P=0.045) were independent predictors of pCR and were significantly associated with higher pCR rate in LARC patients after nCRT (Table 2), and the longitudinal length of the tumor was not found to have independent predictive value, although this factor was found to have significant correlation with pCR in univariate analysis.

ROC analysis

ROC analysis of the longitudinal length of tumor measured by MRI showed that the AUC value, sensitivity and specificity were 0.735, 89.47% and 48.57% respectively, and the optimal cut-off value was 5.5cm. The ROC analysis of the correlation between CEA level before treatment and pCR showed that the AUC value, sensitivity and specificity of pCR prediction using CEA were 0.741, 63.16% and 90.48%, respectively, and the optimal cut-off value was 3.1ng/mL (Figure 1).

Discussion

Colorectal cancer is the third most common malignancy and the second leading cause of cancer death worldwide (17). LARC patients with pCR have higher local control rate, lower distant metastasis rate, and better survival (10). Whereas, there was still no reliable clinical predictor of pCR. This study enrolled 124 LARC patients, which demonstrated that the number of cycles of consolidation chemotherapy, serum CEA level before treatment, and EMVI may be important determinants of LARC patients to reach pCR after nCRT.

CEA is a glycoprotein secreted by colorectal cancer tissues and a common tumor marker of colorectal cancer. It is of great value in clinical screening, disease progression monitoring and prognosis prediction of colorectal cancer patients. At present, some studies have found that pre-treatment CEA level is still of great significance in predicting pCR (18–22). Cheong et al. (18) retrospectively studied 145 LARC patients who received nCRT and found that 92.6% patients with pCR showed pre-treatment CRT CEA levels <5 ng/mL (P<0.001). Pre-treatment CRT CEA levels were important risk factors for pCR (OR=18.71; 95%CI:4.62–129.51, P<0.001), respectively. Li et al. (19) found that the pre-treatment CEA level of patients in the pCR group was significantly lower than that of patients in the non-pCR group (3.82 ± 4.08 vs. 25.33 ± 49.41). It was a significant predictor of pCR, with AUC of 0.785 and optimal cut-off value of 3.35 ng/mL. These results indicated that the level of pre-treatment CEA may be a reasonable biomarker for predicting the pathological response of rectal cancer. However, the optimal cut-off value of pre-treatment CEA level to predict pCR is still inconsistent (19–22). In addition, contrary to the above studies, some studies did not find a correlation between CEA level and pCR (23, 24). The reasons for these divergences may be the differences in the enrolled population and the relatively small sample size of the retrospective studies. Further multi-institutional, prospective studies with a large sample size or meta-analysis studies were needed to confirm these findings.

It is well known that LARC patients who achieve pCR have a good prognosis, but only a small proportion of patients could achieve pCR after nCRT. In order to improve the tumor downstaging rate and achieve higher pCR rate, some studies have proposed total neoadjuvant therapy (TNT), which means the addition of consolidation chemotherapy after nCRT. Earlier study by Garcia-Aguilar et al. (25) proposed that nCRT followed by consolidation chemotherapy could improve pCR rate in a multi-center phase II clinical trial. This study demonstrated that the pCR rate of patients with nCRT and consolidation chemotherapy was higher than that of patients with nCRT alone (P=0.0036). Compared with the nCRT alone group, nCRT followed by 6 cycles of consolidation chemotherapy could bring a significantly higher survival advantage (OR=3.49, 95%CI 1.39-8.75; P=0.011). Liang et al. (26) found that patients in the nCRT followed by consolidation chemotherapy group had significantly higher “pCR rate + near-pCR rate” (32.8% vs. 16.25%; P=0.015), the univariate analysis and multivariate analysis found that consolidation chemotherapy was the independent predictor to achieve high “pCR rate and close to pCR rate”. In addition, the research showed that the consolidation chemotherapy was safe and feasible. There were no difference between the two groups in grade 3 to 4 toxic effects (nausea, vomiting, lower white blood cell count and anemia, etc.). Zhai et al. (27) found that the pCR rate of patients in the nCRT alone group was only 12.8%, while it was

TABLE 1 Characteristics of patients with or without pCR.

Characteristics	Patients Number	pCR	Non-pCR	*P value*
Gender				0.252
Male	95	17	78	
Female	29	2	27	
Age				0.821
30-49	33	4	29	
50-69	75	13	62	
≥70	16	2	14	
Concurrent chemotherapy regimens				0.600
Single-agent fluorouracil	85	14	71	
Oxaliplatin+platinum	39	5	34	
Radiation dose (Gy)				0.630
≤50.4	114	18	96	
>50.4	10	1	9	
Time between nCRT and surgery (week)				0.490
6≤X<8	10	0	10	
8≤X<10	36	5	31	
≥10	78	14	64	
Cycles of consolidation chemotherapy				**0.035**
0	54	4	50	
1-2	54	9	42	
>2	16	6	13	
T staging				0.273
T3	91	12	79	
T4	33	7	26	
N staging				
N0	5	0	5	0.247
N1	21	1	20	
N2	98	18	80	
Distance between tumor and anal border (cm)				0.538
<5	47	7	40	
5≤X<10	68	12	56	
10≤X<15	9	0	9	
Proportion of tumor in enteric cavity				0.097
<1/2	33	8	25	
≥1/2	91	11	80	
EMVI				**0.014**
No	84	18	66	
Yes	40	1	39	
CEA level (ng/mL)				**0.030**
<5	59	15	44	
5≤X<10	24	1	23	
10≤X<20	18	2	16	
≥20	23	1	22	
CA199 level (U/mL)				0.568
<30	100	14	86	
30≤X<60	11	2	9	
≥60	13	3	10	
NLR				0.399
<3	93	14	79	
3≤X<5	25	3	22	
≥5	6	2	4	
PLR				0.477
≤150	68	9	59	
>150	56	10	46	
Length (cm)				**0.027**
<5	50	12	38	
≥5	74	7	67	
The largest thickness (cm)				0.525
<1	10	1	9	
1≤X<2	81	11	70	
≥2	33	7	26	
Pathological type				0.716
mucinous adenocarcinoma	9	1	8	
non-mucinous adenocarcinoma	115	18	97	

pCR, pathological complete response; nCRT, neoadjuvant chemoradiotherapy; EMVI, extramural venous invasion; CEA, carcino-embryonic antigen; NLR, neutrophil to lymphocyte ratio; PLR, platelet-to-lymphocyte ratio. Bolded value means P value < 0.05.

32.7% in the nCRT followed by 3 cycles of XELOX consolidation chemotherapy. Although consolidation chemotherapy improved the pCR rate of patients, the rate of grade 3-4 adverse reactions did not increase. The univariate analysis showed that consolidation chemotherapy was an independent predictor of pCR.

Although some studies showed that the TNT regimen could improve pCR rate, some studies still presented different opinions. A phase II clinical trial of KCSG CO 14-03 by Kim et al. (28) showed

TABLE 2 Logistic multivariate analysis of pCR in LARC patients after nCRT.

Characteristics	OR (95% CI)	P value
Cycle number of consolidation chemotherapy	2.362 (1.031-5.41)	0.042
CEA level(ng/mL)	0.388 (0.199-0.754)	0.005
EMVI or not	0.115 (0.014-0.952)	0.045

pCR, pathological complete response; LARC, locally advanced rectal cancer; nCRT, neoadjuvant chemoradiotherapy; CEA, carcino-embryonic antigen; EMVI, extramural venous invasion.

that the pCR rate of patients in the nCRT group alone was 5.8%, while the pCR rate of patients in the nCRT followed by 2 cycles of XELOX consolidation chemotherapy group was 13.6%. Although the pCR rate of patients in the consolidation chemotherapy group was slightly higher than that of patients in the non-consolidation chemotherapy group, the difference was not statistically significant. Moore et al. analyzed 49 LARC patients and showed that the pCR rate of patients in the nCRT followed by consolidation chemotherapy group was 16%, while that in the nCRT alone group was as high as 25% (29). Therefore, the researcher thought that consolidation chemotherapy was not helpful to improve the pCR rate of patients.

So, could consolidation chemotherapy improve the pCR rate in patients? There were two meta-analysis studies. The study of Riesco-Martinez et al. showed that the pCR rate of patients in the consolidation chemotherapy group was significantly higher than that in the non-consolidation chemotherapy group (22.9% vs 13.2%, P<0.001) (30). In addition, no significant increase in grade 3-4 toxicity was observed in consolidation chemotherapy regimens. The study of Petrelli et al. showed that the addition of TNT treatment with induction chemotherapy and/or consolidation chemotherapy could improve the pCR rate of patients, and the toxicity of TNT regimen was comparable to that of standard treatment regimen (31). These studies suggest that consolidation chemotherapy may be helpful and safe to improve the pCR rate of patients.

EMVI refers to the presence of tumor cells in the blood vessels outside the muscularis propria (32). The characteristics of EMVI on MRI are that tumor signals exist in the vascular structure, blood vessels dilate or tumor infiltrates beyond the vascular wall and destroys the vascular boundary (32, 33). EMVI was associated with a higher risk of distant metastasis and poor prognosis (34, 35). In addition, EMVI was an independent predictor of higher recurrence risk in LARC patients after nCRT (36). At present, there were few studies on EMVI in predicting responsiveness to nCRT in LARC patients with different conclusions. A study of 649 LARC patients undergoing nCRT by the European Colorectal Cancer Association showed that the pCR rate and partial response rate of EMVI positive patients were lower than those of EMVI negative patients (7.5% vs 86.6%, 6.9% vs 83.3%), but the difference was not statistically significant (37). Hammarstrom et al. (38) showed that among patients in the short-course radiotherapy group, the cCR rate of EMVI negative patients was significantly higher than that of EMVI positive patients (11% vs 0%, P=0.017). While in the nCRT group and short-course radiotherapy followed by consolidation chemotherapy group, the cCR rate in EMVI negative patients was comparable to that in EMVI positive patients (16% vs. 18%, 29% vs. 23%). So, researchers suggested that EMVI positive may only be a predictor of poor sensitivity to radiotherapy. Sun et al. (39) analyzed the value of EMVI on the response to nCRT in patients with stage T3. The study showed that the good response rate of EMVI negative patients was about twice that of EMVI positive patients. Multivariate analysis showed that EMVI negative was an independent predictor of good response to rectal cancer. This study showed that the pCR rate of EMVI negative patients was significantly higher than that of EMVI positive patients (21.4% vs

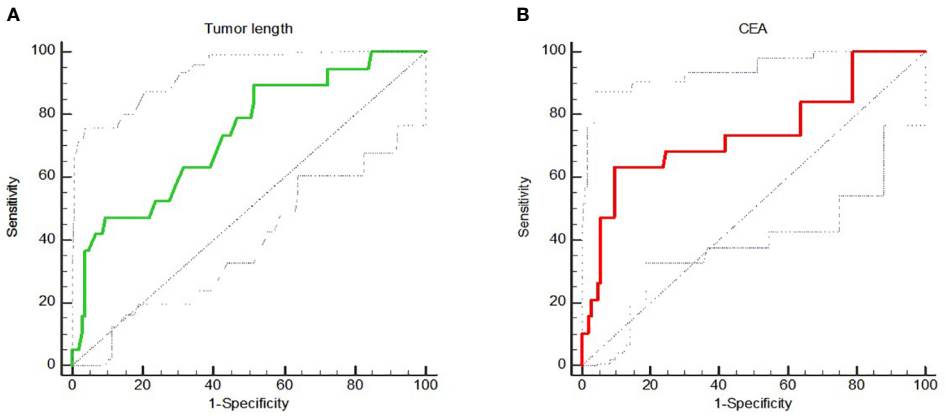

FIGURE 1
(A) showed the ROC analysis of correlation between longitudinal length of tumor measured by MRI and pCR; **(B)** showed the ROC analysis of correlation between CEA level and pCR.

2.5%, P=0.014). Multivariate analysis showed that EMVI negative was an independent predictor of pCR. In conclusion, studies using EMVI to predict the nCRT sensitivity are rare and controversial in LARC patients, further studies are needed to confirm the accuracy of this finding.

Tumor diameter or longitudinal length, which reflect tumor size, may be another clinical factor affecting pCR achievement in LARC patients. Garland et al. (23) studied 297 LARC patients who received nCRT and found that patients with smaller tumors were more likely to achieve pCR (5.0 ± 2.0cm vs. 6.0 ± 2.0, P = 0.008). Multivariate analysis showed that tumor size under endoscopy was an independent predictor of pCR. However, when the analysis was stratified by tumor size of <3.5cm, 3.5-7cm and >7 cm, the results showed that there was no correlation between tumor size and pCR (P=0.094). Park et al. (40) studied 249 LARC patients, and the univariate analysis showed that the proportion of pCR rate in patients with tumor size ≤4cm was significantly higher (37.61% vs. 18.40%, P=0.001), but multivariate analysis showed that tumor size was not a predictor of pCR. In the study of Lee et al. (41), the cut-off value of tumor size was set as 5cm, which was consistent with Park et al. (40), and only the results of univariate analysis showed that tumor size was correlated with pCR. Univariate analysis by Russo et al. (42) showed that patients with smaller tumors were more likely to achieve pCR, but the study did not provide cut-off value for grouping and conduct multivariate analysis to further confirm the accuracy of this conclusion. In this study, univariate analysis showed that patients with longitudinal tumor length <5cm were more likely to achieve pCR than those with longitudinal tumor length ≥5cm (24.00% vs. 9.46%, P=0.027). ROC analysis showed that the AUC value, sensitivity and specificity were 0.735, 89.47% and 48.57% respectively, and the optimal cut-off value was 5.5cm. However, multivariate analysis did not show statistical significance. To sum up, the conclusions of various studies are different, and it is not certain whether tumor size is the factor affecting the pCR achievement of LARC patients. In addition, the cut-off value of tumor size classification may also be an important factor affecting the results, which should be fully paid attention to in future studies.

As we all know, radiotherapy plays a major role in the neoadjuvant treatment of LARC patients. Although the recommended irradiation dose for LARC patients is 45Gy/25F to PTV and 50.4Gy/28F to CTV-H according to NCCN guidelines, there is still controversy about whether further increase of radiotherapy dose can improve the tumor regression. Appelt et al. performed 60Gy external irradiation sequential 5Gy brachytherapy boost on 51 patients with T2-3/N0-1, and found that 40 cases (78.4%) obtained cCR and entered "Watch & Wait" (43). Another prospective study compared the tumor regression of LARC patients receiving 50.4Gy and 60Gy, and found that increased dose did not significantly improve the pCR of patients, but the downstaging and shrinking of primary tumors were more significant in high-dose group of T3 patients (p=0.049), although there was no significant difference in the pathological reaction of lymph nodes between the two groups (44). In our study, the dose of enrolled patients ranged from 45Gy to 70Gy, and the results showed that only 1 out of 10 patients with a dose greater than 50.4Gy obtained pCR, and the tumor regression status of the patients might not benefit from high dose irradiation.

In this retrospective study, considering the reality of low pCR in patients receiving SCRT, we only analyzed patients with long-course nCRT. In addition, since some patients did not undergo genetic testing, the status of RAS, BRAF and MMR was not included, and only the general characteristics and those significant factors mentioned in other studies were analyzed, which might lead to some potential confounders to interfere with our results. We will pay attention to the above limitations and avoid them as much as possible in the design of future prospective studies.

In conclusion, this study demonstrated that the number of cycles of consolidation chemotherapy, serum CEA level before treatment, and EMVI may be important determinants of LARC patients to reach pCR after nCRT. Whereas, this is a retrospective study with small sample. Further multi-institutional, prospective studies with a large sample size or meta-analysis studies are needed to confirm these findings.

Data availability statement

The datasets presented in this study can be found in online repositories. The names of the repository/repositories and accession number(s) can be found in the article/Supplementary Material.

Ethics statement

The studies involving human participants were reviewed and approved by the fourth hospital of Hebei Medical University. Written informed consent for participation was not required for this study in accordance with the national legislation and the institutional requirements.

Author contributions

Conceived and designed the study: FW and LX. Performed the study and analyzed the data: KW, XZ, CY, LX, FQ, JW, XW, CG, and ML. Wrote the paper: KW, LX, CZ, FW, and YX. Supervised the entire study and review the final paper: FW, CZ, LX, and KW. All authors contributed to the article and approved the submitted version.

Funding

This study was funded by the Hebei Provincial Department of Bureau of Science and Technology (22377733D).

Conflict of interest

The authors declare that the research was conducted in the absence of any commercial or financial relationships that could be construed as a potential conflict of interest.

Publisher's note

All claims expressed in this article are solely those of the authors and do not necessarily represent those of their affiliated organizations, or those of the publisher, the editors and the reviewers. Any product that may be evaluated in this article, or claim that may be made by its manufacturer, is not guaranteed or endorsed by the publisher.

Supplementary material

The Supplementary Material for this article can be found online at: https://www.frontiersin.org/articles/10.3389/fonc.2023.1125470/full#supplementary-material

References

1. Benson AB 3rd, Venook AP, Bekaii-Saab T, Chan E, Chen YJ, Cooper HS, et al. Rectal cancer, version 2.2015. *J Natl Compr Canc Netw* (2015) 13(6):719–28. doi: 10.6004/jnccn.2015.0087

2. Sauer R, Liersch T, Merkel S, Fietkau R, Hohenberger W, Hess C, et al. Preoperative versus postoperative chemoradiotherapy for locally advanced rectal cancer: Results of the German CAO/ARO/AIO-94 randomized phase III trial after a median follow-up of 11 years. *J Clin Oncol* (2012) 30(16):1926–33. doi: 10.1200/JCO.2011.40.1836

3. Yang KL, Yang SH, Liang WY, Kuo YJ, Lin JK, Lin TC, et al. Carcinoembryonic antigen (CEA) level, CEA ratio, and treatment outcome of rectal cancer patients receiving pre-operative chemoradiation and surgery. *Radiat Oncol* (2013) 8:43. doi: 10.1186/1748-717X-8-43

4. Tan Y, Fu D, Li D, Kong X, Jiang K, Chen L, et al. Predictors and risk factors of pathologic complete response following neoadjuvant chemoradiotherapy for rectal cancer: A population-based analysis. *Front Oncol* (2019) 9:497. doi: 10.3389/fonc.2019.00497

5. Fernandez-Martos C, Aparicio J, Bosch C, Torregrosa M, Campos JM, Garcera S, et al. Preoperative uracil, teg -afur, and concomitant radiotherapy in operable rectal cancer: A phase II multicenter study with 3 years' follow-up. *J Clin Oncol* (2004) 22 (15):3016–22. doi: 10.1200/JCO.2004.11.124

6. Kim YH, Kim DY, Kim TH, Jung KH, Chang HJ, Jeong SY, et al. Usefulness of magnetic resonance volumetric evaluation in predicting response to preoperative concurrent chemoradiotherapy in patients with resectable rectal cancer. *Int J Radiat Oncol Biol Phys* (2005) 62(3):761–8. doi: 10.1016/j.ijrobp.2004.11.005

7. Edge SB, Compton CC. The American joint committee on cancer: the 7th edition of the AJCC cancer staging manual and the future of TNM. *Ann Surg Oncol* (2010) 17 (6):1471–4. doi: 10.1245/s10434-010-0985-4

8. Maas M, Nelemans PJ, Valentini V, Das P, Rödel C, Kuo LJ, et al. Long-term outcome in patients with a pathological complete response after chemoradiation for rectal cancer: A pooled analysis of individual patient data. *Lancet Oncol* (2010) 11 (9):835–44. doi: 10.1016/S1470-2045(10)70172-8

9. Rödel C, Martus P, Papadoupolos T, Füzesi L, Klimpfinger M, Fietkau R, et al. Prognostic significance of tumor regression after preoperative chemoradiotherapy for rectal cancer. *J Clin Oncol* (2005) 23(34):8688–96. doi: 10.1200/JCO.2005.02.1329

10. Martin ST, Heneghan HM, Winter DC. Systematic review and meta-analysis of outcomes following pathological complete response to neoadjuvant chemoradiotherapy for rectal cancer. *Br J Surg* (2012) 99(7):918–28. doi: 10.1002/bjs.8702

11. Habr-Gama A, Perez RO, Nadalin W, Sabbaga J, Ribeiro U Jr, Silva e Sousa AH Jr, et al. Operative versus nonoperative treatment for stage 0 distal rectal cancer following chemoradiation therapy: Long-term results. *Ann Surg* (2004) 240(4):711–7. doi: 10.1097/01.sla.0000141194.27992.32

12. Yang TJ, Goodman KA. Predicting complete response: is there a role for non-operative management of rectal cancer? *J Gastrointest Oncol* (2015) 6(2):241–6. doi: 10.3978/j.issn.2078-6891.2014.110

13. Habr-Gama A, Perez RO, Nadalin W, Sabbaga J, Ribeiro U Jr, Silva E, Sousa AH Jr, et al. High 1-year complication rate after anterior resection for rectal cancer. *J Gastrointest Surg* (2014) 18(4):831–8. doi: 10.1007/s11605-013-2381-4

14. Hiotis SP, Weber SM, Cohen AM, Minsky BD, Paty PB, Guillem JG, et al. Assessing the predictive value of clinical complete response to neoadjuvant therapy for rectal cancer:an analysis of 488 patients. *J Am Coll Surg* (2002) 194(2):131–5. doi: 10.1016/S1072-7515(01)01159-0

15. Nancy YL, Jiade JL. *Target volume delineation and field setup: A practical guide for conformal and intensity-modulated radiation therapy*. Berlin, Heidelberg: Springer-Verlag (2013) p. 161–8. doi: 10.1007/978-3-642-28860-9

16. Weiser MR. AJCC 8th edition: Colorectal cancer. *Ann Surg Oncol* (2018) 25 (6):1454–5. doi: 10.1245/s10434-018-6462-1

17. Cao W, Chen HD, Yu YW, Li N, Chen WQ. Changing profiles of cancer burden worldwide and in China: A secondary analysis of the global cancer statistics 2020. *Chin Med J (Engl)* (2020) 134(7):783–91. doi: 10.1097/CM9.0000000000001474

18. Cheong C, Shin JS, Suh KW. Prognostic value of changes in serum carcinoembryonic antigen levels for preoperative chemoradiotherapy response in locally advanced rectal cancer. *World J Gastroenterol* (2020) 26(44):7022–35. doi: 10.3748/wjg.v26.i44.7022

19. Li A, He K, Guo D, Liu C, Wang D, Mu X, et al. Pretreatment blood biomarkers predict pathologic responses to neo-CRT in patients with locally advanced rectal cancer. *Future Oncol* (2019) 15(28):3233–42. doi: 10.2217/fon-2019-0389

20. Das P, Skibber JM, Rodriguez-Bigas MA, Feig BW, Chang GJ, Wolff RA, et al. Predictors of tumor response and downstaging in patients who receive preoperative chemoradiation for rectal cancer. *Cancer* (2007) 109(9):1750–5. doi: 10.1002/cncr.22625

21. Peng H, Wang C, Xiao W, Lin X, You K, Dong J, et al. Analysis of clinical characteristics to predict pathologic complete response for patients with locally advanced rectal cancer treated with neoadjuvant chemoradiotherapy. *J Cancer* (2018) 9(15):2687–92. doi: 10.7150/jca.25493

22. Motta R, Ybazeta P, Cordova O. Predictive factors of complete pathological response in operated patients with locally advanced rectal cancer after chemoradiotherapy neoadjuvant treatment in Peru. *Ann Oncol* (2018) 29(Suppl 5): v84. doi: 10.1093/annonc/mdy151.298

23. Garland ML, Vather R, Bunkley N, Pearse M, Bissett IP. Clinical tumour size and nodal status predict pathologic complete response following neoadjuvant chem oradiotherapy for rectal cancer. *Int J Colorectal Dis* (2014) 29(3):301–7. doi: 10.1007/s00384-013-1821-7

24. Wu F, Wang J, Yang C, Zhou C, Niu W, Zhang J, et al. Volumetric imaging parameters are significant for predicting the pathological complete response of pr eoperative concurrent chemoradiotherapy in local advanced rectal cancer. *J Radiat Res* (2019) 60(5):666–76. doi: 10.1093/jrr/rrz035

25. Garcia-Aguilar J, Chow OS, Smith DD, Marcet JE, Cataldo PA, Varma MG, et al. Effect of adding mFOLFOX6 after neoadjuvant chemoradiation in locally advanced rectal cancer: A multicentre, phase 2 trial. *Lancet Oncol* (2015) 16(8):957–66. doi: 10.1016/S1470-2045(15)00004-2

26. Liang HQ, Dong ZY, Liu ZJ, Luo J, Zeng Q, Liao PY, et al. Efficacy and safety of consolidation chemotherapy during the resting period in patients with local advanced rectal cancer. *Oncol Lett* (2019) 17(2):1655–63. doi: 10.3892/ol.2018.9804

27. Zhai Z, Zhang K, Wang C, Zhang T, Wang L, Yao J, et al. Adding three cycles of CAPOX after neoadjuvant chemoradiotherapy increases the rates of complete response for locally advanced rectal cancer. *Curr Oncol* (2021) 28(1):283–93. doi: 10.3390/curroncol28010033

28. Kim SY, Joo J, Kim TW, Hong YS, Kim JE, Hwang IG, et al. A randomized phase 2 trial of consolidation chemotherapy after preoperative chemoradiation therapy versus chemoradiation therapy alone for locally advanced rectal cancer: KCSG CO 14-03. *Int J Radiat Oncol Biol Phys* (2018) 101(4):889–99. doi: 10.1016/j.ijrobp.2018.04.013

29. Moore J, Price T, Carruthers S, Selva-Nayagam S, Luck A, Thomas M, et al. Prospective randomized trial of neoadjuvant chemotherapy during the 'wait period' following preoperative chemoradiotherapy for rectal cancer: Results of the WAIT trial. *Colorectal Dis* (2017) 19(11):973–9. doi: 10.1111/codi.13724

30. Riesco-Martinez MC, Fernandez-Martos C, Gravalos-Castro C, Espinosa-Olarte P, La Salvia A, Robles-Diaz L, et al. Impact of total neoadjuvant therapy vs. standard chemorad-iotherapy in locally advanced rectal cancer: A systematic review and meta-analysis of randomized trials. *Cancers (Basel)* (2020) 12(12):3655. doi: 10.3390/cancers12123655

31. Petrelli F, Trevisan F, Cabiddu M, Sgroi G, Bruschieri L, Rausa E, et al. Total neoadjuvant therapy in rectal smith NJ, shihab O, arnaout a, et al. MRI for detection of extramural vascular invasion in rectal cancer. *AJR Am J Roentgenol* (2008) 191 (5):1517–22. doi: 10.1097/SLA.0000000000003471

32. Smith NJ, Shihab O, Arnaout A, Swift RI, Brown G. MRI For detection of extramural vascular invasion in rectal cancer. *AJR Am J Roentgenol* (2008) 191 (5):1517–22. doi: 10.2214/AJR.08.1298

33. Smith NJ, Barbachano Y, Norman AR, Swift RI, Abulafi AM, Brown G. Prognostic significance of magnetic resonance imaging-detected extramural vascular invasion in rectal cancer. *Br J Surg* (2008) 95(2):229–36. doi: 10.1002/bjs.5917

34. van den Broek JJ, van der Wolf FSW, Heijnen LA, Schreurs WH. The prognostic importance of MRI detected extramural vascular invasion (mrEMVI) in locally advanced rectal cancer. *Int J Colorectal Dis* (2020) 35(10):1849–54. doi: 10.1007/s00384-020-03632-9

35. Chand M, Bhangu A, Wotherspoon A, Stamp GWH, Swift RI, Chau I, et al. EMVI-positive stage II rectal cancer has similar clinical outcomes as stage III disease following pre-operative chemoradiotherapy. *Ann Oncol* (2014) 25(4):858–63. doi: 10.1093/annonc/mdu029

36. Prampolini F, Taschini S, Pecchi A, Sani F, Spallanzani A, Gelsomino F, et al. Magnetic resonance imaging performed before and after preoperative chemoradiotherapy in rectal cancer: predictive factors of recurrence and prognostic significance of MR-detected extramural venous invasion. *Abdom Radiol (NY)* (2020) 45 (10):2941–9. doi: 10.1007/s00261-018-1838-z

37. 2017 European Society of Coloproctology (ESCP) Collaborating Group. Evaluating the incidence of pathological complete response in current international rectal cancer practice: the barriers to widespread safe deferral of surgery. *Colorectal Dis* (2018) 20(Suppl 6):58–68. doi: 10.1111/codi.14361

38. Hammarström K, Imam I, Mezheyeuski A, Ekström J, Sjöblom T, Glimelius B. A comprehensive evaluation of associations between routinely collected staging information and the response to (Chemo)Radiotherapy in rectal cancer. *Cancers (Basel)* (2020) 13(1):16. doi: 10.3390/cancers13010016

39. Sun Y, Li J, Shen L, Wang X, Tong T, Gu Y. Predictive value of MRI-detected extramural vascular invasion in stage T3 rectal cancer patients before neoadjuvant chemoradiation. *Diagn Interv Radiol* (2018) 24(3):128–34. doi: 10.5152/dir.2018.17286

40. Park CH, Kim HC, Cho YB, Yun SH, Lee WY, Park YS, et al. Predicting tumor response after preoperative chemoradiation using clinical parameters in rectal cancer. *World J Gastroenterol* (2011) 17(48):5310–6. doi: 10.3748/wjg.v17.i48.5310

41. Lee SY, Kim CH, Kim YJ, Kwak HD, Ju JK, Kim HR. Obesity as an independent predictive factor for pathologic complete response after neoadjuvant chemor adiation in rectal cancer. *Ann Surg Treat Res* (2019) 96(3):116–22. doi: 10.4174/astr.2019.96.3.116

42. Russo AL, Ryan DP, Borger DR, Wo JY, Szymonifka J, Liang WY, et al. Mutational and clinical predictors of pathologic complete response in the treatment of locally advanced rectal cancer. *J Gastrointest Cancer* (2014) 45(1):34–9. doi: 10.1007/s12029-013-9546-y

43. Appelt AL, Pløen J, Harling H, Jensen FS, Jensen LH, Jørgensen JC, et al. High-dose chemoradiotherapy and watchful waiting for distal rectal cancer: A prospective observational study. *Lancet Oncol* (2015) 16(8):919–27. doi: 10.1016/S1470-2045(15)00120-5

44. Bertocchi E, Barugola G, Nicosia L, Mazzola R, Ricchetti F, Dell'Abate P, et al. A comparative analysis between radiation dose intensification and conventional fractionation in neoadjuvant locally advanced rectal cancer: A monocentric prospective observational study. *Radiol Med* (2020) 125(10):990–8. doi: 10.1007/s11547-020-01189-9

frontiers | Frontiers in Oncology

TYPE Original Research
PUBLISHED 03 April 2023
DOI 10.3389/fonc.2023.1138299

OPEN ACCESS

EDITED BY
Marco Rengo,
Sapienza University of Rome, Italy

REVIEWED BY
Cibele Masotti,
Hospital Sirio Libanes, Brazil
Susannah Ellsworth,
University of Pittsburgh, United States

*CORRESPONDENCE
Tarek Taha
t_taha@rambam.gov.il

SPECIALTY SECTION
This article was submitted to Gastrointestinal Cancers: Colorectal Cancer, a section of the journal Frontiers in Oncology

RECEIVED 05 January 2023
ACCEPTED 21 March 2023
PUBLISHED 03 April 2023

CITATION
Lutsyk M, Taha T and Billan S (2023) Can lymphocytes serve as a predictor of response to preoperative chemoradiation therapy for locally advanced rectal cancer?. *Front. Oncol.* 13:1138299.
doi: 10.3389/fonc.2023.1138299

Can lymphocytes serve as a predictor of response to preoperative chemoradiation therapy for locally advanced rectal cancer?

Myroslav Lutsyk[1], Tarek Taha[2*] and Salem Billan[3]

[1]Ha'Emek Medical Center, Afula, Israel, [2]The Baruch Padeh Medical Center, Poriya, Poriah, Israel, [3]Rambam Health Care Campus, Haifa, Israel

Introduction: The aim of this study is to identify factors that may predict the response of locally advanced rectal cancer tumors (LARC) to neoadjuvant chemoradiotherapy (CRT) and to evaluate the effect of circulating lymphocytes on pathological tumor response.

Methods: This retrospective study included neoadjuvant CRT-treated, LARC-diagnosed patients at the Rambam Health Care Campus in Haifa, Israel. CHAID analysis, t-test, χ^2 test, and ROC curve analyses were performed to explore the association between pathological complete response (pCR) and several factors including patient demographics, tumor characteristics, type of treatment, and levels of circulating lymphocytes measured on a weekly basis.

Results: Out of 198 patients enrolled in the study, pCR was achieved in 50 patients (25%). ROC curve and CHAID analyses showed that absolute lymphopenia was significantly associated with lower pCR rates (p=0.046 and p=0.001, respectively). Other factors that were found to have a significant impact were radiation therapy type (p=0.033) and tumor distance from the anal verge (p= 0.041).

Conclusion: An absolute decrease in the level of circulating lymphocytes during preoperative CRT to LARC is associated with poorer tumor response to treatment and thus may serve as a predictive biomarker for treatment resistance.

KEYWORDS

lymphopenia, neoadjuvant chemo(radio)therapy, pathological complete response (pCR), tumor response, rectal adenocarcinoma

Introduction

Rectal cancer is the seventh most common cancer in the world accounting for 730,000 new cases per year (1). The incidence is higher in men and more common in adults with the average age at diagnosis being 63 years (2). The disease is associated with the Western lifestyle and its incidence is greater in developed countries. Mortality rates, however, are

higher in developing countries, which may reflect the limited health infrastructures in those nations and demonstrate the impact of treatment on survival and life expectancy. By 2030, the global burden of colorectal cancer is expected to rise by 60%, when estimates suggest there will be 2.2 million new cases and 1.1 million deaths (3).

Treatment for rectal adenocarcinoma is determined by the clinical stage of the disease and the location of the tumor in the rectum. In its earliest stages, the standard treatment is local excision, which can be sufficient, without removal of lymph nodes or any further action. The objective is tumor removal with free resection margins that minimizes the chances of local recurrence, which are considered relatively high due to the cancer's anatomical location in the pelvis and its proximity to other organs and structures (4).

According to guidelines issued by the National Comprehensive Cancer Network (NCCN), the American Society of Clinical Oncology (ASCO), and the European Society for Medical Oncology (ESMO) (5–7), the standard of care for locally advanced disease (stages II-III (cT3-4N0 or cTxN1-2)) is the provision of preoperative CRT and radical resection of the rectum – total mesorectal excision (TME). The main surgical approaches to the treatment of tumors at these stages are low anterior resection (LAR), which includes the preservation of sphincters, or abdominoperineal resection (APR) in lower positioned tumors, located within 6 cm from the anal verge, which do not allow preservation of the anus and sphincters (8).

Prior to surgery, neoadjuvant radiation therapy can be given as a short course (total dose of 25Gy using 5Gy fractions for 5 days) or as a long course (total dose of 50-54Gy using 1.8-2.0Gy fractions for 5 weeks), in conjunction with 5-fluorouracil-based chemotherapy or capecitabine, as studies have shown that the addition of chemotherapy significantly improves local control rates (9, 10). The surgery may be performed immediately or 6-8 weeks after neoadjuvant treatment ends.

The goal of neoadjuvant therapy is to reduce the size of the tumor (downgrading) and/or to reduce the stage of the disease (downstaging) to allow more efficient resection with free margins, thus lowering the chances of local recurrence (11, 12). Treatment can lead to downstaging in 50-60% of patients and even pathological complete response (pCR) in 10-20% of cases (13). pCR is defined as the absence of tumor cells in the rectum or lymph nodes and their replacement by fibrotic tissue as observed microscopically in the surgical sample obtained during the surgery (ypT0N0M0). Therefore, pCR is an important prognostic factor in the assessment of rates of recurrence, overall survival (OS), and disease-free survival (DFS) (14, 15).

A wide range of factors are known to affect tumor response to CRT, such as pathological and clinical tumor stage, distance from the anal verge, and the time between the end of neoadjuvant therapy and surgery (12). Studies have also shown that blood lymphocyte levels before, during, and after neoadjuvant therapy predict prognosis and are positively associated with pCR (16, 17). Accordingly, it is greatly important to evaluate measurable variables that may predict treatment efficacy and the likelihood of a pCR. Patients predicted to have good treatment response may cause oncologists to refine or alter their decisions (e.g., opting to intensify preoperative chemotherapy treatment, provide less radiation therapy, etc.), which might result in large differences in the adverse events profile.

Twenty-five percent of the bone marrow of elderly adults' reserve is contained in the pelvic bones, which are considered a metabolically active focus. It is also known that of all blood cells, lymphocytes are the most radiation-sensitive, having an LD50 of 2Gy. Secondary lymphopenia caused by radiation therapy is a common phenomenon among oncology patients in general and patients with rectal cancer in particular (18). The decrease in lymphocyte levels is exponential and begins after the first week of treatment (19, 20). Although it is usually an acute side effect that resolves about 3 months after treatment end, several studies have shown that lymphopenia is a poor prognostic factor for progression-free survival (PFS) and OS in various tumors (16, 21). It is hypothesized that lymphocytes play a significant role in the anticancer activity of the immune system, as a greater density of T cells in the tumor bed has been shown to be associated with higher OS and DFS (22).

The hypothesis of the present investigation is that a decrease in the level of lymphocytes during preoperative neoadjuvant CRT treatment of rectal cancer predicts lower responsiveness of the tumor to treatment.

Materials and methods

This retrospective study was approved by the Ethics Committee of the Rambam Health Care Campus in Haifa, Israel (0315-19-RMB). The inclusion criteria included patients referred to Rambam's Radiation Therapy Unit between September 2015 to January 2020 following diagnosis of rectal adenocarcinoma by histopathological examination, clinical stage IIA-IIIC, per the TNM v8. T-stage was determined using transrectal ultrasonography and pelvic MRI, and N-stage was assessed using MRI and PET-CT. Patients who were treated with induction or consolidation chemotherapy before or after a chemoradiation course, which signifies a total neoadjuvant treatment (TNT) approach, were excluded from this study.

Radiation therapy characteristics

Each patient was administered a total radiation therapy dose of 50Gy to the tumor volume in daily 2Gy increments *via* simultaneous integrated boost (SIB), along with 45Gy in daily 1.8Gy increments to pelvic lymph nodes. Each treatment was planned using the Monaco Treatment Planning System (TPS) and delivered 5 times a week for 5 weeks. The volumetric modulated arch therapy (VMAT) technique was used to deliver 6- or 10- MV photon beam energies with Agility HD MLC transmission optimization. Gross tumor volume (GTV), visualized on a CT-based simulation with fusion of pretreatment MRI or PET-CT images on TPS, was contoured by a radiation oncology expert, revised by radiology and nuclear medicine expert, and approved in

a weekly radiation oncology staff meeting. Clinical target volume (CTV) to tumor SIB was contoured by adding 1.5 -2.0 cm around the GTV and adding 0.5 cm around the CTV -planning target volume for the SIB. Pelvic lymph node volume (CTV45) was created by the contouring of mesorectal fat, the presacral lymph nodes 0.5-0.7 cm anteriorly from the ventral aspect of the sacrum, an 1.0-1.5 cm expansion around the internal iliac, and obturator blood vessels. In cases where there was involvement of the anal canal or the explicit pathologic appearance of lymph nodes, the external iliac nodes and/or common iliac lymph nodes were included in the CTV45. An additional expansion of 0.5 cm around CTV45 thereby established the pelvic planning target volume (PTV45). Volume values were measured automatically by radiation therapy TPS software.

Chemotherapy regimen

Chemotherapy was applied using 5-fluorouracil in a dose of 300 mg/m^2 for 96 hours weekly or capecitabine at 825 mg/m^2, given twice a day, 5 days a week during 5 weeks of the radiation treatment.

Surgery and pathology

Surgery was performed 6-8 weeks after completion of chemoradiation therapy using the total mesorectal excision technique. Resected tissue was examined by a senior pathologist to evaluate the response of the primary tumor and lymph nodes. Complete pathological response was defined as no viable tumor cells in primary tumor tissue and in all resected lymph nodes. Based on the response, two groups of patients were identified: one presenting a pathological complete response (pCR) in both primary tumor and lymph nodes and the other with a less than complete response (no-pCR).

Blood test

Blood tests were performed weekly on each chemoradiation course, and an absolute lymphocyte count (ALC) was registered. Patients having lymphopenia (<1x10^9/L) at the time of chemoradiation start were excluded from the study. Further analysis was performed to compare host, tumor, and treatment characteristics between lymphopenic and non-lymphopenic patients.

Statistical analysis

For the calculation of descriptive and frequency statistics, analyses were performed using IBM SPSS Statistics v.27 software. Crosstab with chi-square tests were used to execute comparisons between the two groups (i.e., with and without pCR). A chi-square test with an independent t-test was carried out to estimate homogeneity between the pCR and non-pCR groups. Presuming nonparametric distribution of observed pCR and lymphopenia, the nonparametric chi-square test was used. To assess the role of chemoradiotherapy-induced lymphopenia in the achievement of pCR, a univariate analysis was used along with age, gender, ethnicity, body weight and height, smoking status, level of tumor in the rectal wall, delivered RT dose, GTV, and PTV45 variables. To evaluate correlations between clinical, blood test, and radiotherapeutic features and to exclude possible collinearity of exploring factors, a factor analysis was performed. The variables included in this analysis were age, GTV, PTV45, level of lower tumor margin, and absolute lymphocyte count at the conclusion of radiotherapy course.

Results

Between 2015 and 2020, 354 patients were referred to our Radiation therapy Unit for neoadjuvant radiotherapy. After collecting data and excluding patients with an absolute lymphocyte count in their blood samples, 202 patients were enrolled in the study. Four additional patients were excluded due to the presence of synchronous metastasis. Patient demographics and characteristics are presented in Table 1. The mean age of the patients at the time of diagnosis was 60.6 ± 11.73 years, with 74 females (37.4%) and 124 males (62.6%); 76 Arab (38.4%) and 122 Jewish (61.6%) patients. There were 150 patients (76%) who were past smokers or had never smoked.

Disease in Stage II or Stage III was diagnosed in 57 and 141 patients, respectively. Mean gross tumor volume (GTV) was 47.81 ± 4.5 cm^3 and PTV was 1066.14 ± 296.61 cm^3. The Mean absolute lymphocyte count for the two last weeks of chemoradiation was 0.8 ± 0.32 10^9/L. The follow-up time was in the range of 9 to 78 months, with a mean of 36.5 ± 1.4 months. The mean delivered radiotherapy dose was 49.9 ± 0.74Gy.

Table 2 presents the pathological outcomes of neoadjuvant chemoradiation therapy.

Taking into consideration that the current TNM system permits a TisN0M0 case to be classified as a Stage 0 disease - 58 patients (28.7%) were diagnosed as pathological Stage 0. Six cases (6.2%) presented a near- complete response (maximal treatment response, MTR) to delivered treatment, where only several islets of viable tumor cells were found on pathological examination. Those MTR cases were formally rendered as non-pCR patients, resulting in pCR in 53 cases (26.2%) (Table 2). During the observation period, there were 29 patients (14.4%) who experienced local or distant recurrences (detected by imaging and/or endoscopic procedures during follow up), while 17 patients (8.4%) died. The results after splitting the patient groups according to observed lymphopenia are presented in Tables 3 and 4. The chi- square test showed a significant difference between observed and expected rates of lymphopenia and pCR ($p<0.001$). Further crosstabulation of T- and N-downstaging rates observed in patients with and without lymphopenia showed statistical significance in the lymph node response rate ($p=0.029$). The primary tumor response rate was not significant between the two groups.

Lymphopenia was observed in 148 patients (75%) having a mean ALC of 0.65 ± 0.01, 10^9/L while in 50 (25%) the mean ALC

was 1.24 ± 0.03, 10^9/L (t-test, p<.0001) (Table 3). Between non-lymphopenic and lymphopenic patients, the t-test showed significant differences in baseline ALC levels, measured a week before treatment start (p<0.0001), patient height (p=0.039), disease-free time (p=0.02) (Table 3). Only a trend was shown in difference in PTV value (p=0.05).

Linear regression analysis showed an inverse dependency of pCR on primary tumor volume and observed lymphopenia (p<0.05). Primary tumor downstaging had the largest impact on pCR (B=.37) with the level of statistical significance standing at less than p<0.001. Univariate analysis of variance showed the absence of heteroscedasticity in White's test. It also showed a statistically significant effect on pCR achievement by lymphopenia at the conclusion of chemoradiation course (p=0.045), GTV (p=0.002), height (p=0.001), weight (p=0.023). pCR dependence on GTV and patient body weight were negative in terms of tumor response to delivered therapy.

Kaplan-Meier disease-free survival graph estimation test results showed no significant differences between the lymphopenic and non-lymphopenic groups, nor in the pCR or non-pCR groups, although visually the two survival lines were well separated (Figure 1). A multivariate Cox regression analysis was performed to further evaluate the effect of factors on the DFS period. It showed PTV as the most influential, DFS-modifying factor (p<0.01).

The factor analysis was performed to study the potential collinearity of variables affecting pCR and to clarify the model. It included patient age, smoking status, height, weight, as well as GTV, distance from the anal verge to the lower tumor margin in the rectal wall, lymphopenia, and tumor response to the neoadjuvant treatment. The analysis showed very low collinearity between the variables. However, statistical significance was observed in the correlation of lymphopenia and the following factors: height (p=0.02), distance to lower tumor margin (p=0.046), PTV45 (p=0.025), and achieved pCR (p=0.033). An inverted correlation was found between lymphopenia and the distance from anal verge to tumor margin and pCR. GTV was directly correlated with PTV (p<0.001) and inversely correlated with pCR (p=0.033). The PTV value directly correlated with body weight (p<0.001) and inversely correlated with the distance from the anal verge to the tumor (p<0.001). Patient body weight directly correlated with patient height (p<0.001).

TABLE 1 Demographic, anthropometric, and clinical characteristics of study participants (n=198).

Characteristic	Mean ± SD
Age (years)	60.6 ± 11.73
Height (cm)	167.45 ± 12.3
Weight (kg)	77.65 ± 15.4
Gender (n, %)	
Female	74 (37.4%)
Male	124 (62.6%)
Ethnicity (n, %)	
Arabs	76 (38.4%)
Jews	122 (61.6%)
Smoking (n, %)	
Light smoker	6 (3%)
Heavy smoker	42 (21.2%)
Past smoker	26 (13.1%)
Never smoked	124 (62.6%)
Clinical Stage (n, %)	
IIa	52 (26.3%)
IIb	4 (2%)
IIc	1 (0.5%)
IIIa	4 (2%)
IIIb	115 (58.1%)
IIIc	22 (11.1%)
GTV (cm^3)	47.81 ± 45
PTV (cm^3)	1066.14 ± 296.61
Distance from anal verge (cm)	6.79 ± 2.77
Delivered dose (Gy)	49.9 ± 0.74
ALC for last 2 weeks of CRT (10^9/L)	0.8 ± 0.32
OS (months)	23.56 ± 14.1

SD, standard deviation; GTV, gross tumor volume; PTV, planning target volume; ALC, absolute lymphocyte count; CRT, chemoradiotherapy; OS, overall survival.

TABLE 2 Pathological outcome of neoadjuvant chemoradiation (n=198).

Characteristic	N (%)
Stage	
0	58 (29.3%)
I	44 (22.2%)
IIa	42 (21.2%)
III	1 (0.5%)
IIIa	19 (9.6%)
IIIb	21 (10.6%)
IIIc	13 (6.6%)
Achieved pCR	
No pCR	145 (73.2%)
pCR	53 (26.8%)
Recurrence	
No recurrence	172 (86.9%)
Recurrent disease	26 (13.1%)
Viability	
Alive	183 (92.4%)
Deceased	15 (7.6%)

pCR; pathological complete response.

TABLE 3 Descriptive statistics of lymphopenic vs. non-lymphopenic participants (n=198).

Characteristic	No lymphopenia (n=50)	Lymphopenia (n=148)	T-test (*p*)
Age (years)	60.8 ± 1.5	60.5 ± 0.09	
Height (cm)	167.08	167.57	0.039
Weight (kg)	78.82	77.26	
Gender n (%)			
Female	18 (36%)	56 (37.8%)	
Male	32 (64%)	92 (62.2%)	
Ethnicity n (%)			
Arabs	23 (46%)	53 (35.8%)	
Jews	27 (54%)	95 (64.2%)	
Smoking n (%)			
Light smoker	2 (4%)	4 (2.7%)	
Heavy smoker	11 (22%)	31 (20.9%)	
Past smoker	8 (16%)	18 (12.2%)	
Never smoked	29 (58%)	95 (64.2%)	
GTV (cm^3)	38.65	50.9	
PTV (cm^3)	973.94 ± 2	1097.28 ± 2	0.05
Distance from anal verge (cm)	7.2	6.65	
Delivered dose (Gy)	49.908	50.003	
ALC for last two weeks of CRT (10^9/L)	1.24 ± 0.03	0.65 ± 0.01	<0.000
DFS (months)	31.4 ± 1.9	28.5 ± 1.7	0.02

SD, standard deviation; GTV, gross tumor volume; PTV, planning target volume; ALC, absolute lymphocyte count; CRT, chemoradiotherapy; DFS, disease-free survival.
Results are shown as mean ± SD or n (%0) as specified.

Discussion

Decreased lymphocyte levels in the bloodstream following radiation therapy were first described in the 1970s (23, 24), but the clinical significance of these declines has not been adequately investigated in rectal cancer. Therefore, the plan of our study was to focus on changes in lymphocytes' levels in the bloodstream during chemoradiation, and their effect on preoperative treatment outcomes.

Microbiological studies have shown that sensitivity to radiation therapy depends not only on the biological characteristics of the tumor but also on its microenvironment (25, 26). Tumor reduction is affected by the immune response of the host in addition to the direct damage to the cancer cells caused by radiation (27). Additional studies have shown that the presence of immune cells in and around the tumor bed is associated with a better therapeutic response in colorectal cancer (28) and may be used as a tool to predict recurrence and survival in this cancer type. Nevertheless, there are studies that suggest a link between the level of lymphocytes in the bloodstream, which assume that blood cell count reflects host conditions and the effectiveness of radiation therapy for rectal cancer (16, 29). It should be noted that the association between lymphopenia after radiation therapy and recurrence rates has been examined in other cancers such as bladder (30) and head and neck tumors (31), but as aforementioned, not investigated adequately yet in rectal cancer.

A study published in the journal BMC Cancer in 2011 (16) examined the relationship between the effectiveness of radiation therapy and the levels of all blood cells withdrawn before and after treatment. Its results support the present study's findings regarding lymphocyte levels. On the other hand, an investigation published in 2017 (32) offered contradictory findings, which suggested a decrease in the level of lymphocytes during preoperative treatment is associated with better tumor regression.

The present investigation found that the level of lymphocytes in the bloodstream decreases during radiation therapy and that this is an independent predictor of treatment efficacy and achievement of a pCR in LARC. Both absolute lymphopenia and relative lymphopenia were found to be associated with lower tumor regression rates. These findings emphasize the importance of follow-up throughout radiation therapy, while addressing the trend of lymphocytes levels during treatment and not just their absolute level at different time points.

Keeping in mind the potential influence of multicollinearity on study's results, we evaluated each factor in terms of its pathophysiological impact on the processes within tumor, lymph nodes and volume of surrounding tissues. Using VMAT techniques

10.3389/fonc.2023.1138299

TABLE 4 Clinical characteristics of non-lymphopenic vs. lymphopenic participants (n=198).

Characteristic	No lymphopenia (n=50)	Lymphopenia (n=148)
Clinical T stage		
T2	1 (2%)	3 (2%)
T3	48 (96%)	133 (89.9%)
T4b	1 (2%)	12 (8.1%)
Clinical N stage		
N 0	17 (34%)	40 (27%)
N 1	27 (54%)	92 (62.2%)
N 2	6 (2%)	16 (10.8%)
Cinical stage		
IIa	16 (32%)	36 (24.3%)
IIc	1 (2%)	4 (2.7%)
IIIa	1 (2%)	3 (2%)
IIIb	26 (52%)	89 (60%)
IIIc	6 (12%)	16 (10.8%)
Achieved pCR		
pCR	20 (40%)	33 (22.3%)
no pCR	30 (60%)	115 (77.7%)
Recurrence		
No recurrence	47 (94%)	125 (84.5%)
Recurrent disease	3 (6%)	23 (15.5%)
Viability		
Alive	47 (97%)	138 (91.9%)
Deceased	5 (3%)	12 (8.1%)

pCR, pathological complete response.
Results are shown as n (%).

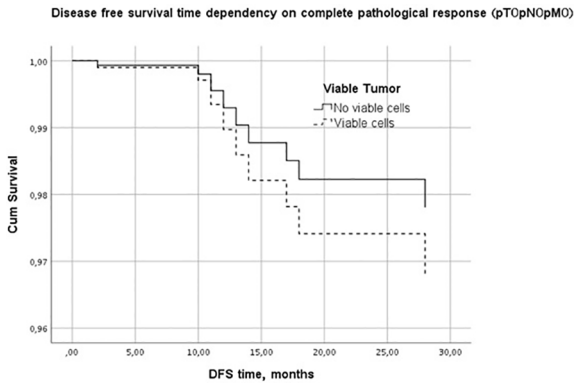

FIGURE 1
Disease free survival time dependency on pathological complete response.

for our patients, we produced the maximal gradient between PTV and surrounding pelvic bones to decrease adverse effects on bone marrow. We suggested that our strict bone marrow irradiation reduction policy is an appropriate way to reduce possible collinearity for study's results.

The present research is a unique investigation that analyses variables throughout the course of antineoplastic treatment while normalizing individual values for each colorectal cancer patient. As there are few studies in the literature that have been conducted using the same methodology, it is critical to examine the lymphocyte level parameter in other cancers and larger sample numbers to establish whether the findings detailed here are random or not.

The information reported in this study may help medical oncologists predict the therapeutic response in this type of cancer. By monitoring lymphocyte levels during treatment and identifying those patients who may respond less well to, for example, the full preoperative treatment approach, they may be guided toward treatment therapeutic strategy adjustments and alternatives that will optimize outcomes. The current analysis was unable to find variables that predict the development of lymphopenia in different patients. Possible reasons for this may be insufficient sample size, analysis of non-real-time results (as the study is retrospective and relies on existing information), and the absence of a control group. More extensive prospective studies with larger sample sizes are needed before a more conclusive answer can be asserted to the question posed by this study – whether lymphopenia affects the response of radiation therapy to rectal cancer and what are the factors that can predict the development of lymphopenia in patients.

Conclusion

Decreased levels of lymphocytes during preoperative CRT treatment of LARC are predictive of a non-pCR. It is associated with lower regression rates and may be a prognostic measure of therapeutic response. This study showed that weekly monitoring of the lymphocyte levels during preoperative treatment reflects the hematopoietic toxicity of radiation therapy and may also predict responsiveness to treatment. Monitoring the immune response to preoperative treatment by blood tests is a convenient and accessible clinical tool for identifying patients who may benefit from preoperative radiation therapy. It is also a practical way to diagnose patients with a lower likelihood of achieving a full response to treatment, thus creating opportunities to customize therapeutic approaches and offer adaptations and alternatives, such as full preoperative radiation therapy. Further prospective studies are needed to better understand the factors that could predict the development of lymphopenia in patients and thereby establish the means for treatment optimization.

Data availability statement

The raw data supporting the conclusions of this article will be made available by the authors, without undue reservation.

Ethics statement

The studies involving human participants were reviewed and approved by Rambam Healthcare Campus. Written informed consent for participation was not required for this study in accordance with the national legislation and the institutional requirements.

Author contributions

ML, TT and SB contributed to conception and design of the study. ML organized the database and performed statistical analysis. TT wrote the manuscript. TT has Equal contribution and first authorship for this paper. ML - the concept and methodology formalization, data base creation, statistical analysis. All authors contributed to manuscript revision, read, and approved the submitted version.

Conflict of interest

The authors declare that the research was conducted in the absence of any commercial or financial relationships that could be construed as a potential conflict of interest.

Publisher's note

References

1. Sung H, Ferlay J, Siegel RL, Laversanne M, Soerjomataram I, Jemal A, et al. Global cancer statistics 2020: GLOBOCAN estimates of incidence and mortality worldwide for 36 cancers in 185 countries. *CA Cancer J Clin* (2021) 71(3):209–49. doi: 10.3322/caac.21660

2. Howlader N, Noone AM, Krapcho M, Miller D, Brest A, Yu M, et al. *SEER cancer statistics review 1975-2016 national cancer institute SEER cancer statistics review 1975-2016*. National Cancer Institute (2016) p. 11–4.

3. Arnold M, Sierra MS, Laversanne M, Soerjomataram I, Jemal A, Bray F. Global patterns and trends in colorectal cancer incidence and mortality. *Gut* (2017) 66(4):683–91. doi: 10.1136/gutjnl-2015-310912

4. Feeney G, Sehgal R, Sheehan M, Hogan A, Regan M, Joyce M, et al. Neoadjuvant radiotherapy for rectal cancer management. *World J Gastroenterol* (2019) 25(33):4850–69. doi: 10.3748/wjg.v25.i33.4850

5. National Comprehensive Cancer Network (NCCN). *Rectal cancer* (2021). Available at: https://www.nccn.org/patients/guidelines/content/PDF/rectal-patient.pdf.

6. American Society of Clinical Oncology. *Gastrointestinal cancer* (2019). Available at: https://www.asco.org/practice-patients/guidelines/gastrointestinal-cancer#/34951.

7. European Society for Medical Oncology (ESMO). *ESMO management and treatment adapted recommendations in the COVID-19 era: Colorectal cancer (CRC)* . Available at: https://www.esmo.org/guidelines/gastrointestinal-cancers/gastrointestinal-cancers-colorectal-cancer-crc-in-the-covid-19-era.

8. Richetti A, Fogliata A, Clivio A, Nicolini G, Pesce G, Salati E, et al. Neo-adjuvant chemo-radiation of rectal cancer with volumetric modulated arc therapy: Summary of technical and dosimetric features and early clinical experience. *Radiat Oncol* (2010) 5 (1):14. doi: 10.1186/1748-717X-5-14

9. Gérard JP, Conroy T, Bonnetain F, Bouché O, Chapet O, Closon-Dejardin M-T, et al. Preoperative radiotherapy with or without concurrent fluorouracil and leucovorin in T3-4 rectal cancers: Results of FFCD 9203. *J Clin Oncol* (2006) 24(28):4620–5. doi: 10.1200/JCO.2006.06.7629

10. Bosset JF, Calais G, Mineur L, Maingon P, Stojanovic-Rundic S, Bensadounet R-J, et al. Fluorouracil-based adjuvant chemotherapy after preoperative chemoradiotherapy in rectal cancer: Long-term results of the EORTC 22921 randomised study. *Lancet Oncol* (2014) 15(2):184–90. doi: 10.1016/S1470-2045(13)70599-0

11. Fokas E, Liersch T, Fietkau R, Ghadimi M, Liersch T, Grabenbauer GG, et al. Tumor regression grading after preoperative chemoradiotherapy for locally advanced rectal carcinoma revisited: Updated results of the CAO/ARO/AIO-94 trial. *J Clin Oncol* (2014) 32(15):1554–62. doi: 10.1200/JCO.2013.54.3769

12. Bitterman DS, Salgado LR, Moore HG, Sanfilippo NJ, Gu P, Hatzaras I, et al. Predictors of complete response and disease recurrence following chemoradiation for rectal cancer. *Front Oncol* (2015) 5:286(DEC). doi: 10.3389/fonc.2015.00286

13. Sung SY, Son SH, Park EY, Kay CS. Prognosis of locally advanced rectal cancer can be predicted more accurately using pre and post-chemoradiotherapy neutrophil lymphocyte ratios in patients who received preoperative chemoradiotherapy. *PloS One* (2017) 12(3). doi: 10.1371/journal.pone.0173955

14. Zorcolo L, Rosman AS, Restivo A, Pisano M, Nigri GR, Fancellu A, et al. Complete pathologic response after combined modality treatment for rectal cancer and long-term survival: A meta-analysis. *Ann Surg Oncol* (2012) 19(9):2822–32. doi: 10.1245/s10434-011-2209-y

15. George TJ, Allegra CJ, Yothers G. Neoadjuvant rectal (NAR) score: a new surrogate endpoint in rectal cancer clinical trials. *Curr Colorectal Cancer Rep* (2015) 11 (5):275–80. doi: 10.1007/s11888-015-0285-2

16. Kitayama J, Yasuda K, Kawai K, Sunami E, Nagawa H. Circulating lymphocyte is an important determinant of the effectiveness of preoperative radiotherapy in advanced rectal cancer. *BMC Cancer* (2011) 11. doi: 10.1186/1471-2407-11-64

17. Heo J, Chun M, Noh OK, Oh Y-T, Suh KW, Park JE, et al. Sustaining blood lymphocyte count during preoperative chemoradiotherapy as a predictive marker for pathologic complete response in locally advanced rectal cancer. *Cancer Res Treat* (2016) 48(1):232–9. doi: 10.4143/crt.2014.351

18. Campian JL, Ye X, Sarai G, Herman J, Grossman SA. Severe treatment-related lymphopenia in patients with newly diagnosed rectal cancer. *Cancer Invest* (2018) 36 (6):356–61. doi: 10.1080/07357907.2018.1499028

19. Ellsworth SG, Zhang H, Mereniuk T, Agrawal N, Zellars RC, Kong FM, et al. Factors affecting kinetics of acute radiation-induced lymphopenia in patients with gastrointestinal cancer. *Int J Radiat Oncol Biol Physics* (2018) 102:2018. doi: 10.1016/j.ijrobp.2018.07.623

20. Shiraishi Y, Fang P, Xu C, Song J, Krishnan S, Koay EJ, et al. Severe lymphopenia during neoadjuvant chemoradiation for esophageal cancer: A propensity matched analysis of the relative risk of proton versus photon-based radiation therapy. *Radiother Oncol* (2018) 128(1):154–60. doi: 10.1016/j.radonc.2017.11.028

21. Venkatesulu BP, Mallick S, Lin SH, Krishnan S. A systematic review of the influence of radiation-induced lymphopenia on survival outcomes in solid tumors. *Crit Rev Oncology/Hematology* (2018) 123(February):42–51. doi: 10.1016/j.critrevonc.2018.01.003

22. Ménétrier-Caux C, Ray-Coquard I, Blay JY, Caux C. Lymphopenia in cancer patients and its effects on response to immunotherapy: An opportunity for combination with cytokines? *J ImmunoTherapy Cancer* (2019) 7(1):1–15. doi: 10.1186/s40425-019-0549-5

23. Stratton JA, Byfield PE, Byfield JE, Small RC, Benfield J, Pilch Y. A comparison of the acute effects of radiation therapy, including or excluding the thymus, on the lymphocyte subpopulations of cancer patients. *J Clin Invest* (1975) 56(1):88–97. doi: 10.1172/JCI108084

24. Stjernswärd J, Jondal M, Vánky F, Wigzell H, Sealy R. Lymphopenia and change in distribution of human b and T lymphocytes in peripheral blood induced by irradiation for mammary carcinoma. *Lancet* (1972) 1(7765):1352–6. doi: 10.1016/s0140-6736(72)91091-4

25. Barcellos-Hoff MH, Park C, Wright EG. Radiation and the microenvironment - tumorigenesis and therapy. *Nat Rev Cancer.* (2005) 5(11):867–75. doi: 10.1038/nrc1735

26. Prise KM, Schettino G, Folkard M, Held KD. New insights on cell death from radiation exposure. *Lancet Oncol* (2005) 6(7):520–8. doi: 10.1016/S1470-2045(05)70246-1

27. Demaria S, Formenti SC. Sensors of ionizing radiation effects on the immunological microenvironment of cancer. *Int J Radiat Biol* (2007) 83(11-12):819–25. doi: 10.1080/09553000701481816

28. Koch M, Beckhove P, Op den Winkel J, Autenrieth D, Wagner P, Nummer D, et al. Tumor infiltrating T lymphocytes in colorectal cancer: Tumor-selective activation and cytotoxic activity in situ. *Ann Surg* (2006) 244(6):986–93. doi: 10.1097/01.sla.0000247058.43243.7b

29. Kitayama J, Yasuda K, Kawai K, Sunami E, Nagawa H. Circulating lymphocyte number has a positive association with tumor response in neoadjuvant chemoradiotherapy for advanced rectal cancer. *Radiat Oncol* (2010) 5:47. doi: 10.1186/1748-717X-5-47

30. O'Toole C, Unsgaard B. Clinical status and rate of recovery of blood lymphocyte levels after radiotherapy for bladder cancer. *Cancer Res* (1979) 39(3):840–3.

31. Kuss I, Hathaway B, Ferris RL, Gooding W, Whiteside TL. Decreased absolute counts of T lymphocyte subsets and their relation to disease in squamous cell carcinoma of the head and neck. *Clin Cancer Res* (2004) 10(11):3755–62. doi: 10.1158/1078-0432.CCR-04-0054

32. Wu Z, Zhang J, Cai Y, Deng R, Yang L, Li J, et al. Reduction of circulating lymphocyte count is a predictor of good tumor response after neoadjuvant treatment for rectal cancer. *Med (United States)* (2018) 97(38). doi: 10.1097/MD.0000000000011435

33. American Cancer Society. *Colorectal cancer facts & figures 2020-2022* (2022). Available at: https://www.cancer.org/content/dam/cancer-org/research/cancer-facts-and-statistics/colorectal-cancer-facts-and-figures/colorectal-cancer-facts-and-figures-2020-2022.pdf.

34. The Jerusalem Post. *Colon cancer awareness month: Early detection rising, mortality falling* (2021). Available at: https://www.jpost.com/health-science/colon-cancer-awareness-month-early-detection-rising-mortality-falling-660561.

frontiers | Frontiers in Oncology

TYPE Case Report
PUBLISHED 08 June 2023
DOI 10.3389/fonc.2023.1187623

OPEN ACCESS

EDITED BY
Marco Rengo,
Sapienza University of Rome, Italy

REVIEWED BY
Luigi Tornillo,
University of Basel, Switzerland
Zheng Liu,
National Cancer Center of China, China

*CORRESPONDENCE
Davide Ciardiello
davide.ciardiello@ieo.it

†These authors have contributed equally to this work

RECEIVED 16 March 2023
ACCEPTED 22 May 2023
PUBLISHED 08 June 2023

CITATION
Ciardiello D, Del Tufo S, Parente P, Gravina AG, Selvaggi F, Panarese I, Franco R, Caterino M, Martini G, Ciardiello F, Grassi R, Cappabianca S, Reginelli A and Martinelli E (2023) Case report of unusual synchronous anal and rectal squamous cell carcinoma: clinical and therapeutic lesson.
Front. Oncol. 13:1187623.
doi: 10.3389/fonc.2023.1187623

Case report of unusual synchronous anal and rectal squamous cell carcinoma: clinical and therapeutic lesson

Davide Ciardiello[1,2*†], Sara Del Tufo[3†], Paola Parente[4], Antonietta Gerarda Gravina[5], Francesco Selvaggi[6], Iacopo Panarese[7], Renato Franco[7], Michele Caterino[8], Giulia Martini[2], Fortunato Ciardiello[2], Roberto Grassi[3], Salvatore Cappabianca[3], Alfonso Reginelli[3†] and Erika Martinelli[2†]

[1]Division of Gastrointestinal Medical Oncology and Neuroendocrine Tumors, European Institute of Oncology (IEO), IRCCS, Milan, Italy, [2]Oncology Unit, Department of Precision Medicine, Università degli Studi della Campania "Luigi Vanvitelli", Napoli, Italy, [3]Radiology Unit, Department of Precision Medicine, Università degli Studi della Campania "Luigi Vanvitelli", Napoli, Italy, [4]Pathology Unit, Fondazione IRCCS Casa Sollievo Della Sofferenza, San Giovanni Rotondo, Foggia, Italy, [5]Gastroenterology Unit, Department of Precision Medicine, Università degli Studi della Campania "Luigi Vanvitelli", Napoli, Italy, [6]Department of Advanced Medical and Surgical Sciences, Università degli Studi della Campania "Luigi Vanvitelli", Napoli, Italy, [7]Pathology UniV, Department of Mental and Physical Health and Preventive Medicine, University of Campania "Luigi Vanvitelli", Napoli, Italy, [8]Clinica Villa delle Querce, Napoli, Italy

Synchronous tumors of the rectum and anus are sporadic. Most cases in the literature are rectal adenocarcinomas with concomitant anal squamous cell carcinoma. To date, only two cases of concomitant squamous cell carcinomas of the rectum and anus are reported, and both were treated with up-front surgery and received abdominoperineal resection with colostomy. Here, we report the first case in the literature of a patient with synchronous HPV-positive squamous cell carcinoma of the rectum and anus treated with definitive chemoradiotherapy with curative intent. The clinical-radiological evaluation demonstrated complete tumor regression. After 2 years of follow-up, no evidence of recurrence was observed.

KEYWORDS

SCC, rectal cancer, anal cancer, HPV, chemo-radiotherapy

Background

Squamous cell carcinoma (SCC) of the rectum is an infrequent malignancy. Only 0.1%–0.3% of rectal cancers (RCs) are represented by the SCC histotype, while adenocarcinoma represents about 90% of RCs (1, 2). Similarly, anal cancer is rare, accounting for less than 1% of all new cancer diagnoses and less than 3% of all

gastrointestinal tract tumors (3). Synchronous tumors of the rectum and anus are sporadic. Most cases in the literature are rectal adenocarcinomas with concomitant anal SCC. Thus, identification of the optimal treatment in this unusual presentation is challenging and has to be defined case by case. To date, only two cases of synchronous SCC of the rectum and anus are reported, and both were treated with up-front surgery (4, 5). Here, we report the first case in the literature of a patient with synchronous SCC of the rectum and anus treated with definitive chemo-radiotherapy (CRT) without subjecting her to radical surgery.

Clinical presentation

A 68-year-old woman came to our observation for the onset of pain in the anal area, weight loss, and nonspecific abdominal pain for about 2 months. The patient, a former smoker and nondrinker, presented in good condition with a performance status (PS) of 0 according to ECOG and without comorbidities. Blood test values were within the range. About a month before, following the indication of a general practitioner, the patient underwent an ultrasound exam of the abdomen, which resulted in a negative, and a colonoscopy. The endoscopic examination showed the presence of two lesions: a polyp of approximately 4 cm about 10 cm from the anal verge and another ulcerated lesion at the anorectal junction. Biopsies of both lesions were performed. The histological examination, conducted in a local laboratory, revealed in both cases nonkeratinizing SCC. No evidence of gynecological tumors was clinically observed.

Due to the unusual endoscopic presentation and histologic report, the case was discussed by a multidisciplinary team to define the best diagnostic and therapeutic flow.

It was decided to repeat the endoscopic examination and revise the tumor samples. The pan-coloscopy showed the presence at the level of the anorectal junction of an ulcerated lesion of approximately 15–20 mm and, about 8 cm from the anal verge, a lesion of about 3 cm with a nonlifting sign. A re-biopsy of each lesion was performed. At the microscopical examination, both rectal and anal biopsies confirmed the diagnosis, documenting infiltration by carcinoma with a solid growth pattern. Immunohistochemistry documented positivity for p40 and CK5/6 and negativity for CK20 and CDX2, leading to squamous, nonkeratinizing histotype, according to the WHO 2019 edition of Digestive System Tumors. Moreover, diffuse p16 immunostaining was shown, as observed in human papillomavirus (HPV) infection (Figure 1).

A baseline total body CT scan with the administration of a contrast medium documented the presence of a polypoid lesion at the level of the rectum, at the right posterolateral wall, and at the level of the anal region, where there was pathological thickening.

The MRI examination of the rectum showed the presence of a parietal formation with a polypoid appearance and a broad implant

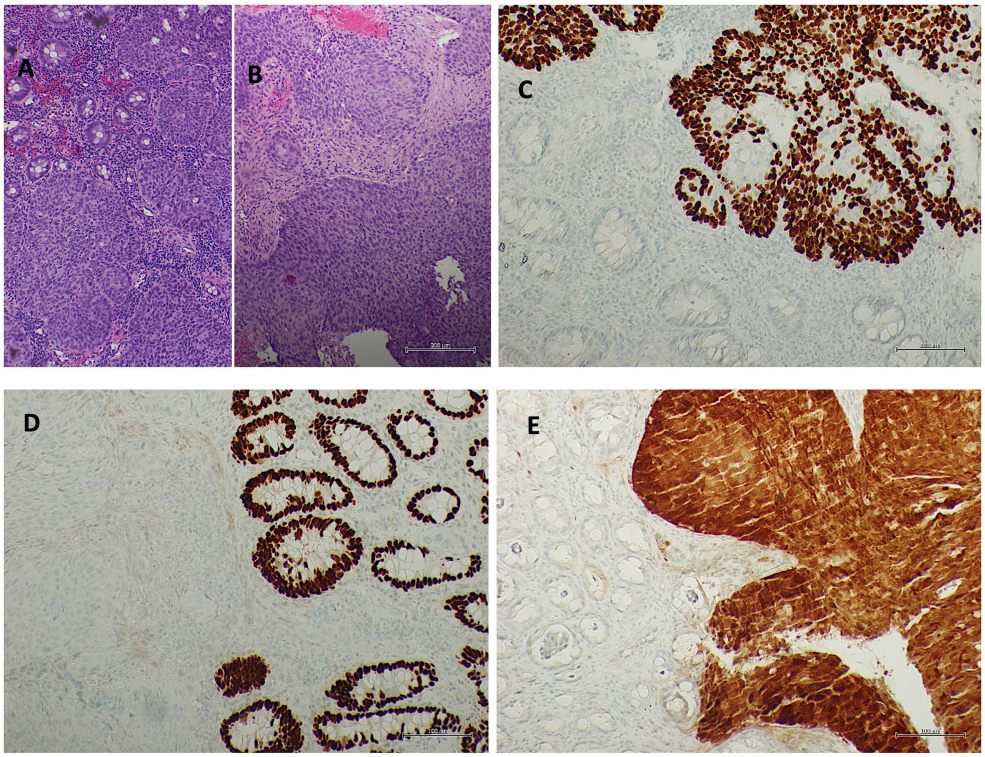

FIGURE 1
Rectal mucosa (**A** hematoxylin/eosin staining) and anal mucosa (**B** hematoxylin/eosin staining) infiltrated by squamous non-keratinizing carcinoma. Squamous differentiation underlined from p40 immunostaining (**C** p40 immunohistochemistry) and negativity for CDX2 (**D** CDX2 immunohistochemistry). Diffuse p16 immunostaining in neoplasia (**E** p16 immunohistochemistry).

base at the level of the mid-rectum, measuring roughly 37 × 37 × 37 mm (AP × LL × CC) of the posterolateral wall right, causing narrowing of the lumen. This formation showed a restriction of the signal in the Diffusion-weighted imaging (DWI)/ADC sequences and clear pathological impregnation in the post-contrastography phases, infiltrating the mesorectum until it exceeds the mesorectal fascia by about 4.5 mm, determining the extramural vascular invasion and the elevator muscle of the right anus. At the level of the anorectal junction, the presence of heteroplastic tissue with dimensions of approximately 18 × 13 × 23 mm (AP × LL × CC) was highlighted, which infiltrates the internal and external anal sphincter, showing inhomogeneous intensity in T2 and signal restriction in DWI. Furthermore, two lymph node formations were found in the right posterolateral mesorectal fat, one 13 mm from the mesorectal fascia and another in the coccygeal area. Thus, both endoscopic examination and MRI demonstrated no contiguity between the two lesions. Therefore, it was not possible to define whether the two lesions have a common origin or whether they are two distinct neoplasms According to MRI evaluation, rectal cancer staging was T4b N1b CMR+ MVI+, while anal cancer staging was T2 N1a.

The multidisciplinary group discussed the case again to define the therapeutic program. Considering that chemoradiotherapy is a standard of care (SOC) for SCC of the anus and that available evidence shows that rectal SCC is also sensitive to this treatment, it was decided to propose concurrent chemoradiotherapy, reserving the option of surgery in the presence of persistence or locoregional progression (1–3).

Thus, the patient started treatment with mitomycin *c* 10 mg/m^2 on days 1–29 scheme plus capecitabine 825 mg/m^2 bis in die (bid) and concomitant radiotherapy on the pelvis and anorectum (total dose, 60 Gy).

During therapy, the patient experienced grade 3 diarrhea and grade 2 anal mucositis, which required suspension of the concomitant therapy for 1 week, and symptomatic treatment for diarrhea and anal mucositis was administrated. After regression to grade 1 toxicity, the chemoradiotherapy treatment was continued. Response to treatment was evaluated with clinical, endoscopic, and instrumental criteria after 6 months from the beginning of chemoradiation. A digital rectal examination showed no evidence of disease, as did an endoscopic evaluation. Biopsies were taken during proctoscopy and were negative. Finally, re-evaluation with contrast-enhanced MRI examination showed complete tumor regression with no sign of a viable tumor in the DWI sequence (Figure 2). After 2 years of follow-up performed according to the European Society of Medical Oncology (ESMO) guidelines for anal cancer, no evidence of disease was observed (3). The patient maintained a good rectal function after CRT without an impact on her daily life.

Discussion

The insurgence of SCC in the lower gastrointestinal tract is rare, with most of the tumors originating from the squamous epithelium of the anal canal (2). Primary SCC from the colon and rectum are rare, representing less than 1% of colorectal malignancies (1–5). So far, while different theories have been proposed, the etiology of rectal SCC is still debated (1, 2). It has been suggested that rectal SCC could originate from pluripotent stem cells that could differentiate into different lineages (6). Other groups suggested a potential malignant evolution from persistent ectopic embryonal nests of ectodermal cells (7). The presence of chronic inflammation such as intestinal bowel disease (IBD) that causes a persistent

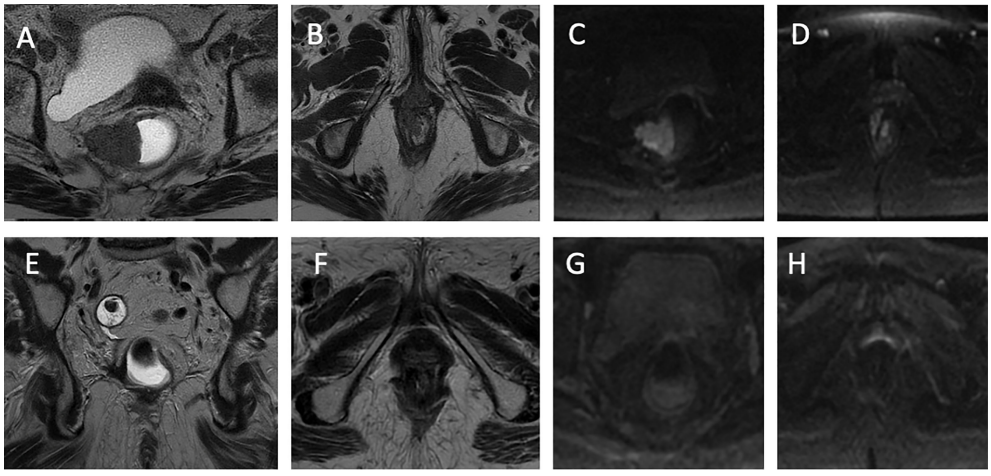

FIGURE 2
Radiologic images. **(A)** The T2-weighted sequence of rectal cancer on the axial plane. Parietal neoplastic formation of the middle rectum with a polypoid appearance and a broad implant base is observed on the right posterolateral wall from 6 to 12 o'clock, which causes the narrowing of the rectal lumen. This rectal formation infiltrates the mesorectum until it exceeds the mesorectal fascia by about 4.5 mm and infiltrates the elevator muscle. **(B)** The T2-weighted sequence of anal cancer on the axial plane. At the level of the rectal junction at 11 o'clock, there is evidence of neoplastic tissue infiltrating the internal and external anal sphincter. **(C)** Sequence weighted in DWI in correspondence with the rectal lesion. Signal restriction in the DWI sequence. **(D)** Sequence weighted in DWI at the level of the anal canal. Signal restriction in the DWI sequence. **(E)** Coronal plane T2-weighted sequence. A clear hypointensity is observed with regard to fibrotic outcomes 6 months after the start of radiochemotherapy (CRT). **(F)** T2-weighted sequence on the axial plane. Anal lesion response after CRT. **(G)** Sequence weighted in DWI in correspondence with the rectal lesion. No signal restriction following CRT. **(H)** Sequence weighted in DWI at the level of the anal canal. No signal restriction following CRT.

irritative stimulus could induce squamous metaplasia and favor the insurgence of rectal SCC (8). HPV and human immunodeficiency virus (HIV) are recognized risk factors for anal cancer (9). Nevertheless, the role of HPV infection in rectal SCC is controversial (10–12). Audeau and colleagues evaluated the association of HPV in a cohort of 20 patients with SCC of the rectum, adenosquamous tumors, or adenocarcinoma with squamous dysplasia; the authors reported no correlation with HPV 6, 11, 16, and 18 (10). On the contrary, other case reports or case series found a correlation with HPV positivity in squamous rectal cancer (11, 12).

Guerra and colleagues conducted a retrospective analysis on the Surveillance Epidemiology and End Results Database (SEER) to investigate the clinical–pathological characteristics of rectal SCC (13). In a large population of 142 patients diagnosed between 1946 and 2015, the median age was 63, with a predominance in women and in diagnosis in the early stage compared with advanced disease. The presence of synchronous rectal and anal SCC is an uncommon condition, and to date, only two cases were described in the literature (4, 5). The first one was a 48-year-old man with an anal and a rectosigmoid SCC with type 2 diabetes as the only comorbidity; no history of smoking or alcohol consumption was described (4). HPV was not tested. The patient underwent abdominoperineal resection, and a permanent colostomy was positioned. Subsequent adjuvant chemoradiotherapy was performed.

The second case was a 78-year-old man with a concurrent anal canal SCC and a rectal SCC (5). The patients had an anamnesis of heavy smoking, alcohol drinking, and opium consumption. No comorbidity or viral infection was reported. While the endoscopic and radiological evaluation demonstrated the presence of rectal and anal lesions, the biopsy results were negative. Thus, the patients underwent up-front diagnostic and therapeutic surgery with an abdominal–perineal resection. Histopathology proved the presence of synchronous rectal and anal SCC. After a multidisciplinary discussion, postoperative chemoradiotherapy was proposed.

In this scenario, our case could be of interest in different aspects. It represents the first case of concomitant HPV-positive rectal anal SCC described in the literature. It is very difficult to assess if the rectal SCC was a metastasis of anal cancer or a second malignancy. Repeated endoscopy evaluation, CT scan, and high-quality RMI do not demonstrate a clear contiguity between the two lesions. Moreover, from a clinical point of view, it is intricate to correlate a small anal cancer with a significantly more advanced rectal SCC. However, in both lesions, the presence of an HPV infection could have clearly contributed to the pathogenesis. Unfortunately, like in the other two cases, due to the lack of an adequate tumor sample, it was not possible to perform a genetic evaluation to discriminate if the two lesions have a common or distinct origin or to evaluate HPV genetic typing. This aspect could represent a limitation that deserves to be investigated by further translational prospective studies/case series. In the last decades, definitive CRT has emerged as the SOC for early and locally advanced anal SCC with curative intent (3). In cases of persistent disease or locoregional recurrent disease, surgery could represent a therapeutic option. Due to its infrequent occurrence, there has been no prospective study investigating the optimal treatment for rectal SCC (1). Historically, up-front surgery was proposed; however, it was complicated by significant comorbidity and mortality (1, 14). Therefore, definitive CRT has been proposed to improve outcomes and preserve organs (1, 15, 16). A French retrospective study included 23 patients treated in two referral institutions. CRT exhibited a really high rate of clinical complete response at 83%. The 5-year disease-free survival rate was 81%, while the 5-year overall survival rate was 86%. Remarkably, the 5-year colostomy-free survival rate was 65%. In another series of nine patients with locally advanced or metastatic rectal SCC, induction with docetaxel, 5-fluorouracil, and cisplatin (DCF) determined a promising response rate that was further increased after chemoradiation (16). For patients with metastatic disease, no evidence based on prospective studies is currently available. In a case series from the Mayo Clinic, 52 patients with advanced rectal SCC were included; however, the exact number of cases with metastatic disease was not indicated (17). Based on these findings, it is reasonable to treat rectal SCC similarly to anal SCC with CRT in cases of locally advanced disease and platinum-based chemotherapy in combination with 5-fluorouracil or taxane for metastatic disease (1).

Intriguingly, our case report is the first one to use a conservative approach for synchronous rectal and anal lesions. The patient received the combination of mitomycin *c* 10 mg/m^2 on days 1 and 29 together with capecitabine 825 mg/m^2 (bid) with concurrent radiotherapy for a total dose of 60 Gy with curative intent. According to the ESMO guidelines, while the optimal dose for curative CRT is not known, for patients with locally advanced anal cancer, the radiotherapy dose should be >50.4 Gy (3). In the absence of prospective studies, we can consider these recommendations also valid for rectal SCC. The definition of the best time for tumor assessment in rectal SCC is not yet defined. In the ACT II study, it has been shown that a significant proportion of patients with anal SCC treated with CRT do not exhibit a complete response when assessed at 10–12 weeks and could display a complete tumor regression at 26 weeks from the beginning of CRT (18).

Clinical and radiological evaluation after 6 months of the beginning of chemoradiation showed no evidence of disease and a complete clinical response. After a longer follow-up of 2 years, no evidence of occurrence was observed without residual toxicity.

Conclusion

Rectal SCC is an uncommon malignancy with limited evidence to guide treatment decisions. In this scenario, we report the first case of synchronous rectal and anal HPV SCC treated with conservative CRT. While more cases are needed to better understand the biology and multidisciplinary approach, we think that our case report could be of interest in this orphan disease.

Patient perspective

When I started my oncological journey, I was full of fears. I met doctors who helped and supported me through the hardest of times. Thanks to teamwork, more than 2 years after the diagnosis, I recovered and went back to living normally.

Data availability statement

The original contributions presented in the study are included in the article/supplementary material. Further inquiries can be directed to the corresponding author.

Ethics statement

Written informed consent was obtained from the individual(s), and minor(s)' legal guardian/next of kin, for the publication of any potentially identifiable images or data included in this article.

Author contributions

Conceptualization: DC. Original writing: DC, ST, and PP. Data collection: all the authors. Supervision: RG, SC, FC, AR, and EM. All authors contributed to the article and approved the submitted version.

Conflict of interest

The authors declare that the research was conducted in the absence of any commercial or financial relationships that could be construed as a potential conflict of interest.

Publisher's note

All claims expressed in this article are solely those of the authors and do not necessarily represent those of their affiliated organizations, or those of the publisher, the editors and the reviewers. Any product that may be evaluated in this article, or claim that may be made by its manufacturer, is not guaranteed or endorsed by the publisher.

References

1. Astaras C, Bornand A, Koessler T. Squamous rectal carcinoma: a rare malignancy, literature review and management recommendations. *ESMO Open* (2021) 6(4):100180. doi: 10.1016/j.esmoop.2021.100180

2. Dyson T, Draganov PV. Squamous cell cancer of the rectum. *World J Gastroenterol* (2009) 15(35):4380–6. doi: 10.3748/wjg.15.4380

3. Rao S, Guren MG, Khan K, Brown G, Renehan AG, Steigen SE, et al. Anal cancer: ESMO clinical practice guidelines for diagnosis, treatment and follow-up☆. *Ann Oncol* (2021) 32(9):1087–100. doi: 10.1016/j.annonc.2021.06.015

4. Madhu YC. Synchronous squamous cell carcinoma of the anorectum and proctosigmoid-a case report. *Indian J Surg* (2018) 80(1):77–80. doi: 10.1007/s12262-017-1716-x

5. Jabbar S, Soni SC, Selvakumar B, Taywade S, Elhence P. Synchronous squamous cell carcinoma of rectum and anal canal- a rare entity. (2022). doi: 10.21203/rs.3.rs-1735444/v1

6. Sundriyal D, Shirsi N, Kotwal S, Dawar R. Squamous cell carcinoma of rectum: how to treat? *Indian J Surg Oncol* (2015) 6(3):300–302. doi: 10.1007/s13193-015-0434-8

7. Williams GT, Blackshaw AJ, Morson BC. Squamous carcinoma of the colorectum and its genesis. *J Pathol* (1979) 129(3):139–47. doi: 10.1002/path.1711290306

8. Almagro UA, Pintar K, Zellmer RB. Squamous metaplasia in colorectal polyps. *Cancer* (1984) 53(12):2679–82. doi: 10.1002/1097-0142(19840615)53:12<2679::aid-cncr2820531219>3.0.co;2-6

9. Lin C, Franceschi S, Clifford GM. Human papillomavirus types from infection to cancer in the anus, according to sex and HIV status: a systematic review and meta-analysis. *Lancet Infect Dis* (2018) 18(2):198–206. doi: 10.1016/S1473-3099(17)30653-9

10. Audeau A, Han HW, Johnston MJ, Whitehead MW, Frizelle FA. Does human papilloma virus have a role in squamous cell carcinoma of the colon and upper rectum? *Eur J Surg Oncol* (2002) 28(6):657–60. doi: 10.1053/ejso.2002.1304

11. Matsuda A, Takahashi K, Yamaguchi T, Matsumoto H, Miyamoto H, Kawakami M, et al. HPV infection in an HIV-positive patient with primary squamous cell carcinoma of rectum. *Int J Clin Oncol* (2009) 14(6):551–4. doi: 10.1007/s10147-009-0890-7

12. Sotlar K, Köveker G, Aepinus C, Selinka HC, Kandolf R, Bültmann B. Human papillomavirus type 16-associated primary squamous cell carcinoma of the rectum. *Gastroenterology* (2001) 120(4):988–94. doi: 10.1053/gast.2001.22523

13. Guerra GR, Kong CH, Warrier SK, Lynch AC, Heriot AG, Ngan SY. Primary squamous cell carcinoma of the rectum: an update and implications for treatment. *World J Gastrointest Surg* (2016) 8(3):252–65. doi: 10.4240/wjgs.v8.i3.252

14. Song EJ, Jacobs CD, Palta M, Willett CG, Wu Y, Czito BG. Evaluating treatment protocols for rectal squamous cell carcinomas: the duke experience and literature. *J Gastrointest Oncol* (2020) 11(2):242–9. doi: 10.21037/jgo.2018.11.02

15. Loganadane G, Servagi-Vernat S, Schernberg A, Schlienger M, Touboul E, Bosset JF, et al. Chemoradiation in rectal squamous cell carcinoma: bi-institutional case series. *Eur J Cancer* (2016) 58:83–9. doi: 10.1016/j.ejca.2016.02.005

16. Hervé L, Kim S, Boustani J, Klajer E, Pernot M, Nguyen T, et al. Modified DCF (Docetaxel, Cisplatin and 5-fluorouracil) chemotherapy is effective for the treatment of advanced rectal squamous cell carcinoma. *Front Oncol* (2022) 12:974108. doi: 10.3389/fonc.2022.974108

17. Frizelle FA, Hobday KS, Batts KP, Nelson H. Adenosquamous and squamous carcinoma of the colon and upper rectum: a clinical and histopathologic study. *Dis Colon Rectum* (2001) 44(3):341–6. doi: 10.1007/BF02234730

18. Glynne-Jones R, Sebag-Montefiore D, Meadows HM, Cunningham D, Begum R, Adab F, et al. Best time to assess complete clinical response after chemoradiotherapy in squamous cell carcinoma of the anus (ACT II): a *post-hoc* analysis of randomised controlled phase 3 trial [published correction appears in lancet oncol. 2017 Apr;18(4):e196]. *Lancet Oncol* (2017) 18(3):347–56. doi: 10.1016/S1470-2045(17)30071-2

frontiers | Frontiers in Oncology

TYPE Original Research
PUBLISHED 12 June 2023
DOI 10.3389/fonc.2023.1118518

OPEN ACCESS

EDITED BY
Vincenza Granata,
IRCCS, Italy

REVIEWED BY
Giuditta Chiloiro,
IRCCS, Italy
Manuel Conson,
University of Naples Federico II, Italy
Joost Nederend,
Catharina Hospital, Netherlands

*CORRESPONDENCE
Li Ding
dingli6@mail.sysu.edu.cn
Yong Bao
baoyong@mail.sysu.edu.cn

†These authors have contributed equally to this work

RECEIVED 07 December 2022
ACCEPTED 16 May 2023
PUBLISHED 12 June 2023

CITATION
Niu S, Chen Y, Peng F, Wen J, Xiong J, Yang Z, Peng J, Bao Y and Ding L (2023) The role of MRI after neochemoradiotherapy in predicting pathological tumor regression grade and clinical outcome in patients with locally advanced rectal adenocarcinoma. *Front. Oncol.* 13:1118518. doi: 10.3389/fonc.2023.1118518

The role of MRI after neochemoradiotherapy in predicting pathological tumor regression grade and clinical outcome in patients with locally advanced rectal adenocarcinoma

Shaoqing Niu[1†], Yan Chen[2†], Fang Peng[1†], Jie Wen[3], Jianqi Xiong[1], Zhuangzhuang Yang[1], Jianjun Peng[4], Yong Bao[1*] and Li Ding[5*]

[1]Department of Radiation Oncology, the First Affiliated Hospital, Sun Yat-sen University, Guangzhou, China, [2]Department of Radiology, the First Affiliated Hospital, Sun Yat-sen University, Guangzhou, China, [3]Department of Interventional Oncology, the First Affiliated Hospital, Sun Yat-sen University, Guangzhou, China, [4]Gastrointestinal Surgery Center, the First Affiliated Hospital, Sun Yat-sen University, Guangzhou, China, [5]Department of Pathology, the First Affiliated Hospital, Sun Yat-sen University, Guangzhou, China

Objective: To evaluate the predictive value of tumor regression grade assessed by MRI (mr-TRG) after neoadjuvant chemoradiotherapy (neo-CRT) for postoperative pathological TRG (pTRG) and prognosis in patients with locally advanced rectal adenocarcinoma (LARC).

Materials and methods: This was a retrospective study from a single center experience. The patients who were diagnosed with LARC and received neo-CRT in our department between January 2016 and July 2021 were enrolled. The agreement between mrTRG and pTRG was assessed with the weighted κ test. Overall survival (OS), progress-free survival (PFS), local recurrence-free survival (LRFS), and distant metastasis-free survival (DMFS) were calculated by Kaplan-Meier analysis and log-rank test.

Results: From January 2016 to July 2021, 121 LARC patients received neo-CRT in our department. Among them, 54 patients had complete clinical data, including MRI of pre- and post-neo-CRT, postoperative tumor samples, and follow-up. The median follow-up time was 34.6 months (range: 4.4-70.6 months). The estimated 3-year OS, PFS, LRFS and DMFS were 78.5%, 70.7%, 89.0%, and 75.2%, respectively. The median time from the completion of neo-CRT to preoperative MRI and surgery was 7.1 weeks and 9.7 weeks, respectively. Out of 54 patients, 5 patients achieved mrTRG1 (9.3%), 37 achieved mrTRG2 (68.5%), 8 achieved mrTRG3 (14.8%), 4 achieved mrTRG4 (7.4%), and no patient achieved mrTRG5 after neo-CRT. Regarding pTRG, 12 patients achieved pTRG0 (22.2%), 10 achieved pTRG1 (18.5%), 26 achieved pTRG2 (48.1%), and 6 achieved pTRG3 (11.1%). The agreement between three-tier mrTRG (mrTRG1 vs. mrTRG2-3 vs. mrTRG4-5) and pTRG (pTRG0 vs. pTRG1-2 vs. pTRG3) was fair (weighted kappa=0.287). In a dichotomous classification, the agreement between mrTRG

(mrTRG1 vs. mrTRG2-5)and pTRG(pTRG0 vs. pTRG1-3) also resulted in fair agreement (weighted kappa=0.391). The sensitivity, specificity, positive, and negative predictive values of favorable mrTRG (mrTRG 1-2) for pathological complete response (PCR) were 75.0%, 21.4%, 21.4%, and 75.0%, respectively. In univariate analysis, favorable mrTRG (mrTRG1-2) and downstaging N were significantly associated with better OS, while favorable mrTRG (mrTRG1-2), downstaging T, and downstaging N were significantly associated with superior PFS (p<0.05). In multivariate analysis, downstaging N was an independent prognostic factor for OS. Meanwhile, downstaging T and downstaging N remained independent prognostic factors for PFS.

Conclusions: Although the consistency between mrTRG and pTRG is only fair, favorable mrTRG after neo-CRT may be used as a potential prognostic factor for LARC patients.

KEYWORDS

rectal cancer, neoadjuvant therapy, magnetic resonance imaging, tumor regression grade, prognosis

Introduction

Colorectal cancer is the third most common type of cancer and the second leading cause of cancer death according to GLOBOCAN 2020 estimates (1). Different treatment strategies were adopted for different tumor-node-metastasis (TNM) stage diseases combined with clinical features, such as the status of circumferential resection margin (CRM) and extramural venous invasion (EMVI) (2). According to the latest NCCN guidelines, neoadjuvant chemoradiotherapy (neo-CRT) followed by surgery and postoperative chemotherapy (ChT) is the standard care for patients with stage II-III rectal cancer (2).

In the whole process of diagnosis and treatment, pelvic MR and postoperative pathological results play a fatal role in making appropriate treatment decisions for locally advanced rectal adenocarcinoma (LARC) patients. Taking advantage of superior soft-tissue contrast and the ability to allow multiplanar imaging and functional evaluation, MRI is not only considered to be the gold standard of rectal cancer staging but also the best way to assess response to neo-CRT and predict prognosis (3–5). Mandard, Dworak, the American Joint Committee on Cancer (AJCC) and the College of American Pathologists (CAP) created different pathology tumor regression grade (pTRG) systems to evaluate different tumor responses to neo-CRT, which were indicated to be effective and prognostic factors in future studies (6–10). Then, the MERCURY study group established an MRI-assessed tumor regression grade (mr-TRG) system that was analogous to pTRG (5).

However, there was no consistent result of the agreement between mrTRG and pTRG (11, 12). Here, we enrolled 54 LARC patients who received neo-CRT and surgery. In addition to complete routine clinicopathological data, all of them had MRI examination pre- and post- neo-CRT, and operative specimens. The responses of each patient were assessed by MRI after neo-CRT (mrTRG) and by postsurgical histopathologic specimens (pTRG). This study aimed to investigate the consistency of mrTRG and pTRG in these pTRG-defined patients, and to evaluate the predictive value of mr-TRG for prognosis. Furthermore, we hope to provide more valuable information for LARC patients before surgery, and even give some patients who were assessed with favorable mrTRG the opportunity to choose “watch and wait”, which is an organ preservation treatment strategy (13).

Materials and methods

Patients

This was an observational study approved by our institutional medical ethics committee (No [2021].125). From January 2016 to July 2021, 121 LARC patients received neo-CRT at Department of Radiotherapy of the First Affiliated Hospital, Sun Yat-sen University. Before treatment, written informed consent was obtained from all patients. All patients were confirmed histologically as adenocarcinoma. Imaging diagnoses of them were stage II or III disease by pelvic MRI, chest/abdominal CT with contrast, and endorectal ultrasound.

Treatment details

The treatment strategies of all patients were managed by the gastrointestinal center multidisciplinary team (MDT). All patients received long-course radiotherapy (LCRT) with concurrent ChT and surgery. Radiotherapy (RT) was delivered with volume modulated arc

therapy (VMAT). Gross tumor volume (GTV) was defined as the primary tumor (GTVp) and positive lymph nodes (GTVn). Clinical target volume (CTV) included the GTV plus areas at risk for microscopic spread from the primary tumor and at-risk nodal areas (14). The prescribed doses delivered to GTVp and GTVn were 50 Gy for 43 patients, 52.5 Gy for 10 patients, 60 Gy for one patient respectively, and the doses delivered to CTV were 45 Gy for 45 patients, 46 Gy for 9 patients respectively, all delivered in 25 daily fractions. The surgical procedures include Dixon, Miles, Parks, Hartmann and local excision.

The concurrent ChT regimens with RT included CapeOx (Oxaliplatin 130 mg/m^2 on Day 1 + Capecitabine 1000 mg/m^2 twice daily for 14 days, repeated for 3 weeks)for 28 patients, Capecitabine (825mg/m^2 twice daily for 5 days a week) for 22 patients, and mFOLFOX (Oxaliplatin 85 mg/m^2 on Day 1, leucovorin 400 mg/m^2 on Day 1, 5-Fu 400 mg/m^2 bolus on Day 1, followed by 1200 mg/m^2/day for 2 days, over 46-48 hours continuous infusion, repeated for 2 weeks) for 4 patients. The adjuvant ChT regimens included CapeOx for 29 patients and mFOLFOX for 4 patients.

MRI examination and evaluation

Appropriate (20-80 mL) ultrasound gel was used to provide enhanced depiction of the tumor, except for patients with low or large rectal tumors. Before imaging, 20 mg of raceanisodamine hydrochloride was intramuscularly injected to decrease intestinal peristalsis artefacts. All rectal MR images were performed using a 3.0 T MR scanner (Magnetom Verio, Siemens Healthcare, Erlangen, Germany) with a 6-channel phased-array surface coil. All patients were imaged in the supine position and oriented feet-first. The imaging protocols comprised (a) axial turbo spin-echo T2-weithed imaging (T2WI); (b) high-spatial-resolution turbo spin-echo T2WI in sagittal, coronal and oblique axial planes with the oblique axial plane perpendicular to the tumor base; and (c) axial diffusion-weighted imaging (DWI) with b factors of 0 and 1000 s/mm^2 using a single-shot echo-planner imaging sequence. Detailed protocols are listed in Table 1.

Two radiologists experienced in rectal MRI (6 and 5 years) independently reviewed the paired MR images (pre- and post-neo-CRT) without knowledge of the postoperative histopathological results. For a consensus or majority decision, discrepancies were resolved by a third radiologist with more than 20 years of experience in rectal MRI.

A semiquantitative MRI-based tumor regression grade has been implemented (3) (Supplementary materials). We combined T2WI and DWI to assess the relative proportions of residual tumor and the degree of morphologic changes such as fibrosis and mucin production on post-neo-CRT MR images (15, 16). On T2WI, tumor fibrosis demonstrates a signal intensity similar to that of the normal muscularis propria, mucin production within a treated tumor manifests as an interval increase in signal intensity, and residual tumor demonstrates a more intermediate signal intensity similar to that on pretreatment MR images. A hyperintense signal on high-b-value (1000 s/mm^2) DWI at the former tumor location, with low signal intensity on the apparent diffusion coefficient map, was considered to be tumor signal. When there was a discrepancy between two image sets, it was resolved through a complementary approach. For example, confusingly high signal intensity of a lesion on DWI that might have been caused by mucinous change or artifacts was interpreted on T2WI and an apparent diffusion coefficient map. In addition, it should give priority to DWI when ambiguously intermediate high signal intensity of a lesion on T2WI that was difficult to decide residual tumor or radiation fibrosis. Two patients who were assessed as mrTRG2 and mrTRG4 after neo-CRT are presented in Figure 1, 2, respectively.

Pathological evaluation

Formalin fixation and paraffin-embedding (FFPE) tissue sections were cut into 5 μm thick slices and fixed in 4% paraformaldehyde PFA for assessment. Subsequently, the slices were used to perform haematoxylin-eosin (HE) staining. The slides were stained following the HE staining kit (Solarbio, G1120) protocol and observed by microscopy. The specimens were examined and analysed by a pathologist with 10 years of experience and were further reviewed by a dedicated gastrointestinal pathologist, both of whom were blinded to the MRI data. The pTRG-based tumor regression grade assessment system recommended by the AJCC Cancer Staging Manual, Eighth Edition and the CAP Guidelines (17, 18) was implemented in this study (Figure 3) (Supplementary material). Pathological complete response (PCR) was defined as the absence of viable tumor cells in the primary tumor and lymph nodes.

TABLE 1 MRI protocols for Rectal Cancer.

Parameters	Axial T2WI	Sagittal T2WI	Coronal T2WI	Oblique axial T2WI	Axial DWI
TR/TE (ms)	3000/87	3000/87	4000/77	3000/84	3800/74.4
Slice thickness(mm)	5	3	3	3	6
Distance factor (%)	20	0	0	0	20
Slices	25	19	25	24	21
FOV(mm^2)	260×260	180×180	220×220	180×180	300×245
Voxel size (mm^3)	0.8× 0.7×5.0	0.7× 0.6×3.0	0.7× 0.6×3.0	0.6× 0.6×3.0	2.7× 2.7×6.0
Time acquisition	2 min 54 s	2 min 30 s	2 min 52 s	3 min 18 s	6 min 1 s

TR, repetition time; TE, echo time; FOV, field of view; T2WI, T2-weighted imaging; DWI, diffusion-weighted imaging.

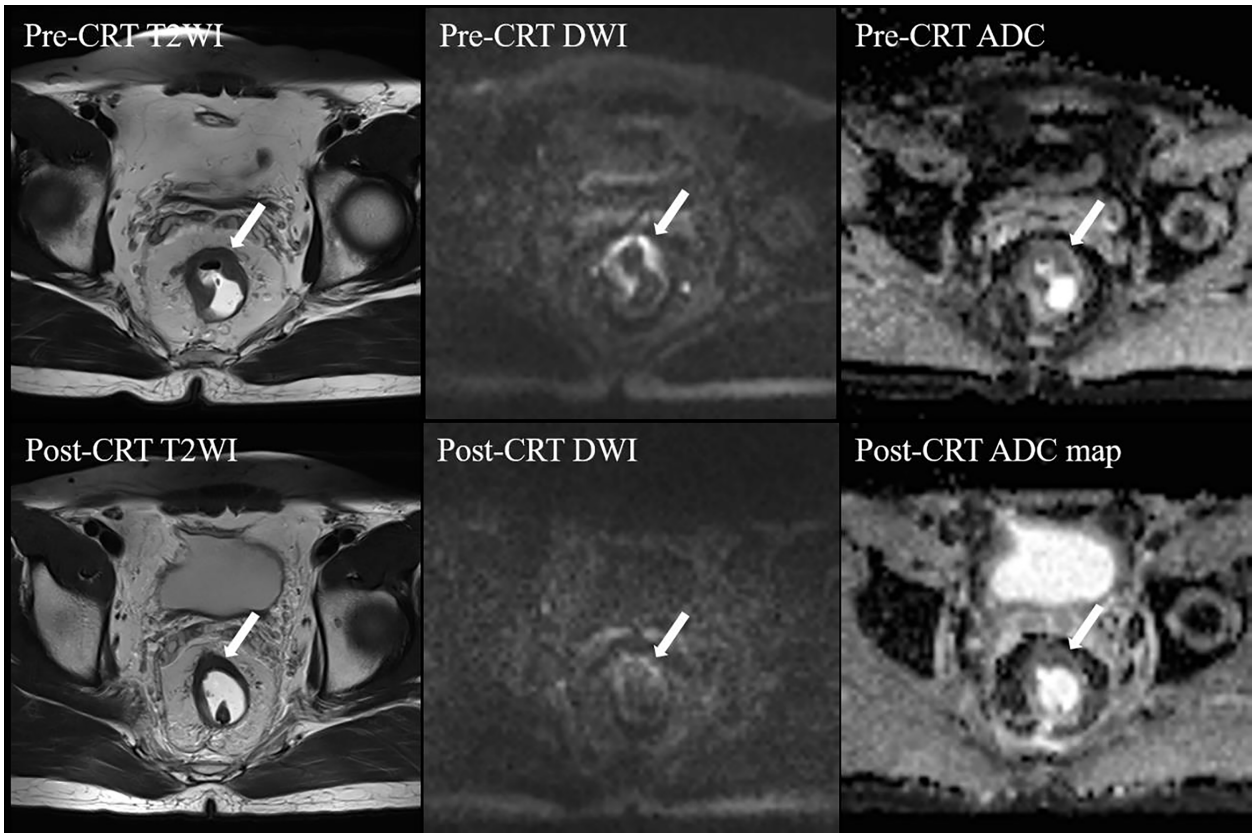

FIGURE 1
MRI tumor regression grade 2 in a 43-year-old man after neo-CRT. Post-neo-CRT T2WI shows a remarkable decrease in the tumor size with the remaining hypointense "fibrotic" thickening of the wall without visible tumor signal, whereas high *b* value post-CRT-DWI shows linear high signal intensity at the tumor bed, with low signal intensity on post-CRT-ADC map, indicating residual tumor. CRT, chemoradiotherapy; T2WI, T2-weighed imaging; DWI, diffusion-weighted imaging; ADC, apparent diffusion coefficient. The white arrows indicate tumor.

Follow-up

The follow-up visits were performed every 3 months during the first 2 years after treatment, every 6 months in the subsequent 3 years, and then yearly thereafter. Patients were followed up by telephone until the last visit on March 10, 2022 or death.

Statistical analysis

The primary end point is the agreement between mrTRG and pTRG. The strength of agreement was assessed using the weighted kappa test. Kappa values were assessed as follows: 0.81-1.00, excellent agreement; 0.61-0.80, good agreement; 0.41-0.60, moderate agreement; 0.21-0.40, fair agreement; and 0.00-0.20, poor agreement. Dichotomous classification for mrTRG (mrTRG1-2 vs. mrTRG 3-5) and pTRG (pTRG 0 vs. pTRG 1-3) was performed to assess the ability of mrTRG to identify PCR by calculating sensitivity, specificity, and positive and negative predictive values.

The secondary end points were the overall survival (OS), local-regional recurrence-free survival (LRFS), progression-free survival (PFS), and distant metastasis-free survival (DMFS) of the enrolled patients. The Kaplan-Meier method and log-rank test were used to assess the differences between favorable (mrTRG1-2) and unfavorable (mrTRG 3-5) patients. *P* values of less than 0.05 with two sides were considered statistically significant. Survival was analyzed with the log-rank test by SPSS software (SPSS. Inc., Version 25, Chicago, IL).

Results

Clinicopathological characteristics

Except for the patients with missing MRI or post surgery specimens or those lost to follow-up, a total of 54 patients with complete clinical data, including MRI information (before and after neo-CRT), postoperative tumor samples, and follow-up, were enrolled in this retrospective study. There were 40 males and 14 females, and the median age at diagnosis was 55 years old (range: 27-74 years). There were 2 patient with stage II disease and 52 patients with stage III disease. There were 42 patients with positive CRM, and 12 patients with negative CRM. There were 38 patients with positive EMVI, 16 patients with negative EMVI. Thirteen patients were diagnosed as peritoneal reflection involved before

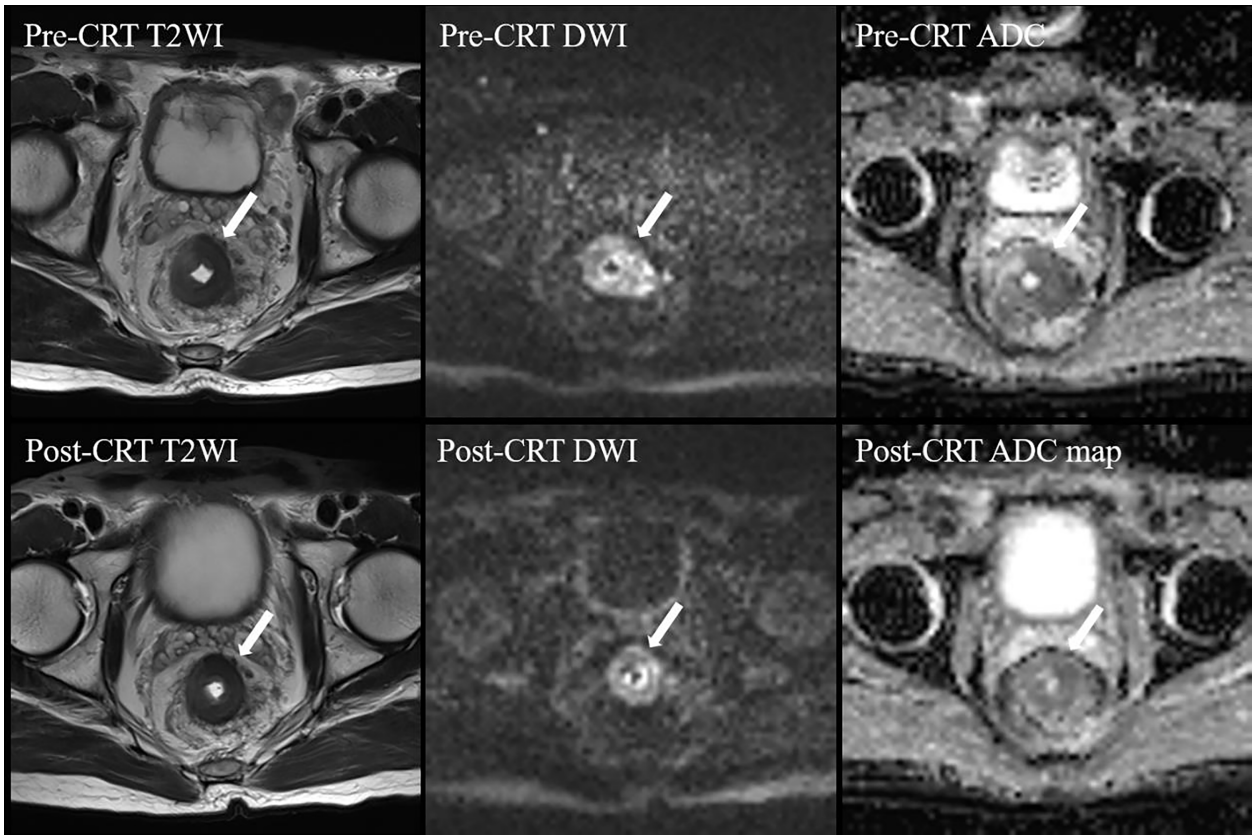

FIGURE 2
MRI tumor regression grade 4 in a 59-year-old man after CRT. Post-CRT T2WI shows a slight reduction (< 50%) in the tumor size with a majority of intermediate signal intensity. On high b value post-CRT-DWI, a thick layer of diffusion restriction was apparent at the tumor bed. CRT, chemoradiotherapy; T2WI, T2-weighed imaging; DWI, diffusion-weighted imaging; ADC, apparent diffusion coefficient.

treatment. The tumor locations included 3 in the upper rectum, 35 in the middle rectum, and 16 in the lower rectum. All clinicopathological characteristics were summarized in Table 2.

Among the 54 patients, 33 patients received neo-CRT and surgery with postoperative ChT, and 21 patients received neo-CRT and surgery. The median RT doses were 50 Gy (range: 50-60 Gy) for GTVp and GTVn, and 45 Gy (range: 45-46 Gy) for CTV, all delivered in 25 daily fractions. The median cycle was 3 for neo-ChT (range: 1-7), and 4 for adjuvant ChT (range: 1-7). The total mesorectal excision (TME) was performed in most (53/54, 98.1%) patients after neo-CRT. The surgical procedures include Dixon (n=41), Miles (n=10), Parks (n=1), Hartmann(n=1), and local excision (n=1).

Of these 54 patients with complete mrTRG and pTRG assessment, 5 patients achieved mrTRG1 (9.3%), 37 achieved mrTRG2 (68.5%), 8 achieved mrTRG3 (14.8%), 4 achieved mrTRG4 (7.4%), and no patient achieved mrTRG5 after neo-CRT. One patient received R1 excision, and the remaining 53 patients received R0 excision. Regarding pTRG, 12 patients achieved pTRG0 (22.2%), 10 patients achieved pTRG1 (18.5%), 26 patients achieved pTRG2 (48.1%), and 6 patients achieved pTRG3 (11.1%) (Table 3).

The agreement between mrTRG and pTRG

The agreement between the three-tier mrTRG (mrTRG1 vs. mrTRG2-3 vs. mrTRG4-5) and pTRG (pTRG0 vs. pTRG1-2 vs. pTRG3) classes was fair (weighted kappa=0.287). In a dichotomous classification, assessment of the agreement between mrTRG (mrTRG1 vs. mrTRG2-5)and pTRG(pTRG0 vs. pTRG1-3) also resulted in fair agreement (weighted kappa =0.391).

When a dichotomous classification (mrTRG 1-2 vs. mrTRG 3-5) was used to assess the ability of mrTRG to predict PCR (pTRG0), 9 out of 12 patients (75.0%) were correctly identified. The sensitivity, specificity, and positive and negative predictive values of mrTRG were 75.0%, 21.4%, 21.4%, and 75.0%, respectively.

Prognosis and survival

The median follow-up time of all patients was 34.6 months (range: 4.4-70.1 months). The estimated 3-year OS, PFS, LRFS and DMFS were 78.5%, 70.7%, 89.0%, and 75.2%, respectively (Figure 4A).

During follow-up, two patients developed local-recurrence, and the tumor site was located anterior to the sacrum. Twelve patients

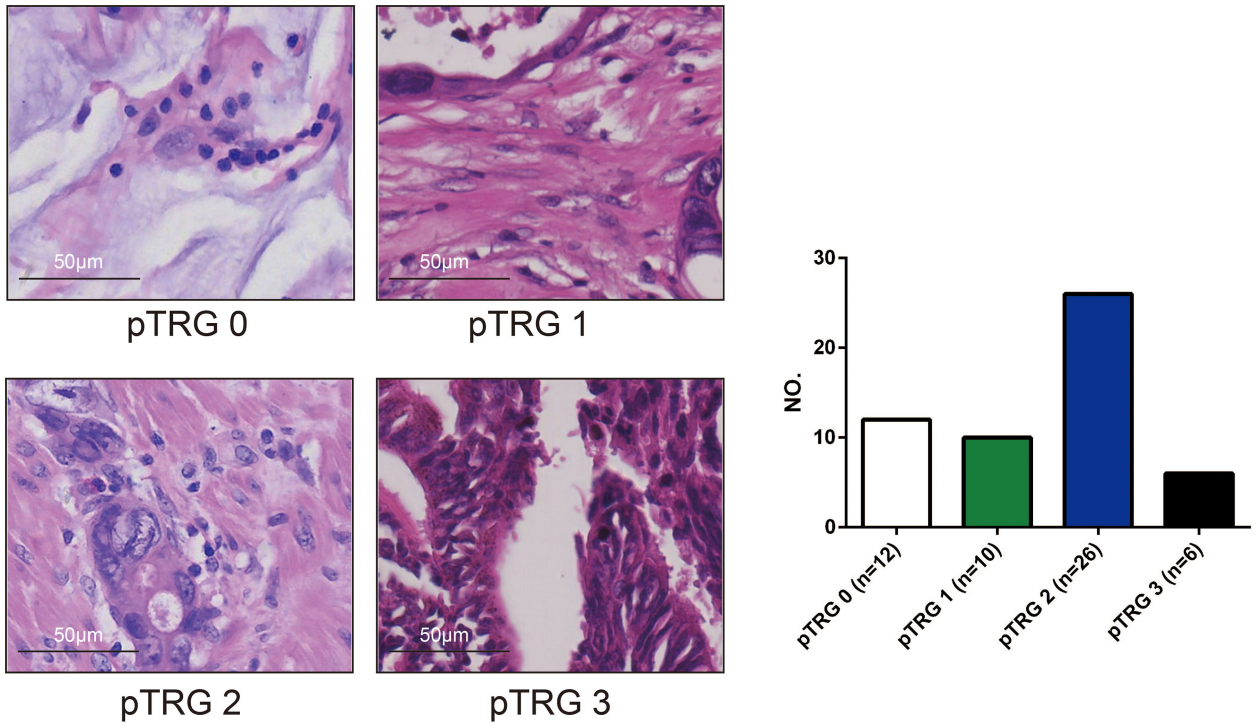

FIGURE 3
The pathological tumour regression (pTRG) assessment results (photomicrograph H and E, 400x). There were 12 patients with pTRG grade 0, 10 patients with pTRG grade 1, 26 patients with pTRG grade 2, and 6 patients with pTRG grade 3, respectively.

TABLE 2 Baseline characteristics and predictive value for prognosis.

Characteristic	N	(%)	OS		PFS		LRFS	
			3-y rate (%)	*P*	3-y rate (%)	*P*	3-y rate (%)	*P*
Age								
≤50y	20	37.0	86.1	0.124	70.4	0.702	95.0	0.843
>50y	34	63.0	73.3		72.0		96.4	
Meidan: 55 years old, rang (27-74)								
Gender								
Male	40	74.1	71.6	0.215	67.5	0.398	94.3	0.404
Female	14	25.9	100		83.6		100	
Tumor location*								
Upper	3	5.6	100	0.318	66.7	0.672	100	0.500
Middle	35	64.8	74.0		66.5		92.8	
Lower	16	29.6	82.0		79.8		100	
cT stage								
T3	35	64.8	78.4	0.569	64.9	0.224	93.1	0.260
T4	19	35.2	79.3		82.5		100	
cN stage								
N0	2	3.7	50.0	0.336	50.0	0.540	100	0.162
N1	20	37.0	82.0		68.8		88.2	

(Continued)

TABLE 2 Continued

Characteristic	N	(%)	OS		PFS		LRFS	
			3-y rate (%)	*P*	3-y rate (%)	*P*	3-y rate (%)	*P*
N2	32	59.3	77.8		74.0		100	
Stage								
II	2	3.7	50.0	0.221	50.0	0.291	100	0.764
III	52	96.3	79.6		72.1		95.6	
CEA level								
Elevated	25	46.3	86.9	0.228	81.1	0.181	95.5	0.915
Normal	29	53.7	70.9		69.2		95.8	
CRM								
Positive	42	77.8	80.9	0.448	69.2	0.697	97.2	0.299
Negative	12	22.2	67.5		81.5		90.0	
EMVI								
Positive	38	70.4	80.0	0.655	77.0	0.766	97.1	0.488
Negative	16	29.6	78.7		69.7		92.3	
Down-stage T/mrTRG/								
Yes	33	61.1	81.8	0.108	81.2	0.019	96.7	0.666
No	21	38.9	73.7		55.0		94.4	
Down-stage N								
Yes	46	85.2	84.3	0.003	76.2	0.019	100	<0.001
No	8	14.8	50.0		42.9		71.4	
mrTRG								
Grade 1	5	9.3	100	0.027	80.0	0.017	100	0.030
Grade 2	37	68.5	85.3		76.6		100	
Grade 3	8	14.8	36.5		66.7		83.3	
Grade 4	4	7.4	50.0		25.0		66.7	
Grade 5	0	0	–		–		–	
pTRG								
Grade 0	12	22.2	71.4	0.798	70.1	0.291	100	0.002
Grade 1	10	18.5	88.9		88.9		100	
Grade 2	26	48.1	75.8		71.1		100	
Grade 3	6	11.1	83.3		50.0		66.7	

OS: overall survival, LRFS: local-regional recurrence-free survival, PFS: progression-free survival, cT stage: clinical T stage, cN stage: clinical N stage, EMVI: extramural venous invasion, CRM: circumferential resection margin, mrTRG: MRI-assessed tumor regression grade, pTRG: pathology-assessed tumor regression grade; CEA: carcinoembryonic antigen.
* The distance form anal verge assessed by MRI (Upper: >10cm; Middle: 5-10cm; Lower: ≤5cm).
"-" means unavailable.

developed distant metastases, and the most common metastatic sites included the lung (n=5), liver (n=3), retroperitoneal lymph nodes (n=3), and bone (n=1).

In univariate analysis, downstage N and favorable mrTRG were significantly associated with better OS (p=0.003 for downstage N, Figure 4B; *p*=0.027 for mrTRG, Figure 4C), while favorable mrTRG, downstage T and downstage N were significantly associated with better PFS (*p*=0.017 for mrTRG, Figure 4D; *p*=0.019 for downstage T, Figure 4E; *p*=0.019 for downstage N, Figure 4F) (Table 2). The factors with a *P* value of less than 0.1 in univariable analysis were included in the multivariable analysis. In multivariate analysis, downstaging N (*p*=0.045) was an independent prognostic factor for OS. Meanwhile, downstaging T (*p*=0.011) and downstaging N (*p*=0.012) were independent prognostic factors for PFS (Table 4).

10.3389/fonc.2023.1118518

TABLE 3 Comparison between mrTRG and pTRG.

		mrTRG					Total
		1	2	3	4	5	
pTRG	0	4	5	2	1	0	12
	1	0	7	2	1	0	10
	2	1	21	3	1	0	26
	3	0	4	1	1	0	6
Total		5	37	8	4	0	54

mrTRG, magnetic resonance tumor regression grade; pTRG, pathological tumour regression grade.

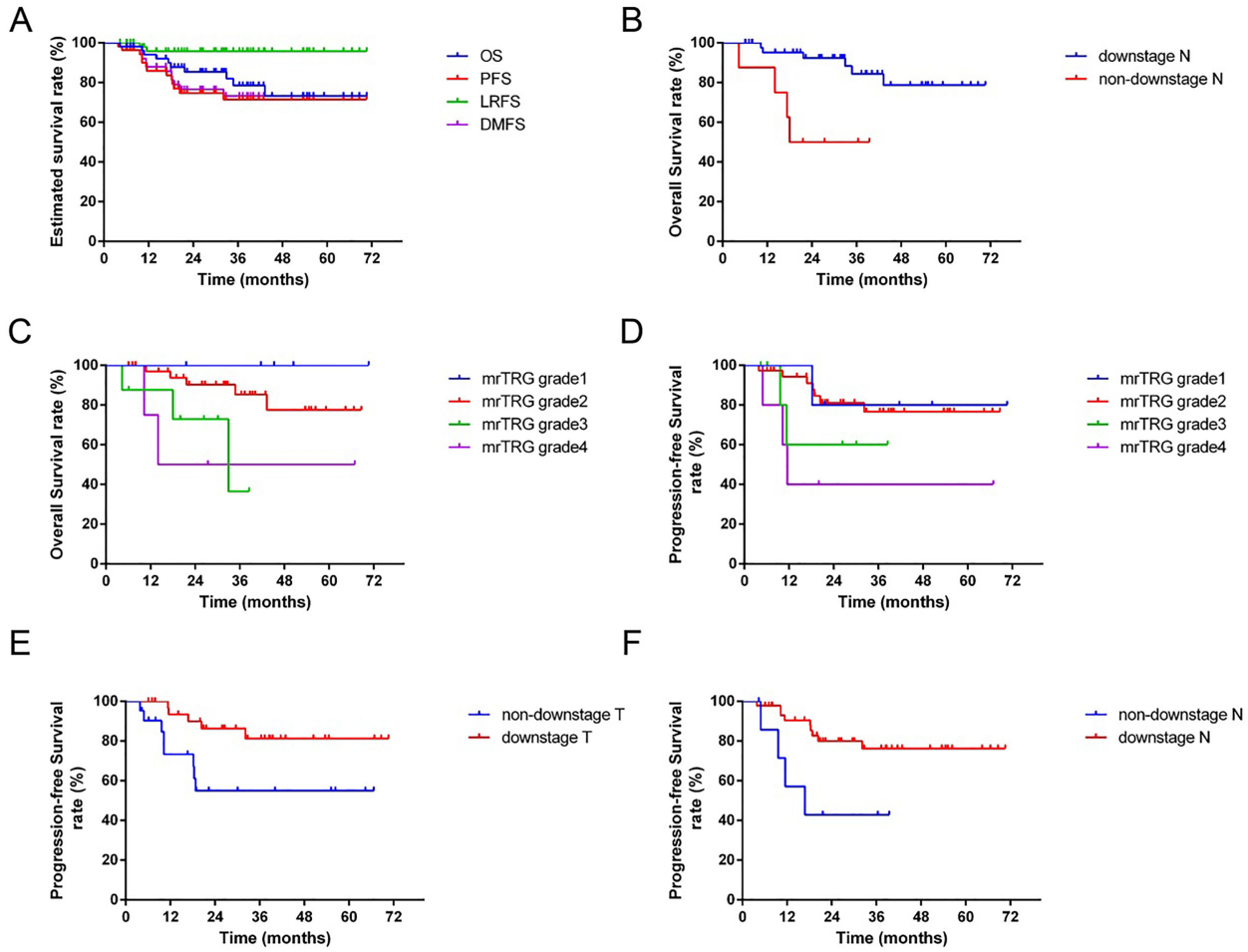

FIGURE 4
The survival curves for 54 patients. **(A)**: The estimated 3-year overall survival (OS), progress-free survival (PFS), local-regional recurrence-free survival (LRFS) and distance metastasis-free survival (DMFS) were 78.5%, 70.7%, 89.0%, and 75.2%, respectively. **(B)**: The 3-year OS of patients with downstage N was significantly better than the non-downstage N group (p=0.003). **(C)**: The 3-year OS of patients with favorable mrTRG was significantly better than the unfavorable group (p=0.027). **(D)**: The 3-year PFS of patients with favorable mrTRG was significantly better than the unfavorable group (p=0.017). **(E)**: The 3-year PFS of patients with downstage T was significantly better than the non-downstaging T group (p=0.019). **(F)**: The 3-year PFS of patients with downstage N was significantly better than the non-downstage N group (p=0.019).

Discussion

The main finding of this research was that favorable mrTRG (mrTRG1-2) after neo-CRT could be used as a potential prognostic factor for LARC patients. Another valuable finding was that although the consistency between mrTRG and pTRG was fair, the sensitivity (75.0%) and negative predictive values (75.0%) of mrTRG 1-2 for PCR were satisfactory.

For LARC patients, neo-CRT followed by surgery and postoperative ChT was the standard care (2), and accurate

TABLE 4 Multivariable Cox analysis of prognostic factors for OS and PFS.

Factors	OS		PFS	
	P value	HR (95%CI)	*P* value	HR (95%CI)
Down-stage T(Yes vs. No)	0.140	0.344 (0.084-1.417)	0.011	0.163 (0.040-0.665)
Down-stage N(Yes vs. No)	0.045	0.209 (0.045-0. 964)	0.012	0.153 (0.036-0.657)
mrTRG (Grade 1-2 vs. 3-4)	0.124	3.203 (0.727-14.118)	0.140	2.577 (0.733-9.059)
pTRG (PCR vs. non-PCR)	0.376	0.515 (0.118-2.240)	0.336	0.475 (0.104-2.164)

OS, Overall survival variable; PFS, Progress-free survival; HR, Hazard ratio; mrTRG, magnetic resonance tumour regression grade; pTRG, pathological tumour regression grade; PCR, pathological complete response.

restaging after neo-CRT and assessment of treatment response were critical to treatment decision-making throughout the process. In routine clinical work, MRI, postoperative pathological results, and hematologic tumor markers (e.g. CEA, CA199) are the most common detection means (19–23). However, there were some limitations in pathological and hematological markers. For example, postoperative pathological results can only be obtained after surgery, and hematology markers have certain fluctuations. With the advantages of high detection accuracy and noninvasiveness, pelvic MRI has become the most commonly used examination, for staging, restaging after neo-CRT and predicting the prognosis (4, 24). In this study, favorable mrTRG (mrTRG1-2) was significantly associated with better OS and PFS in univariate analysis, which was consistent with previous studies. However, pTRG (PCR vs. non-PCR) had no significant effect on prognosis in either univariate or multivariate analysis, which was different from previous research (8, 23, 25, 26). The main reason was that, compared with the PCR group (median cycle was 2, range: 0-5), patients in non-PCR group received more intense adjuvant ChT (median cycle was 4, range: 2-7). The different postoperative treatment strategies and small sample size of this study may reduce the difference in survival between the two groups.

In this study, the consistency between mrTRG and pTRG was fair (weighted kappa=0.287 for three-tier; weighted kappa=0.391 for a dichotomous classification), which was consistent with previous studies (12). However, the sensitivity (75.0%) and negative predictive values (75.0%) of mrTRG 1-2 for PCR were satisfactory. These results suggested that although mrTRG was not a surrogate of pTRG, favorable mrTRG may be a predictor for PCR. Therefore, in clinical work, patients with favorable mrTRG after neo-CRT could be recommended to adopt a "watch-and-wait" strategy, an organ preservation strategy to avoid complications from overtreatment, such as surgery. Previous study results showed no significant difference in recurrence and OS between patients managed with "watch-and-wait" after a clinical complete response and patients with PCR after operation (27).

Restaging MRI is more inclined to over stage of disease after neo-CRT in LARC patients as a result of the difficulties in assessing response within areas of post radiation fibrosis (28). Radiomics refers to the extraction of a vast number of qualitative and quantitative features from routine images using artificial intelligence that are effectively invisible to the human eye. MRI-based radiomics can help clinicians predict whether patients will achieve a PCR after neo-CRT before surgery to avoid excessive treatment (29). MRI-based radiomics has predictive value for the curative effect of neo-CRT on LARC patients and shows good predictive value in terms of tumor staging, postoperative metastasis, and prognosis after treatment (30). In the future, new MRI parameters could be added to mrTRG to increase the accuracy of PCR prediction and provide more valuable information to make treatment decisions.

There are some limitations to this study. First, the use of ultrasound gel is controversial and not recommended by the ESGAR guidelines. However, we filled the rectum with the appropriate amount of gel tailored to the size and location of the tumor. In this circumstance, rectal overdistension was avoided. Therefore, rectal gel filling had a minimal impact on the tumor staging evaluation. Moreover, rectal gel filling will reduce susceptibility artefacts related to luminal gas on DWI and may facilitate detection of smaller and treated tumor (31–33). Thus, rectal gel filling is useful for the mrTRG evaluation based on T2WI and DWI. Second, it was a retrospective study, and the surgical methods and ChT regimen were not completely uniform. Finally, the number of patients who met the criteria was small. In future work, we will produce a prospective study with large sample sizes to verify this result.

In conclusion, although the consistency between mrTRG and pTRG is only fair, favorable mrTRG after neo-CRT may be used as a potential prognostic factor for LARC patients'survival.

Data availability statement

The raw data supporting the conclusions of this article will be made available by the authors, without undue reservation.

Author contributions

SN, YC and FP drafted the manuscript and performed the statistical analysis; JW, JX, ZY and JP collected clinical data; YB and LD conceived the study and participated in its design and coordination. All authors contributed to the article and approved the submitted version.

Funding

Medical Scientific Research Foundation of Guangdong Province of China (A2022121 to SN). Natural Science Foundation of Guangdong Province, China (2023A1515011600 to SN).

Acknowledgments

We appreciate all the help and supports from doctors and patients enrolled from the department of Radiation Oncology, the First Affiliated Hospital, Sun Yat-sen University.

Conflict of interest

The authors declare that the research was conducted in the absence of any commercial or financial relationships that could be construed as a potential conflict of interest.

Publisher's note

Supplementary material

The Supplementary Material for this article can be found online at: https://www.frontiersin.org/articles/10.3389/fonc.2023.1118518/full#supplementary-material

References

1. Sung H, Ferlay J, Siegel RL, Laversanne M, Soerjomataram I, Jemal A, et al. Global cancer statistics 2020: GLOBOCAN estimates of incidence and mortality worldwide for 36 cancers in 185 countries. *CA Cancer J Clin* (2021) 71(3):209–49. doi: 10.3322/caac.21660

2. Benson AB, Venook AP, Al-Hawary MM, Azad N, Chen YJ, Ciombor KK, et al. Rectal cancer, version 2.2022, NCCN clinical practice guidelines in oncology. *J Natl Compr Canc Netw* (2022) 20(10):1139–67.

3. Kalisz KR, Enzerra MD, Paspulati RM. MRI Evaluation of the response of rectal cancer to neoadjuvant chemoradiation therapy. *Radiographics* (2019) 39(2):538–56. doi: 10.1148/rg.2019180075

4. Taylor FG, Quirke P, Heald RJ, Moran B, Blomqvist L, Swift I, et al. Preoperative high-resolution magnetic resonance imaging can identify good prognosis stage I, II, and III rectal cancer best managed by surgery alone: a prospective, multicenter, European study. *Ann Surg* (2011) 253(4):711–9. doi: 10.1097/SLA.0b013e31820b8d52

5. Patel UB, Taylor F, Blomqvist L, George C, Evans H, Tekkis P, et al. Magnetic resonance imaging-detected tumor response for locally advanced rectal cancer predicts survival outcomes: MERCURY experience. *J Clin Oncol* (2011) 29(28):3753–60. doi: 10.1200/JCO.2011.34.9068

6. Fokas E, Strobel P, Fietkau R, Ghadimi M, Liersch T, Grabenbauer GG, et al. Tumor regression grading after preoperative chemoradiotherapy as a prognostic factor and individual-level surrogate for disease-free survival in rectal cancer. *J Natl Cancer Inst* (2017) 109(12). doi: 10.1093/jnci/djx095

7. Dworak O, Keilholz L, Hoffmann A. Pathological features of rectal cancer after preoperative radiochemotherapy. *Int J Colorectal Dis* (1997) 12(1):19–23. doi: 10.1007/s003840050072

8. Erlandsson J, Lorinc E, Ahlberg M, Pettersson D, Holm T, Glimelius B, et al. Tumour regression after radiotherapy for rectal cancer - results from the randomised Stockholm III trial. *Radiother Oncol* (2019) 135:178–86. doi: 10.1016/j.radonc.2019.03.016

9. Mandard AM, Dalibard F, Mandard JC, Marnay J, Henry-Amar M, Petiot JF, et al. Pathologic assessment of tumor regression after preoperative chemoradiotherapy of esophageal carcinoma. clinicopathologic correlations. *Cancer* (1994) 73(11):2680–6. doi: 10.1002/1097-0142(19940601)73:11<2680::aid-cncr2820731105>3.0.co;2-c

10. Jager T, Neureiter D, Urbas R, Klieser E, Hitzl W, Emmanuel K, et al. Applicability of American joint committee on cancer and college of American pathologists regression grading system in rectal cancer. *Dis Colon Rectum* (2017) 60(8):815–26. doi: 10.1097/DCR.0000000000000806

11. Achilli P, Magistro C, Abd El Aziz MA, Calini G, Bertoglio CL, Ferrari G, et al. Modest agreement between magnetic resonance and pathological tumor regression after neoadjuvant therapy for rectal cancer in the real world. *Int J Cancer* (2022) 151(1):120–7. doi: 10.1002/ijc.33975

12. Sclafani F, Brown G, Cunningham D, Wotherspoon A, Mendes LST, Balyasnikova S, et al. Comparison between MRI and pathology in the assessment of tumour regression grade in rectal cancer. *Br J Cancer* (2017) 117(10):1478–85. doi: 10.1038/bjc.2017.320

13. Smith JJ, Strombom P, Chow OS, Roxburgh CS, Lynn P, Eaton A, et al. Assessment of a watch-and-Wait strategy for rectal cancer in patients with a complete response after neoadjuvant therapy. *JAMA Oncol* (2019) 5(4):e185896. doi: 10.1001/jamaoncol.2018.5896

14. Myerson RJ, Garofalo MC, El Naqa I, Abrams RA, Apte A, Bosch WR, et al. Elective clinical target volumes for conformal therapy in anorectal cancer: a radiation therapy oncology group consensus panel contouring atlas. *Int J Radiat Oncol Biol Phys* (2009) 74(3):824–30. doi: 10.1016/j.ijrobp.2008.08.070

15. Jang JK, Lee CM, Park SH, Kim JH, Kim J, Lim SB, et al. How to combine diffusion-weighted and T2-weighted imaging for MRI assessment of pathologic complete response to neoadjuvant chemoradiotherapy in patients with rectal cancer? *Korean J Radiol* (2021) 22(9):1451–61. doi: 10.3348/kjr.2020.1403

16. Park MJ, Kim SH, Lee SJ, Jang KM, Rhim H. Locally advanced rectal cancer: added value of diffusion-weighted MR imaging for predicting tumor clearance of the mesorectal fascia after neoadjuvant chemotherapy and radiation therapy. *Radiology* (2011) 260(3):771–80. doi: 10.1148/radiol.11102135

17. Ryan R, Gibbons D, Hyland JM, Treanor D, White A, Mulcahy HE, et al. Pathological response following long-course neoadjuvant chemoradiotherapy for locally advanced rectal cancer. *Histopathology* (2005) 47(2):141–6. doi: 10.1111/j.1365-2559.2005.02176.x

18. Gavioli M, Luppi G, Losi L, Bertolini F, Santantonio M, Falchi AM, et al. Incidence and clinical impact of sterilized disease and minimal residual disease after preoperative radiochemotherapy for rectal cancer. *Dis Colon Rectum* (2005) 48(10):1851–7. doi: 10.1007/s10350-005-0133-6

19. Horvat N, Carlos Tavares Rocha C, Clemente Oliveira B, Petkovska I, Gollub MJ. MRI Of rectal cancer: tumor staging, imaging techniques, and management. *Radiographics* (2019) 39(2):367–87. doi: 10.1148/rg.2019180114

20. Shin J, Seo N, Baek SE, Son NH, Lim JS, Kim NK, et al. MRI Radiomics model predicts pathologic complete response of rectal cancer following chemoradiotherapy. *Radiology* (2022) 303(2):351–8. doi: 10.1148/radiol.211986

21. Wilson K, Flood M, Narasimhan V, Pham T, Warrier S, Ramsay R, et al. Complete pathological response in rectal cancer utilising novel treatment strategies for neo-adjuvant therapy: a systematic review. *Eur J Surg Oncol* (2021) 47(8):1862–74. doi: 10.1016/j.ejso.2021.03.245

22. Kim JY, Kim NK, Sohn SK, Kim YW, Kim KJ, Hur H, et al. Prognostic value of postoperative CEA clearance in rectal cancer patients with high preoperative CEA levels. *Ann Surg Oncol* (2009) 16(10):2771–8. doi: 10.1245/s10434-009-0651-x

23. Chen HY, Feng LL, Li M, Ju HQ, Ding Y, Lan M, et al. College of American pathologists tumor regression grading system for long-term outcome in patients with locally advanced rectal cancer. *Oncologist* (2021) 26(5):e780–93. doi: 10.1002/onco.13707

24. Taylor FG, Quirke P, Heald RJ, Moran BJ, Blomqvist L, Swift IR, et al. Magnetic resonance imaging in rectal cancer European equivalence study study G: preoperative magnetic resonance imaging assessment of circumferential resection margin predicts disease-free survival and local recurrence: 5-year follow-up results of the MERCURY study. *J Clin Oncol* (2014) 32(1):34–43. doi: 10.1200/JCO.2012.45.3258

25. Sakin A, Sahin S, Sengul Samanci N, Yasar N, Demir C, Geredeli C, et al. The impact of tumor regression grade on long-term survival in locally advanced rectal cancer treated with preoperative chemoradiotherapy. *J Oncol Pharm Pract* (2020) 26(7):1611–20. doi: 10.1177/1078155219900944

26. Fanelli GN, Loupakis F, Smyth E, Scarpa M, Lonardi S, Pucciarelli S, et al. Pathological tumor regression grade classifications in gastrointestinal cancers: role on patients' prognosis. *Int J Surg Pathol* (2019) 27(8):816–35. doi: 10.1177/1066896919869477

27. Dossa F, Chesney TR, Acuna SA, Baxter NN. A watch-and-wait approach for locally advanced rectal cancer after a clinical complete response following neoadjuvant chemoradiation: a systematic review and meta-analysis. *Lancet Gastroenterol Hepatol* (2017) 2(7):501–13. doi: 10.1016/S2468-1253(17)30074-2

28. Jia X, Zhang Y, Wang Y, Feng C, Shen D, Ye Y, et al. MRI For restaging locally advanced rectal cancer: detailed analysis of discrepancies with the pathologic reference standard. *AJR Am J Roentgenol* (2019) 213(5):1081–90. doi: 10.2214/AJR.19.21383

29. Lambregts DMJ, Boellaard TN, Beets-Tan RGH. Response evaluation after neoadjuvant treatment for rectal cancer using modern MR imaging: a pictorial review. *Insights Imaging* (2019) 10(1):15. doi: 10.1186/s13244-019-0706-x

30. Qin Y, Zhu LH, Zhao W, Wang JJ, Wang H. Review of radiomics- and dosiomics-based predicting models for rectal cancer. *Front Oncol* (2022) 12:913683. doi: 10.3389/fonc.2022.913683

31. Beets-Tan RGH, Lambregts DMJ, Maas M, Bipat S, Barbaro B, Curvo-Semedo L, et al. Magnetic resonance imaging for clinical management of rectal cancer: updated recommendations from the 2016 European society of gastrointestinal and abdominal radiology (ESGAR) consensus meeting. *Eur Radiol* (2018) 28(4):1465–75. doi: 10.1007/s00330-017-5026-2

32. Nougaret S, Reinhold C, Mikhael HW, Rouanet P, Bibeau F, Brown G. The use of MR imaging in treatment planning for patients with rectal carcinoma: have you checked the "DISTANCE"? *Radiology* (2013) 268(2):330–44. doi: 10.1148/radiol.13121361

33. Kaur H, Choi H, You YN, Rauch GM, Jensen CT, Hou P, et al. MR imaging for preoperative evaluation of primary rectal cancer: practical considerations. *Radiographics* (2012) 32(2):389–409. doi: 10.1148/rg.322115122

frontiers | Frontiers in Oncology

TYPE Original Research
PUBLISHED 05 September 2023
DOI 10.3389/fonc.2023.1209732

OPEN ACCESS

EDITED BY
Marco Rengo,
Sapienza University of Rome, Italy

REVIEWED BY
Davide Ciardiello,
University of Campania Luigi Vanvitelli, Italy
Anton A. Plekhanov,
Privolzhsky Research Medical University (PIMU), Russia

*CORRESPONDENCE
Stefan D. van der Stel
s.vd.stel@nki.nl

RECEIVED 21 April 2023
ACCEPTED 21 August 2023
PUBLISHED 05 September 2023

CITATION
van der Stel SD, van den Berg JG, Snaebjornsson P, Seignette IM, Witteveen M, Grotenhuis BA, Beets GL, Post AL and Ruers TJM (2023) Size and depth of residual tumor after neoadjuvant chemoradiotherapy in rectal cancer – implications for the development of new imaging modalities for response assessment. *Front. Oncol.* 13:1209732. doi: 10.3389/fonc.2023.1209732

Size and depth of residual tumor after neoadjuvant chemoradiotherapy in rectal cancer – implications for the development of new imaging modalities for response assessment

Stefan D. van der Stel[1,2*], Jose G. van den Berg[3], Petur Snaebjornsson[3,4], Iris M. Seignette[3], Mark Witteveen[1,2], Brechtje A. Grotenhuis[2], Geerard L. Beets[2,5], Anouk L. Post[2,6] and Theo J. M. Ruers[1,2]

[1]Faculty Technische Natuurwetenschappen (TNW), Group Nanobiophysics, Twente University, Enschede, Netherlands, [2]Department of Surgery, Netherlands Cancer Institute, Amsterdam, Netherlands, [3]Department of Pathology, Netherlands Cancer Institute, Amsterdam, Netherlands, [4]Faculty of Medicine, University of Iceland, Reykjavik, Iceland, [5]GROW School for Oncology and Developmental Biology, University of Maastricht, Maastricht, Netherlands, [6]Department of Biomedical Engineering and Physics, Amsterdam Cardiovascular Sciences, Cancer Center Amsterdam, Amsterdam Universitair Medisch Centrum (UMC), University of Amsterdam, Amsterdam, Netherlands

With the shift towards organ preserving treatment strategies in rectal cancer it has become increasingly important to accurately discriminate between a complete and good clinical response after neoadjuvant chemoradiotherapy (CRT). Standard of care imaging techniques such as CT and MRI are well equipped for initial staging of rectal tumors, but discrimination between a good clinical and complete response remains difficult due to their limited ability to detect small residual vital tumor fragments. To identify new promising imaging techniques that could fill this gap, it is crucial to know the size and invasion depth of residual vital tumor tissue since this determines the requirements with regard to the resolution and imaging depth of potential new optical imaging techniques. We analyzed 198 pathology slides from 30 rectal cancer patients with a Mandard tumor regression grade 2 or 3 after CRT that underwent surgery. For each patient we determined response pattern, size of the largest vital tumor fragment or bulk and the shortest distance from the vital tumor to the luminal surface. The response pattern was shrinkage in 14 patients and fragmentation in 16 patients. For both groups combined, the largest vital tumor fragment per patient was smaller than 1mm for 38% of patients, below 0.2mm for 12% of patients and for one patient as small as 0.06mm. For 29% of patients the vital tumor remnant was present within the first 0.01mm from the luminal surface and for 87% within 0.5mm. Our results explain why it is difficult to differentiate between a good clinical and complete response in rectal cancer patients using endoscopy and MRI, since in many patients submillimeter tumor fragments remain below the luminal surface. To detect residual vital tumor tissue in

all patients included in this study a technique with a spatial resolution of 0.06mm and an imaging depth of 8.9mm would have been required. Optical imaging techniques offer the possibility of detecting majority of these cases due to the potential of both high-resolution imaging and enhanced contrast between tissue types. These techniques could thus serve as a complimentary tool to conventional methods for rectal cancer response assessment.

KEYWORDS

tumor response, regression, rectal cancer, fragmentation, neoadjuvant, optical imaging, watch-and-wait

1 Introduction

Over the last decade, rectal cancer treatment has shifted towards organ preserving treatment, having the foremost advantage of improving the patient's quality of life (1, 2). The standard-of-care for intermediate risk and locally advanced rectal cancer is neoadjuvant chemoradiotherapy (CRT) to reduce the size or extent of the tumor, followed by a total mesorectal excision (TME) where the rectum is surgically removed together with surrounding tissue and draining lymph nodes. Moreover, novel advances in rectal cancer treatment indicate the promising role of CRT in patients with bulky and distal tumors of the rectum, providing insights for organ preserving treatment in these complex tumors (3, 4). Since a TME often results in loss of organ function and considerable side effects, there is an increasing interest in organ-sparing treatment to improve the quality of life of patients. Patients with a good clinical response (defined as a near-complete or major response after CRT, with the possibility of residual tumor (5)) could receive additional local tumor treatment (e.g. a local tumor excision or internal boost radiation). In addition to CRT, novel advances in rectal cancer treatment have shown promising results with immunotherapy, especially in patients with microsatellite instable (MSI)-high tumors (6, 7).

In patients with a complete response (without any residual tumor) on the other hand non-operative management can be considered and these patients can be monitored according to watch-and-wait (W&W). After CRT, 20% of patients have a pathological complete response and 42-60% of patients have a good clinical response (8, 9). For organ-sparing treatment to become even more successful, it is important that clinicians can accurately identify the optimal treatment for each patient based on the degree of tumor response to CRT. However, the current workflow for response assessment has difficulty discriminating between patients with a good clinical response and a clinical complete response (10).

Response assessment is currently performed based on a combination of endoscopy, magnetic resonance imaging (MRI) and digital rectal examination. Endoscopic biopsies are only rarely used for initial response assessment because of frequent false positive results. Based on this *clinical* response assessment patients undergo further treatment or are enrolled in W&W. After surgery the resected tissue is analyzed by a pathologist, resulting in a *pathological* response assessment, which remains the gold standard. In approximately 15% of patients that are considered clinical incomplete responders, no residual tumor tissue is present upon histopathological evaluation of the resected specimen (11). These patients undergo major surgery where organ-sparing treatment could have been possible. Additionally, approximately 25% of patients thought to have responded completely based on a clinical evaluation still harbor unrecognized residual tumor (12). Based on the clinical evaluation these patients can be enrolled in W&W, but they developed a local regrowth requiring additional surgery (13). Improving the accuracy of response assessment thus holds the promise of improving treatment decisions and outcome for rectal cancer patients.

The difficulty of MRI to accurately assess tumor response can be explained by the fact that CRT can result in small tumor fragments scattered throughout fibrotic tissue (14). Not only does MRI have difficulty in discriminating between fibrosis and tumor tissue (15, 16) but a major concern in response assessment is also missing small fragments of residual vital tumor tissue, leading to the cautious strategy to perform major surgery whenever residual tumor tissue is suspected (17). CRT treatment can result in response patterns of either shrinkage or fragmentation of rectal tumors. Tumor shrinkage is characterized by a decrease in concentric tumor size, while fragmentation is defined by destruction of the main tumor mass after treatment and formation of small groups of tumor cells embedded in fibrosis. Fragmentation is reported in 40-80% of patients with rectal cancer (18, 19) and increases the chance of radiological understaging because of the difficulty of detecting small tumor fragments (20). While, to the best of our knowledge, the size distribution of tumor fragments in rectal cancer have not been published, a recent study showed that tumor fragment size in esophageal adenocarcinoma can be as small as several micrometers (18). With these dimensions, MR imaging lack resolution and accuracy in visualizing residual tumor fragments. Thus, to improve response assessment and treatment after CRT, an imaging technique is required that can detect small vital tumor fragments within fibrotic tissue.

To identify promising new techniques to improve response assessment in rectal cancer, one requirement placed on such a technique is that it can distinguish between vital tumor tissue and

fibrosis. A second requirement is that the resolution needs to be high enough so it can detect small residual tumor fragments. While techniques like MRI can image the full body, for most other imaging techniques there is a trade-off between the resolution and imaging depth. Therefore, a third requirement is that a new technique needs to be able to image deep enough below the luminal surface so that it can detect residual vital tumor tissue in deeper tissue layers. While general response patterns in rectal cancer have been described in literature, no quantitative description of the size and depth distributions of residual tumor fragments after CRT has been given. Nonetheless, these quantitative measures potentially play a pivotal role in explaining why so many tumors are misclassified by current imaging methods and consequently could provide the theoretical framework more optimal imaging methods in the future. The aim of this study is to provide a quantitative histopathological description of the size and depth distributions of residual tumor tissue after CRT treatment which can be used to select promising new imaging techniques for response assessment based on their resolution and imaging depth.

2 Patients, materials and methods

2.1 Test cohort

Histological slides of rectal resection specimens from 30 patients with rectal tumors that had been treated with CRT and underwent rectal surgery were retrieved from the pathology archive at the Netherlands Cancer Institute. The original pathology report contained information on tumor regression grade (TRG), scored according to Mandard (21). Since we aimed to improve discrimination between a good clinical and a complete response, only cases with a substantial pathological response after CRT treatment were included - scored as Mandard TRG 2 (rare residual tumor cells and clusters scattered through fibrosis) or TRG 3 (increase in the number of residual tumor cells when compared to Mandard TRG 2, while fibrosis still predominates when compared to Mandard TRG 4).

This retrospective medical data/biospecimen study was carried out pursuant to Dutch legislation and international standards. Clinical information such as demographics and tumor characteristics were collected from the medical records (Table 1). Archival H&E slides were scanned using a PANNORAMIC® 1000 scanner from 3DHISTECH at a 40x magnification.

2.2 Assessment of tumor response

Indica Labs' HALO software (v3.4.2986.185) (23) was used to classify tissue, normal mucosa, and tumor areas on the scanned histopathology slides, and to subsequently measure size and volume of tumor cell clusters and distances between tumor cell clusters. The DenseNet AI v2 plugin classifier was trained with 3 complete annotated slides, where a certified pathologist (JGvdB) annotated the full regions of background, normal mucosa, tumor and all other tissues. The classifier was trained for a total of 26345 iterations with a Cross-Entropy of 0.1. After training, performance of the classifier was verified by JGvdB in random slides included in this study. In total, 198 slides were examined, consisting of all H&E tumor slides per case.

First, we determined for each patient whether the response pattern was of fragmentation or shrinkage type. Tumor fragmentation was defined as clusters of cells which do not form a bulk and have at least 3 mm distance between fragments (18). If the response pattern was fragmentation, we measured the width (the short axis) of the widest tumor fragment per patient to be able to determine the ability of different imaging techniques to detect small fragments based on their resolution. We chose the width since that defines the required resolution – a long and narrow fragment of e.g. 3 by 0.05 mm would not be detected by a technique with a

TABLE 1 General patient and tumor characteristics.

Total	30
Gender	
Male	19
Female	11
Age, *median (IQR)*	57 (54 – 69)
Neoadjuvant treatment	
Long course chemoradiation	18
Short course RT and immunotherapy within a trial (22)	5
Short course RT followed by chemotherapy	4
Short course RT	3
Interval between neoadjuvant treatment and surgery (weeks), *median (IQR)*	13 (10 – 17)
Type of surgery	
Abdominoperineal resection (APR)	13
Low anterior resection (LAR)	12
Transanal minimally invasive local excision (TAMIS)	5
Tumor type	
Well/moderately differentiated adenocarcinoma (low grade)	27
Poorly differentiated adenocarcinoma (high grade)	2
Mixed Neuroendocrine Non-Neuroendocrine Neoplasm (miNEN)	1
Mandard tumor regression grade	
2	17
3	13
Tumor invasion in rectum	
Mucosa/submucosa (ypT1)	5
Muscularis propria (ypT2)	16
Pericolic/mesorectal tissue (ypT3)	8
Other organs/structures (ypT4)	1

resolution of 1 mm. We chose the widest fragment per patient since the detection of only that fragment could already be enough to determine an incomplete response. In patients where the response pattern was of shrinkage type we measured the largest width of vital tumor tissue. For all patients we determined the shortest distance from the luminal surface to the vital tumor, in order to determine the ability of different imaging techniques to detect this residual tumor tissue based on the imaging depth. Finally, per patient we measured the tumor volume (based on all slides of a single patient) and the tumor area (based on the single slide with largest tumor area of each patient).

2.3 Statistical analysis

Statistical analysis was performed using IBM SPSS statistics v27 (SPSS Inc., United States). Normal distribution was assessed with the Shapiro-Wilk test. Statistical analysis for normally distributed data was performed with an unpaired t-test, and for non-normally distributed data using a Mann-Whitney test. A p-value ≤ 0.05 was considered statistically significant.

3 Results

3.1 Histopathological evaluation of tumor response

The HALO tissue classification algorithm identified tumor (red), normal mucosa (blue), other tissue types (green) and background (grey) in each histological slide (Figure 1), which was used for a quantitative analysis of the tumor response pattern (Table 2). Examples of the two main tumor response patterns, tumor fragmentation and shrinkage are shown in Figure 2.

Overall, the response pattern was of shrinkage type in 14 patients and of fragmentation type in 16 patients. For both groups combined, the largest vital tumor fragment per patient was smaller than 1 mm for 38% of patients, below 0.2 mm for 12% of patients and for one patient was as small as 0.06 mm. For 29% of patients residual vital tumor was present within the first 0.01 mm from the luminal surface and for 87% within the first 0.5 mm. In one patient there was 8.9 mm of healthy tissue between the residual vital tumor tissue and luminal surface. Moreover, invasion depth for both Mandard TRG 2 and TRG 3 were similarly distributed.

3.2 Tumor fragmentation

The response pattern was of fragmentation type in 65% and 38% in TRG 2 and TRG 3 cases, respectively. The median size of the widest isolated tumor fragments per patient was 0.68 mm for TRG 2 cases, and 1.80 mm in TRG 3 cases. In 63% of patients the widest fragments measured below 1.0 mm and 78% below 2.0 mm in size (Figure 3A). Residual tumor fragments were widely spread throughout the original tumor bed, encapsulated by fibrotic tissue. Individual tumor fragments could be as small as 0.06 mm.

3.3 Tumor shrinkage

The response pattern was of shrinkage type in 35% and 62% in TRG 2 and TRG 3 cases, respectively. The median value of the tumor width per patient was 4.60 mm and 7.55 mm in TRG 2 and TRG 3 cases, respectively. The spread of the width was very large, varying from several hundred micrometers to 1.5 centimeters. Detailed analysis showed that the width of the residual vital tumor bulk was smaller than 1.0 mm in 12% of cases, whereas 50% was smaller than 6.3 mm (Figure 3A).

3.4 Tumor invasion

Residual vital tumor was observed in all layers of the intestine. The most common location was the submucosa or muscle layers,

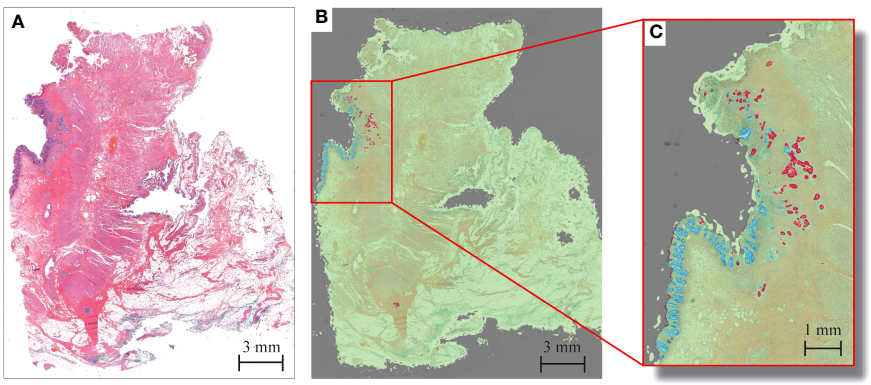

FIGURE 1
Example of tumor response segmentation by artificial intelligence HALO software in rectal cancer after CRT in a patient displaying Mandard TRG 2. **(A)** Haematoxylin and eosin (H&E) snapshot of tissue slide. **(B)** Corresponding tissue labels created by HALO tissue segmentation to enable easy tumor visualization. Red = tumor; blue = mucosa; green = other tissue; gray = background. **(C)** Zoom-in overview of tumor response pattern, with tumor fragments as small as several micrometers.

10.3389/fonc.2023.1209732

TABLE 2 Tumor response patterns based on quantitative analysis of histopathology slides. Data is presented as median with range (smallest to largest).

	Tumor regression grade 2	Tumor regression grade 3	p-value
Total, *n*	17	13	
Tumor response			
Fragmentation, *n*	11	5	
Shrinkage, *n*	6	8	
Fragmentation: maximum width of isolated fragments, *mm*	0.68 (0.06 – 6.90)	1.80 (0.28 – 5.60)	0.054
Shrinkage: maximum width of tumor bulk, *mm*	4.60 (0.18 – 10.90)	7.55 (1.70 – 14.90)	0.019
Shortest distance between vital tumor and luminal surface, *mm*	0.073 (0.001 – 3.30)	0.116 (0.002 – 8.90)	0.36
Area of vital tumor (1 central slide), mm^2	1.92 (0.17 – 6.47)	4.81 (1.09 – 30.99)	0.005
Volume of vital tumor (all tumor containing slides), mm^3	5.72 (0.93 – 25.80)	14.27 (1.87 – 74.87)	0.02

within 1 mm of the mucosal lining of the rectum (ypT1-2), however, vital tumor fragments were also observed in the mesorectal tissue, and extending into other organs (ypT3-4). The tumor invasion depth varied between several micrometers and up to 8.9 mm from the mucosa. In case of fragmentation, residual tumor fragments were present within 0.5 mm from the luminal surface in 95% of cases, whereas for shrinkage this was less, i.e. 75% (Figure 3B).

4 Discussion

This study provides an overview of the quantitative histopathological characteristics of the size and depth distributions of residual vital tumor tissue after CRT treatment in rectal cancer. In our study population, 63% of patients with a TRG 2 response after CRT harbor residual vital tumor fragments of less than 1 mm. Importantly, vital tumor fragments were mostly present within 0.5 mm of the luminal surface, yet could also be located in the mesorectal tissue and extending to other organs. However, in case of a TRG 2 response of large primary tumors, vital tumor fragments were observed extending up to 8.9 mm from the luminal surface.

For years, assessing treatment response in rectal cancer has been investigated intensively, focusing on clinicopathological characteristics or biomarkers as predictors, with mixed results (24, 25). For that reason, alternative approaches for response assessment, such as (novel) optical imaging techniques, should be explored. Optical imaging techniques use light to obtain highly detailed images and signals of organs, tissues, cells or molecules in a minimally invasive or non-invasive way. Optical imaging techniques harbor many advantages, such as the capability of high resolutions, high specificity for set targets and feasibility for real-time imaging. Moreover, optical imaging has the additional benefit that they lack harmful radiation and can therefore be used repeatedly for monitoring of disease progression or treatment effect.

As illustrated in Figure 4, the demand for high resolutions (<1 mm) required to detect small tumor fragments can be achieved with optical imaging. Figure 4 presents only a small sample of

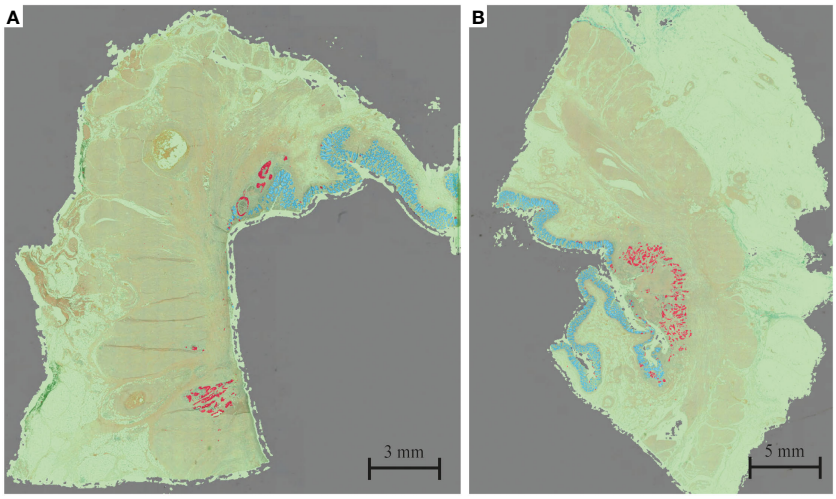

FIGURE 2
Example of **(A)** tumor fragmentation and **(B)** tumor shrinkage. Red = tumor; blue = mucosa; green = other tissue; gray = background.

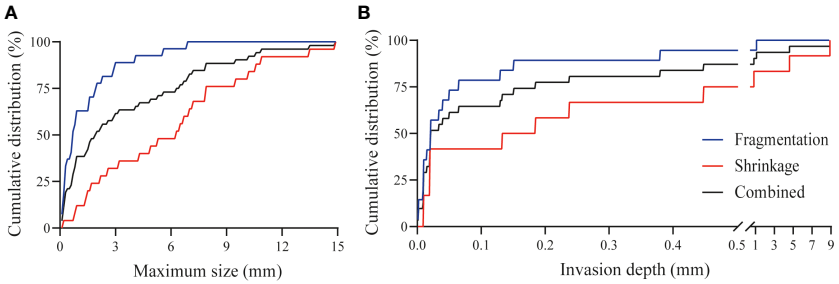

FIGURE 3
Tumor characteristics after CRT. **(A)** Cumulative distribution of the maximum width of tumor fragments in case of tumor fragmentation (n=16, blue line), tumor shrinkage (n=14, red line) and combined cohort (n=30, black line) after CRT. For both groups combined, the largest vital tumor fragment per patient was smaller than 1 mm for 38% of patients, below 0.2 mm for 12% of patients and for one patient was as small as 0.06 mm. **(B)** Cumulative distribution of the minimum invasion depth from the luminal surface in case of tumor fragmentation (n=16, blue line), tumor shrinkage (n=14, red line), and the combined cohort (n=30, black line) after CRT. For 29% of patients residual vital tumor was present within the first 0.01 mm from the luminal surface and for 87% within the first 0.5 mm. In one patient there was 8.9 mm of healthy tissue between the residual tumor tissue and the luminal surface.

available optical imaging techniques, each with their own specific biochemical or structural targets. For example, optical coherence tomography (OCT) uses the refractive properties of light waves in tissue to provide visualization of cross-sectional and 3D images of tissues (26), fluorescence lifetime imaging (FLIm) provides information about the biochemical composition of tissues by measuring the decay of fluorescent molecules (27) and photoacoustic imaging (PAI) utilizes laser-generated ultrasound waves to display tissue morphology and vasculature (28).

It is important to realize that there is an inherent trade-off between resolution and imaging depth. By selecting a technique with a higher resolution, the imaging depth will decrease. However, most optical imaging setups allow for interchanging these parameters, thereby selecting the desired resolution and imaging depths for a specific application. The results from our analysis offers the theoretical framework to evaluate the prospects of different optical imaging techniques. Moreover, challenges such as limitation in field of view, resolution (29) or feasibility for *in vivo* use (30, 31) have been addressed by multiple studies, providing solutions and opportunities for further research. For example, techniques as hyperspectral laparoscopes (32), confocal laser endomicroscopy (33) and tethered capsules (34) have indicated the potential of optical imaging in endoscopic use. Despite these advances, a commercially available optical imaging device is not yet available for tumor response assessment in rectal cancer. Hence, exploration of optical imaging techniques could be the way forward towards accurately defining treatment response assessment in rectal cancer patients. However, it is important to realize that implementation of any technique in the rectal cavity needs an optimized design for intended use.

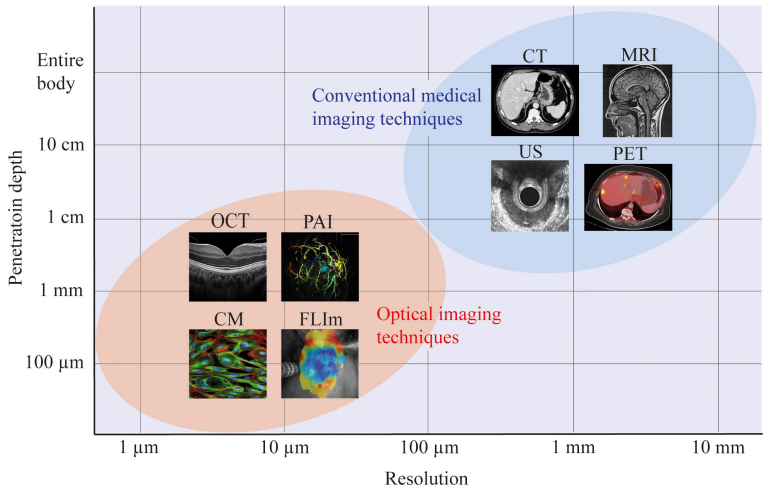

FIGURE 4
Resolution and penetration depths of several imaging modalities. For most optical imaging modalities there is a trade-off between the resolution and imaging depth, achieving more accurate resolutions, at the cost of penetration depth within the tissue of interest. In this figure, a schematic representation is used to indicate the approximate resolution and penetration depth of optical imaging versus conventional medical imaging modalities. For all imaging modalities, the exact resolution and penetration depth will depend on the specific setup. CM, confocal microscopy; FLIm, fluorescence lifetime imaging; OCT, optical coherence tomography; PAI, photoacoustic imaging; US, ultrasound; CT, computed tomography; MRI, magnetic resonance imaging; PET, positron emission tomography.

While the results presented in this study show the potential for optical imaging in treatment response assessment, they also explain why it is difficult to discriminate between a good clinical and a complete response using conventional clinical examination. The foremost reason is that CRT can result in submillimeter residual tumor fragments below the resolution of MRI, and can be scattered throughout the intestinal tissue layers, rendering them invisible for endoscopy.

Currently, MRI is the golden standard for treatment response assessment in rectal cancer. While conventional MRI can achieve a resolution of approximately 1 mm (Figure 4), this is insufficient to identify the submillimeter tumor fragments demonstrated in the present study. Moreover, CRT-induced fibrosis in the tumor bed, replacing vital tumor, decreases the accuracy of MRI to detect residual viable tumor due to the lack of contrast between fibrosis and tumor fragments (35–37). As such, the dimension and distribution of tumor fragments, together with the surrounding fibrosis provides a big challenge for radiologists to accurately assess treatment response with MRI. Currently it is possible to improve this resolution using Ultra High Field (UHF) 7-9 Tesla machines, achieving a resolution below 0.5 mm (38). Even so, in 21% of our patients the largest tumor fragments was less than 0.5 mm. Furthermore, the problem of distinguishing fibrosis from tumor in these UHF scans remains. Another possibility for improving the diagnostic capability of MRI for response imaging of rectal cancer is the use of diffusion-weighted imaging (DWI). DWI offers the possibility to visualize a functional parameter utilizing the diffusion of water molecules within tissues. The advantage of DWI would be the possibility to increase the contrast between tumor and fibrosis. In assessment of breast and renal cancer response to CRT, DWI improved the evaluation of treatment response (39–41). However, the limiting factor of the resolution with respect to the small size of the fragments remains.

In addition to shrinkage and fragmentation of the tumor, in approximately 20% of patients undergoing CRT, microscopic intramural spread (MIS) is present (42), i.e. residual tumor extension beneath normal appearing mucosa. In clinical practice, MIS is commonly used for planning additional radiotherapy, or take into account when selecting the resection plane around the visible tumor. Whilst multiple studies have focused on retrospective assessing the MIS after CRT (42–44), intraoperative assessment remains challenging due to the limited size of the residual tumor fragments in most cases. Moreover, a tumor-positive circumferential resection margin (CRM) after CRT remains an important prognostic factor for local recurrence and overall survival, and can be as high as 31.8% (45). Hence, intraoperative assessment of the MIS potentially allows for more accurate selection of the resection plane, and (novel) optical imaging techniques could provide the tools to decrease tumor-positive CRM rates.

In this study, an AI algorithm was trained for labelling of residual tumor in pathology slides of rectal cancer. Such an algorithm enables the analysis of a large number of slides in detail. Moreover, the same analysis by a pathologist would have taken up a considerable amount of time. In future studies with (novel) imaging techniques, such an AI algorithm could provide key insights into the performance of these techniques by providing detailed histopathological information of the imaged tissue. Furthermore, our detailed analysis revealed that invasion depth of residual tumor fragments/bulk was not related to the Mandard TRG. However, most patients with a TRG 3 response displayed larger tumor volumes and larger tumor diameter than TRG 2 tumors. Thus, Mandard TRG is not only a measure of response, but can also be a measure of residual tumor burden.

There are some limitations to this study. First, 30 patients were included, resulting in 198 pathology slides. The novelty of the segmentation tool required us to manually check the performance of the segmentation in every segmented slice, resulting in a lower patient population. Secondly, an uncertainty remains about what portion of the residual tumor in the histological assessment is still vital and can result in a regrowth. However, in this study we assumed that our assessment of the vital portion of the tumor is right. Moreover, it is important to keep in mind that the AI algorithm was only trained on 3 completely annotated slides, while many more are needed optimizing the algorithm for general application. This could be seen as a limitation, since the trained AI for this study might lack robustness for independent analysis of histology slides. However, the AI was used as a tool for manual annotation, and not as a replacement for an experienced pathologist, and therefore the minimal training size was adequate for the application as used here. Furthermore, the quantitative measurements reported in this paper were verified manually to be accurate, and thus do not rely heavily on the AI for segmentation borders. Moreover, the AI performed well and no major adjustment had to be done to the segmentation once trained.

For successful organ-sparing treatment, it is crucial that clinicians can accurately identify the optimal treatment for each patient based on the response of the tumor to CRT. Resolutions of several micrometers are required for visualizing residual tumor fragments, and an imaging depth of several millimeters is essential for detecting fragments in all layers of the rectal wall. Moreover, it is important to realize that the histopathological characteristics of the tissue are paramount in the selection of an imaging technique. For *in vivo* application, it is important to realize that the imaging technique has to be implemented in an endorectal probe for optimal access to the tumor (46). Many optical imaging techniques have been transformed from table-top setups to endoscopic imaging probes, showing the potential of optical imaging techniques for colorectal response assessment (33, 34, 47–49). results presented in this study show that conventional imaging methods (mainly CT and MRI) lack the resolution for detecting residual vital tumor after CRT in rectal cancer, and hence have limited value in the therapeutic decision-making process around W&W in clinical practice. Our results, however, provide a theoretical basis for novel research in imaging techniques that can achieve the needed resolutions. Depending on the exact application, optical techniques have their own benefits over conventional CT and MR imaging.

To summarize, optical imaging techniques have the prospect of becoming a complimentary tool next to conventional methods for rectal cancer response assessment, since these techniques offer high-resolution imaging with enhanced contrast between tissue types.

Data availability statement

The raw data supporting the conclusions of this article will be made available by the authors, without undue reservation.

Ethics statement

The studies involving humans were approved by Institutional Review Board of the Netherlands Cancer Institute. The studies were conducted in accordance with the local legislation and institutional requirements. The ethics committee/institutional review board waived the requirement of written informed consent for participation from the participants or the participants' legal guardians/next of kin because written informed consent was not required according IRB guidelines.

Author contributions

Study design: AP and TR. Data collection: SS, JB, PS, IS, BG, GB, and AP. Data interpretation: SS, JB, PS and AP. Writing manuscript: SS, AP, and MW. Reviewing manuscript: JB, PS, IS, BG, GB and TR. All authors read and approved the final manuscript.

Acknowledgments

We would like to acknowledge the NKI-AVL Core Facility Molecular Pathology & Biobanking (CFMPB) for supplying NKI-AVL Biobank material and/or lab support.

Conflict of interest

The authors declare that the research was conducted in the absence of any commercial or financial relationships that could be construed as a potential conflict of interest.

Publisher's note

References

1. Tekkis P, Tait D, Cunningham D, Brown G. Is organ preservation in rectal cancer ready for prime time? *Lancet* (2018) 391(10139):2480–2. doi: 10.1016/S0140-6736(18)31324-2

2. Grotenhuis BA, Beets GL. Watch-and-wait is an option in rectal cancer patients: from controversy to common clinical practice. *Clin Oncol* (2022) 35(2):124–9. doi: 10.1016/j.clon.2022.11.011

3. Bahadoer RR, Dijkstra EA, van Etten B, Marijnen CAM, Putter H, Kranenbarg EMK, et al. Short-course radiotherapy followed by chemotherapy before total mesorectal excision (TME) versus preoperative chemoradiotherapy, TME, and optional adjuvant chemotherapy in locally advanced rectal cancer (RAPIDO): a randomised, open-label, phase 3 trial. *Lancet Oncol* (2021) 22(1):29–42. doi: 10.1016/S1470-2045(20)30555-6

4. Fokas E, Schlenska-Lange A, Polat B, Klautke G, Grabenbauer GG, Fietkau R, et al. Chemoradiotherapy plus induction or consolidation chemotherapy as total neoadjuvant therapy for patients with locally advanced rectal cancer: long-term results of the CAO/ARO/AIO-12 randomized clinical trial. *JAMA Oncol* (2022) 8(1):1–10. doi: 10.1001/jamaoncol.2021.5445

5. Custers PA, Geubels BM, Beets GL, Triest Van B, Maas M. Defining near-complete response following (chemo) radiotherapy for rectal cancer: systematic review. *Br J Surg* (2022) 110(1):43–9. doi: 10.1093/bjs/znac372

6. Chen G, Jin Y, Guan W, Zhang R, Xiao W, Cai P, et al. Neoadjuvant PD-1 blockade with sintilimab in mismatch-repair deficient, locally advanced rectal cancer: an open-label, single-centre phase 2 study. *Lancet Gastroenterol Hepatol* (2023) 8(5):422–31. doi: 10.1016/S2468-1253(22)00439-3

7. Cercek A, Lumish M, Sinopoli J, Weiss J, Shia J, Lamendola-Essel M, et al. PD-1 blockade in mismatch repair–deficient, locally advanced rectal cancer. *N Engl J Med* (2022) 386(25):2363–76. doi: 10.1056/NEJMoa2201445

8. Maas M, Nelemans PJ, Valentini V, Das P, Rödel C, Kuo LJ, et al. Long-term outcome in patients with a pathological complete response after chemoradiation for rectal cancer: A pooled analysis of individual patient data. *Lancet Oncol* (2010) 11(9):835–44. doi: 10.1016/S1470-2045(10)70172-8

9. Ryan JE, Warrier SK, Lynch AC, Ramsay RG, Phillips WA, Heriot AG. Predicting pathological complete response to neoadjuvant chemoradiotherapy in locally advanced rectal cancer: A systematic review. *Color Dis* (2016) 18(3):234–46. doi: 10.1111/codi.13207

10. van der Sande ME, Beets GL, Hupkens BJ, Breukink SO, Melenhorst J, Bakers FC, et al. Response assessment after (chemo)radiotherapy for rectal cancer: Why are we missing complete responses with MRI and endoscopy? *Eur J Surg Oncol* (2019) 45(6):1011–7. doi: 10.1016/j.ejso.2018.11.019

11. Haak HE, Maas M, Trebeschi S, Beets-Tan RGH. Modern MR imaging technology in rectal cancer; there is more than meets the eye. *Front Oncol* (2020) 10:1–7. doi: 10.3389/fonc.2020.537532

12. van der Valk MJM, Hilling DE, Bastiaannet E, Meershoek-Klein Kranenbarg E, Beets GL, Figueiredo NL, et al. Long-term outcomes of clinical complete responders after neoadjuvant treatment for rectal cancer in the International Watch & Wait Database (IWWD): an international multicentre registry study. *Lancet* (2018) 391(10139):2537–45. doi: 10.1016/S0140-6736(18)31078-X

13. Deidda S, Elmore U, Rosati R, De Nardi P, Vignali A, Puccetti F, et al. Association of delayed surgery with oncologic long-term outcomes in patients with locally advanced rectal cancer not responding to preoperative chemoradiation. *JAMA Surg* (2021) 156(12):1141–9. doi: 10.1001/jamasurg.2021.4566

14. Nagtegaal ID, Glynne-Jones R. How to measure tumour response in rectal cancer? An explanation of discrepancies and suggestions for improvement. *Cancer Treat Rev* (2020) 84:101964. doi: 10.1016/j.ctrv.2020.101964

15. Beets-Tan RGH, Lambregts DMJ, Maas M, Bipat S, Barbaro B, Curvo-Semedo L, et al. Magnetic resonance imaging for clinical management of rectal cancer: Updated recommendations from the 2016 European Society of Gastrointestinal and Abdominal Radiology (ESGAR) consensus meeting. *Eur Radiol* (2018) 28(4):1465–75. doi: 10.1007/s00330-017-5026-2

16. Barbaro B, Fiorucci C, Tebala C, Valentini V, Gambacorta MA, Vecchio FM, et al. Locally advanced rectal cancer: MR imaging in prediction of response after preoperative chemotherapy and radiation therapy. *Radiology* (2009) 250(3):730–9. doi: 10.1148/radiol.2503080310

17. Maas M, Lambregts DMJ, Nelemans PJ, Heijnen LA, Martens MH, Leijtens JWA, et al. Assessment of clinical complete response after chemoradiation for rectal cancer with digital rectal examination, endoscopy, and MRI: selection for organ-saving treatment. *Ann Surg Oncol* (2015) 22(12):3873–80. doi: 10.1245/s10434-015-4687-9

18. Graham Martinez C, Kus Öztürk S, Al-Kaabi A, Valkema MJ, Bokhorst JM, Rosman C, et al. Shrinkage versus fragmentation response in neoadjuvantly treated oesophageal adenocarcinoma: significant prognostic relevance. *Histopathology* (2022) 80, 982–94. doi: 10.1111/his.14644

19. Gosens MJEM, Klaassen RA, Tan-Go I, Rutten HJT, Martijn H, Van Den Brule AJC, et al. Circumferential margin involvement is the crucial prognostic factor after multimodality treatment in patients with locally advanced rectal carcinoma. *Clin Cancer Res* (2007) 13(22):6617–23. doi: 10.1158/1078-0432.CCR-07-1197

20. Fernández-Aceñero MJ, Muñoz LE, Varela JS, Sánchez JAC, del Arco CD, Paredes BG, et al. Prognostic influence of histopathological regression patterns in rectal adenocarcinoma receiving neoadjuvant therapy. *J Gastrointest Oncol* (2017) 8(1):49–54. doi: 10.21037/jgo.2017.01.02

21. Mandard A -M, Dalibard F, Mandard J -C, Marnay J, Henry-Amar M, Petiot J -F, et al. Pathologic assessment of tumor regression after preoperative chemoradiotherapy of esophageal carcinoma. *Clinicopathologic correlations. Cancer.* (1994) 73(11):2680–6.

22. ClinicalTrials.gov. *Neoadjuvant Treatment in Rectal Cancer With Radiotherapy Followed by Atezolizumab and Bevacizumab*. United States: TARZAN (2019).

23. Sobottka B, Nowak M, Frei AL, Haberecker M, Merki S, Aebersold R, et al. Establishing standardized immune phenotyping of metastatic melanoma by digital pathology. *Lab Investig* (2021) 101(12):1561–70. doi: 10.1038/s41374-021-00653-y

24. Fischer J, Eglinton TW, Richards SJG, Frizelle FA. Predicting pathological response to chemoradiotherapy for rectal cancer: a systematic review. *Expert Rev Anticancer Ther [Internet].* (2021) 21(5):489–500. doi: 10.1080/14737140.2021.1868992

25. Huh JW, Kim HR, Kim YJ. Clinical prediction of pathological complete response after preoperative chemoradiotherapy for rectal cancer. *Dis Colon Rectum.* (2013) 56 (6):698–703. doi: 10.1097/DCR.0b013e3182837e5b

26. Aumann S, Donner S, Fischer J, Müller F. Optical coherence tomography (OCT): principle and technical realization. In: *High Resolution Imaging in Microscopy and Ophthalmology*, vol. p. United States: Springer, Cham (2019). p. 59–85.

27. Datta R, Heaster TM, Sharick JT, Gillette AA, Skala MC. Fluorescence lifetime imaging microscopy: fundamentals and advances in instrumentation, analysis, and applications. *J BioMed Opt.* (2020) 25(07):1. doi: 10.1117/1.JBO.25.7.071203

28. Chapman WC, Mutch M. Co-registered photoacoustic and ultrasound imaging of human colorectal cancer. *J BioMed Opt.* (2019) 24(12):1. doi: 10.1117/1.JBO.24.12.121913

29. Zhang B, Hou W, Jin G, Zhu J. Simultaneous improvement of field-of-view and resolution in an imaging optical system. *Opt Express.* (2021) 29(6):9346. doi: 10.1364/OE.420222

30. Yao L, Zhou Y, Liu K, Yin X, Deng X, Ding Z, et al. Endoscopic OCT angiography using clinical proximal-end scanning catheters. *Photonics* (2022) 9 (5):329. doi: 10.3390/photonics9050329

31. Luo H, Li S, Zeng Y, Cheema H, Otegbeye E, Ahmed S, et al. Human colorectal cancer tissue assessment using optical coherence tomography catheter and deep learning. *J Biophotonics* (2022) 15(6):1–8. doi: 10.1002/jbio.202100349

32. Pfahl A, Köhler H, Thomaßen MT, Maktabi M, Bloße AM, Mehdorn M, et al. Clinical evaluation of a laparoscopic hyperspectral imaging system. *Surg Endosc* (2022) 36(10):7794–9. doi: 10.1007/s00464-022-09282-y

33. Pilonis ND, Januszewicz W, di Pietro M. Confocal laser endomicroscopy in gastro-intestinal endoscopy: Technical aspects and clinical applications. *Transl Gastroenterol Hepatol* (2022) 7(September 2019):1–20. doi: 10.21037/tgh.2020.04.02

34. Liang K, Ahsen OO, Murphy A, Zhang J, Nguyen TH, Potsaid B, et al. Tethered capsule en face optical coherence tomography for imaging Barrett's oesophagus in unsedated patients. *BMJ Open Gastroenterol* (2020) 7(1):1–8. doi: 10.1136/bmjgast-2020-000444

35. Van Der Paardt MP, Zagers MB, Beets-Tan RGH, Stoker J, Bipat S. Patients who undergo preoperative chemoradiotherapy for locally advanced rectal cancer restaged by using diagnostic MR imaging: A systematic review and meta-analysis. *Radiology* (2013) 269(1):101–12. doi: 10.1148/radiol.13122833

36. Tan CH. Use of computed tomography in the management of colorectal cancer. *World J Radiol* (2010) 2(5):151. doi: 10.4329/wjr.v2.i5.151

37. Cote A, Florin GF, Mois E, Elisei R, Badea R, Mare C, et al. The accuracy of endorectal ultrasonography and high-resolution magnetic resonance imaging for restaging rectal cancer after neoadjuvant chemoradiotherapy. *Ann Ital Chir.* (2018) 89:168–76.

38. Stucht D, Danishad KA, Schulze P, Godenschweger F, Zaitsev M, Speck O. Highest resolution in *vivo* human brain MRI using prospective motion correction. *PloS One* (2015) 10(7):1–17. doi: 10.1371/journal.pone.0133921

39. Belli P, Costantini M, Ierardi C, Bufi E, Amato D, Mule' A, et al. Diffusion-weighted imaging in evaluating the response to neoadjuvant breast cancer treatment. *Breast J* (2011) 17(6):610–9. doi: 10.1111/j.1524-4741.2011.01160.x

40. Ahmed SA, Taher MGA, Ali WA, Ebrahem MAES. Diagnostic performance of contrast-enhanced dynamic and diffusion-weighted MR imaging in the assessment of tumor response to neoadjuvant therapy in muscle-invasive bladder cancer. *Abdom Radiol* (2021) 46(6):2712–21. doi: 10.1007/s00261-021-02963-7

41. Akkavak Palazalı G, Yılmaz R, Palazalı O, Dursun M. Magnetic resonance imaging evaluation of pathological response in breast cancer after neoadjuvant chemotherapy. *Indian J Surg* (2022) 85:39–44. doi: 10.1007/s12262-022-03337-z

42. Verrijssen AS, Guillem J, Perez R, Bujko K, Guedj N, Habr-Gama A, et al. Microscopic intramural extension of rectal cancer after neoadjuvant chemoradiation: A meta-analysis based on individual patient data. *Radiother Oncol* (2020) 144:37–45. doi: 10.1016/j.radonc.2019.10.003

43. Guedj N, Maggiori L, Poté N, Norkowski E, Cros J, Bedossa P, et al. Distal intramural and tumor spread in the mesorectum after neoadjuvant radiochemotherapy in rectal cancer: About 124 consecutive patients. *Hum Pathol* (2016) 52:164–72. doi: 10.1016/j.humpath.2016.01.017

44. Sun G, Ye X, Zheng K, Zhang H, Broens P, Trzpis M, et al. Measurement of distal intramural spread and the optimal distal resection by naked eyes after neoadjuvant radiation for rectal cancers. *World J Surg Oncol* (2022) 20(1):1–10. doi: 10.1186/s12957-022-02756-2

45. Detering R, Rutgers MLW, Bemelman WA, Hompes R, Tanis PJ. Prognostic importance of circumferential resection margin in the era of evolving surgical and multidisciplinary treatment of rectal cancer: A systematic review and meta-analysis. *Surg (United States)* (2021) 170(2):412–31. doi: 10.1016/j.surg.2021.02.029

46. Plekhanov AA, Sirotkina MA, Gubarkova EV, Kiseleva EB, Sovetsky AA, Karabut MM, et al. Towards targeted colorectal cancer biopsy based on tissue morphology assessment by compression optical coherence elastography. *Front Oncol* (2023) 13(March):1–15. doi: 10.3389/fonc.2023.1121838

47. Li Y, Zhu Z, Chen JJ, Jing JC, Sun C-H, Kim S, et al. Multimodal endoscopy for colorectal cancer detection by optical coherence tomography and near-infrared fluorescence imaging. *BioMed Opt Express.* (2019) 10(5):2419. doi: 10.1364/BOE.10.002419

48. Elena ET, Gheonea DI, Săftoiu A. Advances in endoscopic ultrasound imaging of colorectal diseases. *World J Gastroenterol* (2016) 22(5):1756–66. doi: 10.3748/wjg.v22.i5.1756

49. Esaki M, Yamamura T, Nakamura M, Maeda K, Sawada T, Mizutani Y, et al. Endoscopic ultrasound elastography as a novel diagnostic method for the assessment of hardness and depth of invasion in colorectal neoplasms. *Digestion* (2021) 102(5):701–13. doi: 10.1159/000511589

frontiers | Frontiers in Oncology

TYPE Original Research
PUBLISHED 26 October 2023
DOI 10.3389/fonc.2023.1212812

OPEN ACCESS

EDITED BY
Marco Rengo,
Sapienza University of Rome, Italy

REVIEWED BY
Davide Ciardiello,
University of Campania Luigi Vanvitelli, Italy
Anton A. Plekhanov,
Privolzhsky Research Medical University (PIMU), Russia

*CORRESPONDENCE
Seun Ja Park
parksj6406@daum.net
Tae Il Kim
taeilkim@yuhs.ac

†These authors have contributed equally to this work

RECEIVED 27 April 2023
ACCEPTED 26 September 2023
PUBLISHED 26 October 2023

CITATION
Kim JH, Yu J, Kim DK, Lee S, Lee SH, Ahn BK, Kim TI and Park SJ (2023) Tumor microbiome analysis provides prognostic value for patients with stage III colorectal cancer.
Front. Oncol. 13:1212812.
doi: 10.3389/fonc.2023.1212812

Tumor microbiome analysis provides prognostic value for patients with stage III colorectal cancer

Jae Hyun Kim[1†], Jongwook Yu[2†], Dong Keon Kim[2], Seunghun Lee[3], Seung Hyun Lee[3], Byung Kwon Ahn[3], Tae Il Kim[2,4*] and Seun Ja Park[1*]

[1]Department of Internal Medicine, Kosin University College of Medicine, Busan, Republic of Korea, [2]Department of Internal Medicine, Yonsei University College of Medicine, Seoul, Republic of Korea, [3]Department of Colorectal Surgery, Kosin University College of Medicine, Busan, Republic of Korea, [4]Brain Korea 21 Project for Medical Science, Yonsei University College of Medicine, Seoul, Republic of Korea

Introduction: Although patients with colorectal cancer (CRC) can receive optimal treatment, the risk of recurrence remains. This study aimed to evaluate whether the tumor microbiome can be a predictor of recurrence in patients with stage III CRC.

Methods: Using 16S rRNA gene sequencing, we analyzed the microbiomes of tumor and adjacent tissues acquired during surgery in 65 patients with stage III CRC and evaluated the correlation of the tissue microbiome with CRC recurrence. Additionally, the tumor tissue microbiome data of 71 patients with stage III CRC from another center were used as a validation set.

Results: The microbial diversity and abundance significantly differed between tumor and adjacent tissues. In particular, *Streptococcus* and *Gemella* were more abundant in tumor tissue samples than in adjacent tissue samples. The microbial diversity and abundance in tumor and adjacent tissues did not differ according to the presence of recurrence, except for one genus in the validation set. Logistic regression analysis revealed that a recurrence prediction model including tumor tissue microbiome data had a better prediction performance than clinical factors (area under the curve [AUC] 0.846 vs. 0.679, p = 0.009), regardless of sex (male patients: AUC 0.943 vs. 0.818, p = 0.043; female patients: AUC 0.885 vs. 0.590, p = 0.017). When this prediction model was applied to the validation set, it had a higher AUC value than clinical factors in female patients.

Conclusion: Our results suggest that the tumor microbiome of patients with CRC be a potential predictor of postoperative disease recurrence.

KEYWORDS

colorectal cancer, microbiome, tissue, prognosis, tumor

1 Introduction

Colorectal cancer (CRC) is the second leading cause of cancer deaths worldwide. Compared with the 2020 estimates, the global burden of CRC is predicted to increase by 63% in 2040 (1). Moreover, the incidence of early-onset CRC (before age 50 years) is increasing in high-income countries (2). For resectable non-metastatic CRC, colectomy with en bloc removal of regional lymph nodes is the preferred treatment; however, several studies reported that approximately 25–30% of patients with stage III CRC experienced disease recurrence within the first 5 years after surgery (3–6). In addition, although adjuvant chemotherapy has demonstrated benefits in patients with stage III CRC, it can reduce the risk of recurrence by only approximately 30% (7, 8). The mortality rates for CRC are consistently higher in men compared to women across different regions worldwide, with men having a mortality rate approximately 25% higher than women (9). Several retrospective studies have shown that female CRC patients typically have longer survival rates than males (10–12). However, some studies have failed to find any survival benefit for women (13). Several prognostic factors for CRC recurrence have been recognized, including a poorly differentiated histology, greater tumor depth, higher number of positive lymph nodes, lymphovascular invasion, perineural invasion, and tumor budding (14–17). In contrast, high microsatellite instability (MSI) and abundant tumor-infiltrating T-cells have been associated with a favorable prognosis in patients with CRC (18–20). Recently, the detection of circulating tumor DNA after surgery has been suggested as a predictor of a high risk of recurrence (21, 22). Nevertheless, a more precise prediction of the risk of CRC recurrence after surgery is still required in clinical practice.

Emerging evidence has demonstrated the microbial composition and ecological changes in patients with CRC and the roles of several bacteria in colorectal carcinogenesis and treatment (23). The gut microbiome, which includes *Faecalibacterium*, *Akkermansia*, and *Bifidobacterium* species, is expected to play an important role in mediating the outcomes of chemotherapy and immunotherapy in patients with melanoma and lung cancer, as it affects immune system activation and tumor responses to treatment (24–26). In particular, the presence of abundant *Fusobacterium nucleatum* (*F. nucleatum*) DNA in tissues has been associated with worse clinical outcomes in patients with CRC (27). One study of patients with pancreatic cancer demonstrated that the diversity and composition of the tumor microbiome are important determinants of long-term survival (28). A recent study of patients with CRC showed that two pathogenic bacteria, *F. nucleatum* and *Bacteroides fragilis* (*B. fragilis*), were more abundant in patients without recurrence than in those with recurrence (29). However, the association between the tumor microbiome and clinical outcomes in patients with CRC remains unclear.

We designed this study to investigate the potential role of the tumor microbiome in predicting postoperative recurrence in patients with stage III CRC. To verify the results, we also analyzed the tumor microbiome data of patients with stage III CRC from another center.

2 Materials and methods

2.1 Patients and sample collection

Two pairs of tumor tissues and adjacent normal-appearing mucosal tissues (hereinafter "adjacent tissues") from patients with CRC who underwent colorectal resection at Kosin University Gospel Hospital (Busan, Republic of Korea) were previously collected and stored immediately in a deep freezer (−80°C). From these samples, we selected and analyzed tumor and adjacent tissues from patients with stage III CRC who underwent adjuvant chemotherapy. Patients with pathological stage I or II CRC who had clinical stage III disease before surgery, those with < 3 months of adjuvant chemotherapy, and those with < 24 months of follow-up were excluded from the analysis. Further, tumor tissue samples from patients with stage III CRC who underwent surgery and adjuvant chemotherapy at Yonsei University Severance Hospital (Seoul, Republic of Korea) were used as a validation set. Detailed clinical data, such as age, sex, height, weight, ABO blood type, history of smoking and alcohol drinking, family history of CRC, comorbid diseases, tumor location, histology, lymphovascular invasion, perineural invasion, Kirsten rat sarcoma viral oncogene homolog (KRAS) mutation, MSI status, T stage, N stage, and laboratory findings (including carcinoembryonic antigen [CEA] level), were assessed. The study protocol was reviewed and approved by the institutional review board of Kosin University Gospel Hospital (approval no. KUGH 2021-01-028).

2.2 Adjuvant chemotherapy and definition of recurrence

Patients with CRC who underwent colorectal resection received were given either FOLFOX, CAPEOX, or FL as adjuvant chemotherapy for a duration of 6 months. The FOLFOX regimen includes intravenous administration of oxaliplatin 85 mg/m^2, leucovorin 400 mg/m^2, and a bolus of 5-fluorouracil 400 mg/m^2 on day 1. This is followed by a continuous infusion of 5-fluorouracil 1200 mg/m^2/day for 2 days. The treatment cycle is repeated every 2 weeks. The CAPEOX regimen includes intravenous administration of oxaliplatin 130 mg/m^2 on day 1 and oral administration of capecitabine 1000 mg/m^2 twice a day for 14 days. The treatment cycle is repeated every 3 weeks. The FL regimen consists of intravenous administration of leucovorin 400 mg/m^2, and a bolus of 5-fluorouracil 400 mg/m^2 on day 1. This is followed by a continuous infusion of 5- fluorouracil 1200 mg/m^2/day for 2 days.

The recurrence of CRC was diagnosed on endoscopic biopsy, surgical resection, and/or radiological imaging study. In this study, we defined recurrence as both locoregional and distant recurrence. Locoregional recurrence was defined as a recurrence at the site of original surgical resection or at the draining lymph nodes. Distant recurrence was defined as a recurrence of CRC developing spread to distant sites including the liver, lung, peritoneum, ovaries, adrenal glands, bone, and brain.

2.3 DNA extraction and bacterial 16S rRNA sequencing

The samples collected at Kosin University Gospel Hospital were transported to Hecto Healthcare Co., Ltd. (Seoul, Korea) and immediately frozen at −80°C. Microbial DNA was extracted using the Maxwell® RSC PureFood GMO and Authentication Kit (Promega, Madison, WI, USA) according to the manufacturer's instructions. To determine DNA concentrations, we used an ultraviolet–visible spectrophotometer (NanoDrop 2000c; Thermo Fisher Scientific, Waltham, MA, USA). QuantiFluor® ONE dsDNA System (Promega) was used for quantification. The DNA samples were stored at −20°C until required for experiments. A sequencing library was prepared according to the Illumina 16S Metagenomic Sequencing Library Preparation Guide (Illumina, San Diego, CA, USA). The V3–V4 region of the bacterial 16S rRNA gene was amplified using primer sets F319 (5′-TCGTCGGCAGCGT-CAGATGTGTATAAGAGACAGCCTACGG-GNGGCWGCAG-3′) and R806 (5′-GTCTCGTGGGCTCGGAGATGTGTATAAGAGAC-AGGACTACHVGGGTATC-TAATCC-3′). The amplified products were purified using Agencourt® AMPure XP beads (Beckman Coulter, Brea, CA, USA), and the quality of the library was confirmed using the Bioanalyzer 2100 system (Agilent, Santa Clara, CA, USA). The pooled libraries were sequenced with 300-bp paired-end reads on the MiSeq platform using the MiSeq version 3 Reagent Kit (Illumina). To prevent contamination, all experimental procedures were conducted inside a biosafety cabinet (BSC). DNA extraction was performed using sterile disposable Petri dishes and surgical blades to cut the sample into appropriate sizes while it was still frozen on dry ice. During the analysis stage, library pooling was performed by mixing Phix control at a 30% ratio with filtered real sequences used as raw data. The resulting data was then subjected to quality filtering, denoising, and sequencing error removal using QIIME2 software before proceeding with further analysis.

2.4 Data analysis and statistical analysis

Raw sequencing data were processed using the Quantitative Insight into Microbial Ecology software package 2 (QIIME 2, version 2021.4; http://qiime2.org). Denoising was performed using the Deblur algorithm, and a taxonomy table was created using the SILVA database (version 138). The non-archaeal/bacterial sequences were removed according to the taxonomic classification results. FASTQ reads were filtered, trimmed, and merged in DADA2 to generate a table of amplicon sequence variants. Taxonomy was assigned to the amplicon sequence variants using a naive Bayes classifier and compared to the SILVA version 138.99 reference database. Alpha diversity was assessed using the Shannon index, Chao1 index, Simpson index, and observed operational taxonomic units, whereas beta diversity was evaluated using principal coordinate analysis based on the Bray–Curtis distance. These analyses were performed using QIIME 2 and R (version 4.1.3; R Foundation for Statistical Computing, Vienna, Austria). To compare the taxa, we selected only those with a mean relative abundance greater than or equal to 1%. Data visualization was performed using the ggplot2 package in R, and statistical analysis was conducted using the Wilcoxon signed rank test and PERMANOVA from the vegan package. Linear discriminant effect size analysis was performed using the online platform, Galaxy (https://huttenhower.sph.harvard.edu/galaxy).

The patients' demographic and clinical data were compared using Student's t-test and Fisher's exact test. Continuous data with a normal distribution are expressed as mean ± standard deviation, and categorical data are presented as numbers (percentage). The Wilcoxon signed-rank test was used to compare microbial abundance between tumor and adjacent tissues, as well as according to the presence of recurrence. Logistic regression analysis was performed to evaluate factors predicting disease recurrence. The 'glm' function in R was used to fit a logistic regression model to our data, including predictors such as clinical variables and microbiome to predict the binary outcome variable of recurrence. The 'step' function was then used to perform backward selection and select the final model. Receiver operating characteristic (ROC) and area under the curve (AUC) analyses were performed to estimate the thresholds of variables. A random forest model was used to assess the mean decrease in the Gini coefficient. To control for the false discovery rate (FDR), statistical significance was determined using the Benjamini-Hochberg procedure with a threshold of FDR-adjusted p value < 0.05. All statistical analyses were performed using R.

3 Results

3.1 Baseline characteristics and evaluation of clinical variables affecting recurrence

Patients with stage III CRC who underwent surgery followed by adjuvant chemotherapy at Kosin University Gospel Hospital (65 patients, discovery set) and Yonsei University Severance Hospital (71 patients, validation set) were enrolled in this study. The baseline characteristics of the patients are summarized in Table 1. The mean age in the discovery set was younger than that in the validation set (60.0 ± 9.3 vs. 64.7 ± 11.4 years, p = 0.010). Additionally, the discovery set had a higher prevalence of current smokers (27.7% vs. 9.9%, p = 0.027) and lymphovascular invasion (63.1% vs. 36.6%, p = 0.004) compared to the validation set. In the discovery set, 60 patients (92.3%) received FOLFOX and 5 patients (7.7%) received CAPEOX. In the validation set, 59 patients (83.1%) received FOLFOX, 8 patients (11.3%) received CAPEOX, and 4 patients (5.6%) received FL. All of the patients received treatment for a minimum of 5 months or more.

We compared the clinical variables according to the presence of recurrence, and no differences were observed in all factors, including tumor location, histology, lymphovascular invasion, perineural invasion, KRAS mutation, MSI status, T stage, N stage, and laboratory findings (Table 2). We evaluated clinical factors as predictors of tumor recurrence; however, none of the factors were found to be significant (Figure 1).

TABLE 1 Baseline characteristics.

Characteristics	Discovery set (n = 65)	Validation set (n = 71)	*p* Value
Age (years)	60.0 ± 9.3	64.7 ± 11.4	0.010
Sex			0.335
Male	34 (52.3)	44 (62.0)	
Female	31 (47.7)	27 (38.0)	
Height (cm)	161.6 ± 9.2	163.1 ± 8.8	0.325
Weight (kg)	61.2 ± 11.5	63.2 ± 11.3	0.303
BMI (kg/m^2)	23.3 ± 3.4	23.7 ± 3.5	0.552
ABO blood type			0.096
A	34 (52.3)	30 (42.3)	
B	9 (13.8)	21 (29.6)	
O	14 (21.5)	16 (22.5)	
AB	8 (12.3)	4 (5.6)	
Smoking			0.027
None	29 (44.6)	41 (57.7)	
Past	18 (27.7)	23 (32.4)	
Current	18 (27.7)	7 (9.9)	
Alcohol drinking			0.299
None	26 (40.0)	33 (46.5)	
Past	23 (35.4)	28 (39.4)	
Current	16 (24.6)	10 (14.1)	
Family history	4 (6.2)	7 (9.9)	0.633
Comorbid diseases			0.204
None	36 (55.4)	34 (47.9)	
DM	11 (18.5)	17 (23.9)	
HTN	17 (33.8)	34 (47.9)	
Dyslipidemia	1 (1.5)	3 (4.2)	
Vascular disorders	7 (10.5)	4 (5.6)	
Hepatitis C	1 (1.5)	0 (0)	
Stomach cancer	1 (1.5)	1 (1.4)	
Tumor location			0.197
Right colon	23 (35.4)	36 (50.7)	
Left colon	28 (43.1)	23 (32.4)	
Rectum	14 (21.5)	12 (16.9)	
Histology			0.794
Well differentiated	4 (6.2)	7 (9.9)	
Moderately differentiated	54 (83.1)	58 (81.7)	
Poorly differentiated	5 (7.7)	5 (7.0)	
SRC/mucinous	2 (3.1)	1 (1.4)	
Lymphovascular invasion	41 (63.1)	26 (36.6)	0.004
Perineural invasion	15 (23.1)	14 (19.7)	0.789
KRAS mutation	11 (42.3)	25 (39.1)	0.962
MSI status			0.223
MSS	40 (61.5)	61 (85.9)	
MSI-low	1 (1.5)	0 (0.0)	
MSI-high	5 (7.8)	3 (4.2)	
N/A	19 (29.2)	7 (9.9)	
Tumor stage			0.060
IIIA	4 (6.2)	10 (14.1)	
IIIB	45 (69.2)	53 (74.6)	
IIIC	16 (24.6)	8 (11.3)	
Adjuvant chemotherapy regimen			0.145
FOLFOX	60 (92.3)	59 (83.1)	
CAPEOX	5 (7.7)	8 (11.3)	
FL	0 (0.0)	4 (5.6)	
CEA (ng/mL)	12.0 ± 18.7	8.2 ± 17.1	0.218

Values are presented as n (%) or mean ± standard deviation.
BMI, body mass index; DM, diabetes mellitus; HTN, hypertension; SRC, signet ring cell carcinoma; KRAS, Kirsten rat sarcoma viral oncogene homolog; MSI, microsatellite instability; MSS, microsatellite stable; N/A, non-available; FOLFOX, consists of oxaliplatin, leucovorin, and 5-fluorouracil; CAPEOX, consists of oxaliplatin and capecitabine; FL, consists of 5-fluorouracil and leucovorin; CEA, carcinoembryonic antigen.

3.2 Microbiome differences between adjacent and tumor tissues

On the basis of previous results (27, 28), we hypothesized that the tissue microbiome of patients with CRC could be a predictor of tumor recurrence after surgery. We focused on the individual differences in the microbiome and attempted to evaluate the possibility that the tissue microbiome can predict recurrence in patients with stage III CRC who underwent surgery and adjuvant chemotherapy. We compared the microbiome differences between adjacent and tumor tissues in patients in the discovery set. Alpha diversity was not different but beta diversity was significantly different between the two tissues, and the taxonomic composition showed differences at the phylum, genus, and species levels (Figure S1). Microbial abundance was remarkably different between adjacent and tumor tissues. At the phylum level, Fusobacteriota, Verrucomicrobiota, and Bacteroidota were more abundant in tumor tissue samples (Figure 2A). At the genus level, *Streptococcus* and *Gemella* were more abundant in tumor tissue samples

(Figure 2B). In contrast, the phyla Firmicutes, Proteobacteria, and Actinobacteriota (Figure 2A), and the genera *Parabacteroides*, *Faecalibacterium*, and *Parasutterella* were more abundant in adjacent tissue samples (Figure 2B). Further, linear discriminant effect size analysis confirmed that the microbial abundance in adjacent tissues was distinct from that in tumor tissues (Figure 2C).

3.3 Microbiome differences according to the presence of recurrence

Figure S2 displays the Kaplan-Meier curves for overall survival and disease-free survival differences between the discovery set and validation set. We assessed differences in the tissue microbiome

TABLE 2 Comparison between patients with and without recurrence.

	Discovery set			Validation set		
Characteristics	No recurrence (n = 40)	Recurrence (n = 25)	*p* Value	No recurrence (n = 52)	Recurrence (n = 19)	*p* Value
Tumor location			0.828			0.640
Rectum	13 (32.5)	10 (40.0)		25 (48.1)	11 (57.9)	
Left colon	18 (45.0)	10 (40.0)		17 (32.7)	6 (31.6)	
Right colon	9 (22.5)	5 (20.0)		10 (19.2)	2 (10.5)	
Histology			0.739			0.288
Well differentiated	3 (7.5)	1 (4.0)		6 (11.5)	1 (5.3)	
Moderately differentiated	32 (80.0)	22 (88.0)		43 (82.7)	15 (78.9)	
Poorly differentiated	4 (10.0)	1 (4.0)		3 (5.8)	2 (10.5)	
SRC/mucinous	1 (2.5)	1 (4.0)		0 (0.0)	1 (5.3)	
Lymphovascular invasion	24 (60.0)	17 (68.0)	0.699	19 (36.5)	7 (36.8)	1.0
Perineural invasion	7 (17.5)	8 (32.0)	0.295	8 (15.4)	6 (31.6)	0.237
KRAS mutation	8 (20.0)	3 (12.0)	0.354	17 (32.7)	8 (42.1)	0.618
MSI status			0.095			0.401
MSS	21 (52.5)	19 (100)		45 (86.5)	16 (84.2)	
MSI-low	1 (2.5)	0 (0)		3 (5.8)	0 (0.0)	
MSI-high	5 (12.5)	0 (0)		4 (7.7)	3 (15.8)	
N/A	13 (32.5)	6 (24.0)				
T stage			0.967			0.719
T1/2	3 (7.5)	1 (4.0)		8 (15.4)	2 (10.5)	
T3/4	37 (92.5)	24 (96.0)		44 (84.6)	17 (89.5)	
N stage			0.829			0.206
N1a/b	20 (50.0)	11 (44.0)		43 (82.7)	13 (68.4)	
N2a/b	20 (50.0)	14 (56.0)		9 (17.3)	6 (31.6)	
Hemoglobin (g/dL)	12.6 ± 1.8	12.7 ± 2.2	0.901			
White blood cells ($\times10^3$/μL)	7.3 ± 1.9	6.8 ± 2.0	0.341			
Platelets ($\times10^3$/μL)	265.7 ± 92.5	255.2 ± 74.4	0.637			
Glucose (mg/dL)	116.5 ± 59.6	118.4 ± 43.5	0.894			
HbA1c (%)	7.4 ± 2.4	7.1 ± 2.0	0.795			
Albumin (g/dL)	4.1 ± 0.4	4.1 ± 0.4	0.768			
HS-CRP (mg/dL)	0.8 ± 2.0	2.0 ± 4.2	0.234			
Cholesterol (mg/dL)	174.1 ± 29.5	170.7 ± 35.2	0.707			
HDL (mg/dL)	46.4 ± 11.5	46.1 ± 12.4	0.918			

(Continued)

TABLE 2 Continued

Characteristics	Discovery set			Validation set		
	No recurrence (n = 40)	Recurrence (n = 25)	*p* Value	No recurrence (n = 52)	Recurrence (n = 19)	*p* Value
Triglyceride (mg/dL)	92.6 ± 36.9	103.1 ± 38.8	0.336			
LDL (mg/dL)	108.4 ± 26.5	105.0 ± 31.4	0.678			
LDH (IU/L)	338.5 ± 63.6	362.5 ± 87.8	0.210			
CEA (ng/mL)	8.8 ± 12.0	17.1 ± 25.5	0.142	7.3 ± 16.3	10.6 ± 19.3	0.484
CA 19-9 (U/mL)	13.1 ± 26.9	18.6 ± 18.5	0.375			

Values are presented as n (%) or mean ± standard deviation.
SRC, signet ring cell carcinoma; KRAS, Kirsten rat sarcoma viral oncogene homolog; MSI, microsatellite instability; MSS, microsatellite stable; N/A, non-available; HbA1c, hemoglobin A1c; HS-CRP, high-sensitivity C-reactive protein; CEA, carcinoembryonic antigen; CA 19-9, carbohydrate antigen 19-9; HDL, high-density lipoprotein; LDL, low-density lipoprotein ; LDH, lactate dehydrogenase.

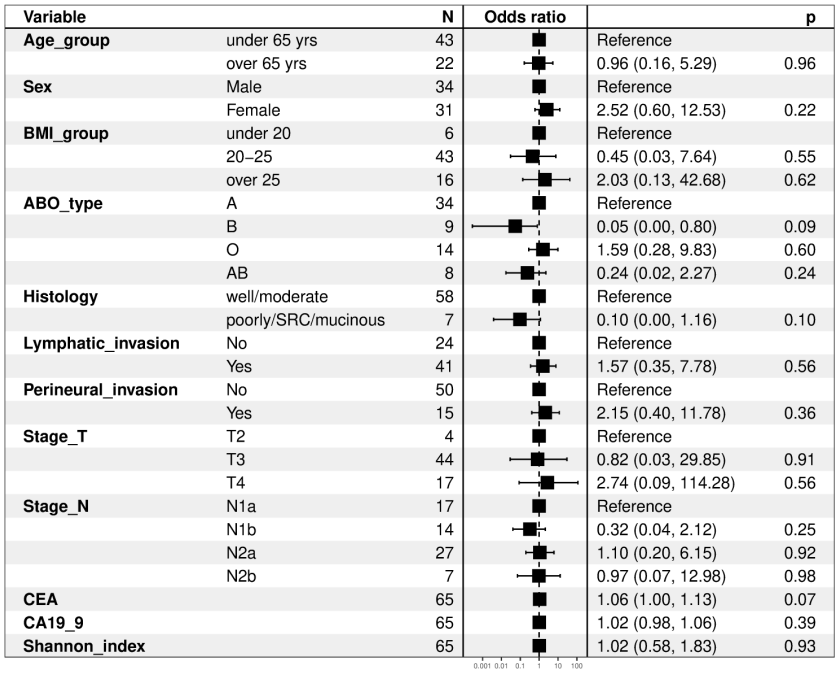

FIGURE 1
Forest plots of clinical factors as predictors of tumor recurrence. BMI, body mass index; SRC, signet ring cell carcinoma; CEA, carcinoembryonic antigen; CA19-9, carbohydrate antigen 19-9.

according to the presence of recurrence. As shown in Figure S3, the taxonomic composition of the tissue microbiome was not different at the phylum, genus, and species levels between patients with and without recurrence in both the discovery and validation sets. In the discovery set, alpha diversity, beta diversity, and microbial abundance at the phylum and genus levels in adjacent and tumor tissues were not significantly different according to the presence of recurrence (Figure 3). Similar results were obtained when the data were divided into male and female groups (Figure S4). In the validation set, alpha and beta diversities did not differ according to the presence of recurrence, and microbial abundance at the phylum and genus levels were also not different, except for the genus *Prevotella* (Figure 4). Similar results were obtained when the data were divided into male and female groups; however, *Prevotella* was more abundant in tumor tissue samples from male patients without recurrence (Figure S5).

3.4 Generation and validation of a prediction model for CRC recurrence

Although we found no significant differences in tissue microbial diversity and abundance between patients with and without recurrence, we attempted to generate a recurrence prediction model including microbiome data using logistic regression analysis in the discovery set. When the analysis was performed by combining clinical factors (age, CEA level, histology, lymphovascular invasion, perineural invasion, stage T, and stage N) and tumor microbiome data (selecting only the genera with a relative abundance greater than or equal to 1%), we found that CEA level, T stage, and perineural invasion (among clinical factors), as well as the tumor tissue microbiome (including *Gemella*, *Parabacteroides*, *Parasutterella*, and *Prevotella*) were significant. We obtained the following estimation formula for the prediction model (see Supplementary Data):

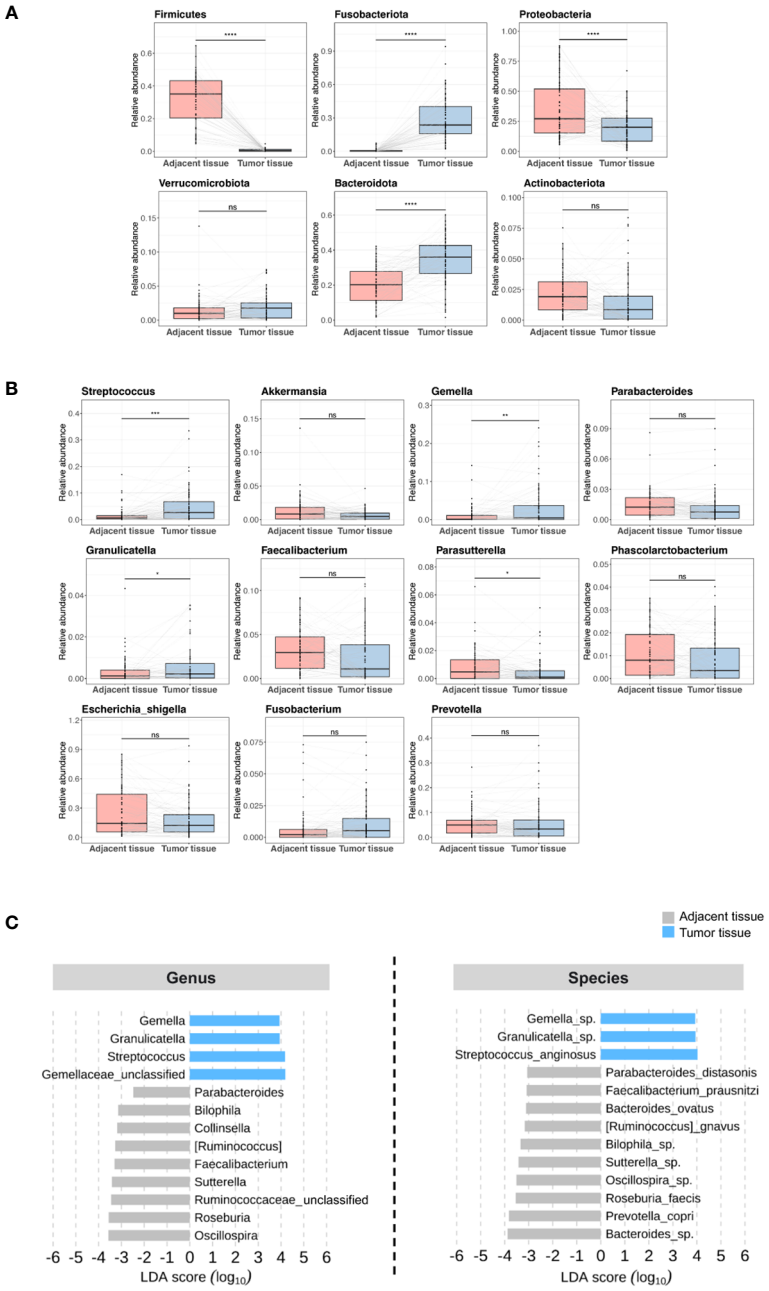

FIGURE 2
Microbial abundance between adjacent and tumor tissues in patients in the discovery set. **(A)** Phylum level. **(B)** Genus level. **(C)** Linear discriminant analysis effect size. ns, non-significant; LDA, linear discriminant analysis. '*', $p < 0.05$; '**', $p < 0.01$; '***', $p < 0.001$; '****', $p < 0.0001$.

$$f(x) = -4.29796 + 0.04667{*}\text{CEA level} + 1.08028 * \text{T stage} + 1.47743 * \text{perineural invasion} - 33.38073 * \textit{Gemella} + 28.07568 * \textit{Parabacteroides} - 141.75533{*}\textit{Parasutterella} + 7.85802 * \textit{Prevotella}$$

(Akaike information criteria : 74.9, Nagelkerke R2 : 47.2%)

We applied the prediction model in generating the ROC curve and compared it to clinical factors (combination of CEA level, T stage, and perineural invasion) without microbiome. The AUC value of this model was 0.846 (95% confidence interval [CI], 0.754–0.938) in the total patients, and a good AUC value was obtained in both male and female patients (Figure 5). When compared with the ROC curve of clinical factors without microbiome, the prediction model showed a significantly better AUC value than clinical factors in the total patients (0.846 vs. 0.679, $p = 0.009$) (Figure 5A), regardless of sex (0.943-0.818, $p = 0.043$ in male; 0.885 vs. 0.590, $p = 0.017$ in female) (Figures 5C, D). In the random forest model analysis, *Gemella*, *Parabacteroides, and Prevotella* had a mean decrease in the Gini coefficient of > 3.0 (Figure 5B).

When the prediction model was applied to the validation set, it showed an AUC value of 0.740 (95% CI, 0.606–0.873), which was not better than the AUC value of clinical factors without microbiome in the analysis of the total patients (Figure 6A). However, the prediction

10.3389/fonc.2023.1212812

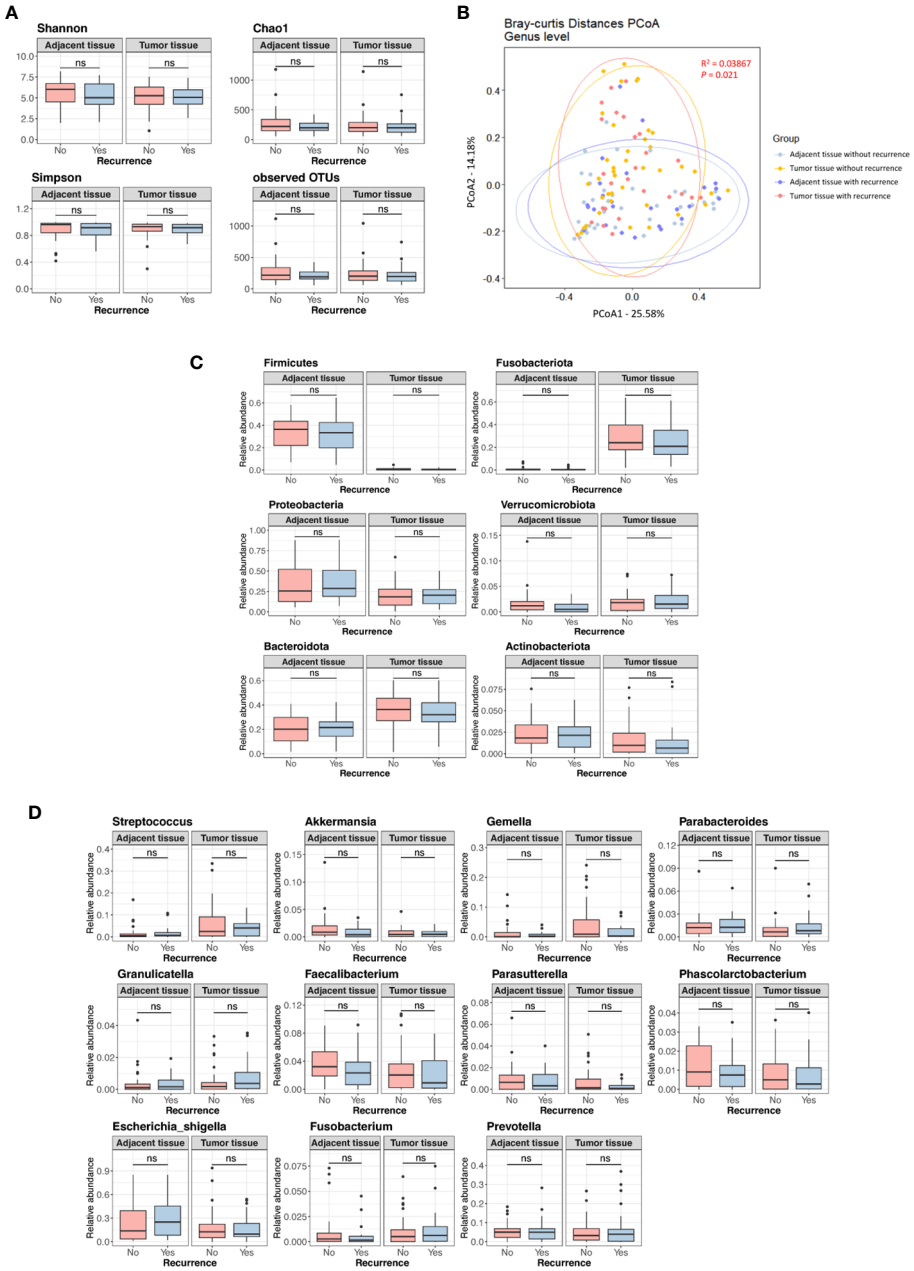

FIGURE 3
Microbial diversity and abundance in adjacent and tumor tissues according to the presence of recurrence in the discovery set. **(A)** Alpha diversity. **(B)** Beta diversity. **(C)** Phylum level. **(D)** Genus level. OTUs, operational taxonomy units; PCoA, principal coordinate analysis; ns, non-significant.

model showed a better AUC value than clinical factors in female patients (0.858 vs. 0.624, p = 0.022) (Figure 6D), but not in male patients (Figure 6C). In the random forest model analysis of the validation set, *Faecalibacterium*, *Prevotella* and *Gemella* had a mean decrease in the Gini coefficient of > 3.0 (Figure 6B).

4 Discussion

In the present study, we assessed a model combining clinical factors and tumor tissue microbiome data for predicting recurrence in patients with stage III CRC. This model showed better AUC values than clinical factors. Our data suggest that analysis of the tumor tissue microbiome combined with clinical factors may help predict recurrence in patients with CRC.

Recent studies have identified *Fusobacterium*, *Bacteroides*, *Peptostreptococcus*, *Gemella*, and *Parvimonas* as genera that are potentially associated with CRC, and emerging evidence has demonstrated their oncogenic functions; however, inter-individual variations in tumor-associated mucosal microbiome remain a barrier to elucidating the role of the microbiome in colorectal tumorigenesis. Concerning intra-individual variations in microbial patterns, several studies have shown that the microbiome structure of cancerous tissues significantly differs from that of the intestinal lumen, and

10.3389/fonc.2023.1212812

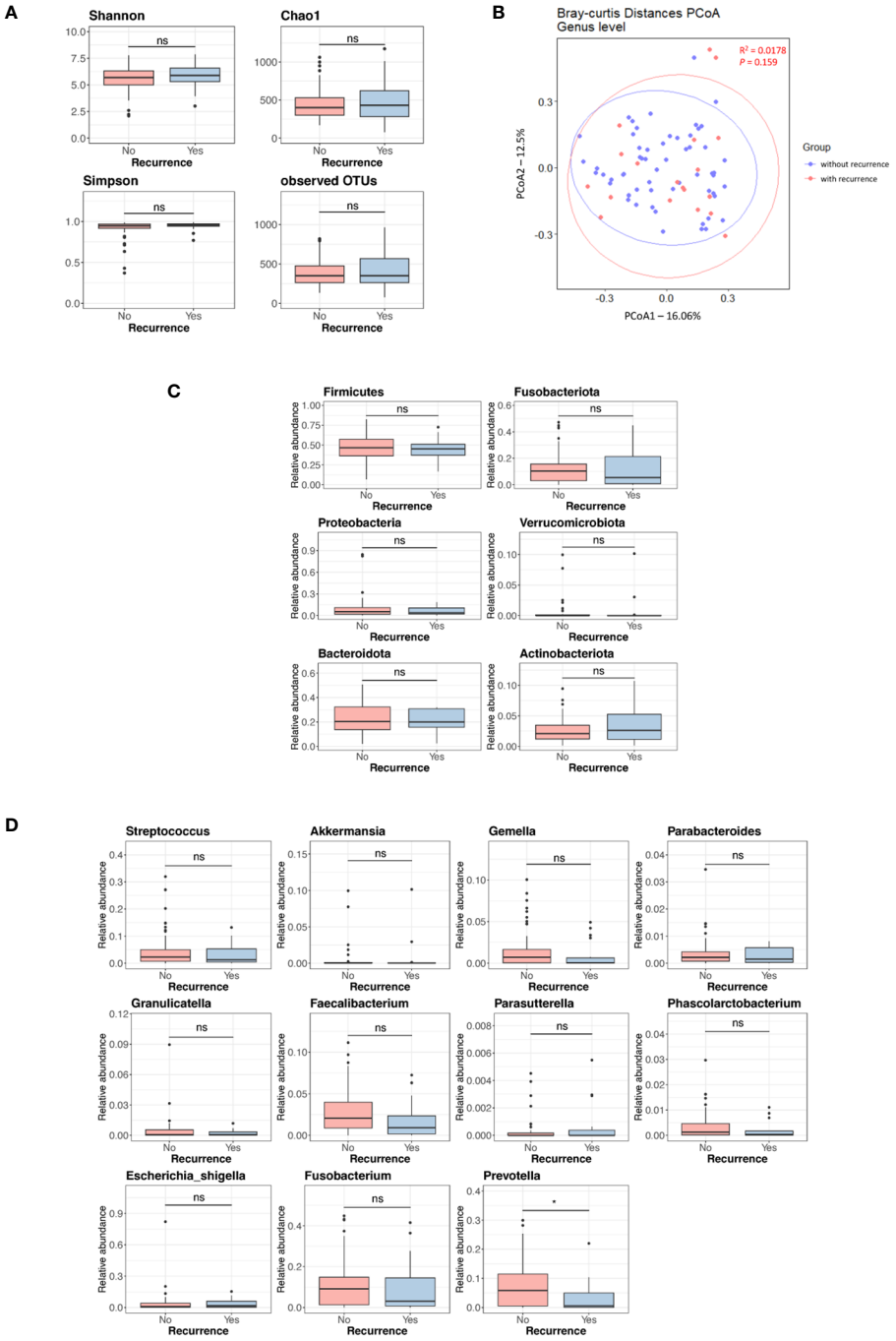

FIGURE 4
Microbial diversity and abundance in tumor tissues according to the presence of recurrence in the validation set. **(A)** Alpha diversity. **(B)** Beta diversity. **(C)** Phylum level. **(D)** Genus level. OTUs, operational taxonomy units; PCoA, principal coordinate analysis; ns, non-significant. '*', $p < 0.05$.

that the microbiome of CRC tissues remarkably differs from that of adjacent tissues (30–32). Consistent with previous studies, our study showed significant differences in the beta diversity and abundance of microbiome between tumor and adjacent tissues. In particular, *Streptococcus* and *Gemella* were more abundant in tumor tissue samples than in adjacent tissue samples. An analysis of paired samples of CRC-adjacent mucosa and colonic mucosa from healthy controls showed differences in microbial community configurations (33). These results suggest that the microbial communities in the colorectal mucosa show distinct alterations according to the stage of colorectal carcinogenesis.

The observed association between the gut microbiome and clinical outcomes has raised the possibility that bacteria can serve as prognostic markers. Several studies reported that increased abundance of *F. nucleatum* and *B. fragilis* was associated with poor clinical outcomes and late-stage CRC (34, 35). In a recent study investigating the profiles of the gut mucosal microbiome in patients with CRC recurrence, a total of 17 bacteria were suggested

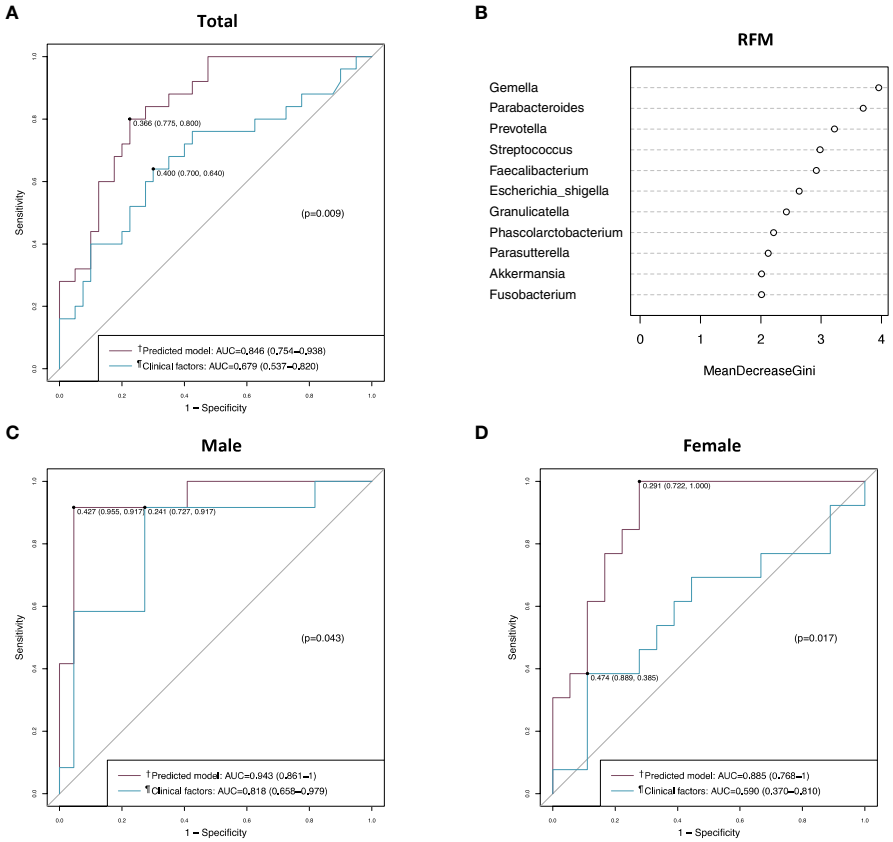

FIGURE 5
Receiver operating characteristic (ROC) curve and random forest model analyses in the discovery set. **(A)** ROC curves of the prediction model and the clinical factors in the total patients. **(B)** Random forest model evaluating tissue microbiomes. **(C)** ROC curves of the prediction model and the clinical factors in male patients. **(D)** ROC curves of the prediction model and the clinical factors in female patients. †Includes clinical factors (CEA level, T stage, and perineural invasion) and tumor tissue microbiome (*Gemella*, *Parabacteroides*, *Parasutterella*, and *Prevotella*). ¶Includes CEA level, T stage, and perineural invasion. AUC, area under the curve; RFM, random forest model.

as potential biomarkers for CRC recurrence and patient prognosis (36). In addition, the persistence of *F. nucleatum* after neoadjuvant chemoradiotherapy in patients with locally advanced rectal cancer was found to be correlated with high relapse rates (37). In the present study, we assessed microbial differences according to the presence of recurrence, and found no significant differences in microbial diversity and the abundance of each microbial group between patients with and without recurrence, except for one genus in the validation set. This lack of difference may be explained by the possibility that a network of numerous microbiomes, rather than the presence of a characteristic microbiome in tumor tissues, contributes to the development of recurrence.

We generated a prediction model for CRC recurrence by combining clinical factors and tumor tissue microbiome data. The model finally included several genera, such as *Gemella*, *Parabacteroides*, *Parasutterella*, and *Prevotella*. This prediction model had a good AUC value in patients with CRC regardless of sex and showed significantly better performance in predicting recurrence than the clinical factors. These results suggest that gut microbiome assessment has a potential role in predicting CRC recurrence; however, further studies with larger sample sizes are needed.

Adjuvant chemotherapy has demonstrated benefits in patients with stage III CRC, it can reduce the risk of recurrence by approximately 30% (7, 8). According to the NCCN guidelines, for low-risk (T1-3, N1) stage III CRC patients, CAPEOX (3 months) or FOLFOX (3-6 months), as well as other options like capecitabine (6 months) or 5-FU (6 months), are recommended. On the other hand, for high-risk (T4, N1-2; any T, N2) stage III CRC patients, the recommended options include CAPEOX (3-6 months) or FOLFOX (6 months), as well as other options like capecitabine (6 months) or 5-FU (6 months) (38). Liquid biopsy is a promising alternative strategy for directly evaluating circulating tumor DNA (ctDNA) from the blood. It aims to detect evidence of minimal residual disease, which could potentially be the source of a later clinical recurrence. Recently, in a study of 455 stage II CRC patients, ctDNA-guided management led to a reduced rate of adjuvant chemotherapy usage, and ctDNA-positive patients who received adjuvant chemotherapy exhibited a three-year recurrence-free survival of 86.4% (39). Although further research is needed, the combined analysis of liquid biopsy and tumor microbiome has the potential to offer more promising insights into predicting patient prognosis and determining the need for additional chemotherapy after surgery in stage III CRC patients.

The strength of our study is that the results obtained by analyzing tumor and adjacent tissue samples from one center were validated by comparing them with tumor tissue data from

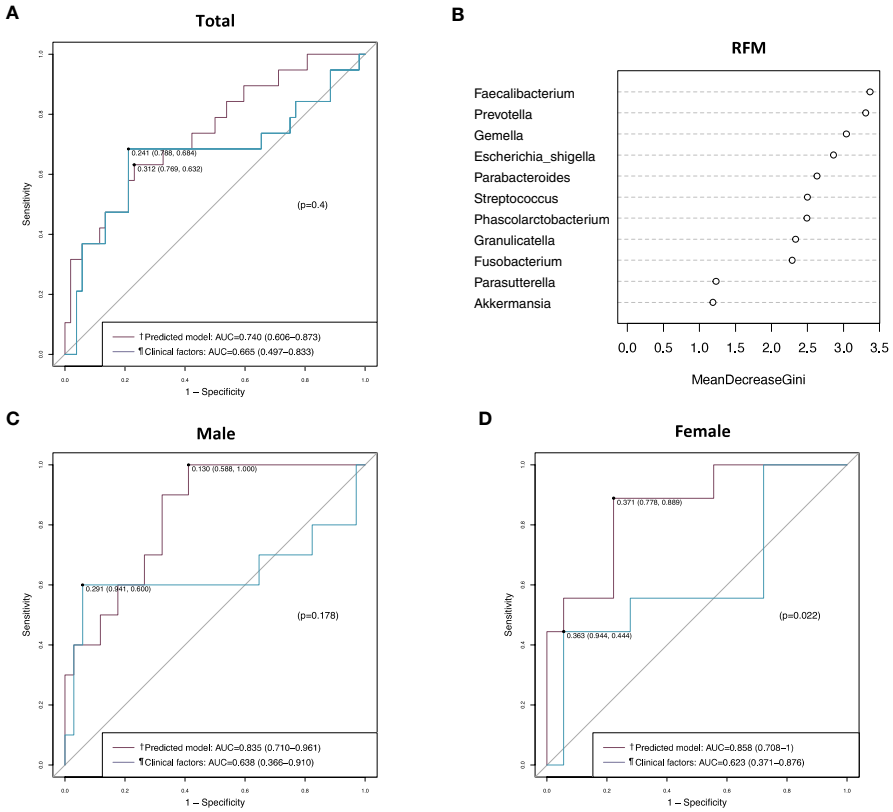

FIGURE 6
Receiver operating characteristic (ROC) curve and random forest model analyses in the validation set. **(A)** ROC curves of the prediction model and the clinical factors in the total patients. **(B)** Random forest model evaluating tissue microbiomes. **(C)** ROC curves of the prediction model and the clinical factors in male patients. **(D)** ROC curves of the prediction model and the clinical factors in female patients. †Includes clinical factors (CEA level, T stage, and perineural invasion) and tumor tissue microbiome (*Gemella*, *Parabacteroides*, *Parasutterella*, and *Prevotella*). ¶Includes CEA level, T stage, and perineural invasion. AUC, area under the curve; RFM, random forest model.

another center. However, our study had several limitations. First, the tumor tissue samples from the two centers were collected at different times and stored in different locations, which may have introduced heterogeneity in the results. Second, we could not compare the microbiomes of adjacent tissues in the validation set because no adjacent tissue data were collected from the other center. Third, the prediction model generated using the discovery set did not show a better AUC value than the clinical factors for the total patients and male patients in the validation set. We believe that this was due to data heterogeneity and the small number of samples. Fourth, the study's sample size was small, which could reduce the reliability of our results. To overcome these limitations, further well-designed studies with larger sample sizes are needed.

In summary, we conducted a comprehensive investigation of the differences in microbial diversity and abundance between tumor and adjacent tissues, as well as their association with recurrence in CRC patients. Additionally, we developed a prediction model using tissue microbiome data to forecast postoperative recurrence. While the predictive performance of our model, measured by AUC values, did not surpass that of the clinical factors alone in the validation set, we did observe a relatively higher AUC value for the new model using microbiome data in female patients. However, we acknowledge the need for further research to explore potential gender-based differences in the microbiome profile's predictive capacity for CRC recurrence. Therefore, the approach for the generalization of these findings should proceed with caution, and we refrain from unequivocally concluding that the tumor microbiome can predict postoperative disease recurrence in all patients. Nevertheless, we believe that our study contributes to emphasizing the importance of the tissue microbiome in diagnosing and predicting the recurrence of CRC.

Data availability statement

The raw data supporting the conclusions of this article will be made available by the authors, without undue reservation.

Ethics statement

The studies involving humans were approved by Kosin University Gospel Hospital (approval no. KUGH 2021-01-028).

The studies were conducted in accordance with the local legislation and institutional requirements. The participants provided their written informed consent to participate in this study.

Author contributions

JK: conceptualization, formal analysis, writing – original, and funding acquisition. JY: conceptualization, formal analysis, and writing – original. DK: methodology and formal analysis. SL, SHL and BA: Resources and data curation. TK: conceptualization, supervision, writing – review & editing. SP: conceptualization, supervision, writing – review & editing, and funding acquisition. All authors contributed to the article and approved the submitted version.

Funding

This study was supported by National Research Foundation of Korea (NRF) grant funded by the Korea government (MSIT), No. 2020R1C1C1012694. This study was supported by Daewon Pharmaceutical Co., Ltd, Seoul, Korea.

The authors declare that this study received funding from Daewon Pharmaceutical Co., Ltd, Seoul, Korea. The funder was not involved in the study design, collection, analysis, interpretation of data, the writing of this article or the decision to submit it for publication.

Acknowledgments

We thank Hecto Healthcare Co., Ltd for their assistance with DNA extraction, 16S rRNA sequencing, and data analysis for the manuscript.

Conflict of interest

The authors declare that the research was conducted in the absence of any commercial or financial relationships that could be construed as a potential conflict of interest.

Publisher's note

Supplementary material

The Supplementary Material for this article can be found online at: https://www.frontiersin.org/articles/10.3389/fonc.2023.1212812/full#supplementary-material

SUPPLEMENTARY FIGURE 1
Microbial diversity and composition in adjacent and tumor tissues of patients in the discovery set. **(A)** Alpha diversity. **(B)** Beta diversity. **(C)** Taxonomic composition at the phylum level. **(D)** Taxonomic composition at the genus level. **(E)** Taxonomic composition at the species level.

SUPPLEMENTARY FIGURE 2
Taxonomic composition of microbiomes. **(A–C)** Taxonomic composition at the phylum, genus, and species levels in the discovery set. **(D–F)** Taxonomic composition at the phylum, genus, and species levels in the validation set.

SUPPLEMENTARY FIGURE 3
Microbial diversity and abundance in adjacent and tumor tissues according to the presence of recurrence in male and female patients in the discovery set. **(A)** Alpha diversity. **(B)** Phylum level. **(C)** Genus level.

SUPPLEMENTARY FIGURE 4
Microbial diversity and abundance in tumor tissues according to the presence of recurrence in male and female patients in the validation set. **(A)** Alpha diversity. **(B)** Phylum level. **(C)** Genus level.

References

1. Xi Y, Xu P. Global colorectal cancer burden in 2020 and projections to 2040. *Transl Oncol* (2021) 14:101174. doi: 10.1016/j.tranon.2021.101174

2. Sinicrope FA. Increasing incidence of early-onset colorectal cancer. *N Engl J Med* (2022) 386:1547–58. doi: 10.1056/NEJMra2200869

3. Osterman E, Hammarström K, Imam I, Osterlund E, Sjöblom T, Glimelius B. Recurrence risk after radical colorectal cancer surgery—less than before, but how high is it? *Cancers (Basel)* (2020) 12:3308. doi: 10.3390/cancers12113308

4. Osterman E, Glimelius B. Recurrence risk after up-to-date colon cancer staging, surgery, and pathology: analysis of the entire swedish population. *Dis Colon Rectum* (2018) 61:1016–25. doi: 10.1097/dcr.0000000000001158

5. Lan YT, Chang SC, Yang SH, Lin CC, Wang HS, Jiang JK, et al. Comparison of clinicopathological characteristics and prognosis between early and late recurrence after curative surgery for colorectal cancer. *Am J Surg* (2014) 207:922–30. doi: 10.1016/j.amjsurg.2013.08.035

6. Benson AB, Venook AP, Al-Hawary MM, Arain MA, Chen YJ, Ciombor KK, et al. Colon cancer, version 2.2021, NCCN clinical practice guidelines in oncology. *J Natl Compr Canc Netw* (2021) 19:329–59. doi: 10.6004/jnccn.2021.0012

7. Abulafi AM, Williams NS. Local recurrence of colorectal cancer: the problem, mechanisms, management and adjuvant therapy. *Br J Surg* (1994) 81:7–19. doi: 10.1002/bjs.1800810106

8. Sargent D, Sobrero A, Grothey A, O'Connell MJ, Buyse M, Andre T, et al. Evidence for cure by adjuvant therapy in colon cancer: observations based on individual patient data from 20,898 patients on 18 randomized trials. *J Clin Oncol* (2009) 27:872–7. doi: 10.1200/jco.2008.19.5362

9. Dekker E, Tanis PJ, Vleugels JLA, Kasi PM, Wallace MB. Colorectal cancer. *Lancet* (2019) 394:1467–80. doi: 10.1016/s0140-6736(19)32319-0

10. Yang Y, Wang G, He J, Ren S, Wu F, Zhang J, et al. Gender differences in colorectal cancer survival: a meta-analysis. *Int J Cancer* (2017) 141:1942–9. doi: 10.1002/ijc.30827

11. Schmuck R, Gerken M, Teegen EM, Krebs I, Klinkhammer-Schalke M, Aigner F, et al. Gender comparison of clinical, histopathological, therapeutic and outcome factors in 185,967 colon cancer patients. *Langenbecks Arch Surg* (2020) 405:71–80. doi: 10.1007/s00423-019-01850-6

12. Sant M, Allemani C, Santaquilani M, Knijn A, Marchesi F, Capocaccia R. EUROCARE-4. Survival of cancer patients diagnosed in 1995-1999. Results and commentary. *Eur J Cancer* (2009) 45:931–91. doi: 10.1016/j.ejca.2008.11.018

13. White A, Ironmonger L, Steele RJC, Ormiston-Smith N, Crawford C, Seims A. A review of sex-related differences in colorectal cancer incidence, screening uptake, routes to diagnosis, cancer stage and survival in the UK. *BMC Cancer* (2018) 18:906. doi: 10.1186/s12885-018-4786-7

14. Konishi T, Shimada Y, Lee LH, Cavalcanti MS, Hsu M, Smith JJ, et al. Poorly differentiated clusters predict colon cancer recurrence: an in-depth comparative analysis of invasive-front prognostic markers. *Am J Surg Pathol* (2018) 42:705–14. doi: 10.1097/pas.0000000000001059

15. Fujita S, Shimoda T, Yoshimura K, Yamamoto S, Akasu T, Moriya Y. Prospective evaluation of prognostic factors in patients with colorectal cancer undergoing curative resection. *J Surg Oncol* (2003) 84:127–31. doi: 10.1002/jso.10308

16. Lugli A, Kirsch R, Ajioka Y, Bosman F, Cathomas G, Dawson H, et al. Recommendations for reporting tumor budding in colorectal cancer based on the International Tumor Budding Consensus Conference (ITBCC) 2016. *Mod Pathol* (2017) 30:1299–311. doi: 10.1038/modpathol.2017.46

17. Lee H, Sha D, Foster NR, Shi Q, Alberts SR, Smyrk TC, et al. Analysis of tumor microenvironmental features to refine prognosis by T, N risk group in patients with stage III colon cancer (NCCTG N0147) (Alliance). *Ann Oncol* (2020) 31:487–94. doi: 10.1016/j.annonc.2020.01.011

18. Gryfe R, Kim H, Hsieh ET, Aronson MD, Holowaty EJ, Bull SB, et al. Tumor microsatellite instability and clinical outcome in young patients with colorectal cancer. *N Engl J Med* (2000) 342:69–77. doi: 10.1056/nejm200001133420201

19. Idos GE, Kwok J, Bonthala N, Kysh L, Gruber SB, Qu C. The prognostic implications of tumor infiltrating lymphocytes in colorectal cancer: A systematic review and meta-analysis. *Sci Rep* (2020) 10:3360. doi: 10.1038/s41598-020-60255-4

20. Nosho K, Baba Y, Tanaka N, Shima K, Hayashi M, Meyerhardt JA, et al. Tumour-infiltrating T-cell subsets, molecular changes in colorectal cancer, and prognosis: cohort study and literature review. *J Pathol* (2010) 222:350–66. doi: 10.1002/path.2774

21. Tie J, Cohen JD, Wang Y, Christie M, Simons K, Lee M, et al. Circulating tumor DNA analyses as markers of recurrence risk and benefit of adjuvant therapy for stage III colon cancer. *JAMA Oncol* (2019) 5:1710–7. doi: 10.1001/jamaoncol.2019.3616

22. Tie J, Cohen JD, Lahouel K, Lo SN, Wang Y, Kosmider S, et al. Circulating tumor DNA analysis guiding adjuvant therapy in stage II colon cancer. *N Engl J Med* (2022) 386:2261–72. doi: 10.1056/NEJMoa2200075

23. Wong SH, Yu J. Gut microbiota in colorectal cancer: mechanisms of action and clinical applications. *Nat Rev Gastroenterol Hepatol* (2019) 16:690–704. doi: 10.1038/s41575-019-0209-8

24. Routy B, Le Chatelier E, Derosa L, Duong CPM, Alou MT, Daillère R, et al. Gut microbiome influences efficacy of PD-1-based immunotherapy against epithelial tumors. *Science* (2018) 359:91–7. doi: 10.1126/science.aan3706

25. Matson V, Fessler J, Bao R, Chongsuwat T, Zha Y, Alegre ML, et al. The commensal microbiome is associated with anti-PD-1 efficacy in metastatic melanoma patients. *Science* (2018) 359:104–8. doi: 10.1126/science.aao3290

26. Gopalakrishnan V, Spencer CN, Nezi L, Reuben A, Andrews MC, Karpinets TV, et al. Gut microbiome modulates response to anti-PD-1 immunotherapy in melanoma patients. *Science* (2018) 359:97–103. doi: 10.1126/science.aan4236

27. Mima K, Nishihara R, Qian ZR, Cao Y, Sukawa Y, Nowak JA, et al. Fusobacterium nucleatum in colorectal carcinoma tissue and patient prognosis. *Gut* (2016) 65:1973–80. doi: 10.1136/gutjnl-2015-310101

28. Riquelme E, Zhang Y, Zhang L, Montiel M, Zoltan M, Dong W, et al. Tumor microbiome diversity and composition influence pancreatic cancer outcomes. *Cell* (2019) 178:795–806.e12. doi: 10.1016/j.cell.2019.07.008

29. Choi S, Chung J, Cho ML, Park D, Choi SS. Analysis of changes in microbiome compositions related to the prognosis of colorectal cancer patients based on tissue-derived 16S rRNA sequences. *J Transl Med* (2021) 19:485. doi: 10.1186/s12967-021-03154-0

30. Leung PHM, Subramanya R, Mou Q, Lee KT, Islam F, Gopalan V, et al. Characterization of mucosa-associated microbiota in matched cancer and non-neoplastic mucosa from patients with colorectal cancer. *Front Microbiol* (2019) 10:1317. doi: 10.3389/fmicb.2019.01317

31. Marchesi JR, Dutilh BE, Hall N, Peters WH, Roelofs R, Boleij A, et al. Towards the human colorectal cancer microbiome. *PloS One* (2011) 6:e20447. doi: 10.1371/journal.pone.0020447

32. Chen W, Liu F, Ling Z, Tong X, Xiang C. Human intestinal lumen and mucosa-associated microbiota in patients with colorectal cancer. *PloS One* (2012) 7:e39743. doi: 10.1371/journal.pone.0039743

33. Nakatsu G, Li X, Zhou H, Sheng J, Wong SH, Wu WKK, et al. Gut mucosal microbiome across stages of colorectal carcinogenesis. *Nat Commun* (2015) 6:1–9. doi: 10.1038/ncomms9727

34. Wei Z, Cao S, Liu S, Yao Z, Sun T, Li Y, et al. Could gut microbiota serve as prognostic biomarker associated with colorectal cancer patients' survival? A pilot study on relevant mechanism. *Oncotarget* (2016) 7:46158–72. doi: 10.18632/oncotarget.10064

35. Colov E?A3B2 show
?>P, Degett TH, Raskov H, Gögenur I. The impact of the gut microbiota on prognosis after surgery for colorectal cancer - a systematic review and meta-analysis. *APMIS* (2020) 128:162–76. doi: 10.1111/apm.13032

36. Huo RX, Wang YJ, Hou SB, Wang W, Zhang CZ, Wan XH. Gut mucosal microbiota profiles linked to colorectal cancer recurrence. *World J Gastroenterol* (2022) 28:1946–64. doi: 10.3748/wjg.v28.i18.1946

37. Serna G, Ruiz-Pace F, Hernando J, Alonso L, Fasani R, Landolfi S, et al. Fusobacterium nucleatum persistence and risk of recurrence after preoperative treatment in locally advanced rectal cancer. *Ann Oncol* (2020) 31:1366–75. doi: 10.1016/j.annonc.2020.06.003

38. National Comprehensive Cancer Network. NCCN clinical practice guidelines in oncology. *Colon Cancer ver* (2023) 2.

39. Tie J, Cohen JD, Lahouel K, Lo SN, Wang Y, Kosmider S, et al. Circulating Tumor DNA analysis guiding adjuvant therapy in stage II colon cancer. *N Engl J Med* (2022) 386:2261–72. doi: 10.1056/NEJMoa2200075

frontiers | Frontiers in Oncology

TYPE Original Research
PUBLISHED 22 November 2023
DOI 10.3389/fonc.2023.1242193

OPEN ACCESS

EDITED BY
Sharon R. Pine,
University of Colorado Anschutz Medical Campus, United States

REVIEWED BY
Anton A. Plekhanov,
Privolzhsky Research Medical University (PIMU), Russia
Francesco Ricchetti,
Sacro Cuore Don Calabria Hospital (IRCCS), Italy

*CORRESPONDENCE
Zhongxue Fu
fzx19990521@126.com

RECEIVED 18 June 2023
ACCEPTED 08 November 2023
PUBLISHED 22 November 2023

CITATION
Yang J, Deng Q, Chen Z, Chen Y and Fu Z (2023) Body composition parameters combined with blood biomarkers and magnetic resonance imaging predict responses to neoadjuvant chemoradiotherapy in locally advanced rectal cancer.
Front. Oncol. 13:1242193.
doi: 10.3389/fonc.2023.1242193

Body composition parameters combined with blood biomarkers and magnetic resonance imaging predict responses to neoadjuvant chemoradiotherapy in locally advanced rectal cancer

Jianguo Yang, Qican Deng, Zhenzhou Chen, Yajun Chen and Zhongxue Fu*

Department of Gastrointestinal Surgery, The First Affiliated Hospital of Chongqing Medical University, Chongqing, China

Aim: To investigate whether body composition parameters combined with systemic inflammatory markers and magnetic resonance imaging (MRI) can predict the pathological complete response (pCR) following neoadjuvant chemoradiotherapy (NCRT) in locally advanced rectal cancer (LARC).

Methods: A retrospective analysis of data on LARC patients treated with NCTR and radical surgery between January 2013 and May 2023 was performed. Body composition parameters were assessed by measuring the skeletal muscle index (SMI), subcutaneous adipose index (SAI), and visceral adipose index (VAI) at the third lumbar vertebra level by computed tomography (CT). Inflammatory markers such as neutrophil to lymphocyte ratio (NLR) were obtained from laboratory tests performed prior to NCRT. MRI was conducted to evaluate MRI tumor regression grading (mrTRG). Logistic regression analyses were employed to identify factors affecting the pCR. The risk score of pCR was computed by a nomogram. The discrimination of the nomogram was determined using C-index and calibration curve.

Results: Two hundred and ninety-one patients with LARC were enrolled in the study, 55 (18.9%) of whom achieved pCR after NCRT. Multivariate analysis suggested that pre-NCRT NLR≥2.6 (OR=0.378, 95% CI 0.164-0.868, P=0.022), mrTRG 3-5 (OR=0.256, 95%CI 0.121-0.54, P<0.001), and pre-NCRT L-SMI (OR=0.292, 95% CI 0.097-0.883, P=0.029) were independent risk factors for pCR. ROC curves analysis demonstrated that the performance of mrTRG combined with pre-NCRT NLR and pre-NCRT L-SMI in predicting pCR was significantly improved compared with mrTRG alone (AUC: 0.763 vs. 0.667). Additionally, mrTRG 3-5 (OR=0.375, 95% CI 0.219-0.641, P<0.001) was also an independent predictor for poor tumor regression.

Conclusion: The pathological complete response of neoadjuvant chemoradiotherapy in locally advanced rectal cancer can be effectively predicted by combining the body composition parameters with blood biomarkers and magnetic resonance imaging.

KEYWORDS

rectal cancer, neoadjuvant chemoradiotherapy, pathological complete response, body composition parameters, blood biomarkers, magnetic resonance imaging

Introduction

The statistics for cancer in 2022 have shown that colorectal cancer (CRC) has the third incidence and second highest mortality rate of all cancers, and its occurrence is rapidly increasing (1). Rectal cancer represents approximately 30% of all CRCs, with most being diagnosed at an already locally advanced stage (2). The standard treatment strategy for locally advanced rectal cancer (LARC) continues to be neoadjuvant chemoradiotherapy (NCRT) in combination with total mesorectal resection (TME) (3, 4). NCRT has been found to significantly improve local control of tumors, R0 resection, and sphincter-preservation rate (5). However, there are significant differences in individualized treatment responses to NCRT in LARC. Although the majority of LARC patients exhibit a pathological tumor regression response after NCRT, only 10%-30% of LARC patients achieve pathological complete response (pCR) (6). Given that tumor regression response after NCRT is closely related to the oncological outcome of patients (7, 8), predicting pCR plays a crucial role in treating LARC.

Body composition and obesity were linked with the occurrence and prognosis of cancer. Obesity was a high-risk factor for developing CRC, as well as the potential risk factor for drug resistance and oncological prognosis (9, 10). LARC patients with obesity have lower pCR and sphincter-preservation rates, and higher postoperative complications (11). Skeletal muscle, subcutaneous adipose, and visceral adipose are important components of the body, and CT has become a popular tool for assessing body composition (12). Compared to body mass index (BMI), body composition parameters are more precise in reflecting the skeletal muscle and adipose status of patients with rectal cancer (13). Low skeletal muscle has been proven to predict poor short-term and long-term clinical outcomes in patients with CRC, gastric cancer, liver cancer, bile duct cancer, and pancreatic cancer (14, 15). Low skeletal muscle also contributes to adverse effects and decreased sensitivity of LARC patients to NCRT (16). Subcutaneous adipose and visceral adipose are also important parameters that reflect the function of the body. High subcutaneous adipose and visceral adipose were independent factors influencing the tumor regression grade (TRG), postoperative complications, and recurrence in LARC (17, 18). Several meta-analyses have shown that CT-based adiposity parameters are better predictors of short-term and long-term oncological outcomes in renal clear cell carcinoma, pancreatic cancer, and gastric cancer (19–23).

Cancer-related systemic inflammation is also connected to the development, treatment sensitivity, and prognosis of many cancers, including colorectal, gastric, prostate, and breast cancers (24). The neutrophil-to-lymphocyte ratio (NLR), monocyte-to-lymphocyte ratio (MLR), systemic immune-inflammatory index (SII), and platelet-to-lymphocyte ratio (PLR) are commonly used blood markers of systemic inflammation (24). Studies have revealed that systemic inflammatory markers are not only important predictors of pathological response to NCRT in LARC but are also influential factors of disease-free survival (DFS) and overall survival (OS) (24–26).

Magnetic resonance imaging (MRI) is widely performed for pre-treatment staging and assessment of tumor regression of rectal cancer. In particular, diffusion-weighted imaging (DWI) further effectively differentiates the residual tumor cells and the level of fibrosis in the treated area after NCRT (27). A previous study revealed that MRI tumor regression grade (mrTRG) was an independent predictor of pCR, with an AUC value of 0.721. In addition, mrTRG combined with NLR, LMR, and carcinoembryonic antigen (CEA) had a significantly higher performance in predicting pCR (AUC=0.913) (28). To date, there has been a lack of research investigating the combination of body composition parameters, mrTRG, and inflammatory markers for the purpose of predicting pCR after NCRT in patients with LARC.

Consequently, the aim of this study was to assess the potential of combining body composition parameters, systemic inflammatory markers, and mrTRG as a predictive tool for pCR following NCRT in LARC patients.

Materials and methods

Patients

We retrospectively analyzed data from 291 patients with LARC who underwent NCTR and radial surgery at The First Hospital of Chongqing Medical University between January 2013 and May 2023. The inclusion criteria were as follows: (1) age >18 years; (2) adenocarcinoma; (3) the distance tumor from the anus <12 cm; (4) clinical T3-4 or N+ and no distant metastasis; (5) completion of

NCRT and radical surgery; (6) completion of imaging (CT and MRI) and laboratory tests before NCRT and surgery. The exclusion criteria were as follows: (1) incomplete clinical data; (2) history of other malignancies; (3) recurrent rectal cancer; (4) history of pelvic radiotherapy; (5) combination with acute or chronic infections, and hematologic diseases. This study was reviewed and approved by the Ethics Committee of the First Affiliated Hospital of Chongqing Medical University and was implemented in accordance with the Helsinki Declaration. Since this study was retrospective, written informed consent was exempted.

Neoadjuvant therapy

The treatment regimens for patients with LARC were developed by a multidisciplinary team (MDT). The radiotherapy regimens included long-course radiotherapy and short-course radiotherapy. Long-course radiotherapy was administered as 45-50Gy in 25 fractions with concurrent oral capecitabine 825 mg/m2 twice a day during radiotherapy. Short-course radiotherapy was administered as 25Gy in 5 fractions with concurrent oral capecitabine 825 mg/m2 twice a day during radiotherapy. After completion of radiotherapy, 1-3 cycles of consolidation chemotherapy were administered. The consolidation chemotherapy regimens were XELOX (Oxaliplatin 130 mg/m2, D1, Capecitabine 1000 mg/m2 twice daily, D1-D14) and XELIRI (Irinotecan 200 mg/m2, D1, Capecitabine 1000 mg/m2 twice daily, D1-D14). All patients underwent surgery according to TME principles after completion of NCRT. The tumor regression was evaluated according to the American Joint Committee on Cancer (AJCC) 8th edition classification criteria [28]. The pathological TRG (pTRG) 0-1 was defined as tumor regression (TR), while pTRG 2-3 is defined as non-tumor regression (non-TR). pCR was defined as the absence of residual tumor cells in the specimen and lymph nodes (T0N0M0).

Body composition

All patients performed abdominal CT within 2 weeks before NCRT and surgery. Two researchers applied SliceOmatic version 5.0 (TomoVision) software to measure skeletal muscle area, subcutaneous adipose area, and visceral adipose area on CT images of cross-sections of the lumbar 3 vertebrae (L3). The Hounsfield Units (HU) range of measured tissues was as follows: skeletal muscle (-29-150 HU), visceral adipose tissue (-15-50 HU), and subcutaneous adipose tissue (-190-30 HU) (Figure 1) (29). The body composition area was normalized by the square of the patient's height. We finally obtained the skeletal muscle area index (SMI), subcutaneous adipose area index (SAI), and visceral adipose area index (VAI). The change in body composition was presented as (post-NCRT-pre-NCRT)/pre-NCRT×100. The low SMI (L-SMI) was defined as the lowest sex-specific quartile cutoff value. The high SAI (H-SAI) and high VAI (H-VAI) were defined as the highest sex-specific quartile cutoff value (16). Therefore, the cut-off values for L-SMI, H-SAI, and H-VAI were 43 cm^2/m^2, 43.18 cm^2/m^2, and 59.07 cm^2/m^2 for males and 36.77 cm^2/m^2, 79.75 cm^2/m^2, and 49.23 cm^2/m^2 for females, respectively.

Baseline hematological variables

The blood routine tests, blood biochemistry, CEA, and carbohydrate antigen 19-9 (CA19-9) were performed 1 week before NCRT. NLR = neutrophil count/lymphocyte count; PLR = platelet count/lymphocyte count; SII = (platelet count × neutrophil count)/lymphocyte count. We defined the cut-off values of NLR, PLR, and SII to maximize the discriminant power between the pCR group and the non-pCR group. Thus, the cut-off values of NLR, PLR, and SII were 2.6, 168.45, and 714.65, respectively (Supplementary Figure 1).

MRI assessment of tumor regression response

The rectal high-resolution MRI was conducted within 2 weeks before NCRT and surgery. The T-stage, N-stage, tumor size, distance from the anal verge, circumferential resection margin, and extra-mural vascular invasion of rectal cancer were assessed by MRI before NCRT. The T-stage, N-stage, circumferential

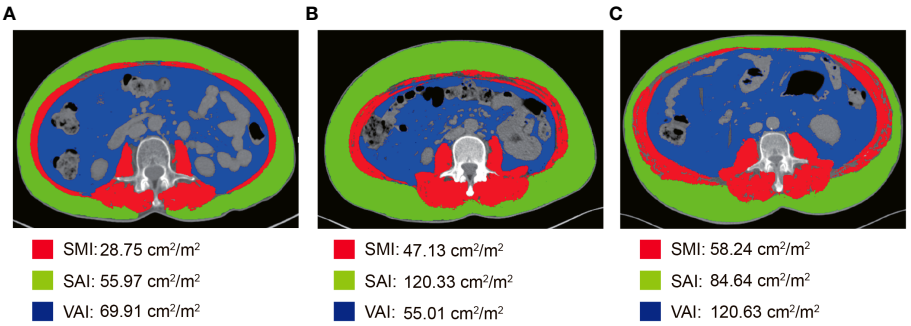

FIGURE 1
Body composition measurement based on CT images at the level of the third lumbar spine. **(A)** L-SMI; **(B)** H-SAI; **(C)** H-VAI.

resection margin, extra-mural vascular invasion, and TRG of rectal cancer were assessed by MRI before surgery. Mandard TRG was used to assess MRI tumor regression response after NCRT (28). mrTRG 1-2 was defined as a good response; mrTRG 3-5 was defined as a poor response. MRI parameters were evaluated by two experienced radiologists.

Statistical analysis

The primary endpoint of the study was pCR and the secondary endpoint was pTRG. The χ^2 test or Fisher's test was used for the analysis of categorical variables. Normally distributed continuous variables were expressed as mean ± standard deviation, and non-normally distributed continuous variables were expressed as median (interquartile range, IQR). The differences between the two samples of continuous variables were analyzed by Student's t-test or Mann-Whitney U test. The Spearman correlation test was performed to compare the relationship between BMI, SMI, SAI, and VAI. Logistic regression was performed to univariate and multivariate analyses. Variables with $p<0.10$ in the univariate analysis were included in the multivariate analysis. The Receiver Operating Curve (ROC) was applied to predict the cut-off values of NLR, PLR, and SII. The nomogram graphs of predicting pCR were built according to the multivariate analysis. The internal validation and area under the curves (AUC) were performed to evaluate the performance of the nomogram graphs, and the C-index was used to test the discriminatory power of the nomogram graphs. $P < 0.05$ was considered statistically significant. SPSS 25, R version 4.1.3, and GraphPad 8 were conducted for statistical analysis.

Results

Basic characteristics of patients

A total of 291 LARC patients (95 female and 196 male) with a median age of 58 years fulfilled the inclusion criteria. Pre-NCRT CEA was elevated in 145 (53.26%) patients. The median of pre-NCRT NLR, PLR, and SII was 2.5 (range, 1.85-3.35), 154.07 (range, 116.91-211.48), and 574.4 (range, 389.21-870), respectively. The median of SMI, SAI, and VAI before NCRT were 45.51 cm2/m2 (range, 40.07-51.5), 36.72 cm2/m2 (range, 26.87-52.51), and 36.64 cm2/m2 (range, 19.92-55.99), respectively. Two hundred and twenty-seven (78.01%) patients with LARC suffered from long-course radiotherapy. The median interval between completion of radiotherapy and surgery was 11 weeks (range, 9-13). Anterior resection was performed in 188 patients. 55 (18.9%) patients achieved pCR after NCRT. Anastomotic leakage occurred in 27 (14.36%) patients who underwent the anterior resection procedure. Eleven (3.78%) patients underwent reoperation due to postoperative complications. Details regarding the baseline characteristics of the patients are shown in Table 1.

TABLE 1 The baseline characteristics.

Characteristics		Number (%)	Median (IQR)
Age,years			58 (50-65)
Sex	Male	196 (67.35%)	
	Female	95 (32.65%)	
Location	Low	146 (50.17%)	
	Middle	145 (49.83%)	
Pre-NCRT CEA	≥5ng/ml	155 (53.26%)	
Pre-NCRT CA19-9	≥27U/ml	74 (25.43%)	
Pre-NCRT NLR			2.5 (1.85-3.35)
Pre-NCRT PLR			154.07 (116.91-211.48)
Pre-NCRT SII			574.4 (389.21-870)
Pre-NCRT Albumin (g/L)			42 (39-45)
Pre-NCRT BMI (kg/m^2)			22.77 (20.31-24.61)
Pre-NCRT SMI (cm^2/m^2)			45.51 (40.07-51.5)
Pre-NCRT SAI (cm^2/m^2)			36.72 (26.87-52.51)
Pre-NCRT VAI (cm^2/m^2)			36.64 (19.92-55.99)
Tumor size (cm)			5 (4.1-6.2)
Clinical T stage	T3	167 (57.39%)	
	T4	124 (42.61%)	
Clinical N stage	N0	37 (12.71%)	
	N1	79 (27.15%)	
	N2	175 (60.14%)	
Radiotherapy regimen	Short-course	64 (21.99%)	
	Long-course	227 (78.01%)	
Chemotherapy regimen	XELOX	255 (87.63%)	
	XELIRI	36 (12.37%)	
Cycle of Consolidation chemotherapy	1	41 (14.09%)	
	2	175 (60.14%)	

(Continued)

TABLE 1 Continued

Characteristics		Number (%)	Median (IQR)
	3	75 (25.77%)	
mrTRG	TRG 1	25 (8.59%)	
	TRG 2	127 (43.64%)	
	TRG 3	109 (37.46%)	
	TRG 4	30 (10.31%)	
Interval between radiotherapy and surgery (weeks)			11 (9-13)
Surgical procedure	Dixon	188 (64.6%)	
	Hartmann	11 (3.78%)	
	Miles	92 (31.62%)	
ypTNM	pCR	55 (18.9%)	
	I	56 (19.24%)	
	II	105 (36.08%)	
	III	75 (25.77%)	
pTRG	TRG 0	55 (18.9%)	
	TRG 1	45 (15.46)	
	TRG 2	126 (43.3%)	
	TRG 3	65 (22.34%)	
Resection category	R0	288 (98.97%)	
Postoperation complications	Overall	84 (28.87%)	
	Anastomotic leakage	27 (14.36%)	
	Surgical site infection	53 (18.21%)	
	Ileus	24 (8.25%)	
	Hemorrhage	4 (1.37%)	
	Pulmonary infection	11 (3.78%)	
	Other	22 (7.56)	
Readmission		26 (8.93%)	
Reoperation		11 (3.78%)	

NCRT, neoadjuvant chemoradiotherapy; IQR, interquartile range; CEA, carcinoembryonic antigen; CA19-9, carbohydrate antigen 19-9; NLR, neutrophil-to-lymphocyte ratio; PLR, platelet-to-lymphocyte ratio; SII, systemic immune-inflammatory index; BMI, Body mass index; SMI, skeletal muscle area index; SAI, subcutaneous adipose area index; VAI, visceral adipose area index; mrTRG, magnetic resonance imaging tumor regression grade; pTRG, pathological tumor regression grade; pCR, pathological complete response.

Changes in BMI and body composition parameters after NCRT

Correlations between body composition parameters (SMI, SAI, and VAI) and BMI before and after NCRT were analyzed using Spearman correlation coefficients. The results showed that BMI was positively correlated with SMI, SAI, and VAI (SMI: r=0.52, P<0.001; SAI: r=0.53, p<0.001; VAI: r=0.67, P<0.001) before NCRT. There was no significant correlation between pre-NCRT VAI and SMI (r=0.02, P=0.76). The correlation between BMI, SMI, SAI, and VAI was not altered by NCRT (Figure 2). The median of BMI, SMI, SAI, and VAI before NCRT were 22.77 kg/m2, 45.51 cm2/m2, 36.72 cm2/m2, and 36.64 cm2/m2, respectively. The median of BMI, SMI, SAI, and VAI after NCRT were 22.58 kg/m2, 44.78 cm2/m2, 37.28 cm2/m2, and 36.06 cm2/m2, respectively. Overall, BMI and body composition parameters decreased in patients with LARC after NCRT. The post-NCRT BMI and SMI were significantly lower than pre-NCRT (P=0.015; P=0.002) (Figure 3). The median of changes in BMI, SMI, SAI, and VAI after NCRT were 0, -0.96%, -1.65%, and -3.04%, respectively (Table 2).

NCRT Baseline characteristics of patients with pCR

Fifty-five (18.9%) patients with LARC attained pCR after NCRT. The median age of the pCR group and the non-pCR group were 56 years (range, 49-66) and 59 years (range, 50.25-65) years, respectively. The proportion of female patients reaching pCR was higher than that of male patients (24.21% vs 16.33%), but the difference was not statistically significant (P=0.11). Patients with NLR < 2.6, PLR < 168.45, and SII < 714.65 before NCRT were more likely to obtain a pCR. There were no significant differences between the two groups in tumor size, clinical T stage, clinical N stage, radiotherapy regimen, chemotherapy regimen, the cycle of consolidation chemotherapy, and the interval between completion of radiotherapy and surgery. The proportion of pCR in patients with mrTRG 1-2 was significantly higher than that in patients with mrTRG 3-4 (52% vs 24.41% vs 9.17% vs 3.33%, P < 0.001). Significantly fewer patients had pre-NCRT L-SMI in the pCR group than in the non-pCR group (7.27% vs 29.34%, P < 0.001). Patients with LARC in the pCR group showed greater changes in BMI (-1.37% vs 0, P=0.021) (Table 3).

Predictors of pCR to NCRT

Univariate and multivariate analyses of LARC patients with pCR after NCRT were shown in Table 4. Univariate analysis indicated that pre-NCRT NLR≥2.6 (OR=0.256, 95% CI 0.129-0.511, P<0.001), pre-NCRT PLR≥168.45 (OR=0.32, 95% CI 0.16-0.637, P=0.001), pre-NCRT SII≥714.15 (OR=0.281, 95% CI 0.127-0.622, P=0.002), mrTRG 3-5(OR= 0.218, 95% CI 0.107-0.443, P<0.001) and pre-NCRT L-SMI (OR=0.19, 95% CI 0.066-0.546, P=0.002) were risk factors for pCR. Multivariate analysis was performed on variables with P<0.1 in the univariate analysis. The analysis results suggested that pre-NCRT NLR≥2.6 (OR= 0.378, 95%CI 0.164-0.868, P=0.022), mrTRG 3-5 (OR=0.256, 95%CI 0.121-0.54, P<0.001), and pre-NCRT L-SMI (OR=0.292, 95% CI 0.097-0.883, P=0.029) were independent risk factors for pCR.

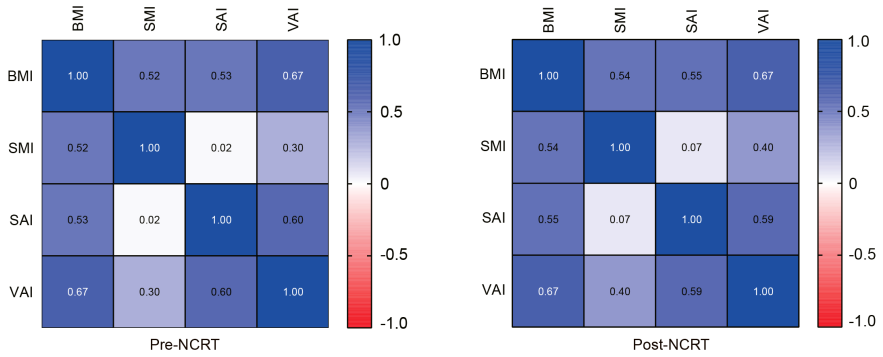

FIGURE 2
Correlation between BMI and body composition parameters before and after NCRT.

ROC curves were used to evaluate the performance of NLR, mrTRG, and L-SMI in predicting pCR. The results demonstrated that the AUC for pre-NCRT NLR, mrTRG, and pre-NCRT L-SMI was 0.667 (95% CI 0.592-0.742, P<0.001), 0.652 (95% CI 0.575-0.728, P<0.001) and 0.61 (95% CI 0.535-0.685, P=0.011), respectively. The performance of mrTRG combined with pre-NCRT NLR and pre-NCRT L-SMI in predicting pCR was significantly improved compared with mrTRG alone (AUC: 0.763 vs. 0.667) (Figure 4, Table 5).

Based on the results of multivariate analysis, pre-NCRT NLR, mrTRG, and pre-NCRT L-SMI were performed to construct a predictive nomogram for pCR after NCRT for LARC (Figure 5A). The probability of pCR prediction after NCRT for LARC patients can be obtained by summing the scores corresponding to pre-NCRT NLR, mrTRG, and pre-NCRT L-SMI, and then plotting a straight line to obtain the probability of achieving pCR. Patients with higher total points were more likely to reach pCR. The model was validated internally and a correction curve was drawn. The validated results showed that the predicted probability of pCR was in good agreement with the actual probability (Figure 5B). The discriminant ability of pCR prediction models was evaluated by the C-index. The results revealed that the C-index of the nomogram was 0.763 (95% CI 0.700-0.826).

Predictors of tumor regression response to NCRT

pTRG 0-1 was defined as tumor regression (TR), while pTRG 2-3 is defined as non-tumor regression (non-TR). Univariate analysis showed that pre-NCRT NLR≥2.6 (OR= 0.523, 95% CI 0.318-0.859, P=0.011), pre-NCRT PLR≥168.45 (OR= 0.461, 95% CI 0.276-0.771, P=0.011), pre-NCRT SII≥714.15 (OR= 0.402, 95%CI 0.229-0.705, P=0.001), and mrTRG 3-5 (OR= 0.336, 95% CI 0.201-0.563, P<0.001) were risk factors for TR. We then conducted multivariate analysis on variables with P<0.1 in univariate analysis. The results indicated that mrTRG 3-5 (OR=0.375, 95% CI 0.219-0.641, P<0.001) was an independent predictor for non-TR (Table 6).

Discussion

The pCR after NCRT is a crucial predictor of favorable prognosis in LARC. Several studies have reported a recurrence rate of 6-17% and a 5-year OS of 87-92.9% for patients who achieved a pCR (30–32). Although NCRT followed by surgery has been shown to reduce local recurrence and improve the clinical

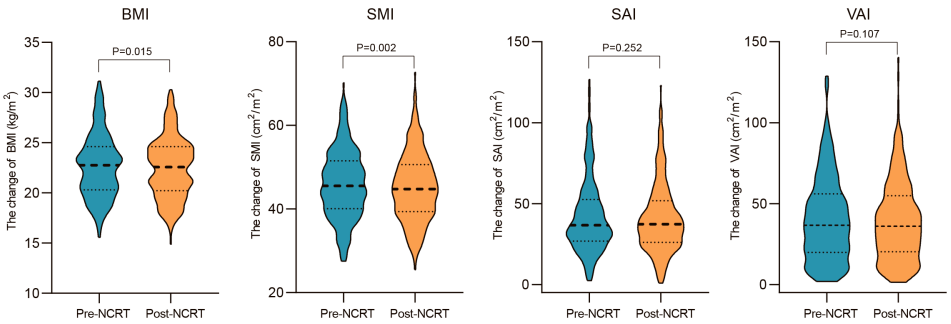

FIGURE 3
Changes in BMI and body composition parameters before and after NCRT.

TABLE 2 The baseline of BMI and body composition parameters.

Variable	Pre-NCRT (IQR)	Post-NCRT (IQR)	Change of body composition (IQR)	*P* value
BMI (kg/m^2)	22.77 (20.31-24.61)	22.58 (20.22-24.61)	0 (-4-2.31)	0.015
SMI (cm^2/m^2)	45.51 (40.07-51.5)	44.78 (39.36-50.61)	-0.96 (-7.15-3.84)	0.002
SAI (cm^2/m^2)	36.72 (26.87-52.51)	37.28 (26.09-51.76)	-1.65 (-14.79-12.5)	0.251
VAI (cm^2/m^2)	36.64 (19.92-55.99)	36.06 (20.30-54.84)	-3.04 (-19.13-22.21)	0.107

NCRT, Neoadjuvant chemoradiotherapy; IQR, interquartile range; BMI, Body mass index; SMI, skeletal muscle area index; SAI, subcutaneous adipose area index; VAI, visceral adipose area index.

TABLE 3 Baseline characteristics of patients with pCR.

		pCR(n=55)	non-pCR(n=236)	P
Age, years	IQR	56 (49-66)	59 (50.25-65)	0.406[m]
Sex	Male	32	164	0.113[f]
	Female	23	72	
Pre-NCRT NLR	<2.60	43	113	<0.001[f]
	≥2.60	12	123	
Pre-NCRT PLR	<168.45	43	126	0.001[f]
	≥168.45	12	110	
Pre-NCRT SII	<714.65	47	147	0.001[f]
	≥714.65	8	89	
Pre-NCRT CEA, ng/ml	≥5	25	130	0.231[f]
Pre-NCRT CA19-9, U/ml	≥27	14	60	1[f]
Size, cm	IQR	4.8 (4-5.8)	5.1 (4.2-6.2)	0.159[m]
Clinical T stage	T3	29	138	0.453[f]
	T4	26	98	
Clinical N stage	N0	9	28	0.601
	N1	13	66	
	N2	33	142	
Clinical TNM	II	9	28	0.372[f]
	III	46	208	
Radiotherapy regimen	Short-course	12	52	1[f]
	Long-course	43	184	
Chemotherapy regimen	XELOX	51	216	1[f]
	XELIRI	4	20	
Cycle of Consolidation chemotherapy	1	4	37	0.271
	2	36	139	
	3	15	60	
Interval between radiotherapy and surgery, weeks	≤10	24	121	0.369[f]
	>10	31	115	
mrTRG	TRG 1	13	12	<0.001

(Continued)

TABLE 3 Continued

		pCR(n=55)	non-pCR(n=236)	P
	TRG 2	31	96	
	TRG 3	10	99	
	TRG 4	1	29	
Pre-NCRT BMI, kg/m^2	>23.9	22	68	0.109[f]
Pre-NCRT L-SMI, cm^2/m^2		4	69	<0.001[f]
Pre-NCRT H-SFI, cm^2/m^2		14	59	1[f]
Pre-NCRT H-VFI, cm^2/m^2		17	56	0.301[f]
ΔBMI	IQR	-1.37 (-5.81-0)	0 (-3.74-3.14)	0.021[m]
ΔSMI	IQR	-2.12 (-8.03-2.14)	-0.525 (-6.83-3.9625)	0.340[m]
ΔSAI	IQR	-3.38 (-18.17-8.08)	-1.235 (-14.17-15.31)	0.221[m]
ΔVAI	IQR	-9.47 (-21.59-16.27)	-1.35 (-17.63-22.88)	0.115[m]

m, Mann-Whitney U test; f, Fisher's test; NCRT, neoadjuvant chemoradiotherapy; IQR, interquartile range; CEA, carcinoembryonic antigen; CA19-9, carbohydrate antigen 19-9; NLR, neutrophil-to-lymphocyte ratio; PLR, platelet-to-lymphocyte ratio; SII, systemic immune-inflammatory index; BMI, Body mass index; L-SMI, low skeletal muscle area index; H-SAI, high subcutaneous adipose area index; H-VAI, high visceral adipose area index; mrTRG, magnetic resonance imaging tumor regression grade; pCR, pathological complete response; ΔBMI, The change of Body mass index; ΔSMI, The change of skeletal muscle area index; ΔSFI, The change of subcutaneous adipose area index; ΔVAI, visceral adipose area index.

TABLE 4 Univariate and multivariate analysis for pCR to NCRT.

		Univariate analysis		Multivariate analysis	
		OR (95% CI)	P	OR (95% CI)	P
Age, years	IQR	0.99(0.966-1.013)	0.386		
Sex	Male	ref	0.109		
	Female	0.611(0.334-1.117)			
Pre-NCRT NLR	<2.60	ref	<0.001	ref	0.022
	≥2.60	0.256(0.129-0.511)		0.378(0.164-0.868)	
Pre-NCRT PLR	<168.45	ref	0.001	ref	0.216
	≥168.45	0.32(0.16-0.637)		0.582(0.247-1.372)	
Pre-NCRT SII	<714.65	ref	0.002	ref	0.93
	≥714.65	0.281(0.127-0.622)		0.953(0.327-2.775)	
Pre-NCRT CEA, ng/ml	≤5	ref	0.199		
	>5	0.679(0.377-1.225)			
Pre-NCRT CA19-9, U/ml	≤27	ref	0.996		
	>27	1.002(0.511-1.965)			
Size, cm		0.94(0.782-1.13)	0.511		
Clinical T stage	T3	ref	0.438		
	T4	1.262(0.7-2.276)			
Clinical N stage	N0	ref	0.604		
	N1	0.613(0.235-1.597)	0.316		
	N2	0.723(0.312-1.677)	0.45		
Clinical TNM	II	ref	0.369		
	III	0.688(0.304-1.556)			

(Continued)

TABLE 4 Continued

		Univariate analysis		Multivariate analysis	
		OR (95% CI)	P	OR (95% CI)	P
Radiotherapy regimen	Short-course	ref	0.972		
	Long-course	1.013(0.498-2.06)			
Chemotherapy regimen	XELOX	ref	0.771		
	XELIRI	0.847(0.277-2.586)			
Cycle of Consolidation chemotherapy	1	ref	0.289		
	2	2.396(0.802-7.16)	0.118		
	3	2.312(0.713-7.5)	0.163		
Interval between radiotherapy and surgery, weeks	≤10	ref	0.309		
	>10	1.359(0.753-2.454)			
mrTRG	TRG 1-2	ref	<0.001	ref	<0.001
	TRG 3-5	0.218(0.107-0.443)		0.256(0.121-0.54)	
Pre-NCRT BMI, kg/m^2	>23.9	1.647(0.896-3.027)	0.108		
Pre-NCRT L-SMI, cm^2/m^2		0.19(0.066-0.546)	0.002	0.292(0.097-0.883)	0.029
Pre-NCRT H-SFI, cm^2/m^2		1.024(0.522-2.011)	0.944		
Pre-NCRT H-VFI, cm^2/m^2		1.438(0.754-2.743)	0.27		
ΔBMI	IQR	0.954(0.909-1.001)	0.054	0.947(0.897-1.001)	0.053
ΔSMI	IQR	1.033(0.996-1.072)	0.082	1.027(0.987-1.069)	0.185
ΔSFI	IQR	0.996(0.986-1.005)	0.373		
ΔVFI	IQR	0.994(0.986-1.002)	0.118		

NCRT, neoadjuvant chemoradiotherapy; IQR, interquartile range; CEA, carcinoembryonic antigen; CA19-9, carbohydrate antigen 19-9; NLR, neutrophil-to-lymphocyte ratio; PLR, platelet-to-lymphocyte ratio; SII, systemic immune-inflammatory index; BMI, Body mass index; L-SMI, low skeletal muscle area index; H-SAI, high subcutaneous adipose area index; H-VAI, high visceral adipose area index; mrTRG, magnetic resonance imaging tumor regression grade; pCR, pathological complete response; ΔBMI, The change of Body mass index; ΔSMI, The change of skeletal muscle area index; ΔSFI, The change of subcutaneous adipose area index; ΔVAI, visceral adipose area index.

outcomes for LARC patients, this approach comes with a significant reduction in the quality of life due to radiotherapy adverse reactions, surgical complications, and permanent stoma (33, 34). Interestingly, radical surgery has been reported to have a similar recurrence rate and OS compared to local resection in LARC patients who achieved clinical complete response (cCR) following NCRT. However, local resection is known to significantly improve quality of life in patients with rectal cancer (35). Furthermore, a "wait-and-watch" approach has also resulted in similar oncological prognosis compared to radical surgery in patients who achieved cCR (36). Several factors contribute to the likelihood of achieving a pCR in LARC. One such factor is the radiation dose, which has a significant impact on the treatment outcome. In particular, tumor response can be enhanced by employing simultaneous integrated boost (SIB) with an up dose of 55-60 Gy (37, 38). Unfortunately, there are currently no reliable markers to accurately predict pCR and cCR for LARC patients after NCRT. This study evaluated the role of body composition parameters, systemic inflammatory markers, and MRI as predicting factors affecting pCR in LARC patients. The findings revealed that L-SMI, NLR, and mrTRG were independent risk factors for achieving pCR. Moreover, mrTRG was also an independent predictor of TR.

The assessment of short-term and long-term clinical outcomes in cancer patients based on L3 cross-sectional body composition parameters is superior to BMI because it provides sex-specific information regarding the patient's skeletal muscle and adipose tissue (39–41). Nevertheless, the cut-off value of the body composition parameter remains controversial due to population differences. The cut-off value of L-SMI in Western populations may be higher than that in Eastern populations. In Western populations, the generally accepted cut-off values for L-SMI are 52.4 cm^2/m^2 for men and 38.5 cm^2/m^2 for women (42). However, two Asian studies defined the cutoff of L-SMI as the sex-specific lowest quartile which was strongly associated with CRC prognosis (43, 44). Therefore, the sex-specific lowest quartile was also defined as the cutoff value for the body composition parameters in this study.

The effect of L-SMI on tumor regression response and prognosis of LARC patients after NCRT is still unclear. A retrospective multicenter study investigated that sarcopenia was an independent risk factor for pCR and cCR but not a predictor of TR (45). In this study, the presence of sarcopenia was assessed by CT scanning of the psoas muscle region at the L3 level which was a minor muscle and cannot imply the entire skeletal muscle level. Olmez et al. analyzed the effect of sarcopenia on the pCR of LARC

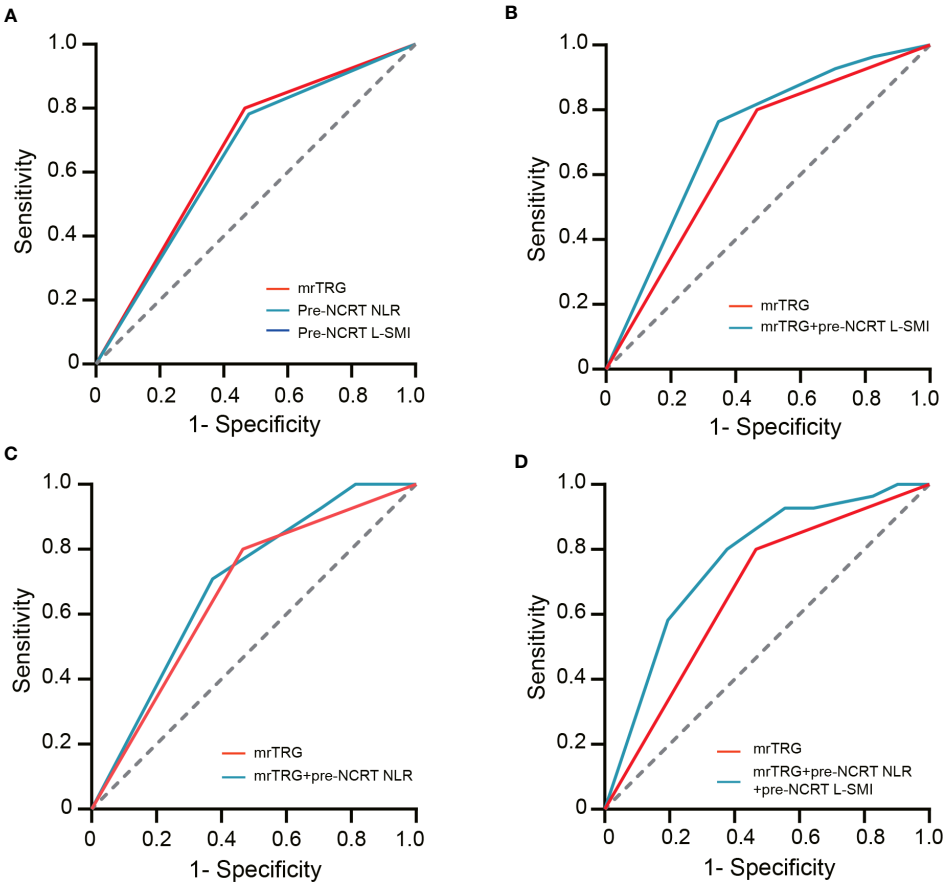

FIGURE 4
The ROC curves of assessing pCR. **(A)** the ROC curves of mrTRG, pre-NCRT NLR and pre-NCRT L-SMI alone; **(B)** the ROC curves of mrTRG + pre-NCRT L-SMI; **(C)** the ROC curves of mrTRG + pre-NCRT NLR; **(D)** the ROC curves of mrTRG+ pre-NCRT L-SMI + pre-NCRT NLR.

TABLE 5 The AUC value of ROC curves.

Parameters	pCR	
	AUC (95% CI)	P Value
mrTRG	0.667 (0.592-0.742)	<0.001
Pre-NCRT NLR	0.652 (0.575-0.728)	<0.001
Pre-NCRT L-SMI	0.61 (0.535-0.685)	0.011
Pre-NCRT NLR+ pre-NCRT L-SMI	0.695 (0.625-0.764)	<0.001
mrTRG+ pre-NCRT NLR	0.739 (0.671-0.808)	<0.001
mrTRG+ pre-NCRT L-SMI	0.72 (0.65-0.79)	<0.001
mrTRG+ pre-NCRT NLR+ pre-NCRT L-SMI	0.763 (0.698-0.829)	<0.001

NCRT, neoadjuvant chemoradiotherapy; NLR, neutrophil-to-lymphocyte ratio; L-SMI, low skeletal muscle area index; mrTRG, magnetic resonance imaging tumor regression grade; pCR, pathological complete response; AUC, the area under the curve; ROC, receiver operating characteristic.

and identified sarcopenia, age≥60 years, the interval between surgery and completion of radiotherapy <8 weeks, and CEA≥2.5 ng/ml as risk factors for pCR through univariate analysis. However, this study did not conduct multivariate analysis of factors affecting pCR (46). It was also observed in our study that L-SMI before NCRT was an independent risk factor for pCR, but it was not a predictor of TR. Furthermore, studies have shown that L-SMI is an independent risk factor for adverse reactions to NCRT, postoperative complications, OS, and DFS in patients with LARC (16–18). However, the underlying reasons for the association between L-SMI and poor oncological outcomes or treatment response to NCRT in LARC remain unclear. Possible explanations for this included the overwhelming distribution of hydrophilic chemotherapeutic drugs such as fluorouracil and oxaliplatin in the lean body which can cause overdose of chemotherapy drugs (47). Loss of skeletal muscle in cancer patients indirectly reflected the strong invasive potential of the tumor (48). Malnutrition was also a principal factor in muscle loss, and patients with malnutrition have impaired immune status and reduced tolerance to chemotherapy (49). Additionally, L-SMI induced the accumulation of M2 macrophages, up-regulation immune checkpoint genes and proinflammatory cytokines (IL-6,

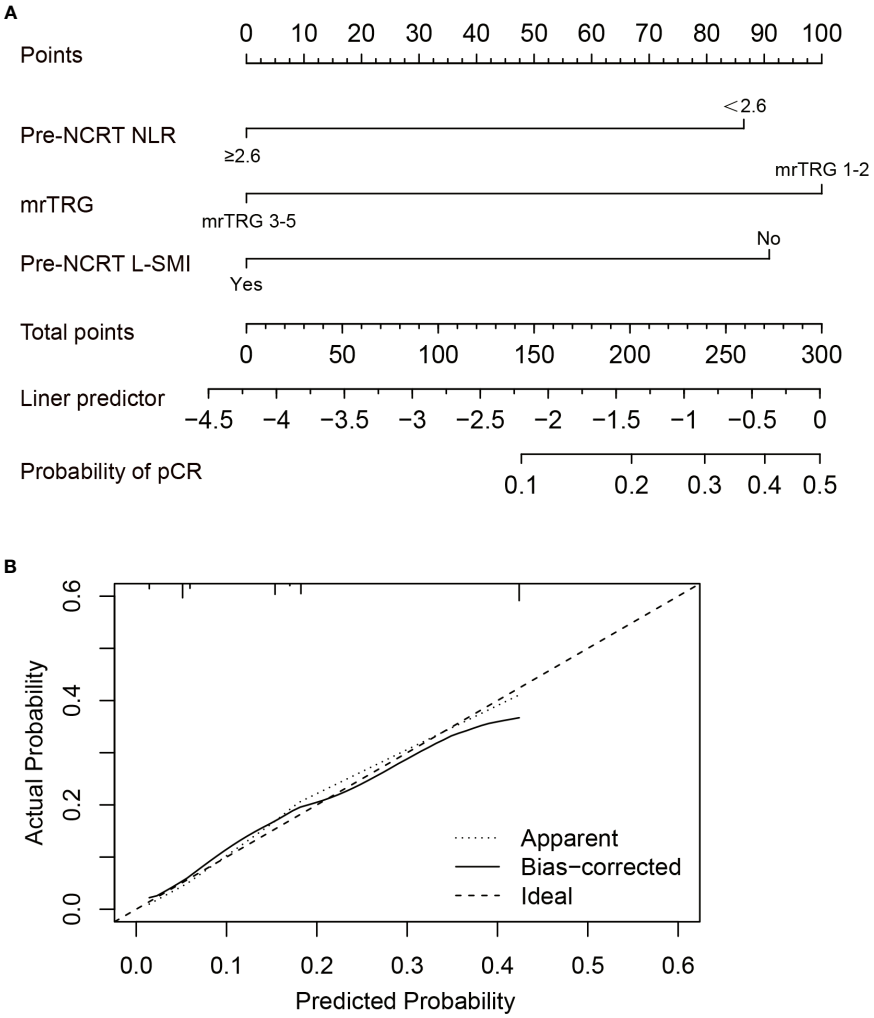

FIGURE 5
Construction of the factors for pCR to NCRT. **(A)** The Nomogram of predicting pCR; **(B)** The curves of internal validation for the nomogram.

IL-10, and TGF-β), and alteration the tumor microenvironment and immune status (50).

Systemic inflammation stimulated cancer cell proliferation, metastasis, immunosuppression, and alteration of the tumor microenvironment through pro-inflammatory factors (24). Several systemic inflammatory markers NLR, PLR, SII, and LMR have been demonstrated to be associated with tumor regression response and prognosis in a variety of cancers (51). A multicenter retrospective study involving 808 patients with LARC indicated that NLR>1.2 and SII>500 were independent risk factors for pCR (52). Furthermore, Liu et al. also confirmed that NLR (AUC=0.794, P=0.024) and PLR (AUC=0.740, P=0.006) were critical predictors of pCR in LARC (53). Sun et al. revealed that low NLR was an independent predictor of TR to NCRT in rectal mucinous adenocarcinoma (OR=4.025, P=0.028), but not SII (54). Our study also suggested that high NLR before NCRT can act as an independent risk factor predictor for pCR in patients with LARC. Although pre-NCRT SII and PLR were not confirmed to be independent risk factors of pCR, in a univariate analysis high SII and PLR were less likely to achieve pCR. However, the ability of systemic inflammatory markers to predict pCR, OS, and DFS in LARC remains controversial. A multicenter study indicated that NLR and PLR were neither risk factors of OS and DFS in LARC patients nor predictors of pCR and TR (26). AN et al. showed that NLR< 2.8 and PLR< 300 were not associated with pCR and 5-year OS, but PLR could be a predictor for 5-year DFS (55). Currently, there was no unified cut-off value of inflammatory markers such as NLR, PLR, and SII to predict pCR and prognosis. The cut-off value of NLR generally between 2-3 can prognosticate the pCR and outcomes (56). In this study, we predicted the optimal cut-off values for obtaining pCR by ROC curves for NLR, PLR, and SII, and ultimately indicated that NLR ≥2.6 was an independent predictor of pCR (AUC= 0.652, P<0.001).

MRI has routinely been applied for staging and treatment response of rectal cancer. Compared with conventional MRI, DWI was more effective in assessing TRG after NCRT for LARC (57). The assessment of mrTRG was also influenced by the radiologist and MRI parameters. Presently, the competence of MRI alone in predicting pCR is still unsatisfactory. Yoo et al. suggested that combination of mrTRG and blood biomarker CEA

10.3389/fonc.2023.1242193

TABLE 6 Univariate and multivariate analysis for TR to NCRT.

		Univariate analysis		Multivariate analysis	
		OR (95% CI)	P	OR (95% CI)	P
Age, years	IQR	0.983 (0.963-1.003)	0.097	0.985 (0.964-1.008)	0.196
Sex	Male	ref	0.378		
	Female	0.795 (0.477-1.324)			
Pre-NCRT NLR	<2.60	ref	0.011	ref	0.471
	≥2.60	0.523 (0.318-0.859)		0.796 (0.428-1.48)	
Pre-NCRT PLR	<168.45	ref	0.003	ref	0.12
	≥168.45	0.461 (0.276-0.771)		0.606 (0.323-1.139)	
Pre-NCRT SII	<714.65	ref	0.001	ref	0.302
	≥714.65	0.402 (0.229-0.705)		0.672 (0.317-1.428)	
Pre-NCRT CEA, ng/ml	≤5	ref	0.856		
	>5	0.956 (0.589-1.553)			
Pre-NCRT CA19-9, U/ml	≤27	ref	0.685		
	>27	0.891 (0.508-1.561)			
Size, cm		0.976 (0.841-1.131)	0.743		
Clinical T stage	T3	ref	0.398		
	T4	1.234 (0.758-2.01)			
Clinical N stage	N0	ref	0.657		
	N1	0.717 (0.316-1.627)	0.426		
	N2	0.901 (0.433-1.876)	0.781		
Clinical TNM	II	ref	0.634		
	III	0.841 (0.412-1.716)			
Radiotherapy regimen	Short-course	ref	0.553		
	Long-course	1.197 (0.661-2.17)			
Chemotherapy regimen	XELOX	ref	0.912		
	XELIRI	0.951 (0.392-2.305)			
Cycle of Consolidation chemotherapy	1	ref	0.192	ref	0.211
	2	2.101 (0.944-4.679)	0.069	2.068 (0.898-4.767)	0.088
	3	1.887 (0.783-4.545)	0.157	1.621 (0.642-4.079)	0.307
Interval between radiotherapy and surgery, weeks	≤10	ref	0.838		
	>10	1.052 (0.648-1.706)			
mrTRG	TRG 1-2	ref	<0.001	ref	
	TRG 3-5	0.336 (0.201-0.563)		0.375 (0.219-0.641)	<0.001
Pre-NCRT BMI, kg/m^2	>23.9	0.805 (0.48-1.352)	0.412		
Pre-NCRT L-SMI, cm^2/m^2		0.651 (0.363-1.167)	0.149		
Pre-NCRT H-SFI, cm^2/m^2		1.292 (0.729-2.287)	0.38		
Pre-NCRT H-VFI, cm^2/m^2		0.733 (0.424-1.267)	0.266		
ΔBMI	IQR	0.802 (0.957-1.035)	0.802		
ΔSMI	IQR	1.017 (0.986-1.049)	0.279		

(Continued)

TABLE 6 Continued

		Univariate analysis		Multivariate analysis	
		OR (95% CI)	P	OR (95% CI)	P
ΔSFI	IQR	0.999 (0.992-1.007)	0.867		
ΔVFI	IQR	0.997 (0.991-1.003)	0.323		

NCRT, neoadjuvant chemoradiotherapy; TR, tumor regression; IQR, interquartile range; CEA, carcinoembryonic antigen; CA19-9, carbohydrate antigen 19-9; NLR, neutrophil-to-lymphocyte ratio; PLR, platelet-to-lymphocyte ratio; SII, systemic immune-inflammatory index; BMI, Body mass index; L-SMI, low skeletal muscle area index; H-SAI, high subcutaneous adipose area index; H-VAI, high visceral adipose area index; mrTRG, magnetic resonance imaging tumor regression grade; pCR, pathological complete response; ΔBMI, The change of Body mass index; ΔSMI, The change of skeletal muscle area index; ΔSFI, The change of subcutaneous adipose area index; ΔVAI, visceral adipose area index.

could better identify the TR to NCRT (AUC: 0.68 vs 0.728) (58). Shi et al. revealed that the proportion of pCR in patients with mrTRG 1-2 was significantly higher than that in patients with mrTRG 3-5 (70% vs 23.1%, P=0.001), and mrTRG could also serve as an independent predictor of pCR (OR=0.074 95% CI 0.011-0.499; P = 0.007). Besides, compared with mrTRG alone, the efficacy of mrTRG combined with NLR in predicting pCR was significantly improved (28). Consistent with this study, we also indicated that mrTRG 1-2 was also an independent predictor of pCR and TR after NCRT for LARC. The performance of mrTRG combined with pre-NCRT NLR and pre-NCRT L-SMI in predicting pCR was greater than that of mrTRG alone (AUC: 0.667 vs 0.763).

Despite the encouraging results observed in this study, we must consider several limitations. Firstly, this study was a single-center retrospective study that may be subject to selection bias and information bias. Secondly, the effect of mrTRG, pre-NCRT NLR, and pre-NCRT L-SMI on OS and DFS in LARC was unclear due to insufficient follow-up time. Thirdly, no uniform cut-off value of systemic inflammatory markers was performed to predict pCR and prognosis, and they were affected by a variety of factors. Finally, the cutoff value of body composition parameters in Asians is unclear, and the sex-specific quartile was conducted as the cutoff value in this study. Therefore, further research is needed to confirm that the selection method of this cut-off value is applicable to the Asian population.

In conclusion, this study demonstrated that MRI tumor regression grading combined with neutrophil-to-lymphocyte ratio and skeletal muscle index can effectively predict the pathological complete response to neoadjuvant chemoradiotherapy in locally advanced rectal cancer. mrTRG was also an independent predictor of tumor regression.

Data availability statement

The original contributions presented in the study are included in the article/Supplementary Material. Further inquiries can be directed to the corresponding author/s.

Ethics statement

The studies involving humans were approved by Ethics Committee of the First Affiliated Hospital of Chongqing Medical University. The studies were conducted in accordance with the local legislation and institutional requirements. The participants provided their written informed consent to participate in this study.

Author contributions

YJ: Research conception, data collection, data analysis, and manuscript writing. QC: Data collection and analysis. CZ: Data collection and literature search. YC: Literature retrieval and data extraction. ZF: conception, supervision, review, editing.

Funding

The author(s) declare financial support was received for the research, authorship, and/or publication of this article. This work is supported by Chongqing key disease Research and Application Demonstration Program (No. 2019ZX003).

Conflict of interest

The authors declare that the research was conducted in the absence of any commercial or financial relationships that could be construed as a potential conflict of interest.

Publisher's note

Supplementary material

The Supplementary Material for this article can be found online at: https://www.frontiersin.org/articles/10.3389/fonc.2023.1242193/full#supplementary-material

References

1. Siegel RL, Miller KD, Fuchs HE, Jemal A. Cancer statistics, 2022. *CA Cancer J Clin* (2022) 72(1):7–33. doi: 10.3322/caac.21708

2. Siegel RL, Wagle NS, Cercek A, Smith RA, Jemal A. Colorectal cancer statistics, 2023. *CA Cancer J Clin* (2023) 73(3):233–54. doi: 10.3322/caac.21772

3. Benson AB, Venook AP, Al-Hawary MM, Azad N, Chen YJ, Ciombor KK, et al. Rectal cancer, version 2.2022, NCCN clinical practice guidelines in oncology. *J Natl Compr Canc Netw* (2022) 20(10):1139–67. doi: 10.6004/jnccn.2022.0051

4. Glynne-Jones R, Wyrwicz L, Tiret E, Brown G, Rödel C, Cervantes A, et al. Rectal cancer: ESMO Clinical Practice Guidelines for diagnosis, treatment and follow-up. *Ann Oncol* (2018) 29(Suppl 4):iv263. doi: 10.1093/annonc/mdy161

5. Sauer R, Becker H, Hohenberger W, Rödel C, Wittekind C, Fietkau R, et al. Preoperative versus postoperative chemoradiotherapy for rectal cancer. *N Engl J Med* (2004) 351:1731–40. doi: 10.1056/NEJMoa040694

6. van der Valk MJM, Hilling DE, Bastiaannet E, Meershoek-Klein Kranenbarg E, Beets GL, Figueiredo NL, et al. Long-term outcomes of clinical complete responders after neoadjuvant treatment for rectal cancer in the International Watch & Wait Database (IWWD): an international multicentre registry study. *Lancet* (2018) 391 (10139):2537–45. doi: 10.1016/S0140-6736(18)31078-X

7. Rullier A, Laurent C, Capdepont M, Vendrely V, Bioulac-Sage P, Rullier E. Impact of tumor response on survival after radiochemotherapy in locally advanced rectal carcinoma. *Am J Surg Pathol* (2010) 34(4):562–8. doi: 10.1097/PAS.0b013e3181d438b0

8. Hasan S, Renz P, Wegner RE, Finley G, Raj M, Monga D, et al. Microsatellite instability (MSI) as an independent predictor of pathologic complete response (PCR) in locally advanced rectal cancer: A national cancer database (NCDB) analysis. *Ann Surg* (2020) 271(4):716–23. doi: 10.1097/SLA.0000000000003051

9. Sun Y, Xu Z, Lin H, Lu X, Huang Y, Huang S, et al. Impact of body mass index on treatment outcome of neoadjuvant chemoradiotherapy in locally advanced rectal cancer. *Eur J Surg Oncol* (2017) 43(10):1828–34. doi: 10.1016/j.ejso.2017.07.022

10. Avgerinos KI, Spyrou N, Mantzoros CS, Dalamaga M. Obesity and cancer risk: Emerging biological mechanisms and perspectives. *Metabolism* (2019) 92:121–35. doi: 10.1016/j.metabol.2018.11.001

11. Diefenhardt M, Ludmir EB, Hofheinz RD, Ghadimi M, Minsky BD, Fleischmann M, et al. Impact of body-mass index on treatment and outcome in locally advanced rectal cancer: A secondary, *post-hoc* analysis of the CAO/ARO/AIO-04 randomized phase III trial. *Radiother Oncol* (2021) 164:223–31. doi: 10.1016/j.radonc.2021.09.028

12. Zopfs D, Theurich S, Große Hokamp N, Knuever J, Gerecht L, Borggrefe J, et al. Single-slice CT measurements allow for accurate assessment of sarcopenia and body composition. *Eur Radiol* (2020) 30(3):1701–8. doi: 10.1007/s00330-019-06526-9

13. Bao QR, Crimì F, Valotto G, Chiminazzo V, Bergamo F, Prete AA, et al. Obesity may not be related to pathologic response in locally advanced rectal cancer following neoadjuvant chemoradiotherapy. *Front Oncol* (2022) 12:994444. doi: 10.3389/fonc.2022.994444

14. Martin L, Birdsell L, Macdonald N, Reiman T, Clandinin MT, McCargar LJ, et al. Cancer cachexia in the age of obesity: skeletal muscle depletion is a powerful prognostic factor, independent of body mass index. *J Clin Oncol* (2013) 31(12):1539–47. doi: 10.1200/JCO.2012.45.2722

15. Lin JX, Tang YH, Zhou WX, Desiderio J, Parisi A, Xie JW, et al. Body composition parameters predict pathological response and outcomes in locally advanced gastric cancer after neoadjuvant treatment: A multicenter, international study. *Clin Nutr* (2021) 40(8):4980–7. doi: 10.1016/j.clnu.2021.06.021

16. Liu Z, Lu S, Wang Y, Lin X, Ran P, Zhou X, et al. Impact of body composition during neoadjuvant chemoradiotherapy on complications, survival and tumor response in patients with locally advanced rectal cancer. *Front Nutr* (2022) 9:796601. doi: 10.3389/fnut.2022.796601

17. Liu J, Yu X, Huang X, Lai Q, Chen J. Associations of muscle and adipose tissue parameters with long-term outcomes in middle and low rectal cancer: a retrospective cohort study. *Cancer Imaging* (2023) 23(1):5. doi: 10.1186/s40644-022-00514-x

18. Choi MH, Oh SN, Lee IK, Oh ST, Won DD. Sarcopenia is negatively associated with long-term outcomes in locally advanced rectal cancer. *J Cachexia Sarcopenia Muscle* (2018) 9(1):53–9. doi: 10.1002/jcsm.12234

19. Fujiwara N, Nakagawa H, Kudo Y, Tateishi R, Taguri M, Watadani T, et al. Sarcopenia, intramuscular fat deposition, and visceral adiposity independently predict the outcomes of hepatocellular carcinoma. *J Hepatol* (2015) 63(1):131–40. doi: 10.1016/j.jhep.2015.02.031

20. Bandera EV, John EM. Obesity, body composition, and breast cancer: an evolving science. *JAMA Oncol* (2018) 4(6):804–5. doi: 10.1001/jamaoncol.2018.0125

21. Kamarajah SK, Bundred J, Tan BHL. Body composition assessment and sarcopenia in patients with gastric cancer: a systematic review and meta-analysis. *Gastric Cancer* (2019) 22(1):10–22. doi: 10.1007/s10120-018-0882-2

22. Vrieling A, Kampman E, Knijnenburg NC, Mulders PF, Sedelaar JPM, Baracos VE, et al. Body composition in relation to clinical outcomes in renal cell cancer: A systematic review and meta-analysis. *Eur Urol Focus* (2018) 4(3):420–34. doi: 10.1016/j.euf.2016.11.009

23. Bundred J, Kamarajah SK, Roberts KJ. Body composition assessment and sarcopenia in patients with pancreatic cancer: a systematic review and meta-analysis. *HPB (Oxford)* (2019) 21(12):1603–12. doi: 10.1016/j.hpb.2019.05.018

24. Zhang Y, Liu X, Xu M, Chen K, Li S, Guan G. Prognostic value of pretreatment systemic inflammatory markers in patients with locally advanced rectal cancer following neoadjuvant chemoradiotherapy. *Sci Rep* (2020) 10(1):8017. doi: 10.1038/s41598-020-64684-z

25. Zhang X, Li J, Peng Q, Huang Y, Tang L, Zhuang Q, et al. Association of markers of systemic and local inflammation with prognosis of patients with rectal cancer who received neoadjuvant radiotherapy. *Cancer Manag Res* (2018) 11:191–9. doi: 10.2147/CMAR.S187559

26. Dudani S, Marginean H, Tang PA, Monzon JG, Raissouni S, Asmis TR, et al. Neutrophil-to-lymphocyte and platelet-to-lymphocyte ratios as predictive and prognostic markers in patients with locally advanced rectal cancer treated with neoadjuvant chemoradiation. *BMC Cancer* (2019) 19(1):664. doi: 10.1186/s12885-019-5892-x

27. Tang Z, Zhang XY, Liu Z, Li XT, Shi YJ, Wang S, et al. Quantitative analysis of diffusion weighted imaging to predict pathological good response to neoadjuvant chemoradiation for locally advanced rectal cancer. *Radiother Oncol* (2019) 132:100–8. doi: 10.1016/j.radonc.2018.11.007

28. Shi X, Zhao M, Shi B, Chen G, Yao H, Chen J, et al. Pretreatment blood biomarkers combined with magnetic resonance imaging predict responses to neoadjuvant chemoradiotherapy in locally advanced rectal cancer. *Front Oncol* (2022) 12:916840. doi: 10.3389/fonc.2022.916840

29. van Vugt JL, Levolger S, Gharbharan A, Koek M, Niessen WJ, Burger JW, et al. A comparative study of software programmes for cross-sectional skeletal muscle and adipose tissue measurements on abdominal computed tomography scans of rectal cancer patients. *J Cachexia Sarcopenia Muscle* (2017) 8(2):285–97. doi: 10.1002/jcsm.12158

30. van der Sluis FJ, Couwenberg AM, de Bock GH, Intven MPW, Reerink O, van Leeuwen BL, et al. Population-based study of morbidity risk associated with pathological complete response after chemoradiotherapy for rectal cancer. *Br J Surg* (2020) 107(1):131–9. doi: 10.1002/bjs.11324

31. Wasmuth HH, Rekstad LC, Tranø G. The outcome and the frequency of pathological complete response after neoadjuvant radiotherapy in curative resections for advanced rectal cancer: a population-based study. *Colorectal Dis* (2016) 18(1):67–72. doi: 10.1111/codi.13072

32. Zorcolo L, Rosman AS, Restivo A, Pisano M, Nigri GR, Fancellu A, et al. Complete pathologic response after combined modality treatment for rectal cancer and long-term survival: a meta-analysis. *Ann Surg Oncol* (2012) 19(9):2822–32. doi: 10.1245/s10434-011-2209-y

33. Shiraishi T, Ito M, Sasaki T, Nishizawa Y, Tsukada Y, Ikeda K. Association between urinary function and resected pattern of the autonomic nerve system after transanal total mesorectal excision for rectal cancer. *Colorectal Dis* (2021) 23(2):405–14. doi: 10.1111/codi.15416

34. Borelli B, Germani MM, Carullo M, Mattioni R, Manfredi B, Sainato A, et al. Total neoadjuvant treatment and organ preservation strategies in the management of localized rectal cancer: A narrative review and evidence-based algorithm. *Crit Rev Oncol Hematol* (2023) 186:103985. doi: 10.1016/j.critrevonc.2023.103985

35. Rullier E, Rouanet P, Tuech JJ, Valverde A, Lelong B, Rivoire M, et al. Organ preservation for rectal cancer (GRECCAR 2): a prospective, randomised, open-label, multicentre, phase 3 trial. *Lancet* (2017) 390(10093):469–79. doi: 10.1016/S0140-6736(17)31056-5

36. Renehan AG, Malcomson L, Emsley R, Gollins S, Maw A, Myint AS, et al. Watch-and-wait approach versus surgical resection after chemoradiotherapy for patients with rectal cancer (the OnCoRe project): a propensity-score matched cohort analysis. *Lancet Oncol* (2016) 17(2):174–83. doi: 10.1016/S1470-2045(15)00467-2

37. Bertocchi E, Barugola G, Nicosia L, Mazzola R, Ricchetti F, Dell'Abate P, et al. A comparative analysis between radiation dose intensification and conventional fractionation in neoadjuvant locally advanced rectal cancer: a monocentric prospective observational study. *Radiol Med* (2020) 125(10):990–8. doi: 10.1007/s11547-020-01189-9

38. Alongi F, Fersino S, Mazzola R, Fiorentino A, Giaj-Levra N, Ricchetti F, et al. Radiation dose intensification in pre-operative chemo-radiotherapy for locally advanced rectal cancer. *Clin Transl Oncol* (2017) 19(2):189–96. doi: 10.1007/s12094-016-1522-0

39. Albano D, Messina C, Vitale J, Sconfienza LM. Imaging of sarcopenia: old evidence and new insights. *Eur Radiol* (2020) 30(4):2199–208. doi: 10.1007/s00330-019-06573-2

40. Brown JC, Caan BJ, Prado CM, Cespedes Feliciano EM, Xiao J, Kroenke CH, et al. The association of abdominal adiposity with mortality in patients with stage I-III colorectal cancer. *J Natl Cancer Inst* (2020) 112(4):377–83. doi: 10.1093/jnci/djz150

41. Hilmi M, Jouinot A, Burns R, Pigneur F, Mounier R, Gondin J, et al. Body composition and sarcopenia: The next-generation of personalized oncology and pharmacology? *Pharmacol Ther* (2019) 196:135–59. doi: 10.1016/j.pharmthera.2018.12.003

42. De Nardi P, Giani A, Maggi G, Braga M. Relation between skeletal muscle volume and prognosis in rectal cancer patients undergoing neoadjuvant therapy. *World J Gastrointest Oncol* (2022) 14(2):423–33. doi: 10.4251/wjgo.v14.i2.423

43. Takeda Y, Akiyoshi T, Matsueda K, Fukuoka H, Ogura A, Miki H, et al. Skeletal muscle loss is an independent negative prognostic factor in patients with advanced lower rectal cancer treated with neoadjuvant chemoradiotherapy. *PloS One* (2018) 13 (4):e0195406. doi: 10.1371/journal.pone.0195406

44. Miyamoto Y, Baba Y, Sakamoto Y, Ohuchi M, Tokunaga R, Kurashige J, et al. Sarcopenia is a negative prognostic factor after curative resection of colorectal cancer. *Ann Surg Oncol* (2015) 22(8):2663–8. doi: 10.1245/s10434-014-4281-6

45. Bedrikovetski S, Traeger L, Price TJ, Carruthers S, Selva-Nayagam S, Moore JW, et al. Can sarcopenia predict complete response after total neoadjuvant therapy in advanced rectal cancer? A multicentre observational cohort study. *J Surg Oncol* (2023) 128(1):75–84. doi: 10.1002/jso.27251

46. Olmez T, Ofluoglu CB, Sert OZ, Keser SH, Gulmez S, Senger AS, et al. The impact of sarcopenia on pathologic complete response following neoadjuvant chemoradiation in rectal cancer. *Langenbecks Arch Surg* (2020) 405(8):1131–8. doi: 10.1007/s00423-020-01983-z

47. Prado CM, Lima IS, Baracos VE, Bies RR, McCargar LJ, Reiman T, et al. An exploratory study of body composition as a determinant of epirubicin pharmacokinetics and toxicity. *Cancer Chemother Pharmacol* (2011) 67(1):93–101. doi: 10.1007/s00280-010-1288-y

48. Dodson S, Baracos VE, Jatoi A, Evans WJ, Cella D, Dalton JT, et al. Muscle wasting in cancer cachexia: clinical implications, diagnosis, and emerging treatment strategies. *Annu Rev Med* (2011) 62:265–79. doi: 10.1146/annurev-med-061509-131248

49. Papadopoulou SK, Papadimitriou K, Voulgaridou G, Georgaki E, Tsotidou E, Zantidou O, et al. Exercise and nutrition impact on osteoporosis and sarcopenia-the incidence of osteosarcopenia: A narrative review. *Nutrients* (2021) 13(12):4499. doi: 10.3390/nu13124499

50. Abe S, Nozawa H, Kawai K, Sasaki K, Murono K, Emoto S, et al. Poor nutrition and sarcopenia are related to systemic inflammatory response in patients with rectal cancer undergoing preoperative chemoradiotherapy. *Int J Colorectal Dis* (2022) 37 (1):189–200. doi: 10.1007/s00384-021-04039-w

51. Grivennikov SI, Greten FR, Karin M. Immunity, inflammation, and cancer. *Cell* (2010) 140:883–99. doi: 10.1016/j.cell.2010.01.025

52. Chiloiro G, Romano A, Mariani S, Macchia G, Giannarelli D, Caravatta L, et al. Predictive and prognostic value of inflammatory markers in locally advanced rectal cancer (PILLAR) - A multicentric analysis by the Italian Association of Radiotherapy and Clinical Oncology (AIRO) Gastrointestinal Study Group. *Clin Transl Radiat Oncol* (2023) 9:100579. doi: 10.1016/j.ctro.2023.100579

53. Liu M, Feng Y, Zhang Y, Liu H. Evaluation of neutrophil-lymphocyte ratio and platelet-lymphocyte ratio on predicting responsiveness to neoadjuvant chemoradiotherapy in locally advanced rectal cancer patients. *BioMed Res Int* (2022) 2022:3839670. doi: 10.1155/2022/3839670

54. Sun Y, Huang Z, Chi P. An inflammation index-based prediction of treatment response to neoadjuvant chemoradiotherapy for rectal mucinous adenocarcinoma. *Int J Clin Oncol* (2020) 25(7):1299–307. doi: 10.1007/s10147-020-01670-5

55. An SH, Kim IY. Can pretreatment platelet-to-lymphocyte and neutrophil-to-lymphocyte ratios predict long-term oncologic outcomes after preoperative chemoradiation followed by surgery for locally advanced rectal cancer? *Ann Coloproctol* (2022) 38(3):253–61. doi: 10.3393/ac.2021.00633.0090

56. Colloca G, Venturino A, Guarneri D. Neutrophil-to-lymphocyte ratio predicts survival of patients with rectal cancer receiving neo-adjuvant chemoradiation followed by radical resection: a meta-analysis. *Expert Rev Anticancer Ther* (2023) 23(4):421–9. doi: 10.1080/14737140.2023.2194635

57. Enkhbaatar NE, Inoue S, Yamamuro H, Kawada S, Miyaoka M, Nakamura N, et al. MR imaging with apparent diffusion coefficient histogram analysis: evaluation of locally advanced rectal cancer after chemotherapy and radiation therapy. *Radiology* (2018) 288(1):129–37. doi: 10.1148/radiol.2018171804

58. Yoo GS, Park HC, Yu JI, Choi DH, Cho WK, Park YS, et al. Carcinoembryonic antigen improves the performance of magnetic resonance imaging in the prediction of pathologic response after neoadjuvant chemoradiation for patients with rectal cancer. *Cancer Res Treat* (2020) 52(2):446–54. doi: 10.4143/crt.2019.261

frontiers | Frontiers in Oncology

TYPE Original Research
PUBLISHED 24 January 2024
DOI 10.3389/fonc.2023.1231508

OPEN ACCESS

EDITED BY
Marco Rengo,
Sapienza University of Rome, Italy

REVIEWED BY
Cibele Masotti,
Hospital Sirio Libanes, Brazil
Charles Ternent,
Methodist Physicians Clinic, United States

*CORRESPONDENCE
Yueping Liu
liuyp@hebmu.edu.cn
Yongqiang Zhang
zyq@hebust.edu.cn
Guiying Wang
wangguiying@hebmu.edu
wangguiyingtgzy@163.com

RECEIVED 20 June 2023
ACCEPTED 28 December 2023
PUBLISHED 24 January 2024

CITATION
Hu J, Sheng Y, Ma J, Tang Y, Liu D, Zhang J, Wei X, Yang Y, Liu Y, Zhang Y and Wang G (2024) Construction and validation of a progression prediction model for locally advanced rectal cancer patients received neoadjuvant chemoradiotherapy followed by total mesorectal excision based on machine learning.
Front. Oncol. 13:1231508.
doi: 10.3389/fonc.2023.1231508

Construction and validation of a progression prediction model for locally advanced rectal cancer patients received neoadjuvant chemoradiotherapy followed by total mesorectal excision based on machine learning

Jitao Hu[1], Yuanyuan Sheng[2], Jinlong Ma[2], Yujie Tang[1], Dong Liu[3], Jianqing Zhang[1], Xudong Wei[4], Yang Yang[3], Yueping Liu[5]*, Yongqiang Zhang[2]* and Guiying Wang[1,6]*

[1]Department of General Surgery, The Fourth Hospital of Hebei Medical University, Shijiazhuang, China, [2]School of Information Science and Engineering, Hebei University of Science and Technology, Shijiazhuang, China, [3]Department of Gastrointestinal Surgery, The Third Hospital of Hebei Medical University, Shijiazhuang, China, [4]Department of General Surgery, The Third Hospital of Hebei Medical University, Shijiazhuang, China, [5]Department of Pathology, The Fourth Hospital of Hebei Medical University, Shijiazhuang, China, [6]The Second Hospital of Hebei Medical University, Shijiazhuang, Hebei, China

Background: We attempted to develop a progression prediction model for local advanced rectal cancer(LARC) patients who received preoperative neoadjuvant chemoradiotherapy(NCRT) and operative treatment to identify high-risk patients in advance.

Methods: Data from 272 LARC patients who received NCRT and total mesorectal excision(TME) from 2011 to 2018 at the Fourth Hospital of Hebei Medical University were collected. Data from 161 patients with rectal cancer (each sample with one target variable (progression) and 145 characteristic variables) were included. One Hot Encoding was applied to numerically represent some characteristics. The K-Nearest Neighbor (KNN) filling method was used to determine the missing values, and SmoteTomek comprehensive sampling was used to solve the data imbalance. Eventually, data from 135 patients with 45 characteristic clinical variables were obtained. Random forest, decision tree, support vector machine (SVM), and XGBoost were used to predict whether patients with rectal cancer will exhibit progression. LASSO regression was used to further filter the variables and narrow down the list of variables using a Venn diagram. Eventually, the prediction model was constructed by multivariate logistic regression, and the performance of the model was confirmed in the validation set.

Results: Eventually, data from 135 patients including 45 clinical characteristic variables were included in the study. Data were randomly divided in an 8:2 ratio into a data set and a validation set, respectively. Area Under Curve (AUC) values of 0.72 for the decision tree, 0.97 for the random forest, 0.89 for SVM, and 0.94 for

XGBoost were obtained from the data set. Similar results were obtained from the validation set. Twenty-three variables were obtained from LASSO regression, and eight variables were obtained by considering the intersection of the variables obtained using the previous four machine learning methods. Furthermore, a multivariate logistic regression model was constructed using the data set; the ROC indicated its good performance. The ROC curve also verified the good predictive performance in the validation set.

Conclusions: We constructed a logistic regression model with good predictive performance, which allowed us to accurately predict whether patients who received NCRT and TME will exhibit disease progression.

KEYWORDS

deep learning, artificial intelligence, total mesorectal excision, neoadjuvant chemoradiotherapy, local advanced rectal cancer

1 Introduction

Colorectal cancer is the third most common cancer worldwide and the second leading cause of cancer-related deaths. In 2020, rectal cancer accounted for 6.0% of newly diagnosed cancer cases and 3.4% of cancer deaths (1). The last decades witnessed the development of multidiscipline, individualization, and precision in treatments for rectal cancer. NCRT followed by TME has been recommended for patients diagnosed with LARC, which is correlated to lower treatment-related toxicity rate, lower local recurrence rate, and higher sphincter preserve rate (2).

However, in clinical research, the sensitivity of patients with rectal cancer to preoperative neoadjuvant therapy varies significantly, and more than half of the patients are not sensitive to neoadjuvant therapy (3, 4) and exhibit disease progression after preoperative neoadjuvant therapy and operative treatment (5). Thus, we need to accurately predict disease progression in this group of patients to target the high-risk patients for focused care and related interventions.

Current methods used for predicting the outcomes of preoperative neoadjuvant therapy include MRI imaging (6), molecular marker examination (7), blood levels (8), and the assessment of pathological and clinical characteristics (9). However, the predictions are unsatisfactory and are primarily useful for determining the effects of preoperative neoadjuvant therapy. Meanwhile, no significant progress has been made in the prediction of disease progression after preoperative neoadjuvant therapy and surgical treatment. Moreover, the routine preoperative examination of patients usually involves blood tests, such as those for neutrophil or leukocyte levels, among others. The routine preoperative examination may have better effects on predicting disease progression if multiple variables, including those available from initial tests (conducted at admission) and post-neoadjuvant examination and tests, can be used comprehensively. This would help avoid the omission of important variables and the deletion or selection of critical variables for predicting disease progression after treatment.

The significance of joint work between medcine and machine learning has been more and more recognised (10). Artificial intelligence (AI) and machine learning have been widely used to screen, diagnose, and treat patients with cancer (11). The AI risk assessment of pulmonary lymph nodes is an example. Compared to traditional statistical methods, AI techniques are more effective for handling complex data (12). Moreover, AI tools can also be built to predict the prognosis of liver cancer (13), lung cancer (14), colorectal squamous cell carcinoma (15), or breast cancer (16) in patients based on pathological images or clinicopathological characteristics. AI application represents a significant trend with potential applications in predicting the outcomes of preoperative neoadjuvant therapy and disease progression after operative treatment (17).

The prediction of disease progression after preoperative neoadjuvant therapy and operative treatment is of great significance. Moreover, previous studies had reported the prediction of the effect of preoperative neoadjuvant, such as MRI (18), circulating DNA (19), tumor microsatellite stability (20), immune cell infiltration (21), etc. However, these studies only considered a few variables, and the true magnitude of the effect needed to be clarified. Chemotherapy has become one of the most important elements in the treatment of rectal cancer (22). Preoperative neoadjuvant therapy and postoperative chemotherapy can improve the prognosis of rectal cancer patients (23). The guidelind suggest the patients recieved a total durationg of 6 months before and after operation (24), we excluded the patients didn't recieved sufficent chemotheratpy. Here, we included information on the patients collected at admission, after

neoadjuvant treatment and postoperative information such as the tumor location, colonoscopy results, imaging and postoperative pathology results. We included multiple variables in the study. We further filtered eight variables using various machine learning methods for analysis, attempting to avoid the loss of important variables. We believed this would help build a prediction model with good predictive ability, which would help predict the outcomes of neoadjuvant treatment and disease progression after operative treatment.

2 Materials and methods

2.1 Patients

A retrospective study was conducted. 272 patients diagnosed with LARC, who received NCRT and underwent TME at the 4th hospital of Hebei Medical University(Shijiazhuang, Hebei, China) were enrolled from 2011-2018 were enrolled. Data included 145 clinical variables were collected.

After considering the inclusion and exclusion criteria, data from 135 patients with rectal cancer, which included 45 clinical characteristic variables, were included in the study. All patients had undergone R0 resection after NCRT. Inclusion criteria: 1) location in the rectum, within 12 cm from the anal verge; 2) pathologically malignant and diagnosed as adenocarcinoma; 3) preoperative neoadjuvant treatment before imaging diagnosis of stage II-III disease; 4) availability of complete clinical data; 5) received standard radiotherapy: 5 days a week at 1.8 Gy per day for 5;weeks to a dose of 45 Gy, followed by a boost of 5.4 Gy, for a total dose of 50.4 Gy; 6)received complete preoperative and post-operative therapy with a duration of 6 months. Exclusion criteria: 1) Concomitant with other serious diseases, such as myocardial infarction; 2) Not receiving standard NCRT; 3) Refuse follow-up; 4)refuse to receive TME after NCRT. The patients in our study recieved standard XELOX regimen in pre-operative and post-operative chemotherapy. The research scheme was approved by the Ethics Committee of the Fourth Hospital of Hebei Medical University (Approval Code: 2023KS015).

2.2 Data processing

Sample data from 272 patients with rectal cancer were screened. Data from 161 patients with rectal cancer followed up for 2 years, who subsequently underwent TME after neoadjuvant therapy, were included.

One target quantity (progression) and 145 characteristic variables were selected per sample. Concurrently, One Hot Encoding was applied to certain numerical characteristics in data processing to facilitate model training. Moreover, the KNN filling method was applied for missing data attributes, whereas SmoteTomek comprehensive sampling (25–27) was used to solve the data imbalance problem to improve the classification accuracy in a few classes. Eventually, 135 patients were selected, and the final model was constructed using four machine learning methods (ten-fold cross-validation) to screen important variables for constructing the prediction model and validating it using a ROC curve.

The 145 variables were shown as followed, Gender, age, previous medical history, chief complaint, family history, smoking history, drinking history were retrospectively collected from the medical history database. As digital rectal examination, blood test, MRI, coloscopy were perfomed both before NCRT and before TME, variables from these tests were recorded twice. In digital rectal examination, the distance between toumor and anus, whether blood was observed after examination were recorded. For the tumors failed to reach through digital rectal examination, the distance was recorded through colonscopy. Variables from coloscope include: whether stenosis, edema or mucus was observed, the morphology of tumor, the status of mucosa. The level of blood tumor biomarkers inclued CEA, CA-199, CA-724, ferroprotein, β2-microglobulin were recorded. The counting of red blood cell, white blood cell, neutrophil, lymphocyte, platelet was recorded. The serum level of albumin was also recorded. Variables from MRI inculded cricumferential invasion, tumor size, clinical TNM staging, vessel invasion. For the pathological results of coloscopy biopsy, the pathological diagnosis, tumor differentiation were recorded. The exact operating method of TME and post-operative complication was also recorded. The mutation status of KRAS, NRAS, BRAF, and the expresstion status of Her-2 MLH1, MSH2, PMS2 were record through the pathological results of the operative specimens. Variable from operative specimens also included tumor size, morphology, tumor differentiation, histological grade, pathological TNM stage, blood vessel invasion, perineural invasion, tumor regression grade. The total number of post-operative The survival and progression information was collected through telephone follow-up.

2.3 Statistical analysis

Statistical work were completed by statistical experts (School of Information Science and Engineering, Hebei University of Science and Technology). The decision tree analysis was conducted using rpart package, random forest analysis was conducted using randomForest package, SVM was conducted using e1071 package, XGBoost was conducted using xgboost package, and LASSO regression was conducted using glmnet package. The predictive ability of the prediction models was assessed based on the AUC values of the ROC curves. $P<0.05$ was considered statistically significant.

3 Results

3.1 Baseline clinical characteristics

We included data from 135 patients from the Fourth Hospital of Hebei Medical University who had undergone preoperative neoadjuvant therapy. Forty-five independent variables, such as gender, age, and others, were included in this study. They were randomly divided into the training and test sets in a ratio of 8:2 for subsequent analysis. There were no difference between the groups (Supplementary Table 1). The detailed information of 135 patients

(with 45 variables) had been shown in Supplementary Table 2. The process was shown in Figure 1.

3.2 Machine learning model construction and validation

All 45 baseline characteristics, including initial hospitalization data and preoperative data, were used to construct a model to predict whether the disease had progressed. Moreover, four machine learning methods were used in the training set to construct the models. In this model, as shown in Figure 2, the AUC values were 0.72 ± 0.11 for decision trees (Figure 2A), 0.97 ± 0.04 for random forests (Figure 2B), 0.89 ± 0.11 for SVM (Figure 2C), and 0.94 ± 0.10 for XGBoost (Figure 2D). To confirm the potential of the four machine learning models, we tested them in a test set and obtained similar results (Figure 3). Our results indicated the excellent predictive ability of the four machine learning models.

3.3 Predictor construction and validation

The predictive ability of the four machine learning models werre good; however, with so many variables, it was not very convenient for practical applications. To further reduce the number of variables, we performed LASSO regression analysis, which yielded 23 variables identified (Figures 4A, B) and eight critical variables (tumor size, pre-operative serium CEA, distant metastasis in NCRT, nerve invasion, age, vascular invasion, preoperative lymph node metastasis, MLH1) were identified using a Venn diagram by four methods (Figure 4C). The MLH1-status was assessed by immunohistochemistry(IHC). These eight variables were subsequently used for multivariate logistics regression to construct a diagnostic prediction model with a discriminant optimal cutoff value of 0.314, suggesting that patients with scores <0.314 could be considered progression-free and patients with scores >0.314 could be considered to exhibit progression. In the training set, ROC analysis revealed a sensitivity of 94% and a

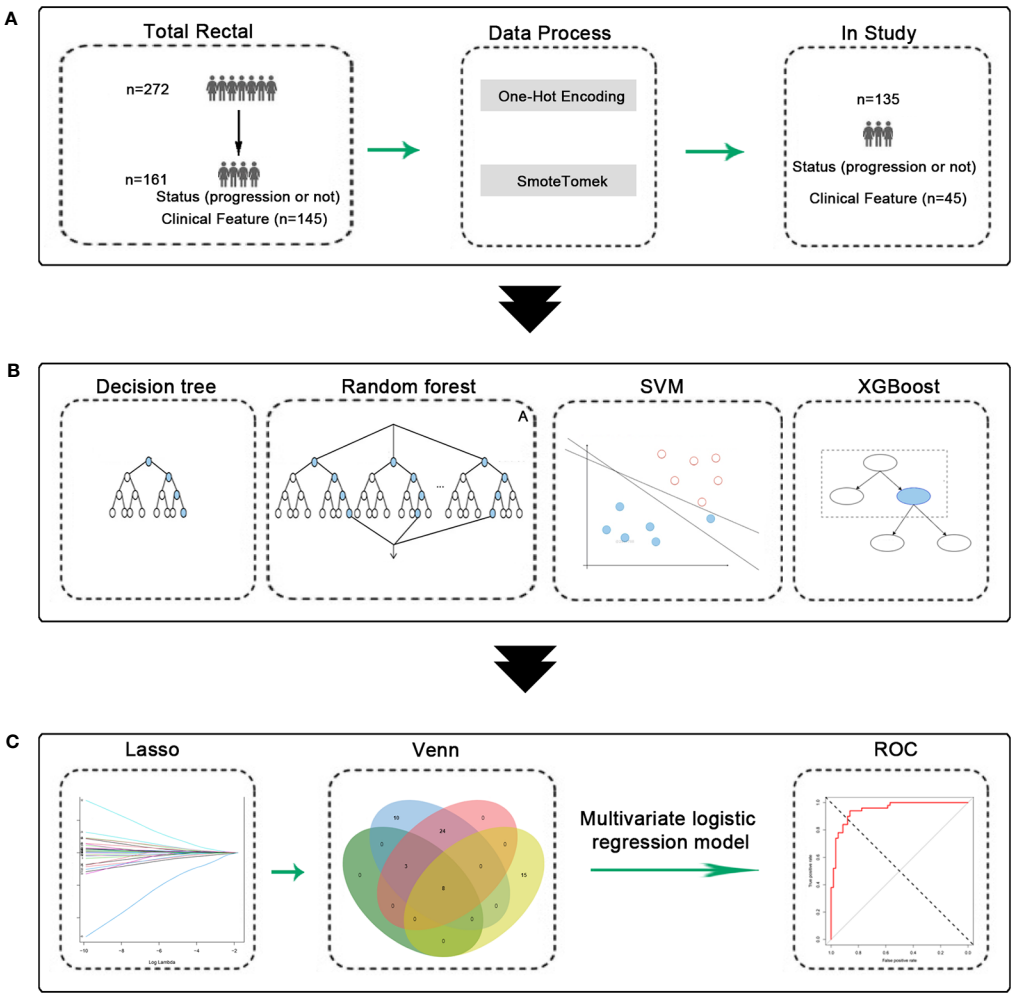

FIGURE 1
Experimental flow chart. **(A)** Data process, 135 patients were obtained. **(B)** Machine learning model construction and validation. **(C)** Construction and validation of predictive models.

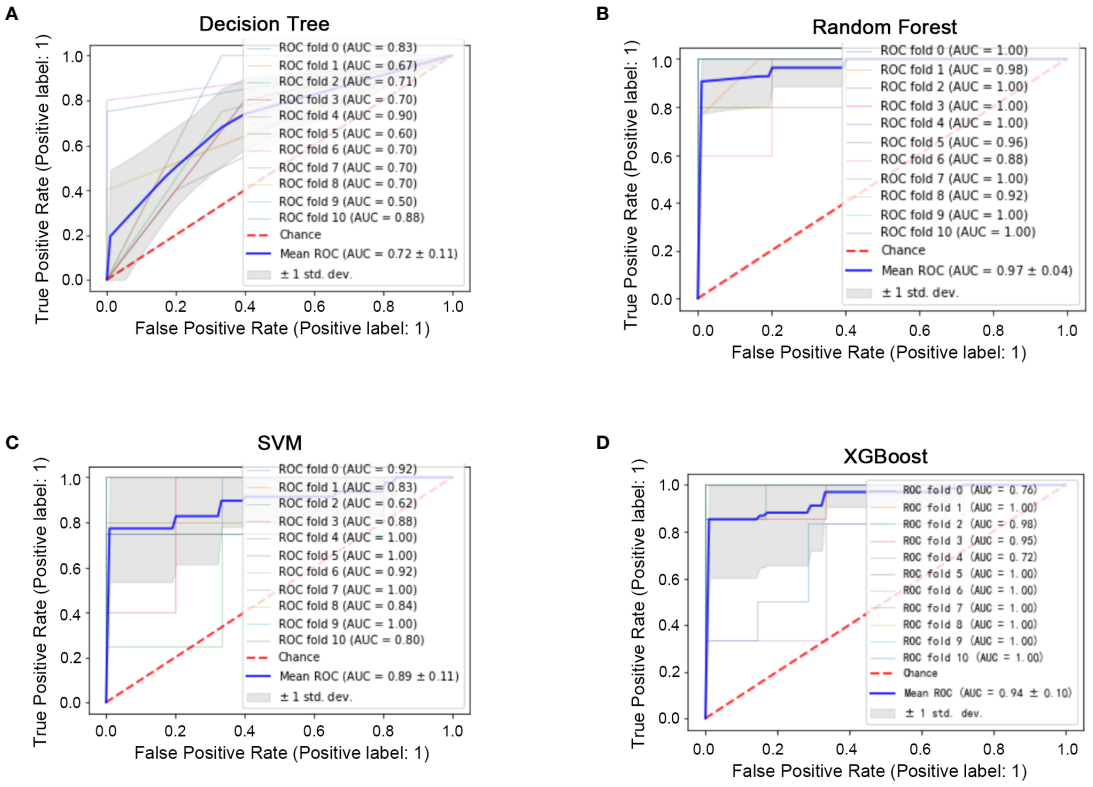

FIGURE 2
Machine learning model construction (ten-fold cross-validation) in the training set. **(A)** ROC diagram of the decision tree in the training set. **(B)** ROC diagram of the random forest in the training set. **(C)**: ROC diagram of the support vector machine in the training set. **(D)** ROC diagram of XGBoost in the training set.

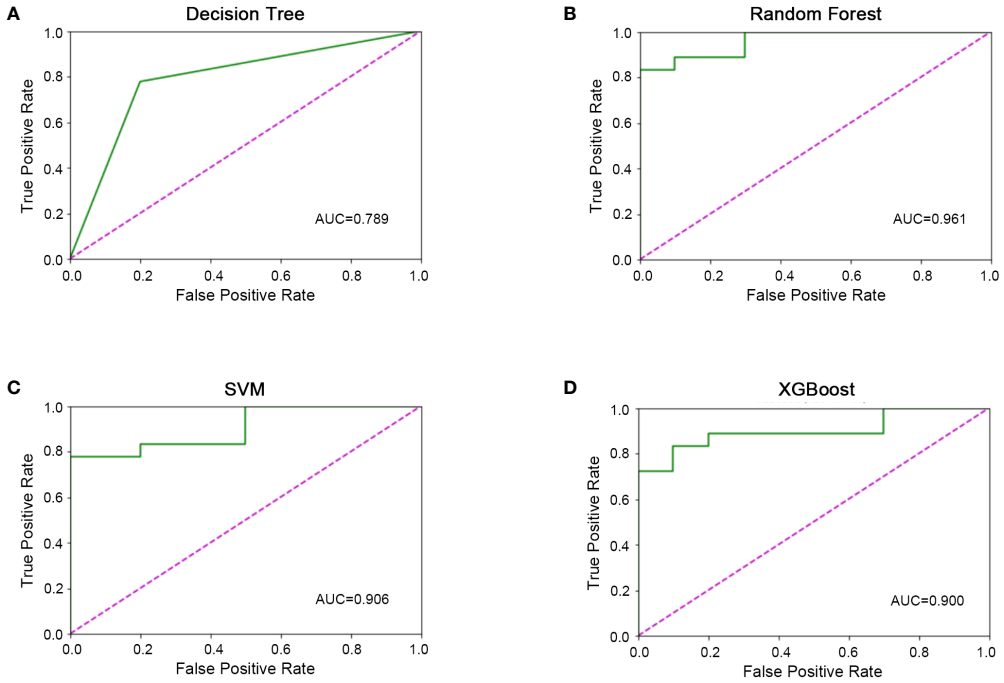

FIGURE 3
Machine learning model validation in the validation set. **(A)** ROC diagram of the decision tree in the validation set. **(B)** ROC diagram of the random forest in the validation set. **(C)** ROC diagram of support vector machine in the validation set. **D)** ROC diagram of XGBoost in the validation set.

10.3389/fonc.2023.1231508

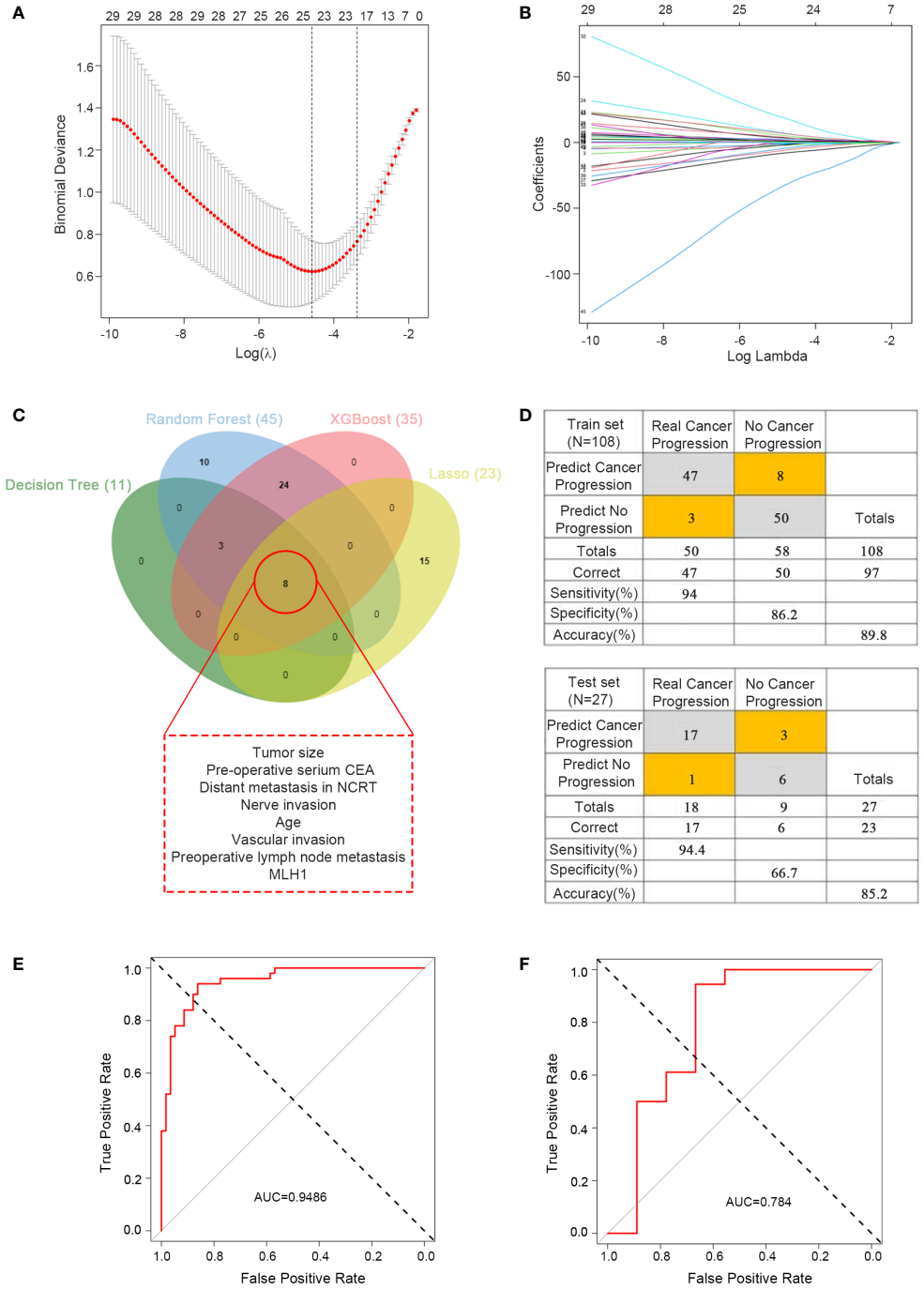

Train set (N=108)	Real Cancer Progression	No Cancer Progression	
Predict Cancer Progression	47	8	
Predict No Progression	3	50	Totals
Totals	50	58	108
Correct	47	50	97
Sensitivity(%)	94		
Specificity(%)		86.2	
Accuracy(%)			89.8

Test set (N=27)	Real Cancer Progression	No Cancer Progression	
Predict Cancer Progression	17	3	
Predict No Progression	1	6	Totals
Totals	18	9	27
Correct	17	6	23
Sensitivity(%)	94.4		
Specificity(%)		66.7	
Accuracy(%)			85.2

FIGURE 4
Predictor construction and validation. **(A)** Clinical characteristics of patients with rectal cancer in the LASSO model. **(B)** Selection of the tuning parameter (λ) in the LASSO model required cross-validation using the maximum criteria. **(C)** Venn diagram of the outcomes of the four machine learning methods for filtering variables. **(D)** Confusion matrix of binary outcomes after logistic regression for predicting patient progression in rectal cancer, the predictor for the train set (upper) and test set (lower). **(E)** ROC curves for predicting disease progression in patients with rectal cancer undergoing preoperative neoadjuvant therapy and after surgical treatment to distinguish whether progression; the training set. **(F)** ROC curves for predicting disease progression in patients with rectal cancer undergoing preoperative neoadjuvant therapy and after surgical treatment to distinguish whether progression; the test set.

specificity of 86.2% for the differentiation between progression and non-progression (Figure 4D upper), with an AUC value of 0.9486 (Figure 4E). Similar results were obtained in the validation set, with a sensitivity of 94.4%, a specificity of 66.7% (Figure 4D down), and an AUC value of 0.784 (Figure 4F).

4 Disscussion

Preoperative neoadjuvant chemoradiotherapy was an important part of rectal cancer treatment (28), and many previous studies had reported prediction models for the response

of rectal cancer to preoperative neoadjuvant therapy (18, 29, 30). However, cases of progression after preoperative neoadjuvant therapy could not be ignored. To rule out the differences caused by chemotherapy, we ultimately included patients who had undergone sufficient chemotherapy in the study to minimize the bias caused by individual chemotherapy as much as possible. In our study, we obtained eight critical variables using four machine learning methods to construct a prediction model for progression after preoperative neoadjuvant therapy, which can reasonably predict the disease progression of patients. This can help improve the focus and increase the frequency of reviews in such cases. Additionally, once signs of progression were detected, the treatment plan could be altered immediately. This can help avoid delays in treatment and improve patient prognosis.

Machine learning have been widely applied in clinical decision-making (10). For example, machine learning had been previously applied to readmission after elective laparoscopic colorectal surgery (31). Tumor burden before and after NCRT are depcited through cTNM before NCRT stage and ypTNM respectively. However, the joint effects of pre and after NCRT stage is not well-studied. A system that is able to integret multiple information may better predict the prognosis of patients (32).

In our study, we included more than 100 variables and tested comprehensive data to avoid missing variables that can influence disease progression. To our knowledge, the variables included in our study were numerous.

We initially constructed four machine learning models. Even though the AUC values were high, they all showed good predictive functions in the training set and test set, but the value of 0.9 did not meet our requirements. Hence, we further screened the variables by LASSO regression and then using Venn diagram to further screen variables. We eventually selected eight important variables. The AUC value of the final prediction model was considerably high at 0.9486, indicating the excellent function of our model. The applicability of these eight variables was high because they were mandatory examinations or tests for patients who require hospitalization.

Feature selection plays a crucial role in the field of machine learning, as it can select the most informative features from raw data, improve model performance, reduce overfitting, and accelerate model training and prediction speed. In large-scale datasets and high-dimensional data, feature selection is particularly important because unnecessary features increase computational complexity and introduce redundant information (33, 34). When selecting univariate and multivariate regression analysis, we need to have an adequate sample size, with a positive sample size at least 10 times the number of variables. The more the better, in order to meet the meaningful results. In addition, we believed that the feature selectionn of univariate and multivariate regression carries subjectivity (subjective selection of p-value), while the feature selection of machine learning relies on computation and is more observable. In sum, univariate and multivariate regression focus more on analyzing the impact of independent variables on outcomes, while feature selection is a part of machine learning.

In the features selection for model construction, SVM was excluded from the analysis. The machine learning of this study were based on the sklearn framework. Decision trees, random forests, and XGBoost were all based on the important features of tree models, so the important features can be obtained from the model. However, SVM did not have important features in the algorithm, so important features were not be obtained. Therefore, in the selection of the variables, SVM was excluded from the analysis.

Currently, nearly all the prediction models for rectal cancer patients undergoing neoadjuvant treatment are used to predict tumor response to identify sensitive patients. Here, we aimed to predict tumor progression after neoadjuvant treatment, to identify high-risk patients. Thus, we pay more attention to these high-risk patients, benefiting for early detection and early treatment. CEA, known as a biomarker in colorectal cancer, had been reported to be associated with pathological complete remission after neoadjuvant treatment for rectal cancer, and tumor size and preoperative CEA are related to tumor downstaging (35). So tumor size and preoperative CEA had the potential to predict tumor progression. Similarly, distant metastasis, nerve invasion, age, vascular invasion, and preoperative lymph node metastasis are all related to tumor prognosis (36, 37), revealing the potential to predict tumor progression. These 7 variables are routine preoperative examination items, indicating that our model had good generality.

However, the time point at which progression occurred and was concentrated remains unascertained, which was also a limitation of this study. In our future studies, we will focus on this aspect of the research topic to determine the period in which the disease is more prone to progression. In addition, This study was a single center retrospective study, and the model constructed lacked external data validation. There was also a selection bias in this study due to the missing cases in the study. In the future, we would collaborate with other centers to further increase the sample size, validate and optimize the model constructed in this study. This will help reduce the frequency at which reviews are conducted and help focus on reviews during critical periods. This is also conducive to adjustments in treatment plans based on the availability of medical resources. In conclusion, we have constructed a model with good predictive function and wide applicability, which can help improve the focus on critical patients and their prognosis.

5 Conclusion

We constructed a logistic regression model with good predictive performance, which allowed us to accurately predict whether patients who received NCRT (sufficent standard XELOX regimen) and TME will exhibit disease progression.

Data availability statement

The original contributions presented in the study are included in the article/Supplementary Material. Further inquiries can be directed to the corresponding authors.

Ethics statement

The studies involving humans were approved by The research scheme was approved by the Ethics Committee of the Fourth Hospital of Hebei Medical University (Approval Code: 2023KS015). The studies were conducted in accordance with the local legislation and institutional requirements. Written informed consent for participation was not required from the participants or the participants' legal guardians/next of kin because Our research was a retrospective study and did not require the written informed consent.

Author contributions

All authors contributed to the research conception and design. Conceptualization, GW, YZ and YL; methodology, YS, JH; software, YS, YZ, GW; validation, JZ; formal analysis, YT; investigation, JH, DL; resources, GW; data curation, JM; writing—original draft preparation, YY; writing—review and editing, YL; visualization, XW; supervision, JH; project administration, JH; funding acquisition, GW. All authors have read and agreed to the published version of the manuscript.

Funding

The author(s) declare financial support was received for the research, authorship, and/or publication of this article. This research was funded by Hebei Natural Science Foundation (H2020206485), (H2022206355).

Acknowledgments

Thanks to everyone who has supported and helped with this research.

Conflict of interest

The authors declare that the research was conducted in the absence of any commercial or financial relationships that could be construed as a potential conflict of interest.

Publisher's note

All claims expressed in this article are solely those of the authors and do not necessarily represent those of their affiliated organizations, or those of the publisher, the editors and the reviewers. Any product that may be evaluated in this article, or claim that may be made by its manufacturer, is not guaranteed or endorsed by the publisher.

Supplementary material

The Supplementary Material for this article can be found online at: https://www.frontiersin.org/articles/10.3389/fonc.2023.1231508/full#supplementary-material

References

1. Sung H, Ferlay J, Siegel RL, Laversanne M, Soerjomataram I, Jemal A, et al. Global cancer statistics 2020: GLOBOCAN estimates of incidence and mortality worldwide for 36 cancers in 185 countries. *CA: Cancer J Clin* (2021) 71(3):209–49. doi: 10.3322/caac.21660

2. Sauer R, Becker H, Hohenberger W, Rödel C, Wittekind C, Fietkau R, et al. Preoperative versus postoperative chemoradiotherapy for rectal cancer. *N Engl J Med* (2004) 351(17):1731–40. doi: 10.1056/NEJMoa040694

3. Pohl M, Schmiegel W. Therapeutic strategies in diseases of the digestive tract - 2015 and beyond targeted therapies in colon cancer today and tomorrow. *Dig Dis* (2016) 34(5):574–9. doi: 10.1159/000445267

4. Peng SH, Mbarak HS, Li YH, Ma C, Shang QL, Chen Z, et al. Neoadjuvant intra-arterial versus intravenous chemotherapy in colorectal cancer. *Med (Baltimore)* (2021) 100(51):e28312. doi: 10.1097/MD.0000000000028312

5. Subbiah IM, Blackmon SH, Correa AM, Kee B, Vaporciyan AA, Swisher SG, et al. Preoperative chemotherapy prior to pulmonary metastasectomy in surgically resected primary colorectal carcinoma. *Oncotarget* (2014) 5(16):6584–93. doi: 10.18632/oncotarget.2172

6. Yang R, Zhao H, Wang X, Ding Z, Tao Y, Zhang C, et al. Magnetic resonance imaging radiomics modeling predicts tumor deposits and prognosis in stage T3 lymph node positive rectal cancer. *Abdom Radiol (NY)* (2023) 48(4):1268–79. doi: 10.1007/s00261-023-03825-0

7. Wang H, Ji D, Tian H, Gao Z, Song C, Jia J, et al. Predictive value of proteomic markers for advanced rectal cancer with neoadjuvant chemoradiotherapy. *BMC Cancer* (2022) 22(1):868. doi: 10.1186/s12885-022-09960-z

8. Martín-Carnicero A, Ramalle-Gomara E, Rubio-Mediavilla S, Alonso-Lago M, Zorrilla-Larraga M, Manrique-Abós, et al. Prognostic and predictive biomarkers in patients with locally advanced rectal cancer (LARC) treated with preoperative chemoradiotherapy. *J Clin Med* (2022) 11(20):6091. doi: 10.3390/jcm11206091

9. Karimi M, Osterlund P, Hammarström K, Imam I, Frodin JE, Glimelius B. Associations between response to commonly used neo-adjuvant schedules in rectal cancer and routinely collected clinical and imaging parameters. *Cancers (Basel)* (2022) 14(24):6238. doi: 10.3390/cancers14246238

10. Ichimasa K, Kudo SE, Mori Y, Misawa M, Matsudaira S, Kouyama Y, et al. Artificial intelligence may help in predicting the need for additional surgery after endoscopic resection of T1 colorectal cancer. *Endoscopy* (2018) 50(3):230–40. doi: 10.1055/s-0043-122385

11. Mitsala A, Tsalikidis C, Pitiakoudis M, Simopoulos C, Tsaroucha AK. Artificial intelligence in colorectal cancer screening, diagnosis and treatment. A new era. *Curr Oncol* (2021) 28(3):1581–607. doi: 10.3390/curroncol28030149

12. Schmidt C. M. D. Anderson breaks with IBM watson, raising questions about artificial intelligence in oncology. *J Natl Cancer Inst* (2017) 109(5):djx113. doi: 10.1093/jnci/djx113

13. Qu WF, Tian MX, Lu HW, Zhou YF, Liu WR, Tang Z, et al. Development of a deep pathomics score for predicting hepatocellular carcinoma recurrence after liver transplantation. *Hepatol Int* (2023) 17(4):927–41. doi: 10.1007/s12072-023-10511-2

14. Hu W, Zhang X, Saber A, Cai Q, Wei M, Wang M, et al. Development and validation of a nomogram model for lung cancer based on radiomics artificial intelligence score and clinical blood test data. *Front Oncol* (2023) 13:1132514. doi: 10.3389/fonc.2023.1132514

15. Yang Y, Yu J, Hu J, Zhou C, Niu J, Ma H, et al. A systematic and comprehensive analysis of colorectal squamous cell carcinoma: Implication for diagnosis and treatment. *Cancer Med* (2022) 11(12):2492–502. doi: 10.1002/cam4.4616

16. Wang J, Liu Y, Zhang R, Liu Z, Yi Z, Guan X, et al. Multi-omics fusion analysis models with machine learning predict survival of HER2-negative metastatic breast cancer: a multicenter prospective observational study. *Chin Med J (Engl)* (2023) 136(7):863–5. doi: 10.1097/CM9.0000000000002625

17. Colorectal Surgery Group of the Surgery Branch in the Chinese Medical Association; Beihang University State Key Laboratory of Virtual Reality Technology and Systems. Expert consensus on the surgical clinical application of rectal cancer neoadjuvant therapy effect evaluation system based on artificial intelligence platform (2022 edition). *Zhonghua Wai Ke Za Zhi* (2022) 60(8):732–5. doi: 10.3760/cma.j.cn112139-20220326-00125

18. Miranda J, Horvat N, Assuncao AN Jr., de M Machado FA, Chakraborty J, Pandini RV, et al. MRI-based radiomic score increased mrTRG accuracy in predicting rectal cancer response to neoadjuvant therapy. *Abdom Radiol (NY)* (2023) 48(6):1911–20. doi: 10.1007/s00261-023-03898-x

19. Truelsen CG, Kronborg CS, Sørensen BS, Callesen LB, Spindler KG. Circulating cell-free DNA as predictor of pathological complete response in locally advanced rectal cancer patients undergoing preoperative chemoradiotherapy. *Clin Transl Radiat Oncol* (2022) 36:9–15. doi: 10.1016/j.ctro.2022.06.002

20. Bando H, Tsukada Y, Inamori K, Togashi Y, Koyama S, Kotani D, et al. Preoperative Chemoradiotherapy plus Nivolumab before Surgery in Patients with Microsatellite Stable and Microsatellite Instability-High Locally Advanced Rectal Cancer. *Clin Cancer Res* (2022) 28(6):1136–46. doi: 10.1158/1078-0432.CCR-21-3213

21. Sekizawa K, Nakagawa K, Ichikawa Y, Suwa H, Ozawa M, Momiyama M, et al. Relationship between stromal regulatory T cells and the response to neoadjuvant chemotherapy for locally advanced rectal cancer. *Surg Today* (2022) 52(2):198–206. doi: 10.1007/s00595-021-02311-8

22. Tamburini E, Tassinari D, Ramundo M, De Stefano A, Viola MG, Romano C, et al. Adjuvant chemotherapy after neoadjuvant chemo-radiotherapy and surgery in locally advanced rectal cancer. A systematic review of literature with a meta-analysis of randomized clinical trials. *Crit Rev Oncol Hematol* (2022) 172:103627. doi: 10.1016/j.critrevonc.2022.103627

23. Bachet JB, Benoist S, Mas L, Huguet F. Neoadjuvant treatment for rectal cancer. *Bull Cancer* (2021) 108(9):855–67. doi: 10.1016/j.bulcan.2021.03.018

24. Benson AB, Venook AP, Al-Hawary MM, Azad N, Chen YJ, Ciombor KK, et al. Rectal cancer, version 2.2022, NCCN clinical practice guidelines in oncology. *J Natl Compr Canc Netw* (2022) 20(10):1139–67. doi: 10.6004/jnccn.2022.0051

25. Kumar V, Lalotra GS, Sasikala P, Rajput DS, Kaluri R, Lakshmanna K, et al. Addressing binary classification over class imbalanced clinical datasets using computationally intelligent techniques. *Healthcare (Basel)* (2022) 10(7):1293. doi: 10.3390/healthcare10071293

26. Fitriyani NL, Syafrudinet M, Alfian G, Rhee J. Development of disease prediction model based on ensemble learning approach for diabetes and hypertension. *IEEE Access* (2019) 7:144777–89. doi: 10.1109/ACCESS.2019.2945129

27. Rana C, Chitre N, Poyekar B, Bide P. Stroke prediction using smote-tomek and neural network, in: *2021 12th International Conference on Computing Communication and Networking Technologies (ICCCNT)*, Kharagpur, India. (2021), pp. 1-5. doi: 10.1109/ICCCNT51525.2021.9579763

28. Oronsky B, Reid T, Larson C, Knox SJ. Locally advanced rectal cancer: The past, present, and future. *Semin Oncol* (2020) 47(1):85–92. doi: 10.1053/j.seminoncol.2020.02.001

29. Peng J, Wang W, Jin H, Qin X, Hou J, Yang Z, et al. Develop and validate a radiomics space-time model to predict the pathological complete response in patients undergoing neoadjuvant treatment of rectal cancer: an artificial intelligence model study based on machine learning. *BMC Cancer* (2023) 23(1):365. doi: 10.1186/s12885-023-10855-w

30. Sun Y, Zhang X, Jin C, Yue K, Sheng D, Zhang T, et al. Prospective, longitudinal analysis of the gut microbiome in patients with locally advanced rectal cancer predicts response to neoadjuvant concurrent chemoradiotherapy. *J Transl Med* (2023) 21(1):221. doi: 10.1186/s12967-023-04054-1

31. Francis NK, Luther A, Salib E, Allanby L, Messenger D, Allison AS, et al. The use of artificial neural networks to predict delayed discharge and readmission in enhanced recovery following laparoscopic colorectal cancer surgery. *Tech Coloproctol* (2015) 19(7):419–28. doi: 10.1007/s10151-015-1319-0

32. Song C, Chung JH, Kang SB, Kim DW, Oh HK, Lee HS, et al. Impact of tumor regression grade as a major prognostic factor in locally advanced rectal cancer after neoadjuvant chemoradiotherapy: A proposal for a modified staging system. *Cancers (Basel)* (2018) 10(9):319. doi: 10.3390/cancers10090319

33. Kourou K, Exarchos TP, Exarchos KP, Karamouzis MV, Fotiadis DI. Machine learning applications in cancer prognosis and prediction. *Comput Struct Biotechnol J* (2015) 13:8–17. doi: 10.1016/j.csbj.2014.11.005

34. Pudjihartono N, Fadason T, Kempa-Liehr AW, O'Sullivan JM. A review of feature selection methods for machine learning-based disease risk prediction. *Front Bioinform* (2022) 2:927312. doi: 10.3389/fbinf.2022.927312

35. Moureau-Zabotto L, Farnault B, de Chaisemartin C, Esterni B, Lelong B, Viret F, et al. Predictive factors of tumor response after neoadjuvant chemoradiation for locally advanced rectal cancer. *Int J Radiat Oncol Biol Phys* (2011) 80(2):483–91. doi: 10.1016/j.ijrobp.2010.02.025

36. Wang H, Hong R, Niu G, Hu Z, Ke C. Clinical study on risk factors related to postoperative recurrence or metastasis of rectal cancer: a retrospective cohort study. *J Gastrointest Oncol* (2022) 13(6):2973–88. doi: 10.21037/jgo-22-942

37. Gheybi K, Buckley E, Vitry A, Roder D. Associations of advanced age with comorbidity, stage and primary subsite as contributors to mortality from colorectal cancer. *Front Public Health* (2023) 11:1101771. doi: 10.3389/fpubh.2023.1101771

Frontiers in Oncology

Advances knowledge of carcinogenesis and tumor progression for better treatment and management

The third most-cited oncology journal, which highlights research in carcinogenesis and tumor progression, bridging the gap between basic research and applications to imrpove diagnosis, therapeutics and management strategies.

Discover the latest Research Topics

See more →

Frontiers

Avenue du Tribunal-Fédéral 34
1005 Lausanne, Switzerland
frontiersin.org

Contact us

+41 (0)21 510 17 00
frontiersin.org/about/contact